7 NSSS ACCIDENT ANALYSIS

This section provides the results of the analyses and/or evaluations which were completed for the NSSS accident analyses in support of the power uprate. These analyses include the emergency core cooling system analysis in Section 7.1 (large and small break LOCA), the containment response analysis in Section 7.2 (LOCA and main steam line break mass and energy releases), the SAR Chapter 15 analyses in Section 7.3 (steam generator tube rupture and various non-LOCA transients), and a review of the plant protection system in Section 7.4 (RPS, ESFAS, and COLSS).

7.1 ECCS PERFORMANCE ANALYSIS

An emergency core cooling system (ECCS) performance analysis demonstrated conformance to the ECCS acceptance criteria for light water nuclear power reactors, 10 CFR 50.46 (Reference 7.1-1), for ANO-2 at the power uprate rated core power of 3026 MWt (3087 MWt including a 2% power measurement uncertainty). Analyses were performed for a spectrum of large break and small break loss-of-coolant accidents (LOCAs). SAR Section 6.3 describes the ECCS performance analysis for ANO-2.

Section 7.1.1 of this report describes the objective of the ECCS performance analysis. Section 7.1.2 identifies the regulatory basis of the analysis. Sections 7.1.3 through 7.1.5 summarize the large break LOCA, small break LOCA, and the long-term ECCS performance analysis. The summaries include a description of the methodology, the plant design data, and the results of the analyses. The conclusions of the ECCS performance analysis are presented in Section 7.1.6.

7.1.1 Objective

The objective of the ECCS performance analysis is to demonstrate conformance to the ECCS acceptance criteria of 10 CFR 50.46(b):

Criterion 1: Peak Cladding Temperature: The calculated maximum fuel element cladding temperature shall not exceed 2200°F.

Criterion 2: Maximum Cladding Oxidation: The calculated total oxidation of the cladding shall nowhere exceed 0.17 times the total cladding thickness before oxidation.

Criterion 3: Maximum Hydrogen Generation: The calculated total amount of hydrogen generated from the chemical reaction of the cladding with water or steam shall not exceed 0.01 times the hypothetical amount that would be generated if all of the metal in the cladding cylinders surrounding the fuel, excluding the cladding surrounding the plenum volume, were to react.

Criterion 4: Coolable Geometry: Calculated changes in core geometry shall be such that the core remains amenable to cooling.

Criterion 5: Long-Term Cooling: After any calculated successful initial operation of the ECCS, the calculated core temperature shall be maintained at an acceptably low value and decay heat shall be removed for the extended period of time required by the long-lived radioactivity remaining in the core.

7.1.2 Regulatory Basis

As required by 10 CFR 50.46(a)(1)(i), the ECCS performance analysis must conform to the ECCS acceptance criteria identified in Section 7.1.1. Additionally, the ECCS performance must be calculated in accordance with an acceptable evaluation model and must be calculated for a number of postulated LOCAs of different sizes, locations, and other properties sufficient to provide assurance that the most severe postulated LOCAs are calculated. The evaluation model may either be a realistic evaluation model as described in 10 CFR 50.46(a)(1)(i) or must conform to the required and acceptable features of Appendix K ECCS Evaluation Models (Reference 7.1-2). The evaluation models used to perform the ANO-2 power uprate ECCS performance analysis are Appendix K evaluation models.

7.1.3 Large Break LOCA Analysis

7.1.3.1 Methodology

The large break LOCA ECCS performance analysis used the CE Nuclear Power 1999 Large Break LOCA ECCS Evaluation Model, herein referred to as the 1999 EM. The current ANO-2 large break LOCA ECCS performance analysis, described in Section 6.3.3.2.2 of the ANO-2 Safety Analysis Report (SAR) (Reference 7.1-3), employs the June 1985 version of the CE Nuclear Power Large Break LOCA ECCS Evaluation Model (Reference 7.1-4), which is the version of the evaluation model upon which the 1999 EM is built.

Several computer codes are used in the 1999 EM. The computer codes are described in the references cited with additional descriptive information provided in the 1999 EM topical report (Reference 7.1-9). The CEFLASH-4A computer code (Reference 7.1-10) is used to perform the blowdown hydraulic analysis of the reactor coolant system (RCS) and the COMPERC-II computer code (Reference 7.1-11) is used to perform the RCS refill/reflood hydraulic analysis and to calculate the containment minimum pressure. It is also used in conjunction with the methodology described in Reference 7.1-12 to calculate the FLECHT-based reflood heat transfer coefficients used in the hot rod heatup analysis. The HCROSS (Reference 7.1-13) and PARCH (Reference 7.1-14) computer codes are used to calculate steam cooling heat transfer coefficients. The hot rod heatup analysis, which calculates the peak cladding temperature and maximum cladding oxidation, is performed with the STRIKIN-II computer code (Reference 7.1-15). Core-wide cladding oxidation is calculated using the COMZIRC computer code (Appendix C of Supplement 1 of Reference 7.1-11). The initial steady state fuel rod conditions used in the analysis are determined using the FATES3B computer code (Reference 7.1-16).

The 1999 EM topical report (Reference 7.1-5) was submitted to the NRC for review and acceptance in Reference 7.1-6. In support of its review, the NRC issued a Request for Additional Information (RAI) (Reference 7.1-7). CE Nuclear Power responded to the RAI in Reference 7.1-8. The information provided in the response to the RAI was incorporated into Revision 1 of the 1999 EM topical report (Reference 7.1-9). The 1999 EM as described in Revision 1 of the topical report was used in the ANO-2 power uprate large break LOCA ECCS performance analysis.

The NRC issued the Safety Evaluation Report for the 1999 EM on December 15, 2000. The Safety Evaluation Reports for the June 1985 version of the CE Nuclear Power Large Break LOCA ECCS Evaluation Model and its versions of the computer codes are documented in References 7.1-17 through 7.1-23. The Safety Evaluation Reports for the FATES3B computer code are documented in References 7.1-24 through 7.1-26.

The limiting initial fuel rod conditions used in the large break LOCA analysis (i.e., the conditions that result in the highest calculated peak cladding temperature) were determined by performing burnup dependent calculations with STRIKIN-II using initial fuel rod conditions calculated by FATES3B.

A study was performed to determine the most limiting single failure of ECCS equipment under power uprate conditions. The study analyzed no failure, failure of an emergency diesel generator, and failure of a low pressure safety injection (LPSI) pump. Maximum safety injection pump flow rates were used in the no failure case; minimum safety injection pump flow rates were used in the emergency diesel generator and LPSI pump failure cases. The pumps were actuated on a safety injection actuation signal (SIAS) generated by low pressurizer pressure with a startup delay of 45 seconds. Minimum refueling water tank temperature was used in all three cases. The most limiting single failure (i.e., the failure that resulted in the highest calculated peak cladding temperature) was no failure of ECCS equipment. This is the same limiting single failure described in the SAR for the current analysis. No failure is the worst condition because it maximizes the amount of safety injection that spills into the containment. This acts to minimize containment pressure which, in turn, minimizes the rate at which the core is reflooded. The failure of either an emergency diesel generator or a LPSI pump is not the most damaging failure because, in both cases, there is sufficient safety injection pump flow to keep the reactor vessel downcomer filled to the cold leg nozzles. This maintains the same driving force for reflooding the core as for no failure, but results in less spillage into the containment. The study also investigated the impact of variation in safety injection tank (SIT) pressure and water volume on peak cladding temperature. Maximum SIT pressure and water volume were determined to result in the highest peak cladding temperature.

A spectrum of guillotine breaks in the reactor coolant pump discharge leg was analyzed. As described in Section 3.4 of Reference 7.1-9, the discharge leg is the most limiting break location and a guillotine break is more limiting than a slot break. In particular, the 0.3, 0.4, 0.6, 0.8, and 1.0 Double-Ended Guillotine breaks in the reactor coolant Pump Discharge leg (DEG/PD) were analyzed. The 0.4 DEG/PD break was determined to be the limiting large break LOCA (i.e., the break that results in the highest calculated peak cladding temperature), rather than the 0.6

DEG/PD that was limiting in previous cycles. The 0.3 DEG/PD was added to the analysis spectrum to confirm that the 0.4 DEG/PD was limiting.

7.1.3.2 Plant Design Data

Important core, RCS, ECCS, and containment design data used in the large break LOCA analysis are listed in Tables 7.1.3-1 and 7.1.3-2. The listed fuel rod conditions are for rod average burnup of the hot rod that produced the highest calculated peak cladding temperature. Plant design data for the containment (e.g., data for the containment initial conditions, containment volume, containment heat removal systems, and containment passive heat sinks) were selected to minimize the transient containment pressure.

7.1.3.3 Results

Table 7.1.3-3 lists the peak cladding temperature and oxidation percentages for the spectrum of large break LOCAs. Times of interest are listed in Table 7.1.3-4. The variables listed in Table 7.1.3-5 are plotted as a function of time for each break size in Figures 7.1.3-1 through 7.1.3-36 and Figures 7.1.3-47 through 7.1.3-55. The additional variables listed in Table 7.1.3-6 are plotted for the 0.4 DEG/PD break, the limiting large break LOCA, in Figures 7.1.3-37 through 7.1.3-46. The results for Cycle 16 demonstrate conformance to the ECCS acceptance criteria as summarized below. The results for Cycle 15 are provided for comparison.

Parameter	Criterion	Cycle 16 Results	Cycle 15 Results
Peak Cladding Temperature	≤2200°F	2154°F	2029°F
Maximum Cladding Oxidation	≤17%	7.8%	5.4%
Maximum Core-Wide Oxidation	≤1%	<0.99%	<0.99%
Coolable Geometry	Yes	Yes	Yes

The results are applicable to ANO-2 for a peak linear heat generation rate (PLHGR) of 13.7 kW/ft and a rated core power of 3026 MWt (3087 MWt including a 2% power measurement uncertainty).

7.1.4 Small Break LOCA Analysis

7.1.4.1 Methodology

The small break LOCA ECCS performance analysis used the Supplement 2 version (referred to as the S2M or Supplement 2 Model) of the CE Nuclear Power Small Break LOCA ECCS Evaluation Model (Reference 7.1-27). This is the same methodology used in the current ANO-2 small break LOCA ECCS performance analysis described in Section 6.3.3.2.3 of the ANO-2

SAR (Reference 7.1-3). The Safety Evaluation Reports documenting NRC acceptance of the S2M are contained in References 7.1-17, 7.1-28, and 7.1-29.

In the S2M evaluation model, the CEFLASH-4AS computer program (Reference 7.1-30) is used to perform the hydraulic analysis of the RCS until the time the safety injection tanks (SITs) begin to inject. After injection from the SITs begins, the COMPERC-II computer program (Reference 7.1-11) is used to perform the hydraulic analysis. However, COMPERC-II was not run in this analysis because the breaks sizes analyzed were too small for the SITs to begin injecting until after the peak cladding temperature was calculated to occur. The hot rod cladding temperature and maximum cladding oxidation are calculated by the STRIKIN-II computer program (Reference 7.1-15) during the initial period of forced convection heat transfer and by the PARCH computer program (Reference 7.1-14) during the subsequent period of pool boiling heat transfer. Core-wide cladding oxidation is conservatively represented as the rod-average cladding oxidation of the hot rod. The initial steady state fuel rod conditions used in the analysis are determined using the FATES3B computer program (Reference 7.1-16). The Safety Evaluation Reports for the small break LOCA ECCS performance analysis computer codes are documented in References 7.1-17, and 7.1-20 through 7.1-22. The Safety Evaluation Reports for the FATES3B computer code are documented in Reference 7.1-24 through 7.1-26.

The analysis was performed using the failure of an emergency diesel generator as the most limiting single failure of the ECCS. This is the same limiting failure as the current analysis. This failure causes the loss of both a high pressure safety injection (HPSI) pump and a LPSI pump and results in a minimum of safety injection water being available to cool the core. Based on this failure and the design of the ANO-2 ECCS, 75% of the flow from one HPSI pump is credited in the small break LOCA analysis. The LPSI pumps are not explicitly credited in the small break LOCA analysis since the RCS pressure never decreases below the LPSI pump shutoff head during the portion of the transient that is analyzed. However, 50% of the flow from one LPSI pump is available to cool the core given a failure of an emergency diesel generator and a break in the reactor coolant pump discharge leg.

As in the previous analysis, a spectrum of three break sizes in the reactor coolant pump discharge (PD) leg was analyzed. The reactor coolant pump discharge leg is the limiting break location because it maximizes the amount of spillage from the ECCS. In particular, the 0.03, 0.04, and 0.05 ft^2/PD breaks were analyzed. These break sizes are within the range of break sizes for which the hot rod cladding heatup transient is terminated solely by injection from a HPSI pump. It is within this range of break sizes that the limiting small break LOCA resides. Smaller breaks are too small to experience as much core uncovery as these breaks. Larger breaks are sufficiently large to allow injection from the SITs to recover the core and terminate the heatup of the cladding before the cladding temperature approaches the peak cladding temperature of the limiting small break LOCA.

7.1.4.2 Plant Design Data

Important core, RCS, and ECCS design data used in the small break LOCA analysis are listed in Tables 7.1.4-1 and 7.1.4-2. The listed fuel rod conditions are for the hot rod burnup that produces the maximum initial stored energy.

7.1.4.3 Results

Table 7.1.4-3 lists the peak cladding temperature and oxidation percentages for the spectrum of small break LOCAs. Times of interest are listed in Table 7.1.4-4. The variables listed in Table 7.1.4-5 are plotted as a function of time for each break in Figures 7.1.4-1 through 7.1.4-24. The Cycle 16 results for the 0.04 ft^2/PD break, the limiting small break LOCA, demonstrate conformance to the ECCS acceptance criteria as summarized below. Cycle 15 results are given for comparison.

Parameter	Criterion	Cycle 16 Results	Cycle 15 Results
Peak Cladding Temperature	≤2200°F	2066°F	1905°F
Maximum Cladding Oxidation	≤17%	10.78%	6.68%
Maximum Core-Wide Oxidation	≤1%	<0.67%	<0.50%
Coolable Geometry	Yes	Yes	Yes

The results are applicable to ANO-2 for a PLHGR of 13.7 kW/ft and a rated core power of 3026 MWt (3087 MWt including a 2% power measurement uncertainty).

7.1.5 Long-Term ECCS Performance

7.1.5.1 Methodology

Long-term post-LOCA residual heat removal is accomplished by continuous boil-off of fluid in the reactor vessel until the fuel decay heat is sufficiently reduced to prevent boil-off. As borated water is delivered to the core region via safety injection and virtually pure water escapes as steam, unacceptably high concentrations of boric acid and other solution additives may accumulate in the reactor vessel unless a flush path is provided.

For a hot leg break, safety injection flow introduced via the cold legs will travel down the annulus, through the core, and out the break. Thus, a flushing path is established through the reactor vessel, precluding the buildup of solids in the core region. However, for a cold leg break, only that amount of injected water required for decay heat removal actually makes it to the core, because the remainder spills out the break. Therefore, because of the geometry of the RCS, there is no flushing through the core for a cold leg break until an alternate flow path is established.

The post-LOCA boric acid precipitation analysis uses the BORON computer program from the CE Nuclear Power Post-LOCA Long Term Cooling Evaluation Model (Reference 7.1-31). This is a different methodology than the methodology used in the boric acid precipitation analysis performed for Cycle 1 that is described in Section 6.3.3.15 of the ANO-2 SAR (Reference 7.1-3).

In the evaluation model, the BORON computer program (Appendix C of Reference 7.1-31) is used to calculate the boric acid concentration in the core as a function of time following the limiting large break LOCA.

The analysis uses a boric acid concentration of 27.6 wt% as the solubility limit of boric acid in the core. This is the solubility limit of boric acid in saturated water at atmospheric pressure. Atmospheric pressure is a conservative minimum value for the core pressure following a large break LOCA.

7.1.5.2 Plant Design Data

Important plant design data used in the post-LOCA boric acid precipitation analysis are listed in Table 7.1.5-1.

7.1.5.3 Results

The post-LOCA boric acid precipitation analysis determined that a minimum flow rate of 250 gpm from a HPSI pump to both the hot and cold legs of the RCS, initiated between two and five hours post-LOCA, maintains the boric acid concentration in the core below the solubility limit of 27.6 wt% for the limiting break, i.e., a large cold leg break. The analysis also determined that the potential for entrainment of the hot side injection by the steam flowing in the hot legs ends prior to two hours post-LOCA.

Figure 7.1.5-1 compares the core boiloff rate with the minimum simultaneous hot and cold leg injection flow rate of 250 gpm. It shows that the initiation of 250 gpm of hot and cold leg injection at five hours post-LOCA provides a substantial and time-increasing flushing flow through the core. Figure 7.1.5-2 presents the core boric acid concentration as a function of time for the limiting break. It shows that without simultaneous hot and cold leg injection, the boric acid concentration in the core exceeds the solubility limit at approximately 7.3 hours post-LOCA. When 250 gpm of simultaneous hot and cold leg injection is initiated at five hours post-LOCA, the maximum boric acid concentration in the core is 23.3 wt% at 5.9 hours post-LOCA, as compared to the solubility limit of 27.6 wt%. Figure 7.1.5-2 also shows that a flushing flow rate of 20 gpm started by five hours post-LOCA is sufficient to prevent the core boric acid concentration from reaching the solubility limit.

In summary, the results of the post-LOCA boric acid precipitation analysis demonstrate conformance to Criterion 5 of the ECCS acceptance criteria. The results are applicable to ANO-2 for a rated core power of 3026 MWt (3087 MWt including a 2% power measurement uncertainty).

7.1.6 Conclusion

An ECCS performance analysis was completed for ANO-2 at the power uprate rated core power of 3026 MWt (3087 MWt including a 2% power measurement uncertainty). The analysis included consideration of large break LOCA, small break LOCA, and post-LOCA boric acid precipitation. The limiting break size, i.e., the break size that resulted in the highest peak cladding temperature, was determined to be the 0.4 DEG/PD break.

The results of the analysis demonstrate conformance to the ECCS acceptance criteria at a PLHGR of 13.7 kW/ft as follows:

Criterion 1: Peak Cladding Temperature: The calculated maximum fuel element cladding temperature shall not exceed 2200°F.

Result: The ECCS performance analysis calculated a peak cladding temperature of 2154 °F for the 0.4 DEG/PD break.

Criterion 2: Maximum Cladding Oxidation: The calculated total oxidation of the cladding shall nowhere exceed 0.17 times the total cladding thickness before oxidation.

Result: The ECCS performance analysis calculated a maximum cladding oxidation of 0.108 times the total cladding thickness before oxidation for the 0.04 ft^2/PD break.

Criterion 3: Maximum Hydrogen Generation: The calculated total amount of hydrogen generated from the chemical reaction of the cladding with water or steam shall not exceed 0.01 times the hypothetical amount that would be generated if all of the metal in the cladding cylinders surrounding the fuel, excluding the cladding surrounding the plenum volume, were to react.

Result: The ECCS performance analysis calculated a maximum hydrogen generation of less than 0.0099 times the hypothetical amount for the 0.4 DEG/PD break.

Criterion 4: Coolable Geometry: Calculated changes in core geometry shall be such that the core remains amenable to cooling.

Result: The cladding swelling and rupture models used in the ECCS performance analysis account for the effects of changes in core geometry that would occur if cladding rupture is calculated to occur. Adequate core cooling was demonstrated for the changes in core geometry that were calculated to occur as a result of cladding rupture. In addition, the transient analysis was performed to a time when cladding temperatures were decreasing and the RCS was depressurized, thereby precluding any further cladding deformation. Therefore, a coolable geometry was demonstrated.

Criterion 5: Long-Term Cooling: After any calculated successful initial operation of the ECCS, the calculated core temperature shall be maintained at an acceptably low value and decay heat shall be removed for the extended period of time required by the long-lived radioactivity remaining in the core.

Result: The large break and small break LOCA ECCS performance analyses demonstrated that the ANO-2 ECCS successfully maintains the fuel cladding temperature at an acceptably low value in the short term. Subsequently, for the extended period of time required by the long-lived radioactivity remaining in the core, the ECCS continues to supply sufficient cooling water from the refueling water tank and then from the sump to remove decay heat and maintain the core temperature at an acceptably low value. In addition, at the appropriate time, the operator realigns a HPSI pump for simultaneous hot and cold leg injection in order to maintain the core boric acid concentration below the solubility limit.

7.1.7 References

7.1-1 Code of Federal Regulations, Title 10, Part 50, Section 50.46, "Acceptance Criteria for Emergency Core Cooling Systems for Light Water Nuclear Power Reactors".

7.1-2 Code of Federal Regulations, Title 10, Part 50, Appendix K, "ECCS Evaluation Models".

7.1-3 Safety Analysis Report for ANO-2, through Amendment 15.

7.1-4 CENPD-132P, "Calculative Methods for the C-E Large Break LOCA Evaluation Model," August 1974.

CENPD-132P, Supplement 1, "Calculational Methods for the C-E Large Break LOCA Evaluation Model," February 1975.

CENPD-132-P, Supplement 2-P, "Calculational Methods for the C-E Large Break LOCA Evaluation Model," July 1975.

CENPD-132, Supplement 3-P-A, "Calculative Methods for the C-E Large Break LOCA Evaluation Model for the Analysis of C-E and W Designed NSSS," June 1985.

7.1-5 CENPD-132, Supplement 4-P, "Calculative Methods for the ABB CENP Large Break LOCA Evaluation Model," April 1999.

7.1-6 LD-99-026, I. C. Rickard (ABB CENP) to Document Control Desk (NRC), "Revisions to ABB CENP ECCS Performance Appendix K Evaluation Model," April 30, 1999.

7.1-7 J. Cushing (NRC) to I. C. Rickard (ABB CENP), "Request for Additional Information (RAI) Regarding CENPD-132-P, Supplement 4-P (TAC No. MA5660)," December 14, 1999.

7.1-8 LD-2000-0011, I. C. Rickard (ABB CENP) to Document Control Desk (NRC), "ABB CENP Response to NRC Request for Additional Information Regarding CENPD-132-P, Supplement 4-P," February 22, 2000.

7.1-9 CENPD-132, Supplement 4-P, Revision 1, "Calculative Methods for the CE Nuclear Power Large Break LOCA Evaluation Model," August 2000.

7.1-10 CENPD-133P, "CEFLASH-4A, A FORTRAN-IV Digital Computer Program for Reactor Blowdown Analysis," August 1974.

CENPD-133P, Supplement 2, "CEFLASH-4A, A FORTRAN-IV Digital Computer Program for Reactor Blowdown Analysis (Modifications)," February 1975.

CENPD-133, Supplement 4-P, "CEFLASH-4A, A FORTRAN-IV Digital Computer Program for Reactor Blowdown Analysis," April 1977.

CENPD-133, Supplement 5-A, "CEFLASH-4A, A FORTRAN77 Digital Computer Program for Reactor Blowdown Analysis," June 1985.

7.1-11 CENPD-134 P, "COMPERC-II, A Program for Emergency-Refill-Reflood of the Core," August 1974.

CENPD-134 P, Supplement 1, "COMPERC-II, A Program for Emergency Refill-Reflood of the Core (Modifications)," February 1975.

CENPD-134, Supplement 2-A, "COMPERC-II, A Program for Emergency Refill-Reflood of the Core," June 1985.

7.1-12 CENPD-213-P, "Application of FLECHT Reflood Heat Transfer Coefficients to C-E's 16x16 Fuel Bundles," January 1976.

7.1-13 LD-81-095, Enclosure 1-P-A, "C-E ECCS Evaluation Model, Flow Blockage Analysis," December 1981.

7.1-14 CENPD-138P, "PARCH, A FORTRAN-IV Digital Program to Evaluate Pool Boiling, Axial Rod and Coolant Heatup," August 1974.

CENPD-138P, Supplement 1, "PARCH, A FORTRAN-IV Digital Program to Evaluate Pool Boiling, Axial Rod and Coolant Heatup (Modifications)," February 1975.

CENPD-138, Supplement 2-P, "PARCH, A FORTRAN-IV Digital Program to Evaluate Pool Boiling, Axial Rod and Coolant Heatup," January 1977.

7.1-15 CENPD-135P, "STRIKIN-II, A Cylindrical Geometry Fuel Rod Heat Transfer Program," August 1974.

CENPD-135P, Supplement 2, "STRIKIN-II, A Cylindrical Geometry Fuel Rod Heat Transfer Program (Modifications)," February 1975.

CENPD-135, Supplement 4-P, "STRIKIN-II, A Cylindrical Geometry Fuel Rod Heat Transfer Program," August 1976.

CENPD-135-P, Supplement 5, "STRIKIN-II, A Cylindrical Geometry Fuel Rod Heat Transfer Program," April, 1977.

7.1-16 CENPD-139-P-A, "C-E Fuel Evaluation Model," July 1974.

CEN-161(B)-P-A, "Improvements to Fuel Evaluation Model," August 1989.

CEN-161(B)-P, Supplement 1-P-A, "Improvements to Fuel Evaluation Model," January 1992.

7.1-17 O. D. Parr (NRC) to F. M. Stern (C-E), June 13, 1975.

7.1-18 O. D. Parr (NRC) to A. E. Scherer (C-E), December 9, 1975.

7.1-19 D. M. Crutchfield (NRC) to A. E. Scherer (C-E), "Safety Evaluation of Combustion Engineering ECCS Large Break Evaluation Model and Acceptance for Referencing of Related Licensing Topical Reports," July 31, 1986.

7.1-20 K. Kniel (NRC) to A. E. Scherer (C-E), "Combustion Engineering Emergency Core Cooling System Evaluation Model," November 12, 1976.

7.1-21 R. L. Baer (NRC) to A. E. Scherer (C-E), "Evaluation of Topical Report CENPD-135 Supplement No. 5," September 6, 1978.

7.1-22 K. Kniel (NRC) to A. E. Scherer (C-E), "Evaluation of Topical Report CENPD-138, Supplement 2-P," April 10, 1978.

7.1-23 K. Kniel (NRC) to A. E. Scherer (C-E), August 2, 1976.

7.1-24 O. D. Parr (NRC) to F. M. Stern (C-E), December 4, 1974.

7.1-25 A. C. Thadani (NRC) to A. E. Scherer (C-E), "Acceptance for Generic Referencing of the Topical Report CEN-161 'Improvements to Fuel Evaluation Model (FATES3)'," May 22, 1989.

7.1-26 A. C. Thadani (NRC) to A. E. Scherer (C-E), "Generic Approval of C-E Fuel Performance Code FATES3B (CEN-161(B)-P, Supplement 1-P) (TAC No. M81769)," November 6, 1991.

7.1-27 CENPD-137P, "Calculative Methods for the C-E Small Break LOCA Evaluation Model," August 1974.

CENPD-137, Supplement 1-P, "Calculative Methods for the C-E Small Break LOCA Evaluation Model," January 1977.

CENPD-137, Supplement 2-P-A, "Calculative Methods for the ABB CE Small Break LOCA Evaluation Model," April 1998.

7.1-28 K. Kniel (NRC) to A. E. Scherer (C-E), "Evaluation of Topical Reports CENPD-133, Supplement 3-P and CENPD-137, Supplement 1-P," September 27, 1977.

7.1-29 T. H. Essig (NRC) to I. C. Rickard (ABB), "Acceptance for Referencing of the Topical Report CENPD-137(P), Supplement 2, Calculative Methods for the C-E Small Break LOCA Evaluation Model (TAC No. M95687)," December 16, 1997.

7.1-30 CENPD-133P, Supplement 1, "CEFLASH-4AS, A Computer Program for the Reactor Blowdown Analysis of the Small Break Loss of Coolant Accident," August 1974.

CENPD-133, Supplement 3-P, "CEFLASH-4AS, A Computer Program for the Reactor Blowdown Analysis of the Small Break Loss of Coolant Accident," January 1977.

7.1-31 CENPD-254-P-A, "Post-LOCA Long Term Cooling Evaluation Model," June 1980.

Table 7.1.3-1

Large Break LOCA ECCS Performance Analysis
Core and Plant Design Data

Quantity	Value	Units
Reactor power level (102% of rated power)	3087	MWt
Peak linear heat generation rate (PLHGR) of the hot rod	13.7	kW/ft
PLHGR of the average rod in assembly with hot rod	12.98	kW/ft
Gap conductance at the PLHGR(1)	2168	BTU-hr-ft^2-°F
Fuel centerline temperature at the PLHGR(1)	3378	°F
Fuel average temperature at the PLHGR(1)	2090	°F
Hot rod gas pressure(1)	1175	psia
Moderator temperature coefficient at initial density	$+0.5 \times 10^{-4}$	$\Delta\rho$/°F
RCS flow rate	118.0×10^6	lbm/hr
Core flow rate	113.9×10^6	lbm/hr
RCS pressure	2200	psia
Cold leg temperature	540.0	°F
Hot leg temperature	607.1	°F
Plugged tubes per steam generator	10	%
Low pressurizer pressure SIAS setpoint	1400	psia
Safety injection tank pressure (min/max)	500/700	psia
Safety injection tank water volume (min/max)	1000/1600	ft^3
LPSI pump flow rate (min, 1 pump/max, 2 pump)	3222/7310	gpm
HPSI pump flow rate (min, 1 pump/max, 2 pump)	728/1667	gpm
Containment pressure	13.2	psia
Containment temperature	60	°F
Containment humidity	100	%
Containment net free volume	1.82×10^6	ft^3
Containment spray pump flow rate	2518	gpm/pump
Refueling water tank temperature	38	°F
Containment passive heat sinks	Table 7.1.3-2	--

(1) These quantities correspond to the rod average burnup of the hot rod (5000 MWD/MTU) that yields the highest peak cladding temperature.

Table 7.1.3-2

Large Break LOCA ECCS Performance Analysis
Containment Passive Heat Sink Data

Wall No.	Description	Material	Thickness (ft)	Surface Area (ft^2)
1	Containment walls and dome	Type B coating Steel Concrete	0.0004 0.0225 3.56	62,050
2	Containment walls [1]	Type A coating Steel Concrete	0.0004 0.0224 3.78	20,000
3	Base slab	Type C coating Concrete	0.0107 10.5	10,000
4	Refueling canal [2]	Stainless steel Concrete	0.0217 2.02	10,000
5	Sheet metal and pipes [1][2]	Galvanized coating Steel	0.00008 0.0049	110,500
6	Concrete walls and floors[1][2]	Type C coating Concrete	0.0063 1.38	28,000
7	Structural Steel [1][2]	Type A coating Steel	0.0004 0.0349	119,300
8	Crane girders and misc. steel [1][2]	Type D coating Steel	0.0005 0.0108	77,000
9	Concrete [1][2]	Concrete	2.70	68,000
10	Stainless steel [1][2]	Stainless steel	0.0179	7,000

(1) Thickness is effective thickness as a result of combining similar thickness walls.
(2) One side of wall is exposed to containment atmosphere, one side is insulated.

Table 7.1.3-3

Large Break LOCA ECCS Performance Analysis Results

Break Size	Peak Cladding Temperature (°F)	Maximum Cladding Oxidation (%)	Maximum Core-Wide Cladding Oxidation (%)
1.0 DEG/PD	2080	6.2	<0.99
0.8 DEG/PD	2081	6.3	<0.99
0.6 DEG/PD	2108	6.9	<0.99
0.4 DEG/PD	2154	7.8	<0.99
0.3 DEG/PD	2112	6.9	<0.99

Table 7.1.3-4

Large Break LOCA ECCS Performance Analysis Times of Interest (seconds after break)

Break Size	SITs On	End of Bypass	Start of Reflood	SITs Empty	Hot Rod Rupture
1.0 DEG/PD	8.9	17.0	31.3	88.2	41.0
0.8 DEG/PD	9.7	18.2	32.4	89.2	39.5
0.6 DEG/PD	11.4	19.5	33.5	90.8	36.0
0.4 DEG/PD	14.4	23.3	37.1	94.6	46.7
0.3 DEG/PD	17.8	27.4	41.0	98.9	58.9

Table 7.1.3-5

Large Break LOCA ECCS Performance Analysis
Each Break
Variables Plotted as a Function of Time

Variable
Core Power
Pressure in Center Hot Assembly Node
Leak Flow Rate
Hot Assembly Flow Rate (Below Hot Spot)
Hot Assembly Flow Rate (Above Hot Spot)
Hot Assembly Quality
Containment Pressure
Mass Added to Core During Reflood
Peak Cladding Temperature[1]

Note:
(1) The cladding temperature at the elevation of cladding rupture is also shown for the limiting break.

Table 7.1.3-6

Large Break LOCA ECCS Performance Analysis
Limiting Break
Variables Plotted as a Function of Time

Variable
Mid Annulus Flow Rate
Quality Above and Below the Core
Core Pressure Drop
Safety Injection Flow Rate into Intact Discharge Legs
Water Level in Downcomer During Reflood
Hot Spot Gap Conductance
Maximum Local Cladding Oxidation Percentage
Fuel Centerline, Fuel Average, Cladding, and Coolant Temperature at the Hot Spot
Hot Spot Heat Transfer Coefficient
Hot Pin Pressure

Table 7.1.4-1

Small Break LOCA ECCS Performance Analysis
Core and Plant Design Data

Quantity	Value	Units
Reactor power level (102% of rated power)	3087	MWt
Peak linear heat generation rate (PLHGR)	13.7	kW/ft
Axial shape index	-0.3	—
Gap conductance at PLHGR[(1)]	1700	BTU-hr-ft^2-°F
Fuel centerline temperature at PLHGR[(1)]	3486	°F
Fuel average temperature at PLHGR[(1)]	2184	°F
Hot rod gas pressure[(1)]	1138	psia
Moderator temperature coefficient at initial density	0.0×10^{-4}	$\Delta\rho$/°F
RCS flow rate	117.4×10^6	lbm/hr
Core flow rate	113.3×10^6	lbm/hr
RCS pressure	2200	psia
Cold leg temperature	556.7	°F
Hot leg temperature	621.1	°F
Plugged tubes per steam generator	10	%
MSSV first bank opening pressure	1130.9	psia
Low pressurizer pressure reactor trip setpoint	1400	psia
Low pressurizer pressure SIAS setpoint	1400	psia
HPSI Flow Rate	Table 7.1.4-2	gpm
Safety injection tank pressure	500	psia

Note:
(1) These quantities correspond to the rod average burnup of the hot rod (1000 MWD/MTU) that yields the maximum initial stored energy.

Table 7.1.4-2

High Pressure Safety Injection Pump
Minimum Delivered Flow to RCS
(Assuming Failure of an Emergency Diesel Generator)

RCS Pressure, psia	Flow Rate, gpm
14.7	738.7
22	736.6
31	733.3
35	732.2
46	729.0
191	680.4
327	631.8
456	583.2
577	534.6
692	486.0
800	437.4
899	388.8
990	340.2
1071	291.6
1142	237.6
1201	172.8
1248	102.6
1269	54.0
1281	0.0

Notes:
1. The flow is assumed to be split equally to each of the four discharge legs.
2. The flow to the broken discharge leg is assumed to spill out the break.

Table 7.1.4-3

Small Break LOCA ECCS Performance Analysis Results

Break Size	Peak Cladding Temperature (°F)	Maximum Cladding Oxidation (%)	Maximum Core-Wide Cladding Oxidation (%)
0.03 ft^2/PD	1842	3.3	<0.43
0.04 ft^2/PD	2066	10. 8	<0.67
0.05 ft^2/PD	1882	10.6	<0.63

Table 7.1.4-4

Small Break LOCA ECCS Performance Analysis Times of Interest (seconds after break)

Break Size	HPSI Flow Delivered to RCS	LPSI Flow Delivered to RCS	SIT Flow Delivered to RCS	Peak Cladding Temperature Occurs
0.03 ft^2/PD	281	(a)	(c)	2275
0.04 ft^2/PD	222	(a)	(c)	1825
0.05 ft^2/PD	187	(a)	1763 (b)	1633

(a) Calculation completed before LPSI flow delivery to RCS begins.
(b) SIT injection calculated to begin but not credited in analysis.
(c) Calculation completed before SIT injection begins.

Table 7.1.4-5

Small Break LOCA ECCS Performance Analysis
Variables Plotted as a Function of Time for Each Break

Variable
Core Power
Inner Vessel Pressure
Break Flow Rate
Inner Vessel Inlet Flow Rate
Inner Vessel Two-Phase Mixture Level
Heat Transfer Coefficient at Hot Spot
Coolant Temperature at Hot Spot
Cladding Temperature at Hot Spot

Table 7.1.5-1

Post-LOCA Boric Acid Precipitation Analysis
Core and Plant Design Data

Quantity	Value	Units
Reactor power level (102% of rated power)	3087	MWt
RCS liquid mass (maximum)	493,000	lbm
RCS boron concentration (maximum)	2000	ppm
Boric acid makeup tanks		
liquid volume, total (maximum)	23,400	gal
boric acid concentration (maximum)	3.5	wt%
liquid temperature (minimum)	53	°F
Refueling water tank		
liquid volume (maximum)	503,300	gal
boron concentration (maximum)	3000	ppm
liquid temperature (minimum)	38	°F
Safety injection tanks		
number (maximum)	4	—
liquid volume per tank (maximum)	1600	ft^3
boron concentration (maximum)	3000	ppm
liquid temperature (minimum)	40	°F
pressure (maximum)	700	psia
Charging pumps		
number (maximum)	3	—
flow rate per pump (maximum)	46	gpm
Flow rates for emptying the RWT		
HPSI pump flow rate (minimum)	724	gpm
LPSI pump flow rate (minimum)	3222	gpm
CS pump flow rate (minimum)	1875	gpm

Figure 7.1.3-1
Large Break LOCA ECCS Performance Analysis
1.0 DEG/PD Break
Core Power

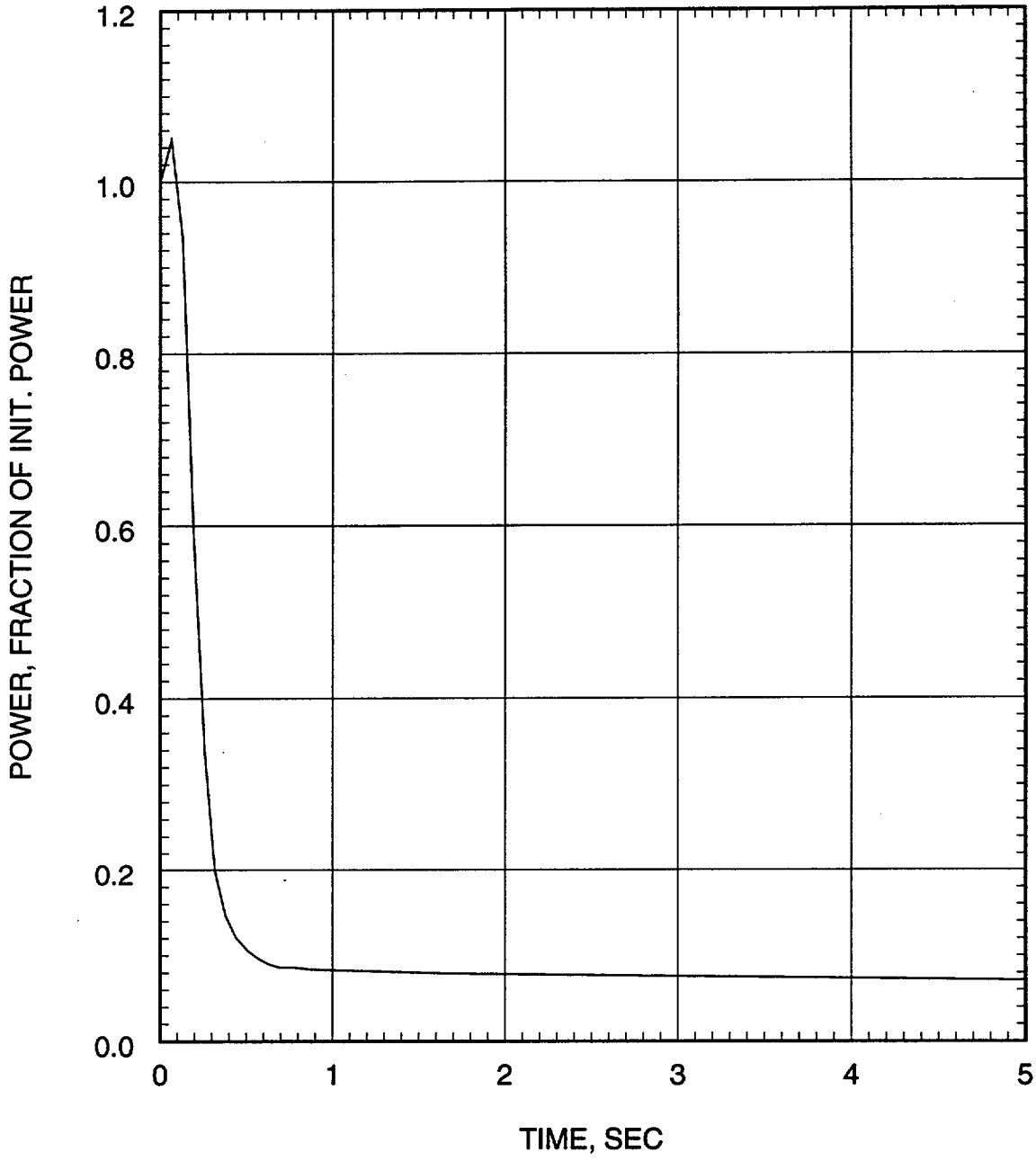

Figure 7.1.3-2
Large Break LOCA ECCS Performance Analysis
1.0 DEG/PD Break
Pressure in Center Hot Assembly Node

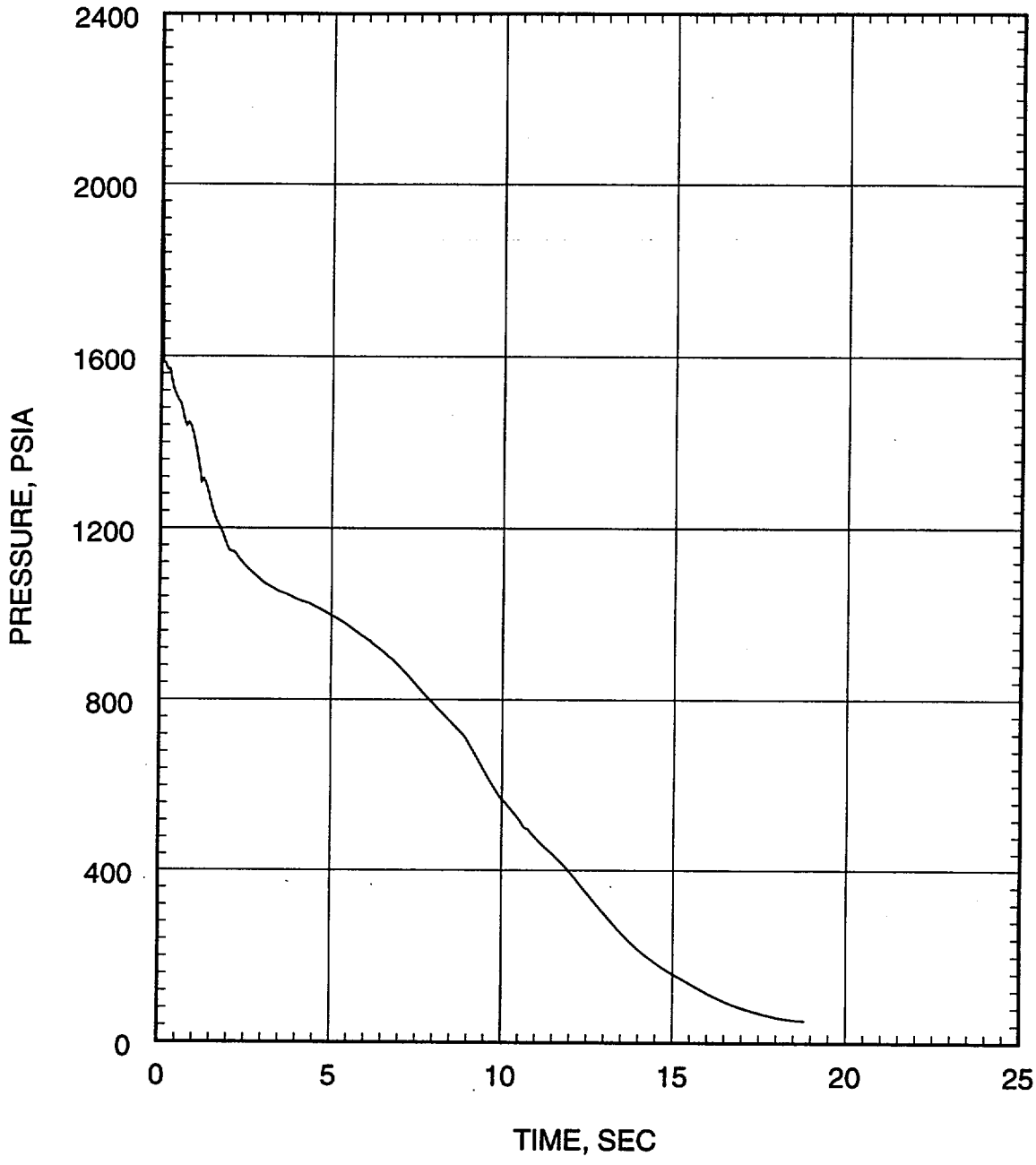

Figure 7.1.3-3
Large Break LOCA ECCS Performance Analysis
1.0 DEG/PD Break
Leak Flow Rate

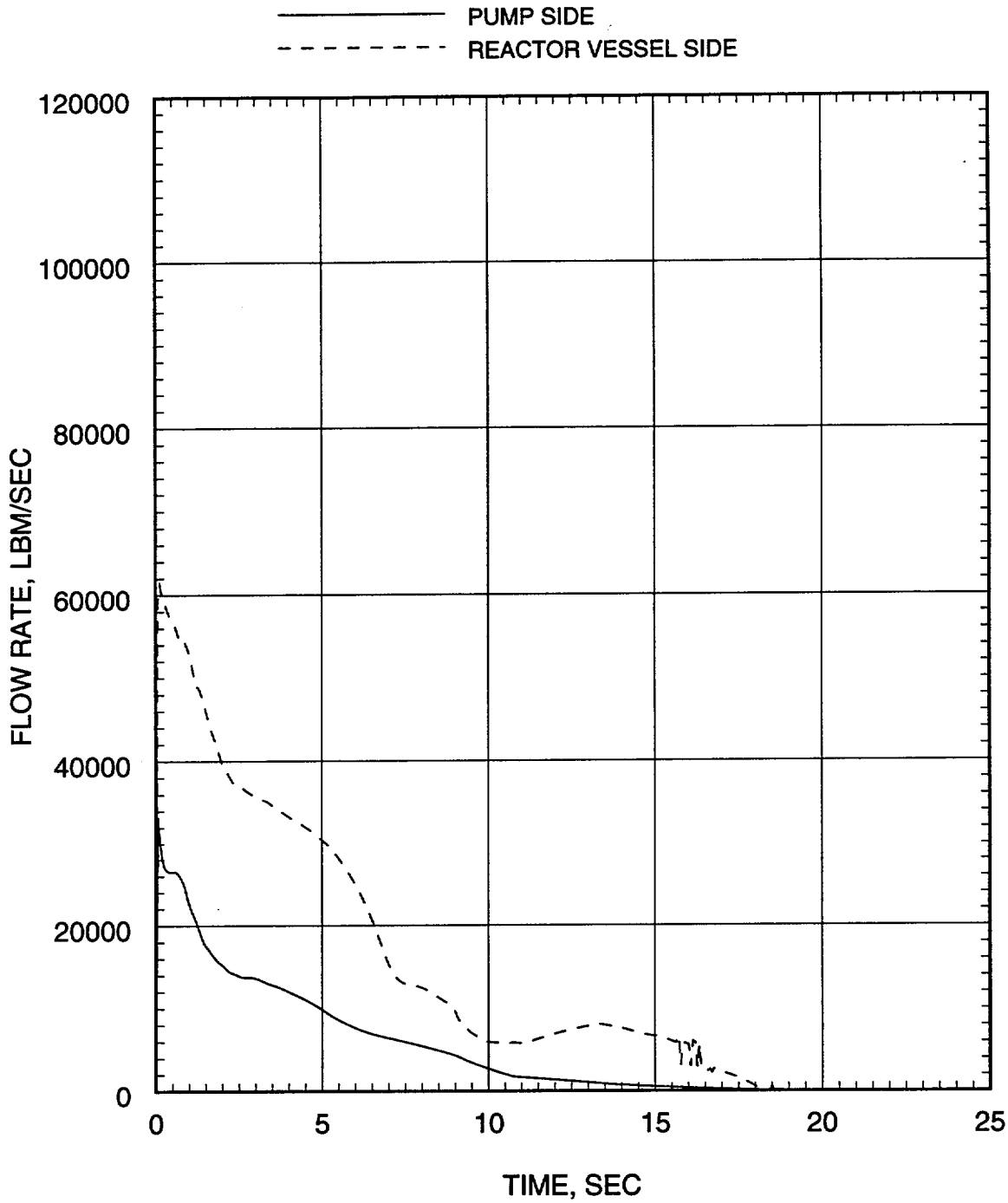

Figure 7.1.3-4
Large Break LOCA ECCS Performance Analysis
1.0 DEG/PD Break
Hot Assembly Flow Rate (Below Hot Spot)

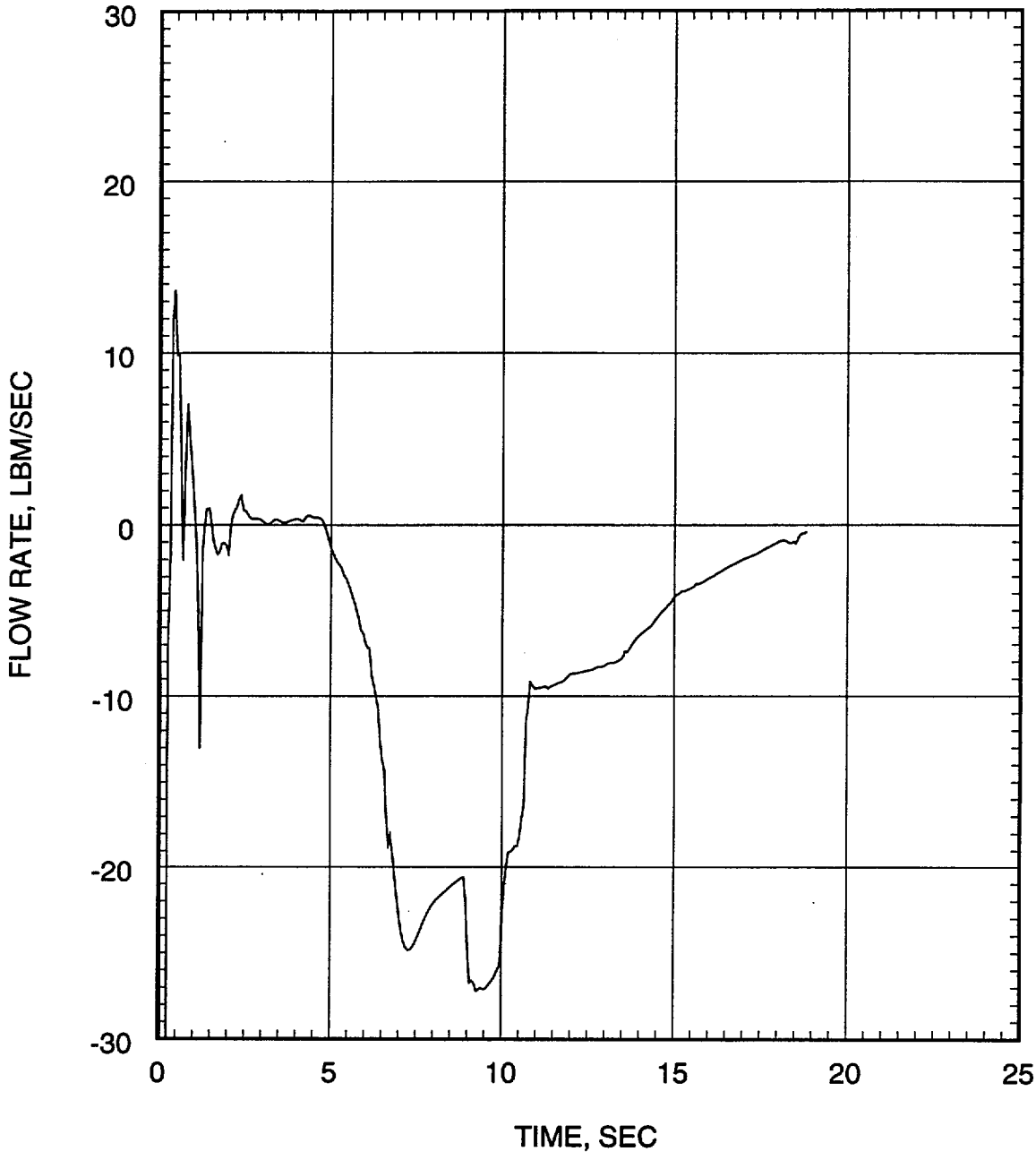

Figure 7.1.3-5
Large Break LOCA ECCS Performance Analysis
1.0 DEG/PD Break
Hot Assembly Flow Rate (Above Hot Spot)

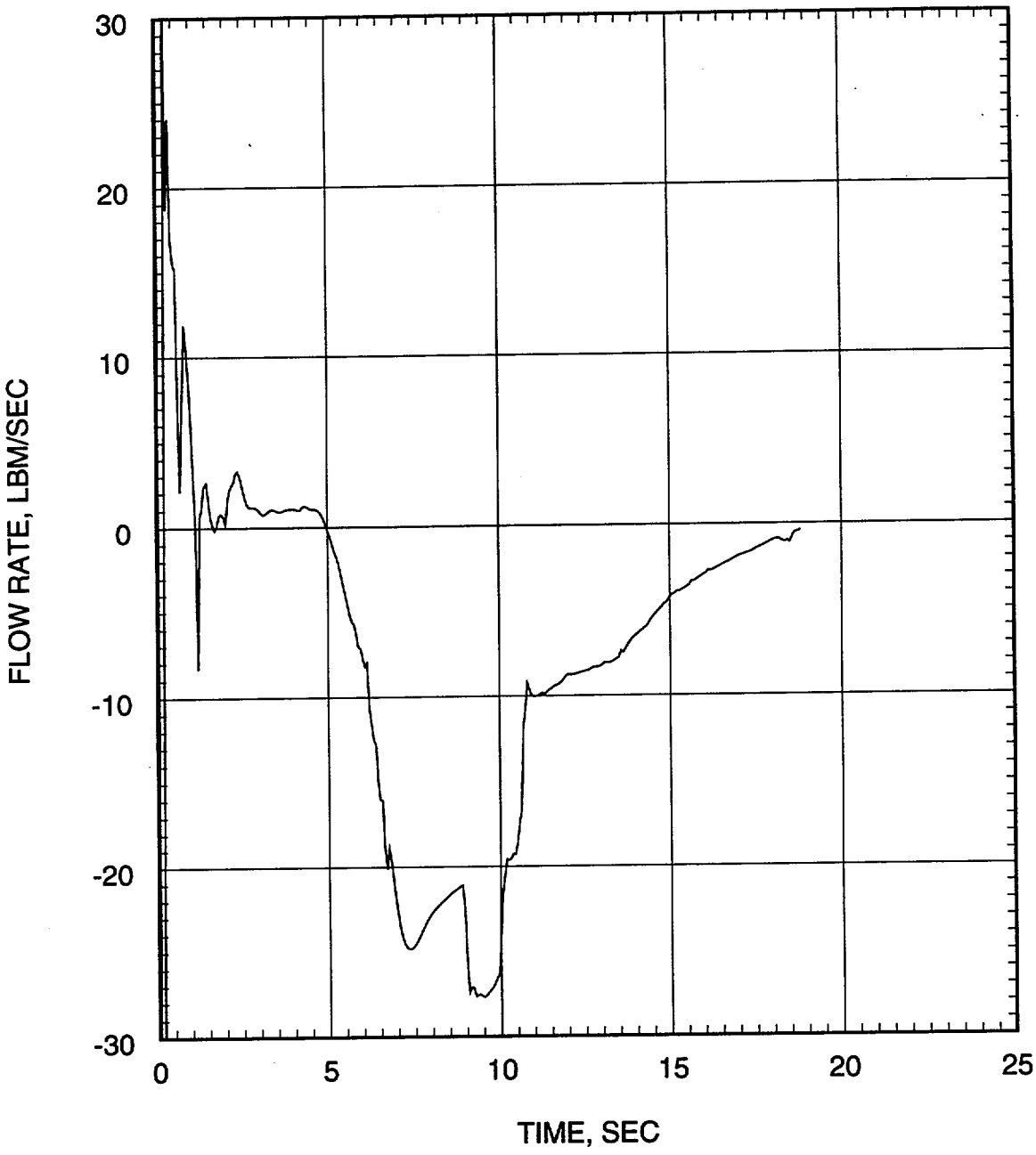

Figure 7.1.3-6
Large Break LOCA ECCS Performance Analysis
1.0 DEG/PD Break
Hot Assembly Quality

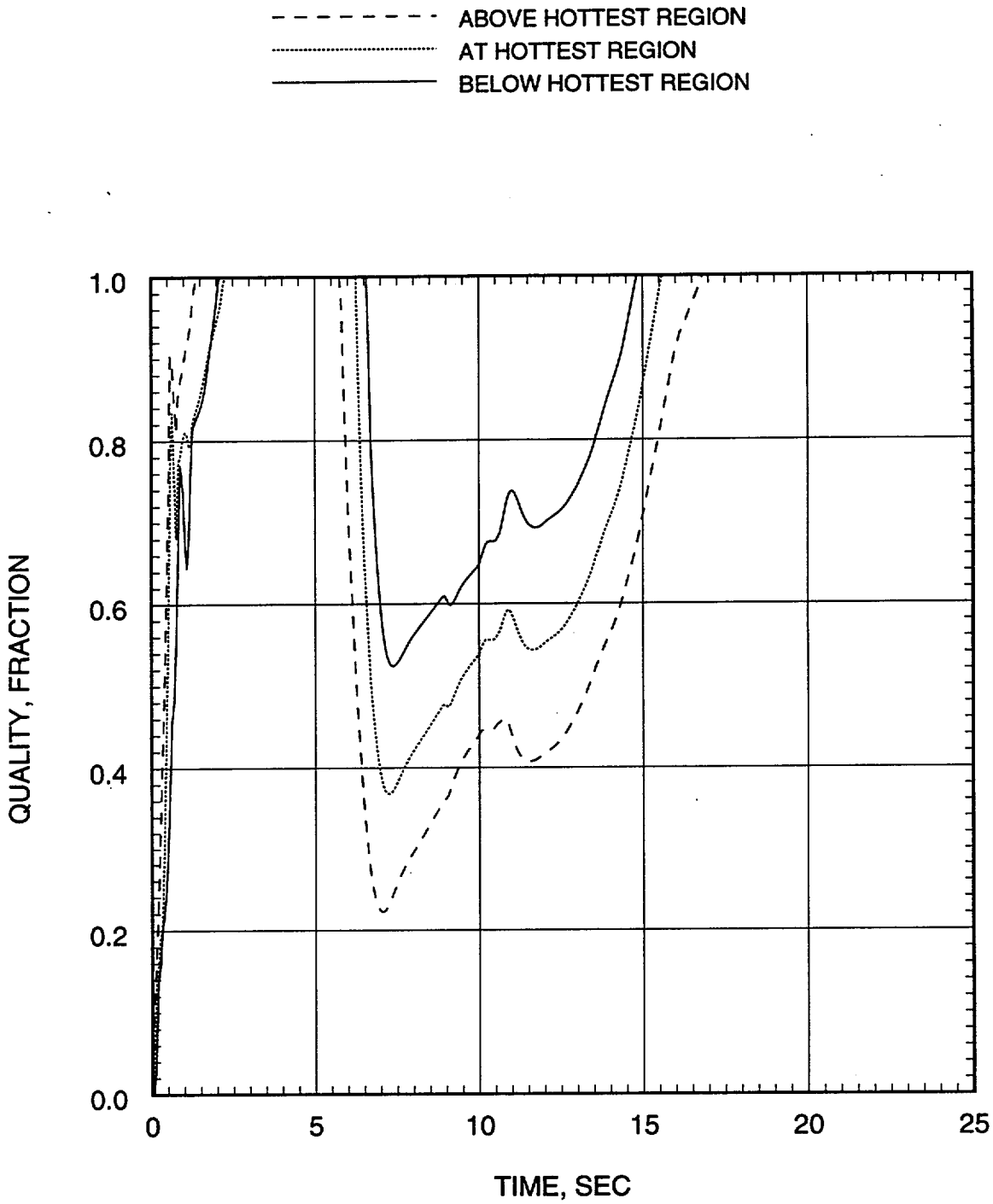

Figure 7.1.3-7
Large Break LOCA ECCS Performance Analysis
1.0 DEG/PD Break
Containment Pressure

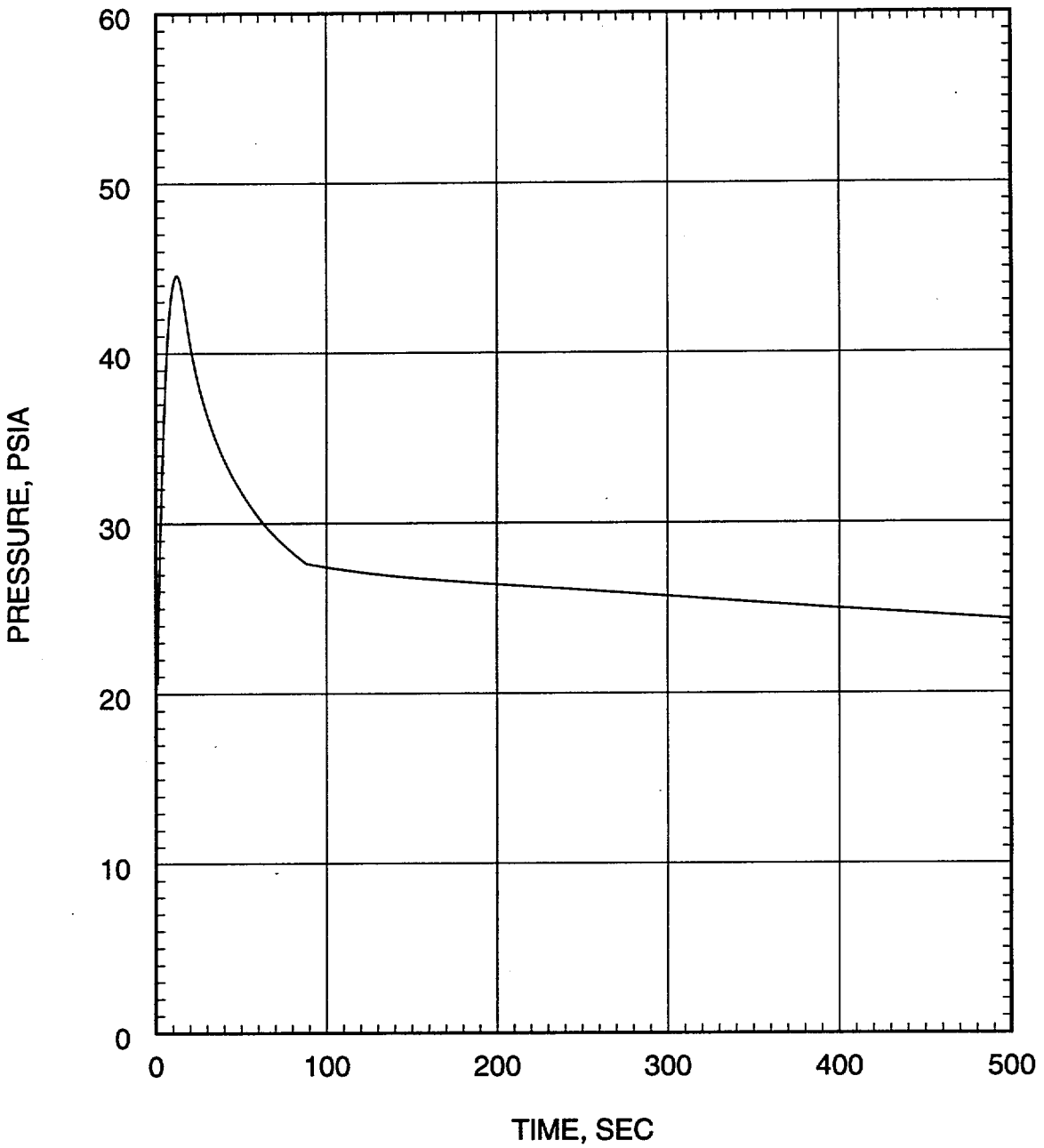

Figure 7.1.3-8
Large Break LOCA ECCS Performance Analysis
1.0 DEG/PD Break
Mass Added to Core During Reflood

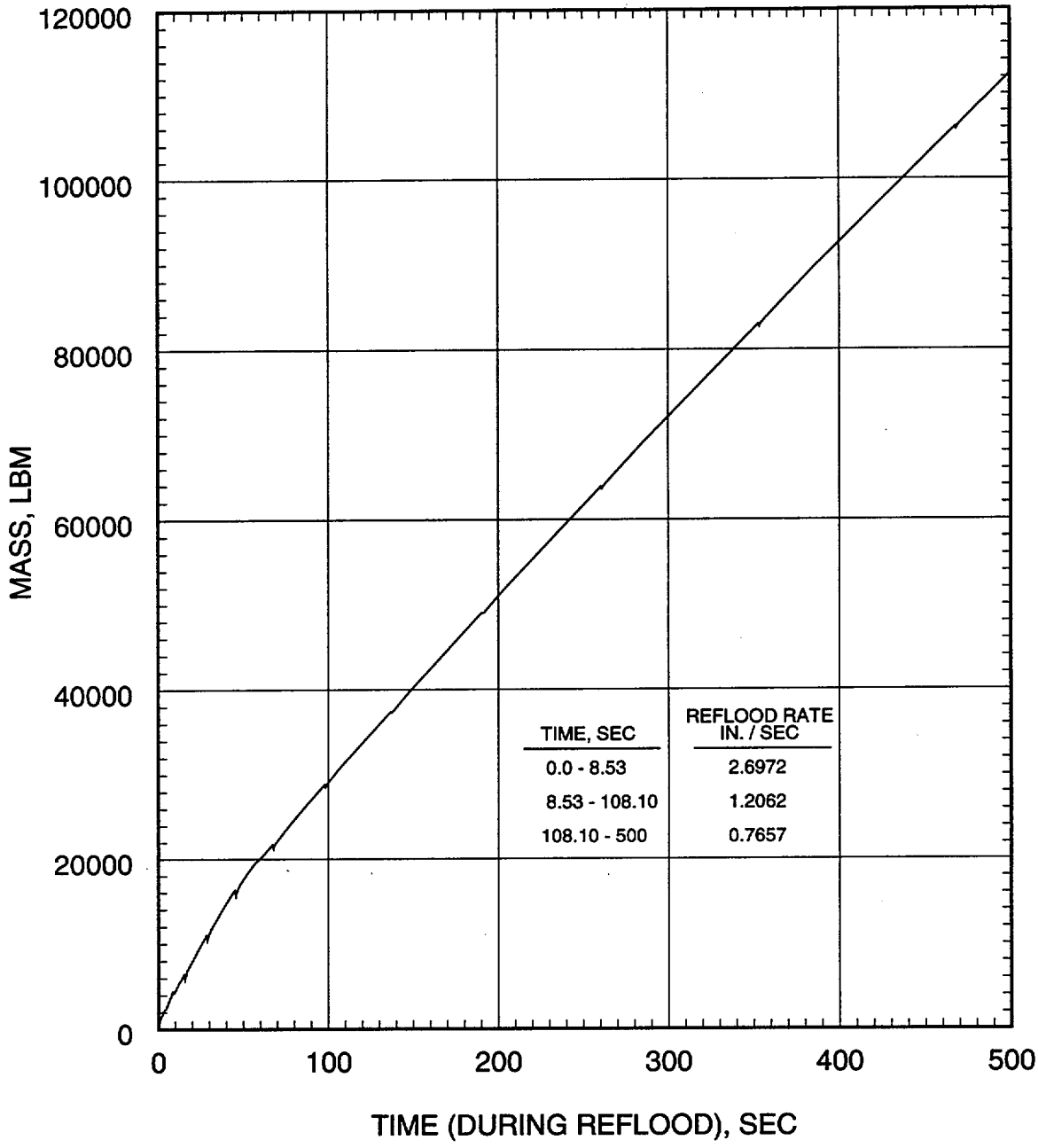

Figure 7.1.3-9
Large Break LOCA ECCS Performance Analysis
1.0 DEG/PD Break
Peak Cladding Temperature

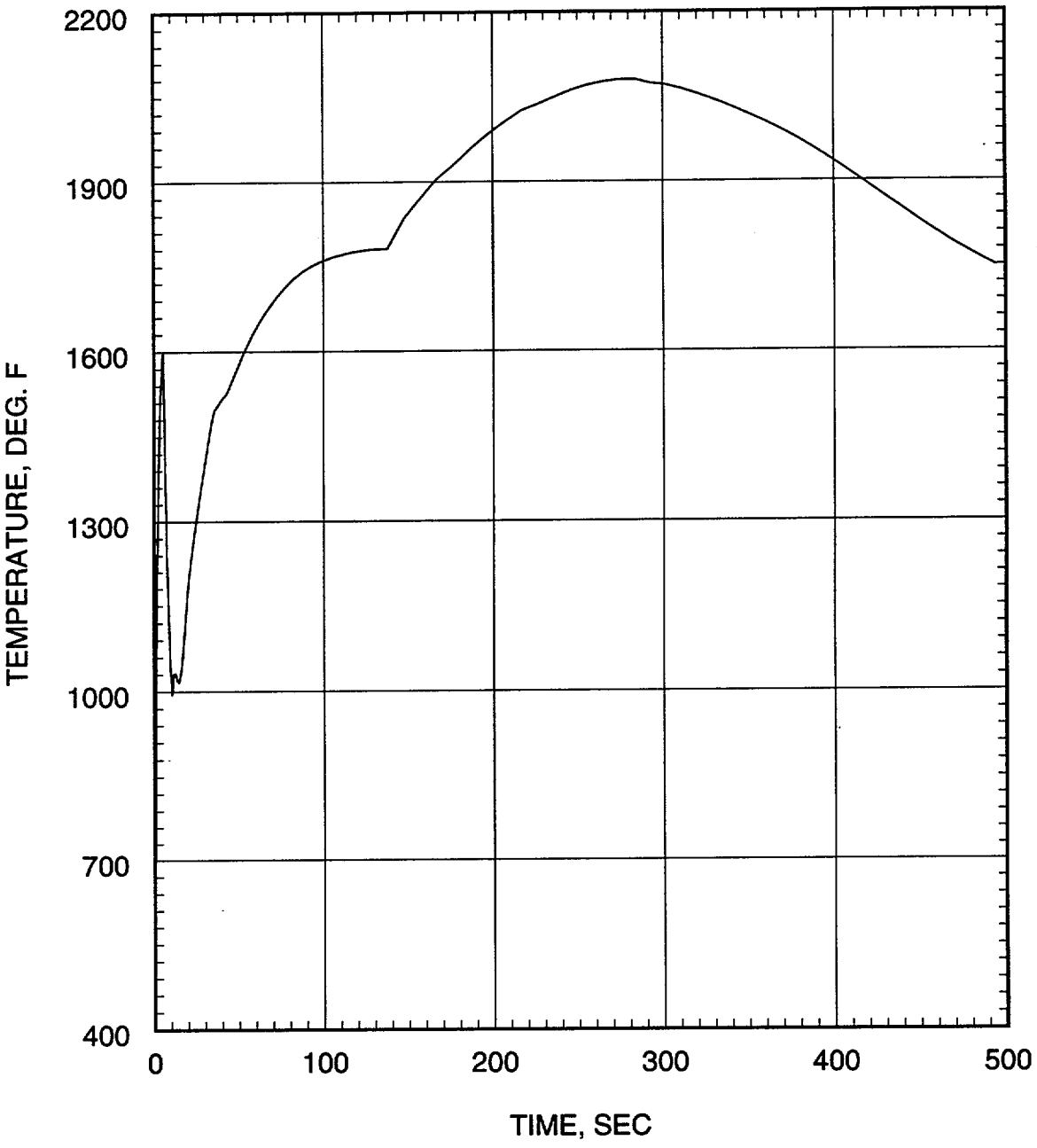

Figure 7.1.3-10
Large Break LOCA ECCS Performance Analysis
0.8 DEG/PD Break
Core Power

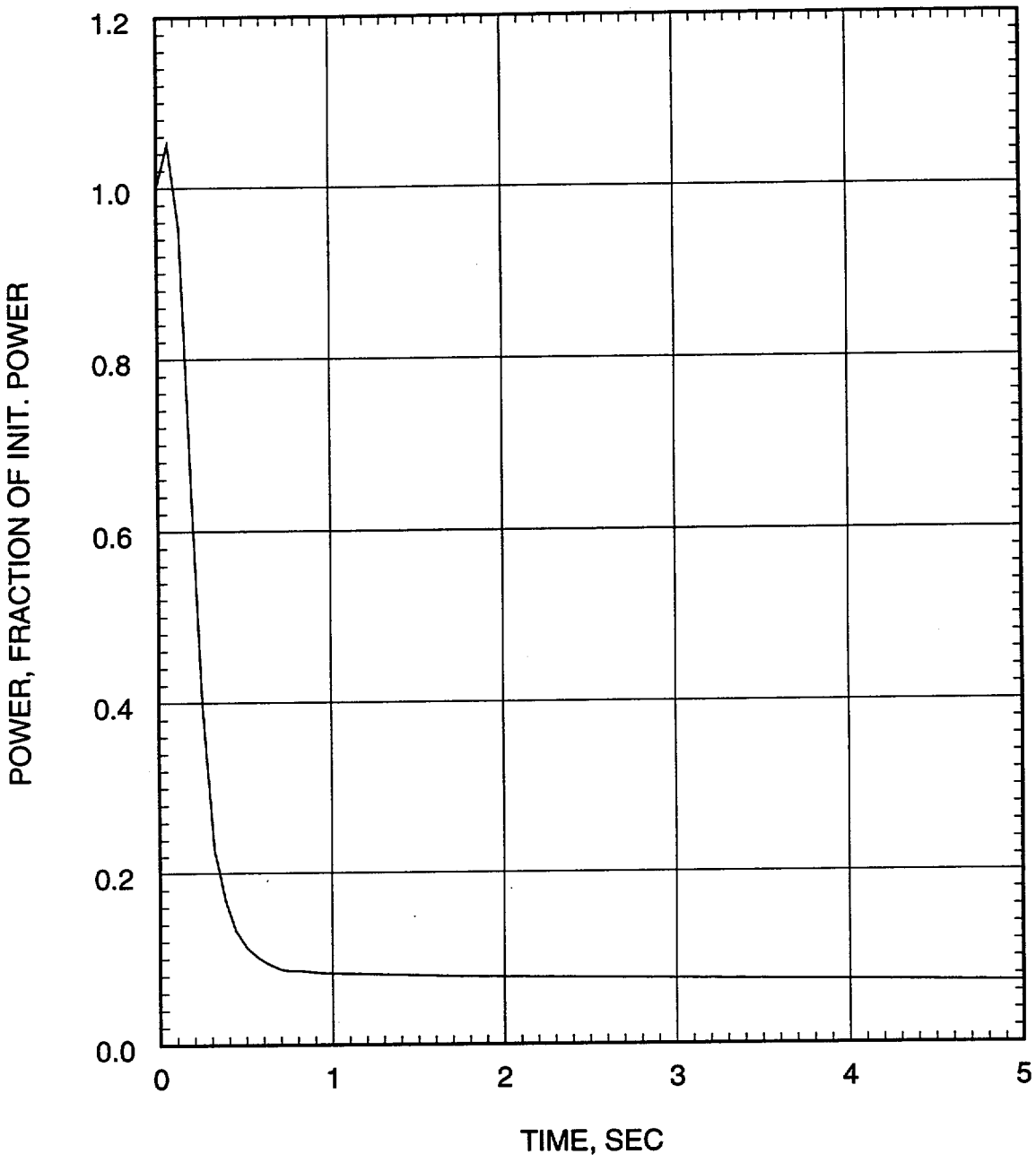

Figure 7.1.3-11
Large Break LOCA ECCS Performance Analysis
0.8 DEG/PD Break
Pressure in Center Hot Assembly Node

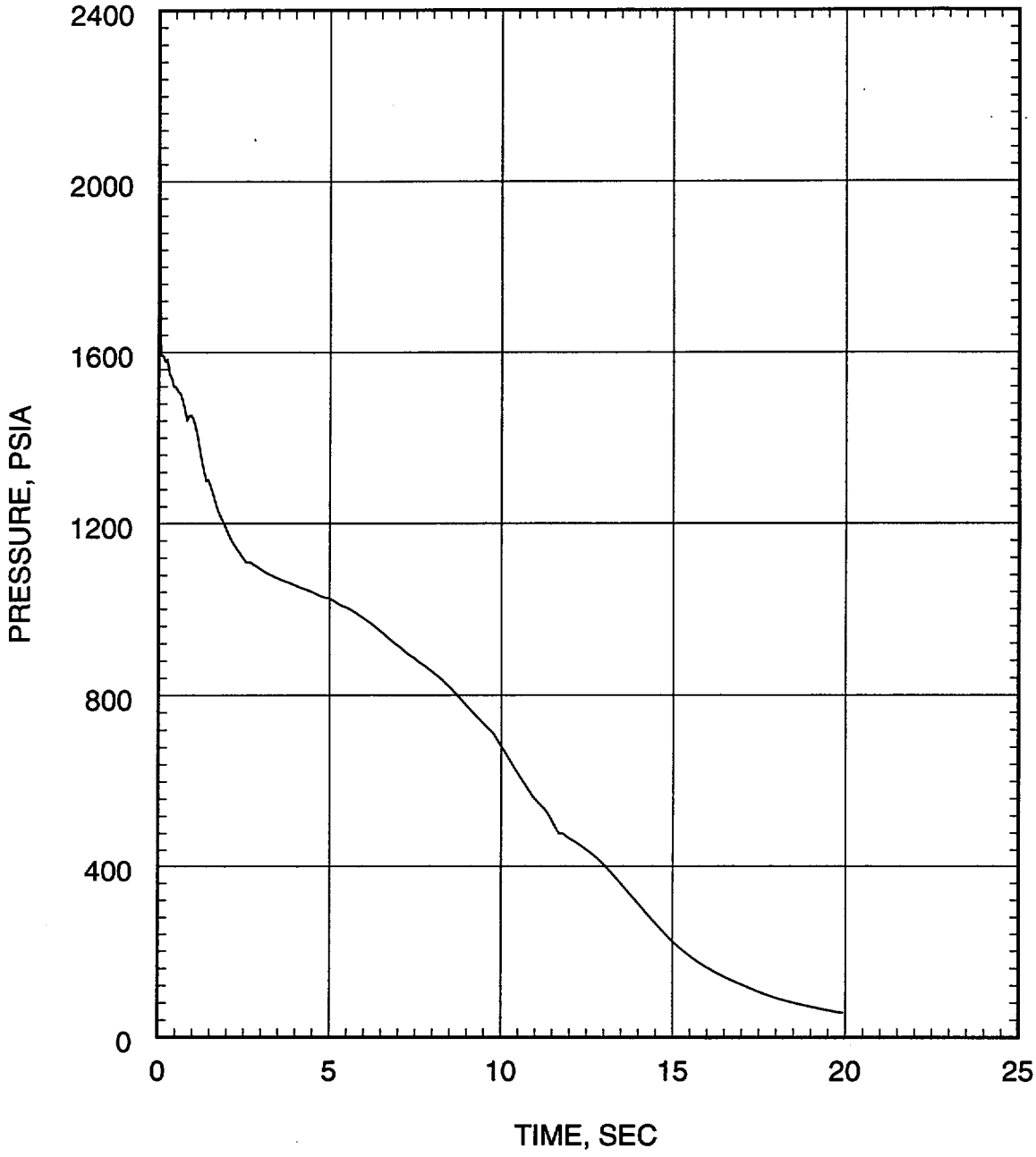

Figure 7.1.3-12
Large Break LOCA ECCS Performance Analysis
0.8 DEG/PD Break
Leak Flow Rate

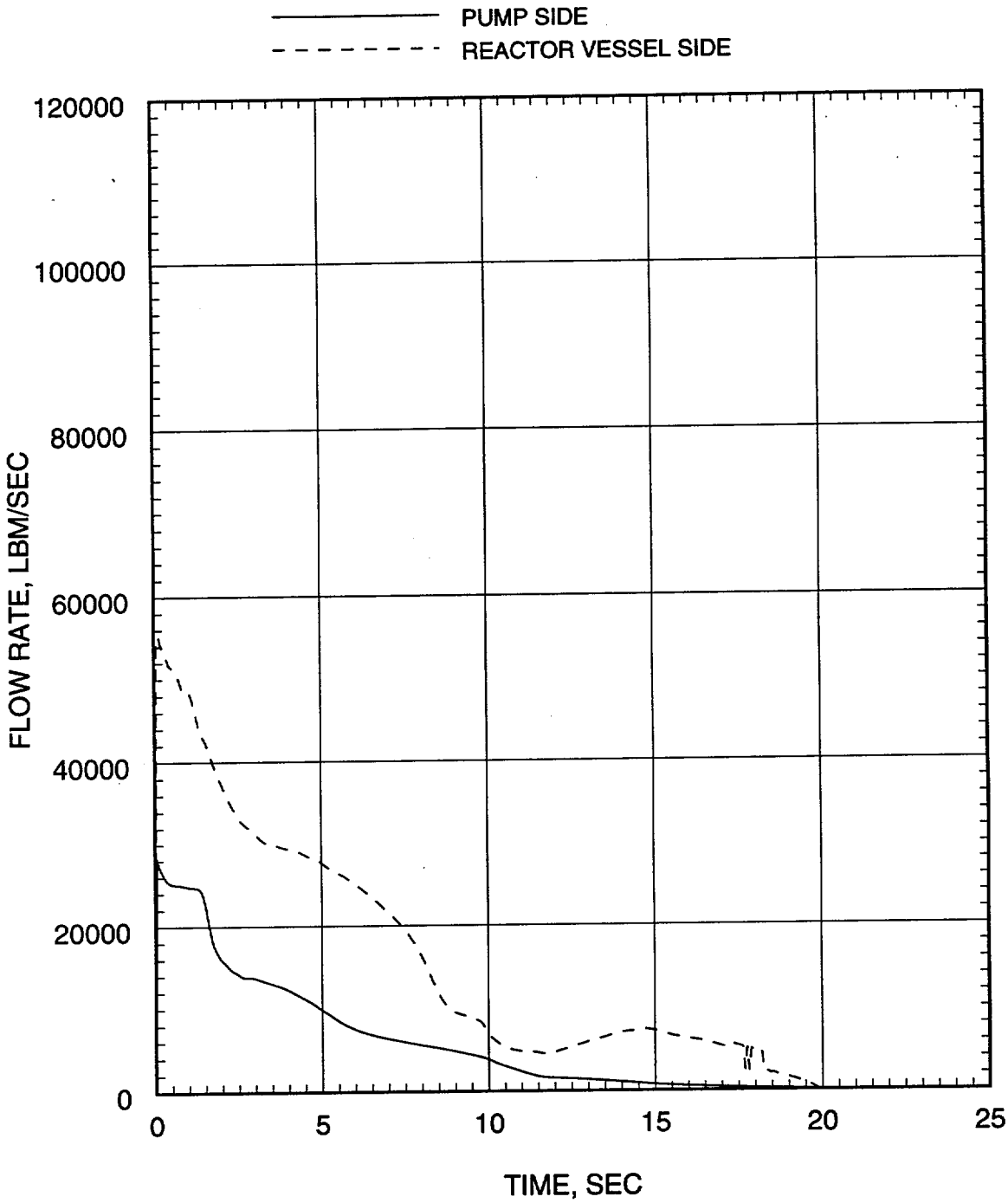

Figure 7.1.3-13
Large Break LOCA ECCS Performance Analysis
0.8 DEG/PD Break
Hot Assembly Flow Rate (Below Hot Spot)

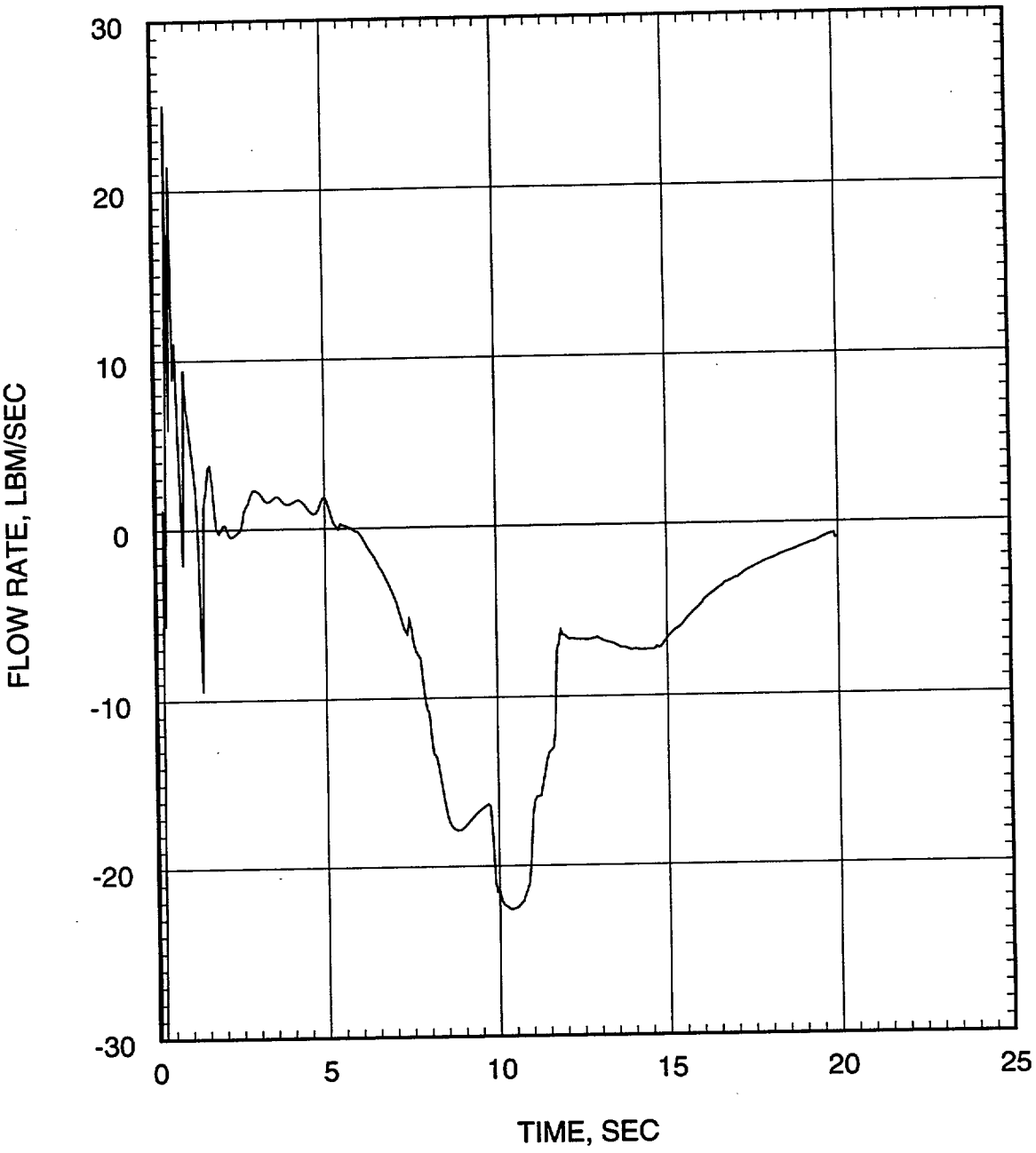

Figure 7.1.3-14
Large Break LOCA ECCS Performance Analysis
0.8 DEG/PD Break
Hot Assembly Flow Rate (Above Hot Spot)

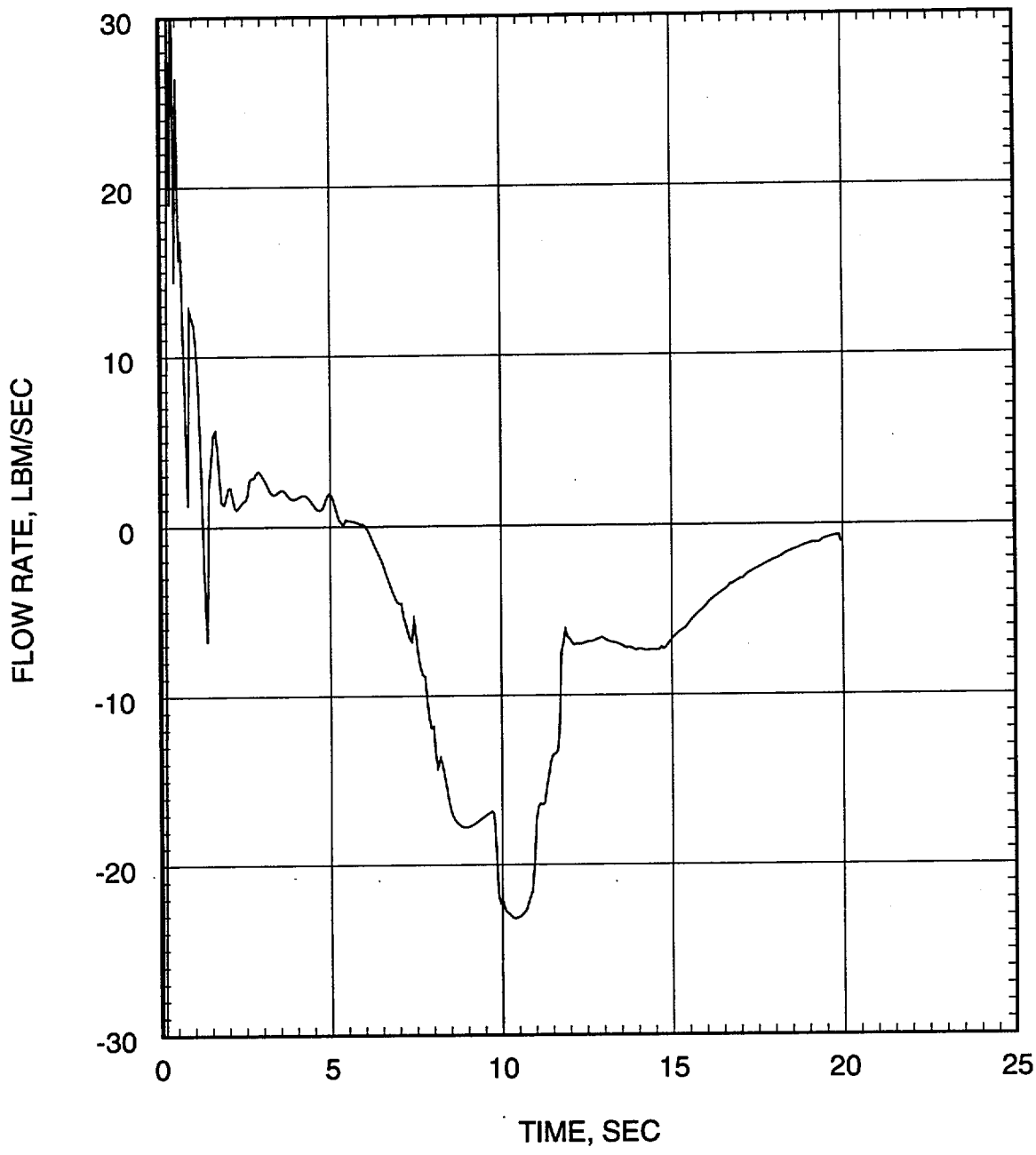

Figure 7.1.3-15
Large Break LOCA ECCS Performance Analysis
0.8 DEG/PD Break
Hot Assembly Quality

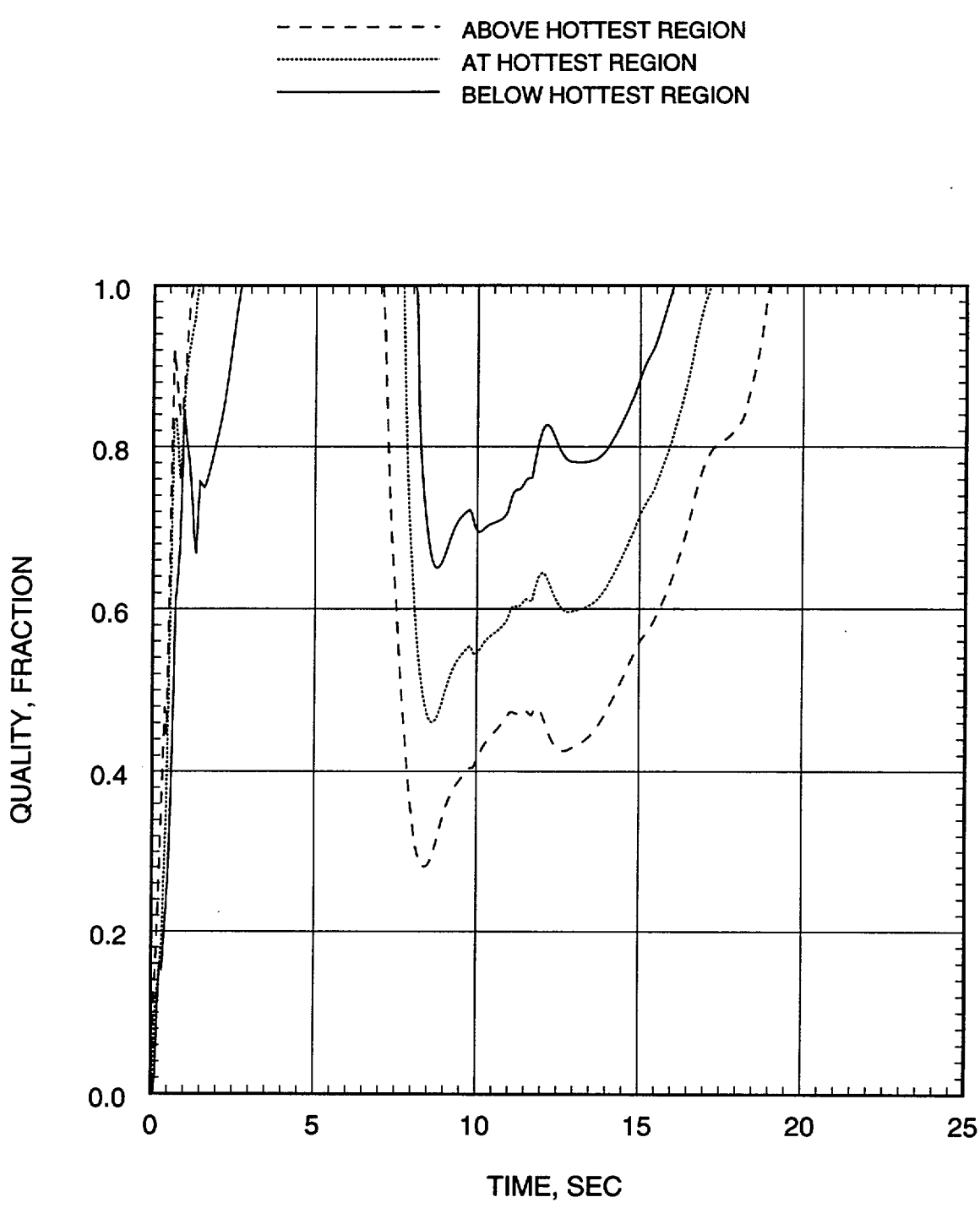

Figure 7.1.3-16
Large Break LOCA ECCS Performance Analysis
0.8 DEG/PD Break
Containment Pressure

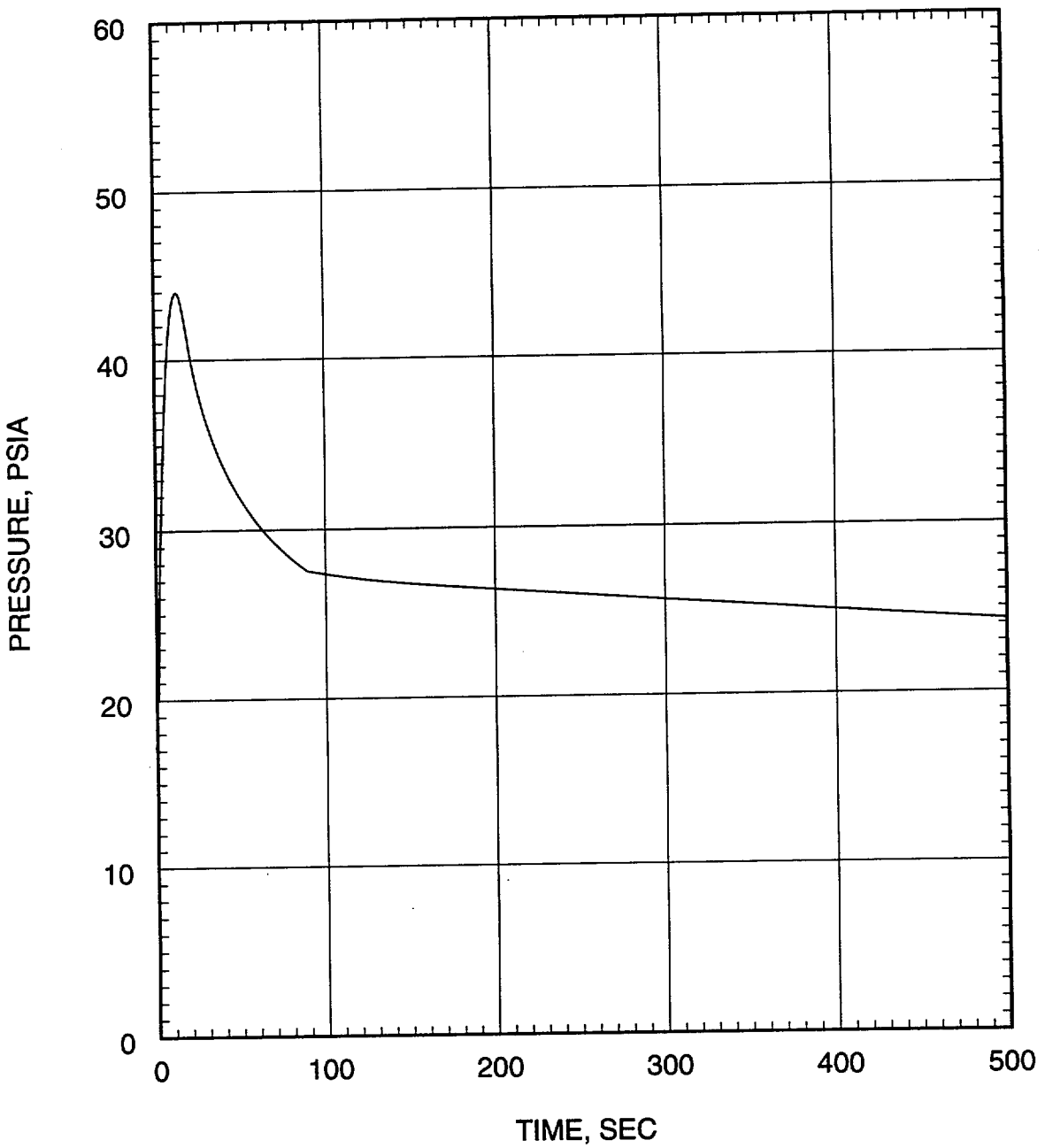

Figure 7.1.3-17
Large Break LOCA ECCS Performance Analysis
0.8 DEG/PD Break
Mass Added to Core During Reflood

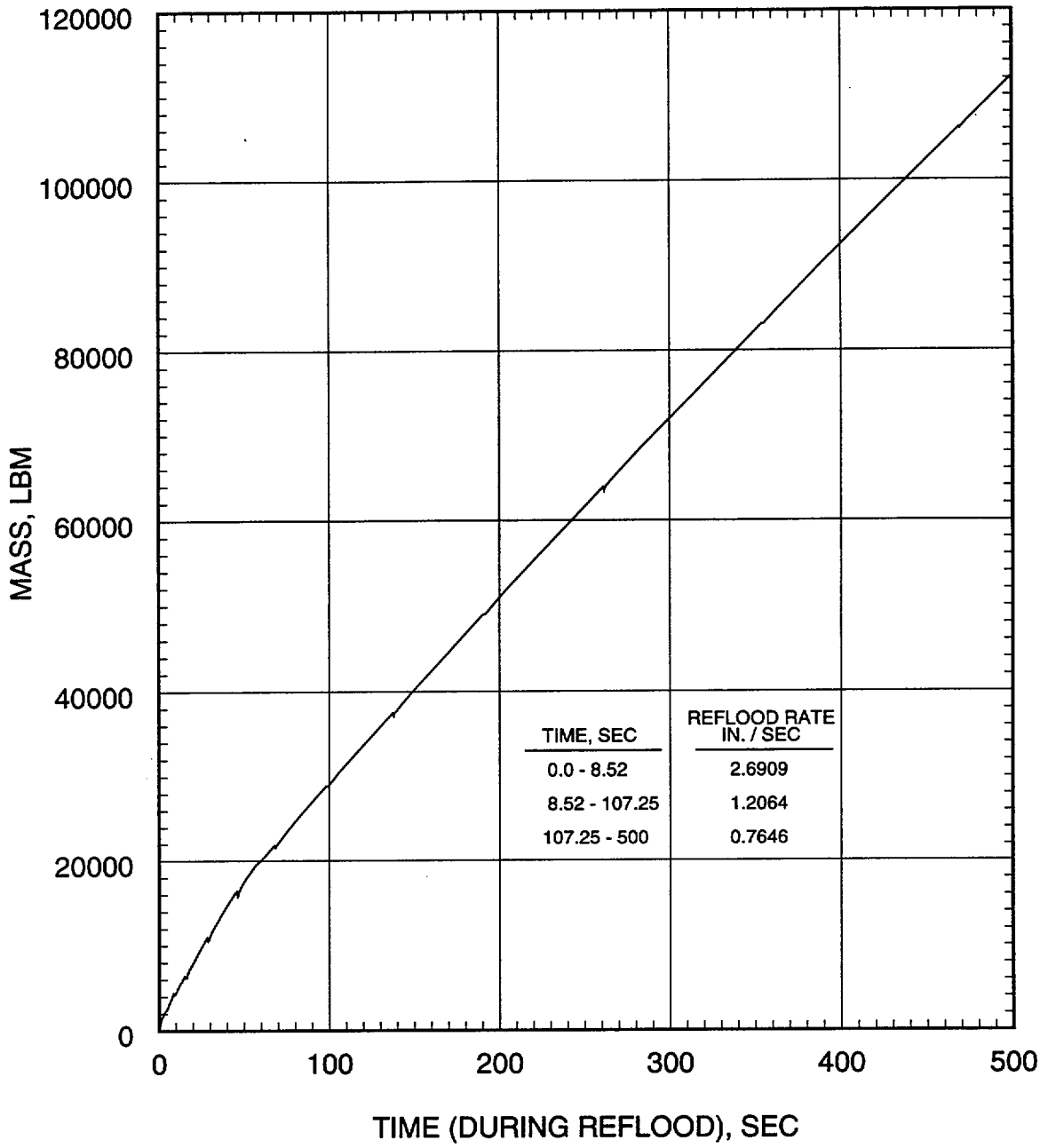

Figure 7.1.3-18
Large Break LOCA ECCS Performance Analysis
0.8 DEG/PD Break
Peak Cladding Temperature

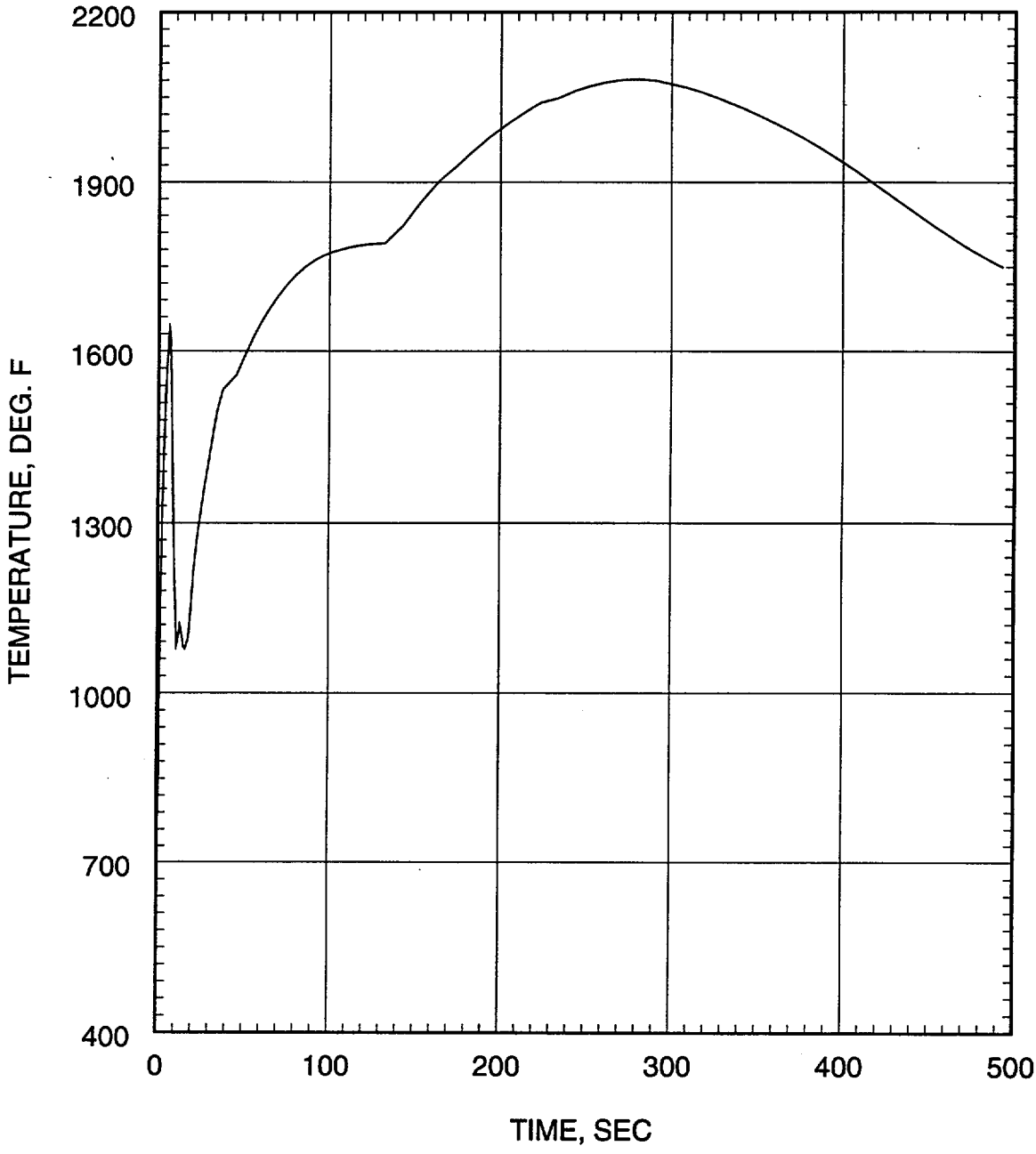

Figure 7.1.3-19
Large Break LOCA ECCS Performance Analysis
0.6 DEG/PD Break
Core Power

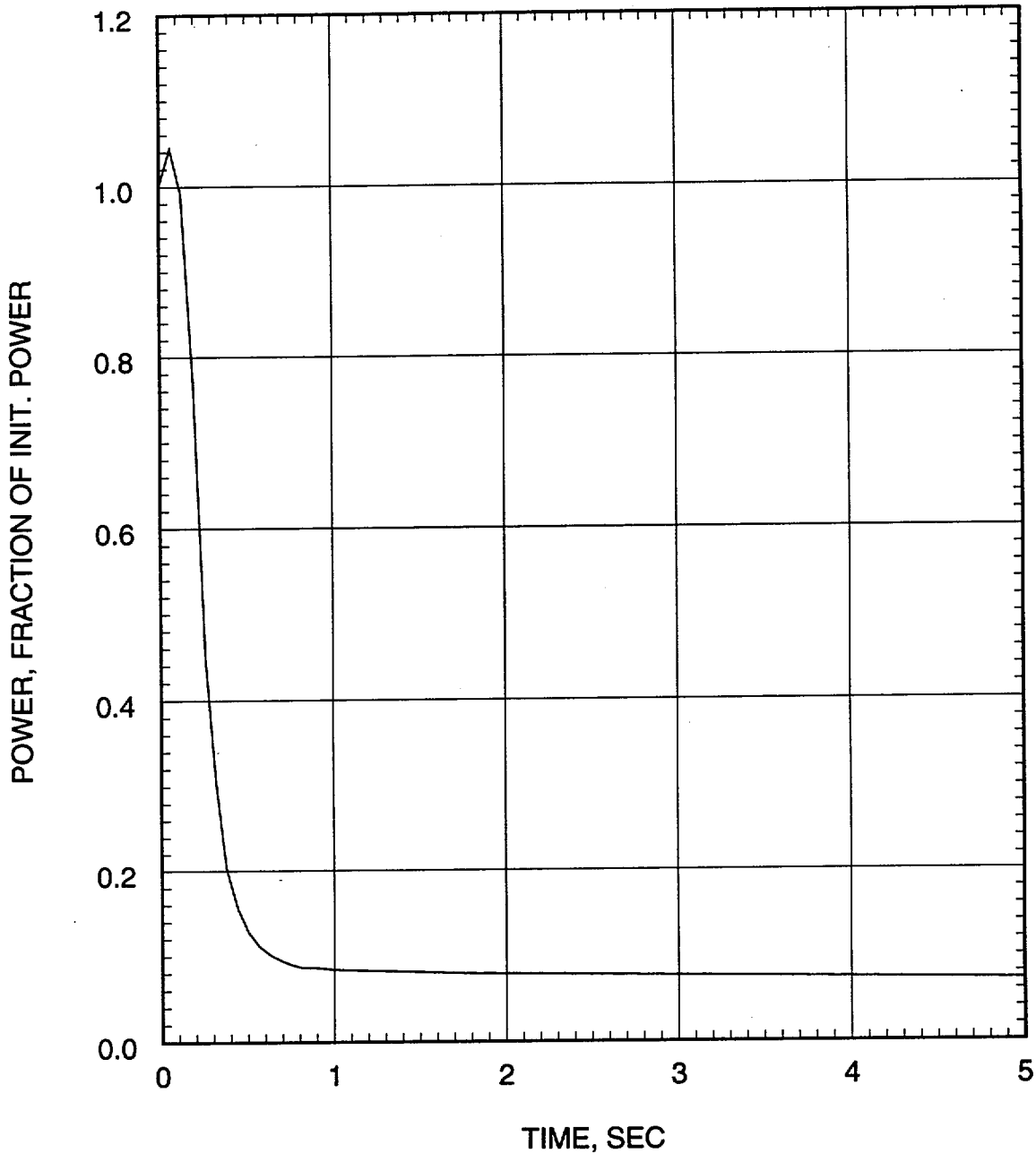

Figure 7.1.3-20
Large Break LOCA ECCS Performance Analysis
0.6 DEG/PD Break
Pressure in Center Hot Assembly Node

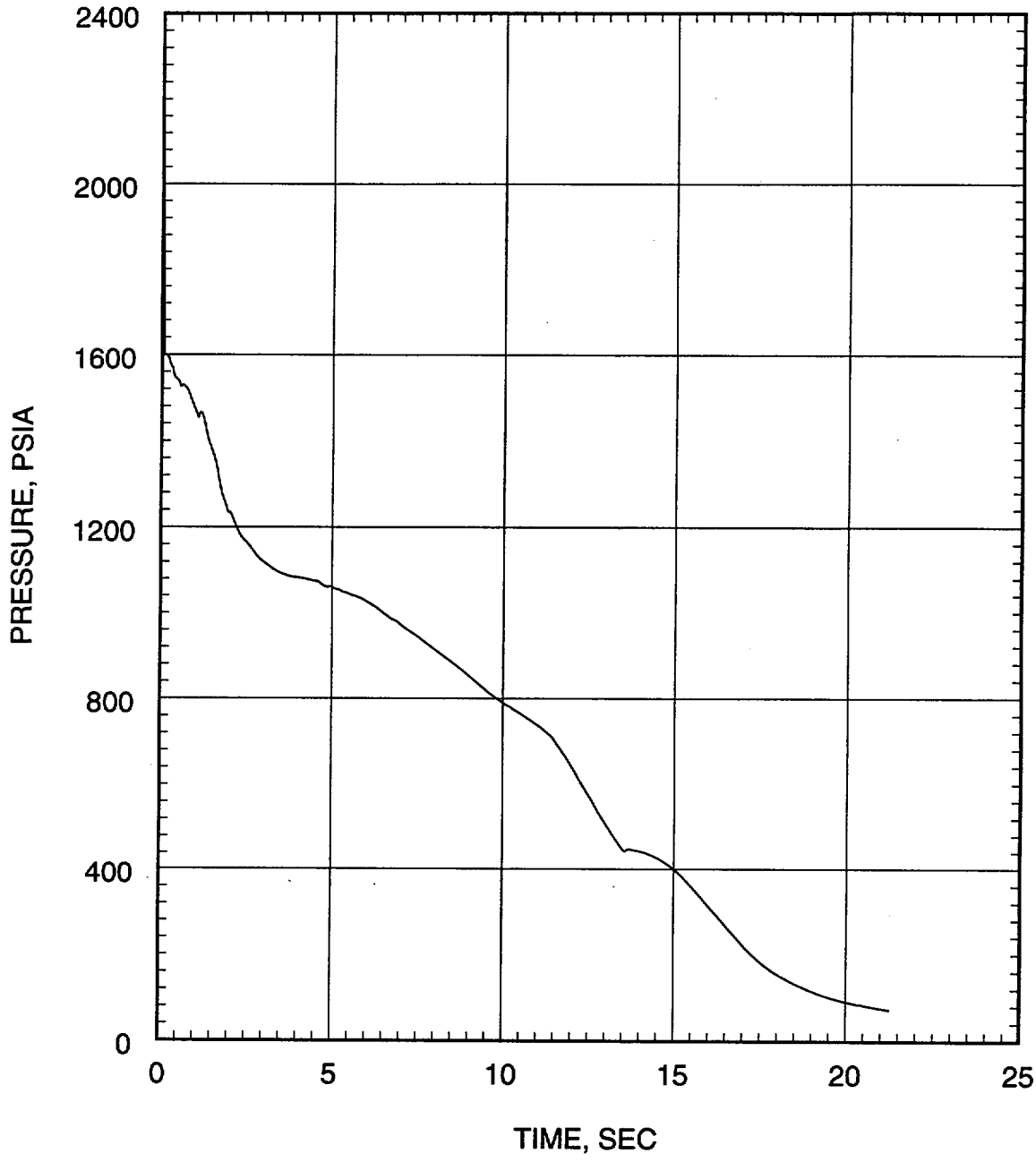

Figure 7.1.3-21
Large Break LOCA ECCS Performance Analysis
0.6 DEG/PD Break
Leak Flow Rate

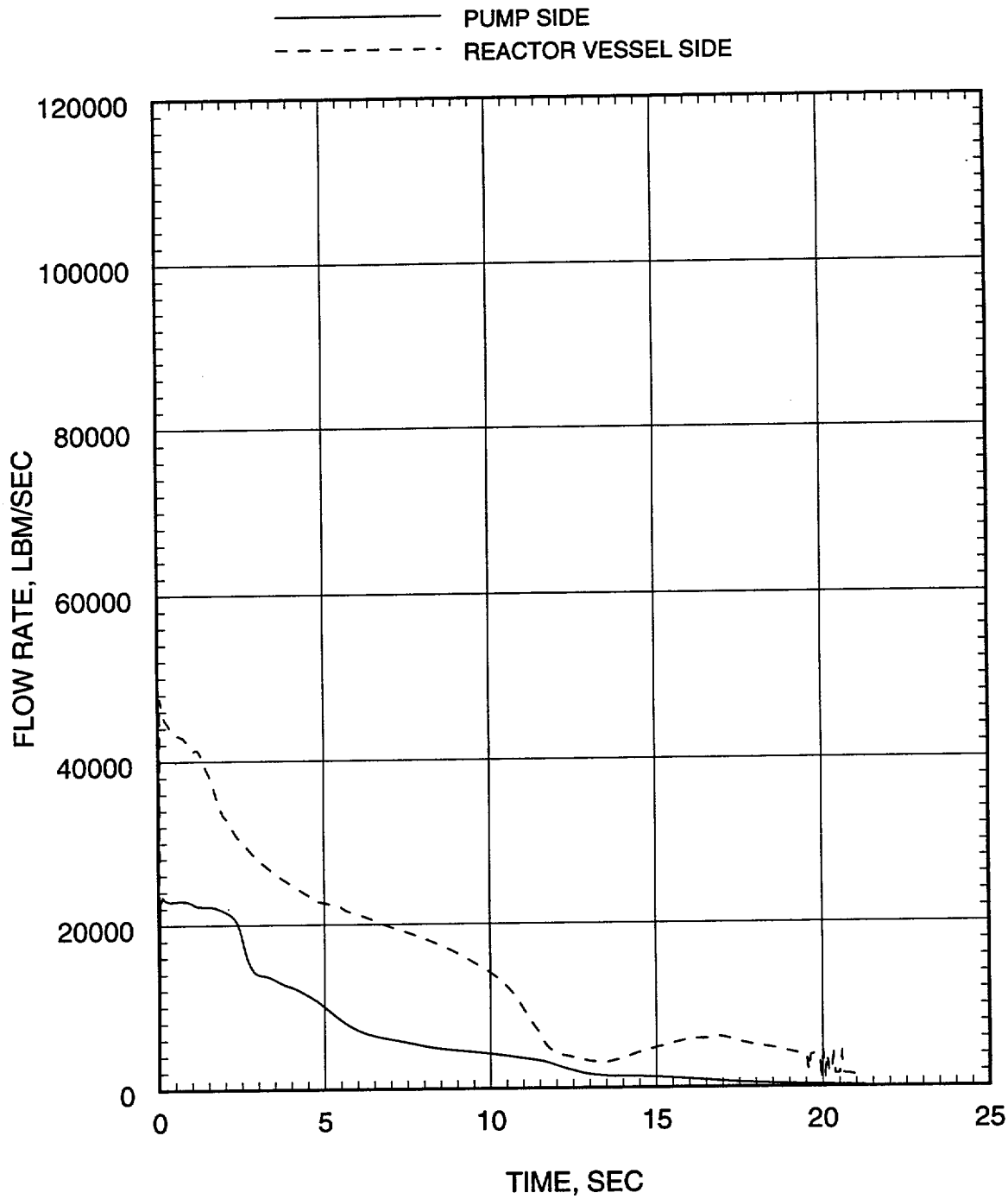

Figure 7.1.3-22
Large Break LOCA ECCS Performance Analysis
0.6 DEG/PD Break
Hot Assembly Flow Rate (Below Hot Spot)

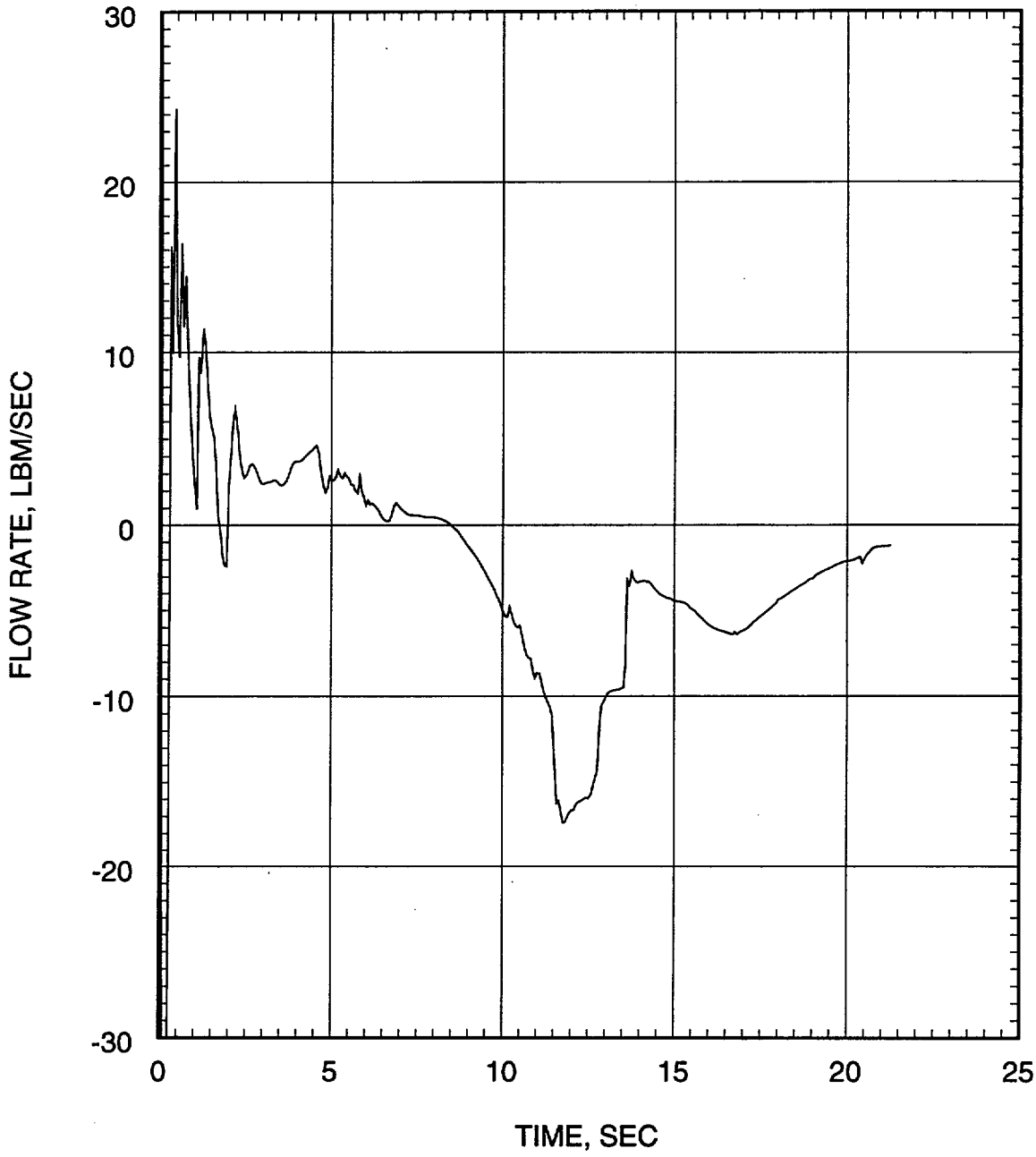

Figure 7.1.3-23
Large Break LOCA ECCS Performance Analysis
0.6 DEG/PD Break
Hot Assembly Flow Rate (Above Hot Spot)

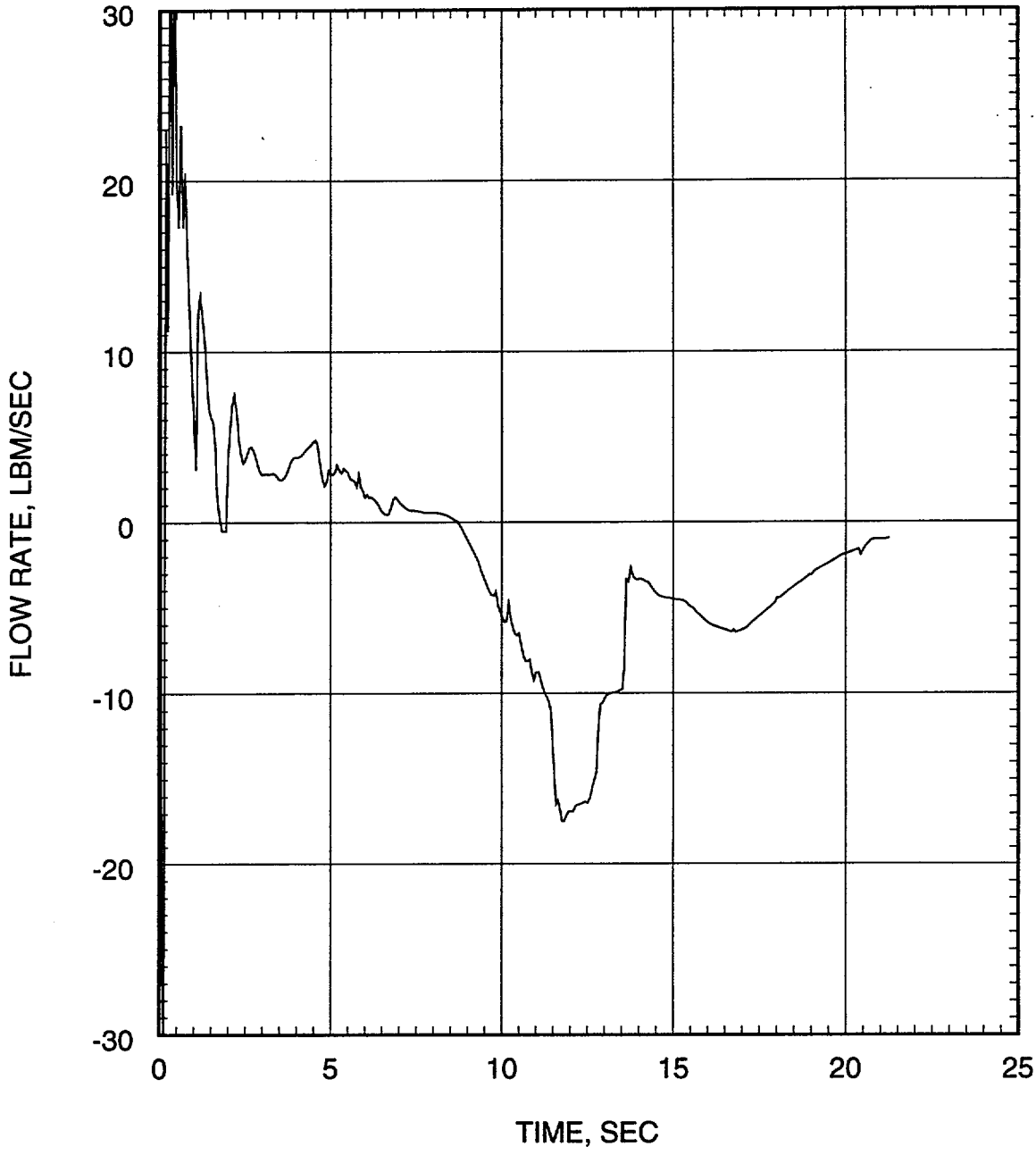

Figure 7.1.3-24
Large Break LOCA ECCS Performance Analysis
0.6 DEG/PD Break
Hot Assembly Quality

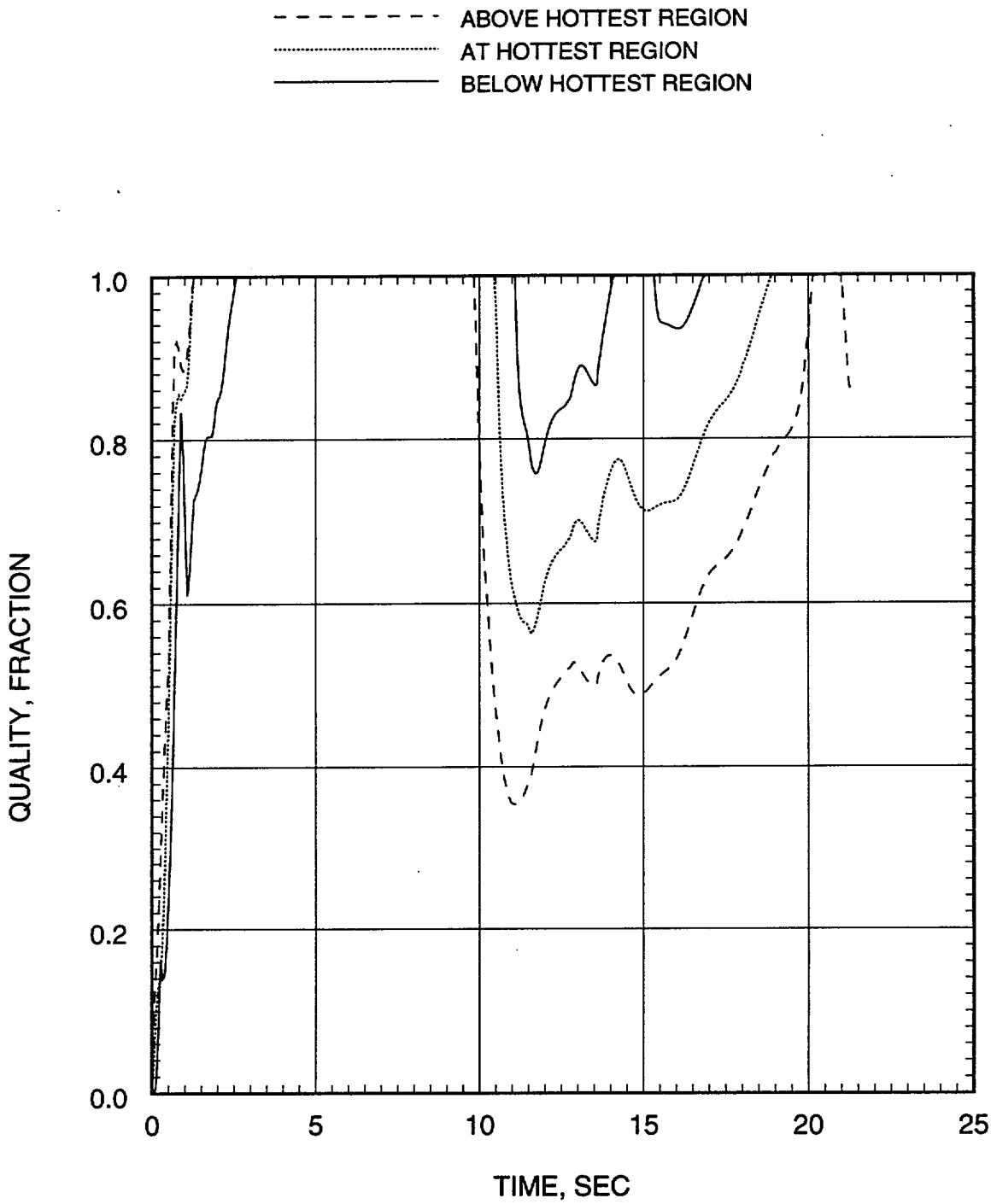

Figure 7.1.3-25
Large Break LOCA ECCS Performance Analysis
0.6 DEG/PD Break
Containment Pressure

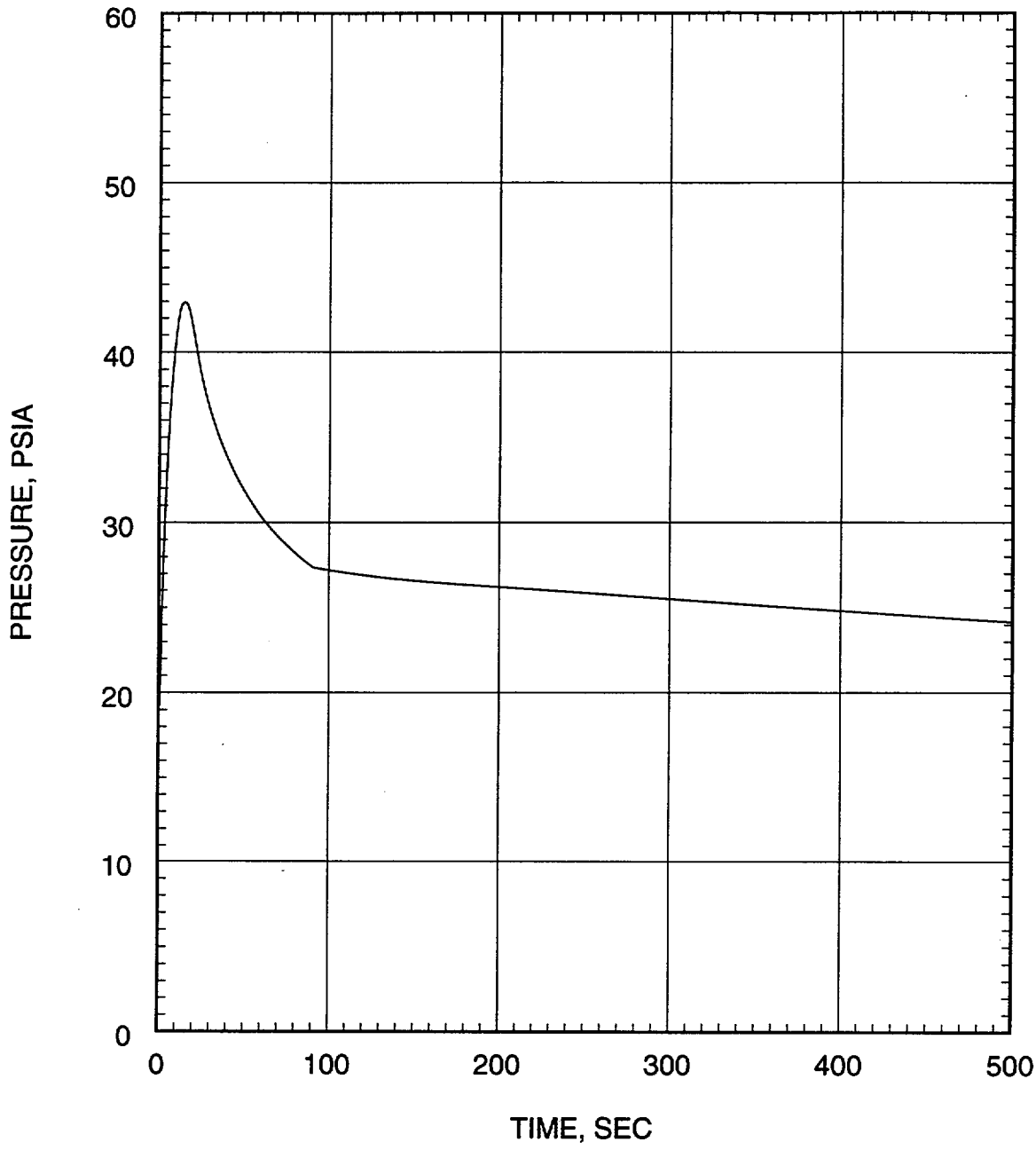

Figure 7.1.3-26
Large Break LOCA ECCS Performance Analysis
0.6 DEG/PD Break
Mass Added to Core During Reflood

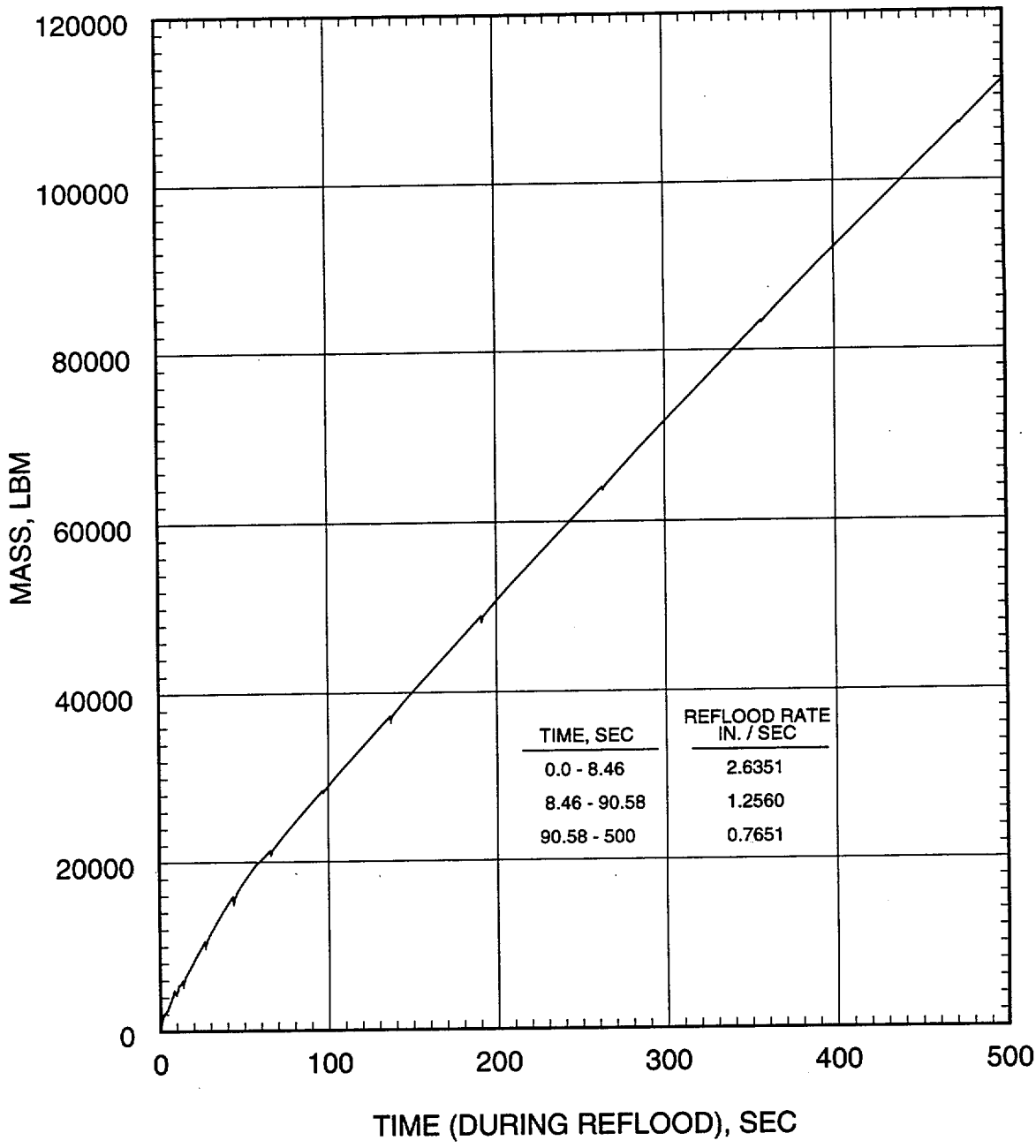

Figure 7.1.3-27
Large Break LOCA ECCS Performance Analysis
0.6 DEG/PD Break
Peak Cladding Temperature

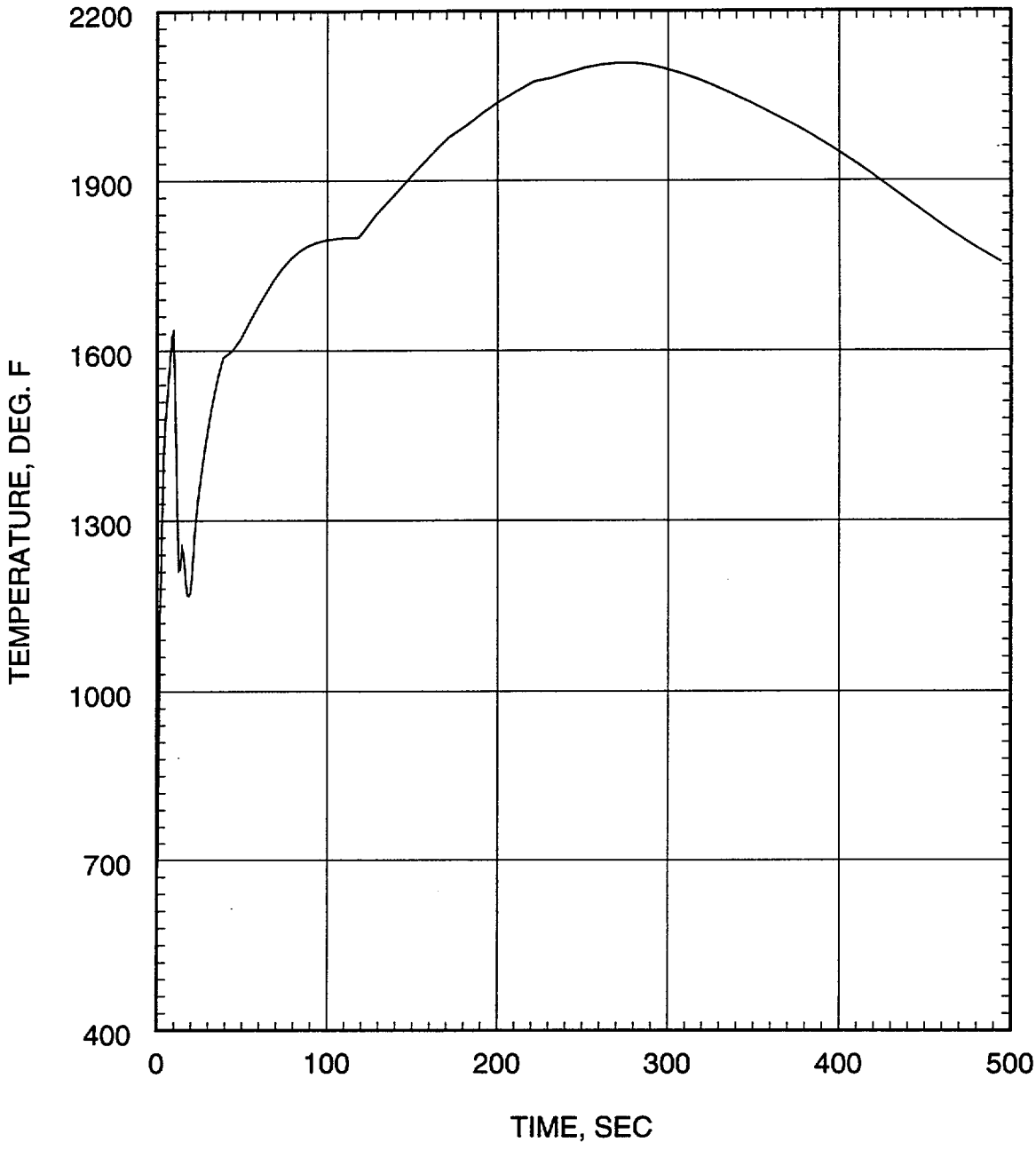

Figure 7.1.3-28
Large Break LOCA ECCS Performance Analysis
0.4 DEG/PD Break
Core Power

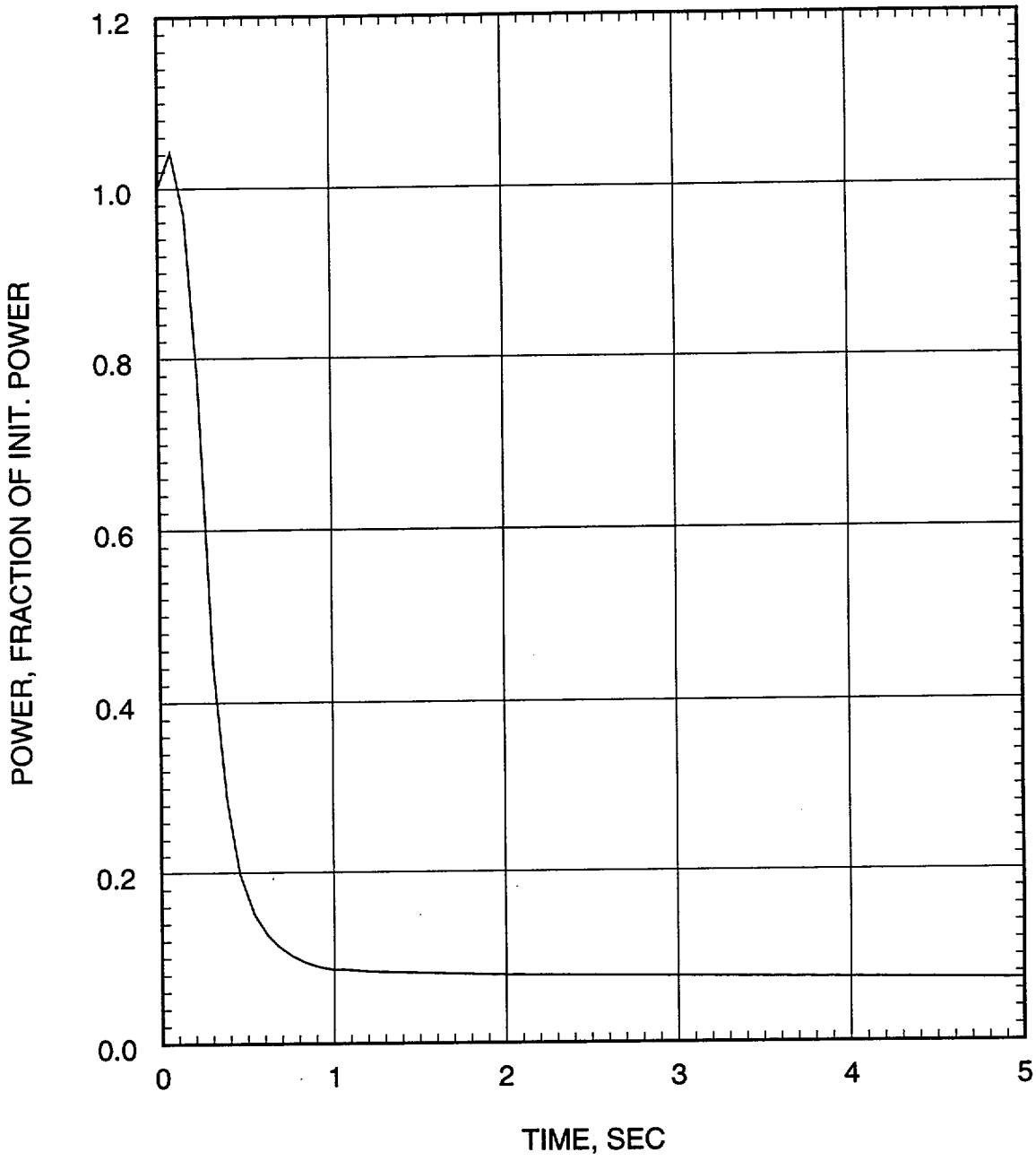

Figure 7.1.3-29
Large Break LOCA ECCS Performance Analysis
0.4 DEG/PD Break
Pressure in Center Hot Assembly Node

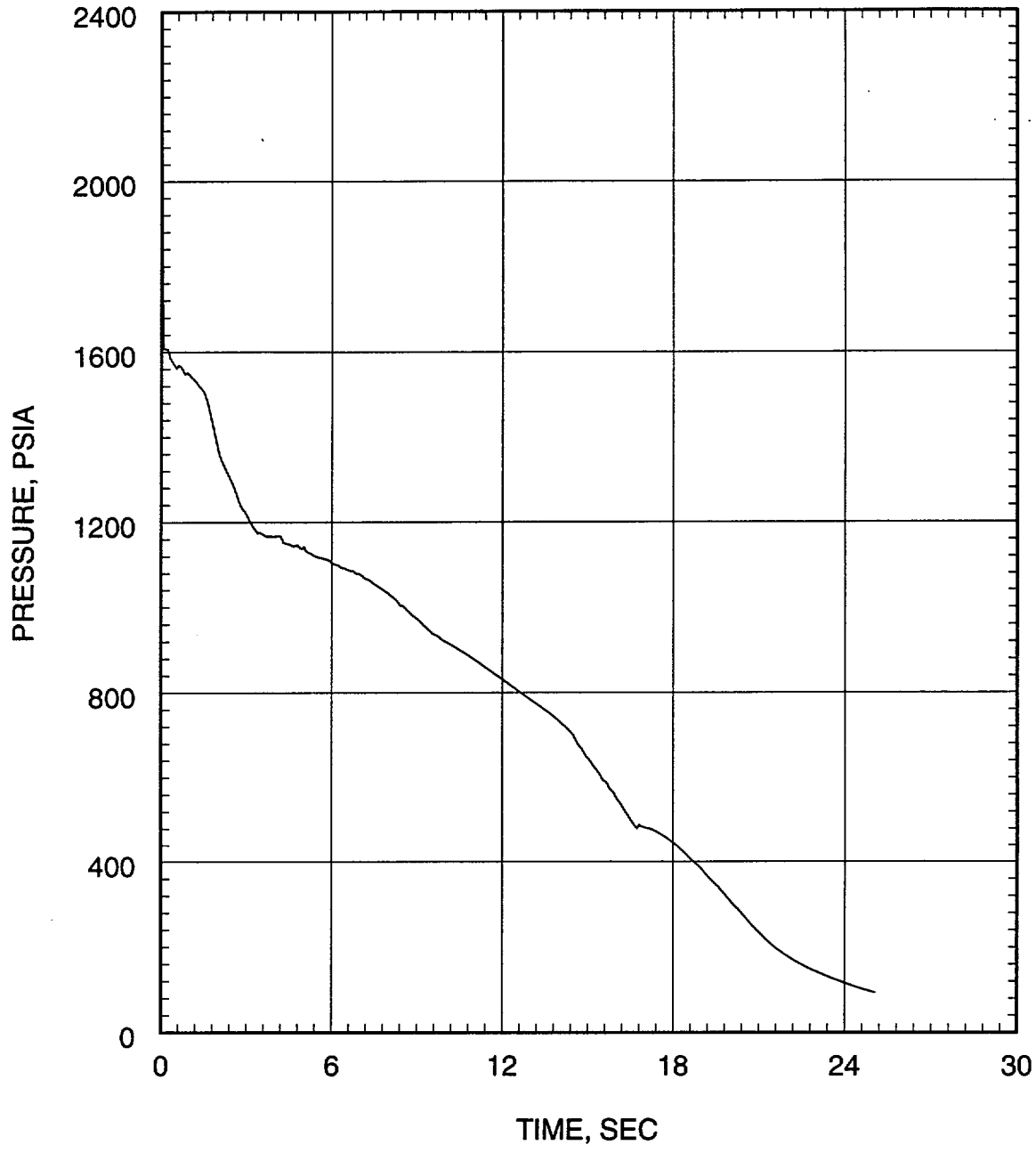

Figure 7.1.3-30
Large Break LOCA ECCS Performance Analysis
0.4 DEG/PD Break
Leak Flow Rate

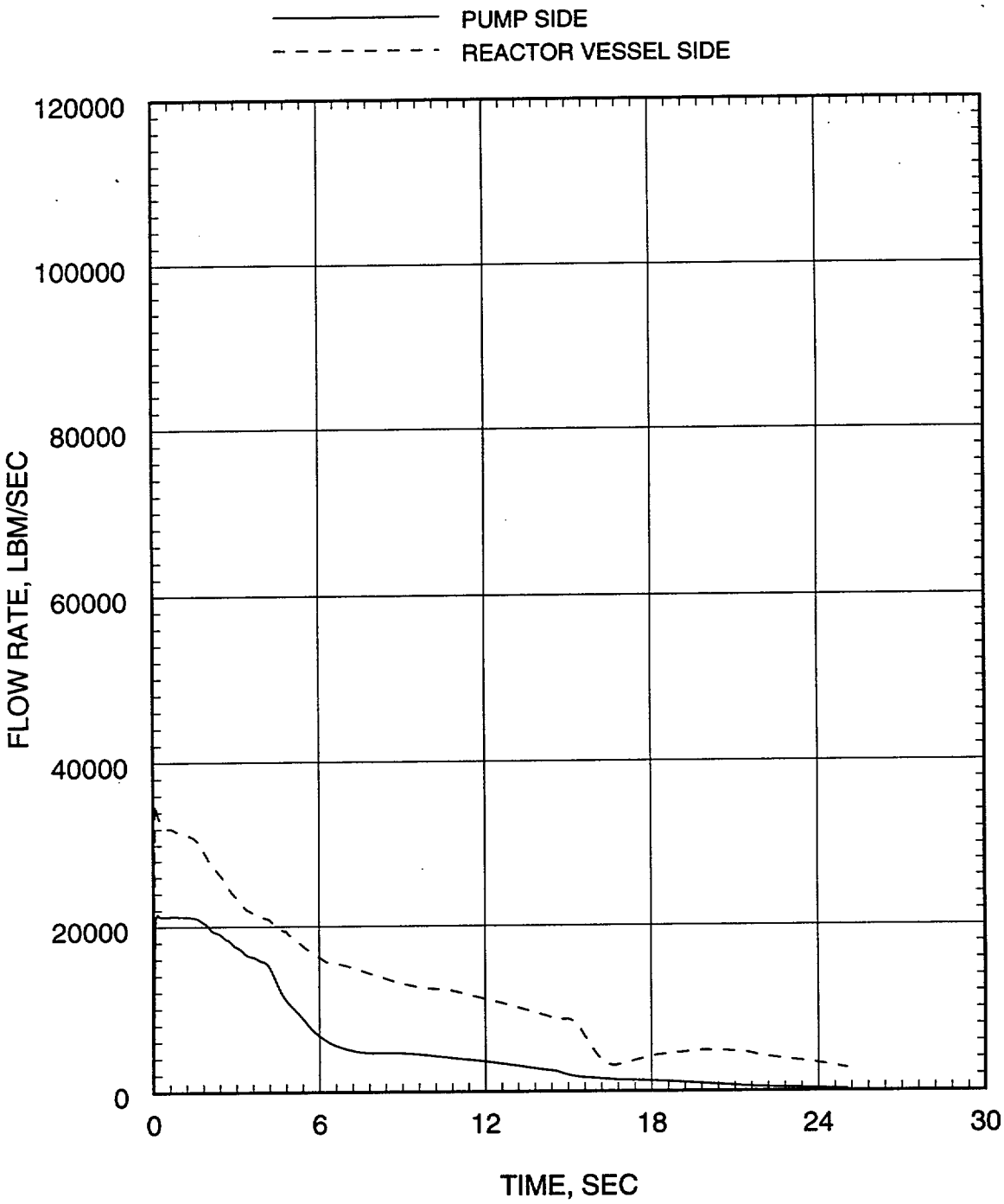

Figure 7.1.3-31
Large Break LOCA ECCS Performance Analysis
0.4 DEG/PD Break
Hot Assembly Flow Rate (Below Hot Spot)

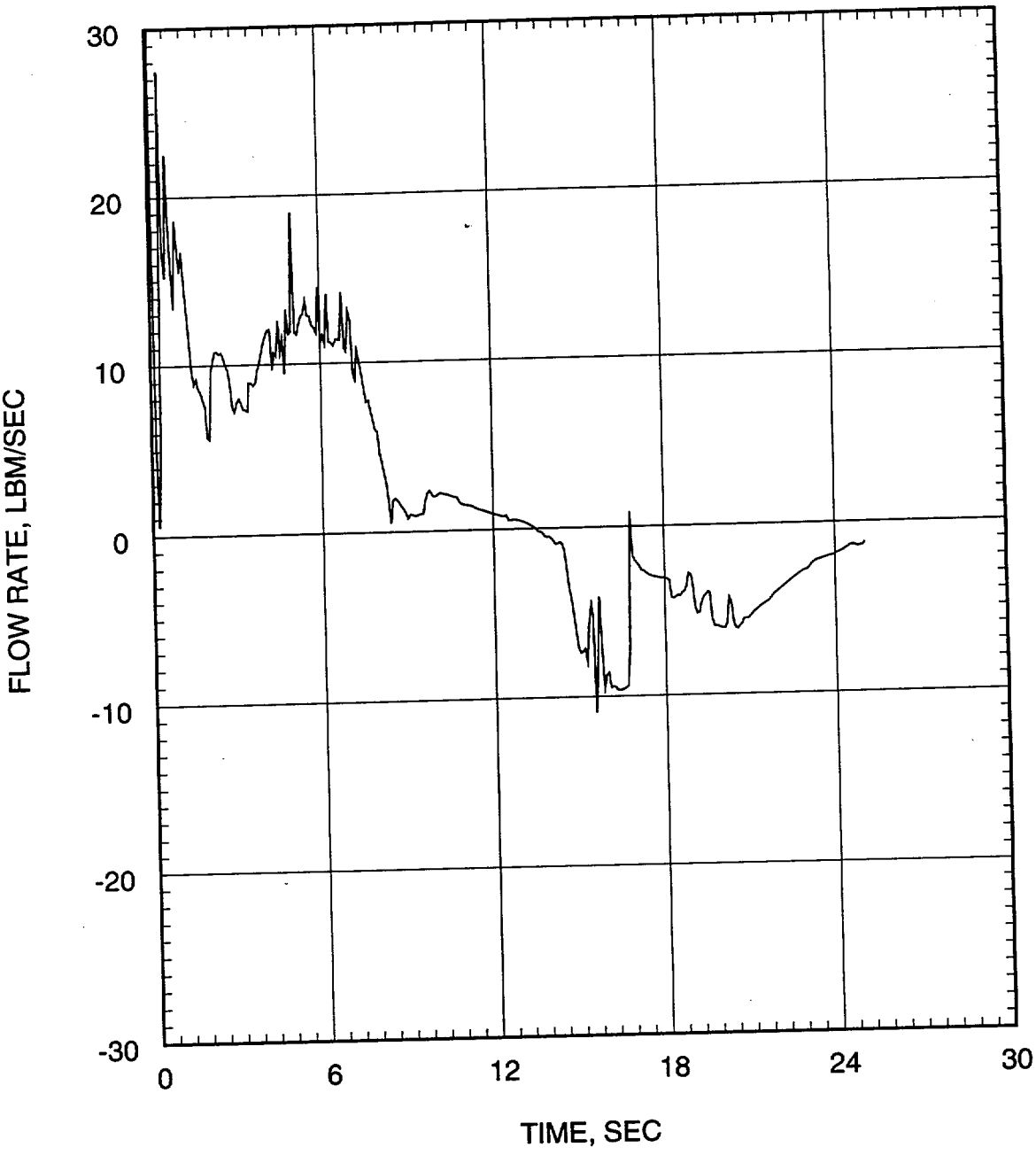

Figure 7.1.3-32
Large Break LOCA ECCS Performance Analysis
0.4 DEG/PD Break
Hot Assembly Flow Rate (Above Hot Spot)

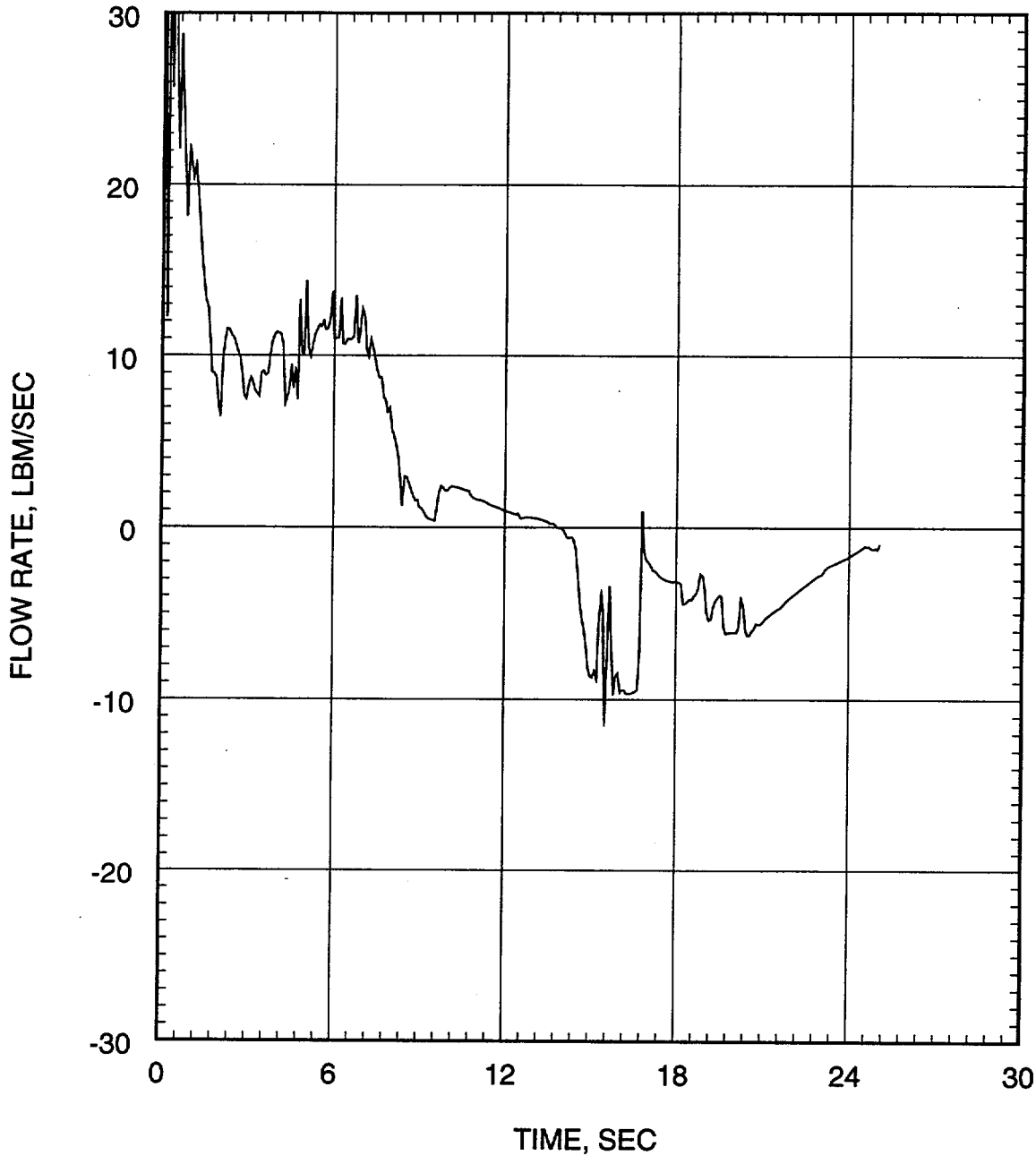

Figure 7.1.3-33
Large Break LOCA ECCS Performance Analysis
0.4 DEG/PD Break
Hot Assembly Quality

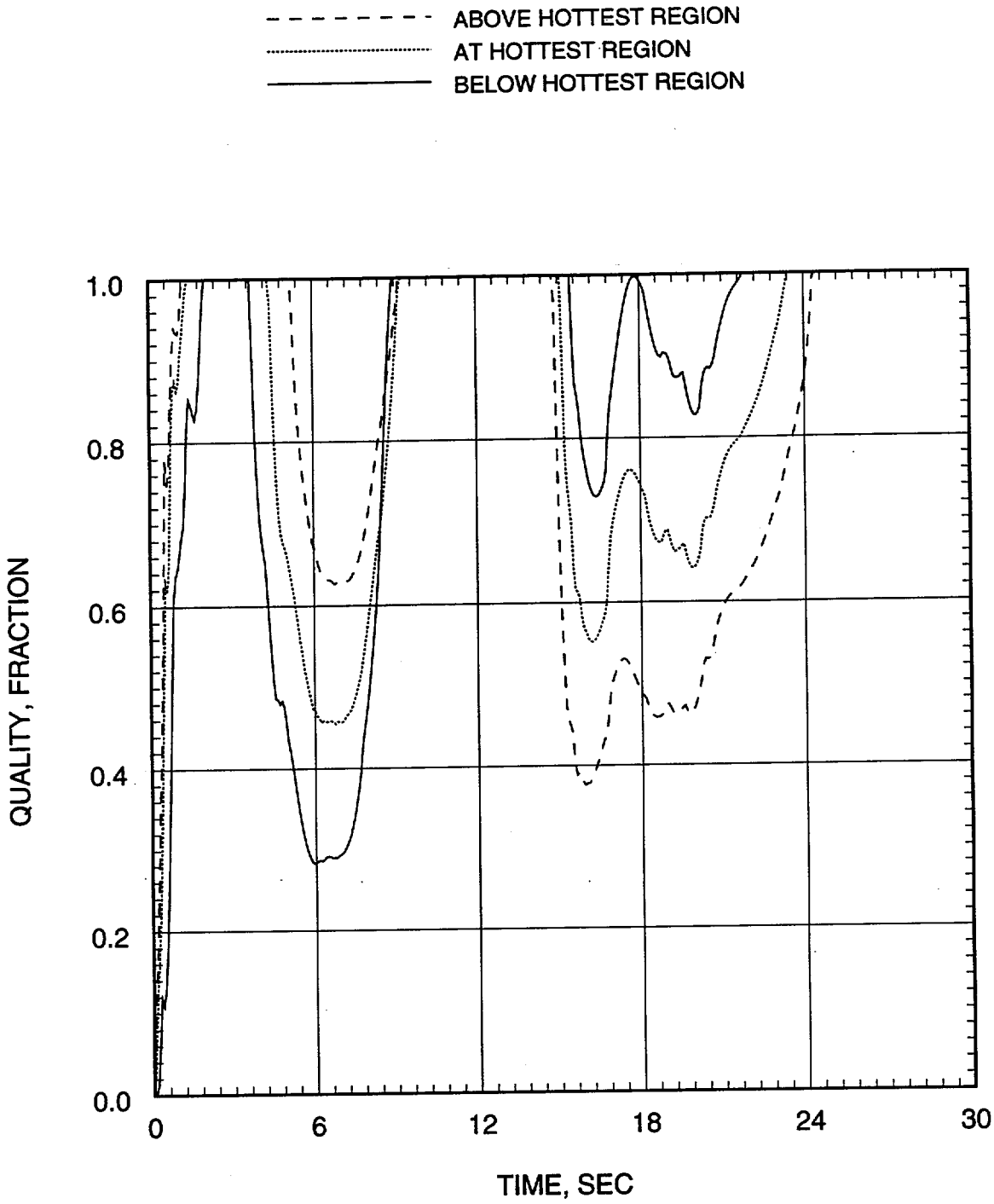

Figure 7.1.3-34
Large Break LOCA ECCS Performance Analysis
0.4 DEG/PD Break
Containment Pressure

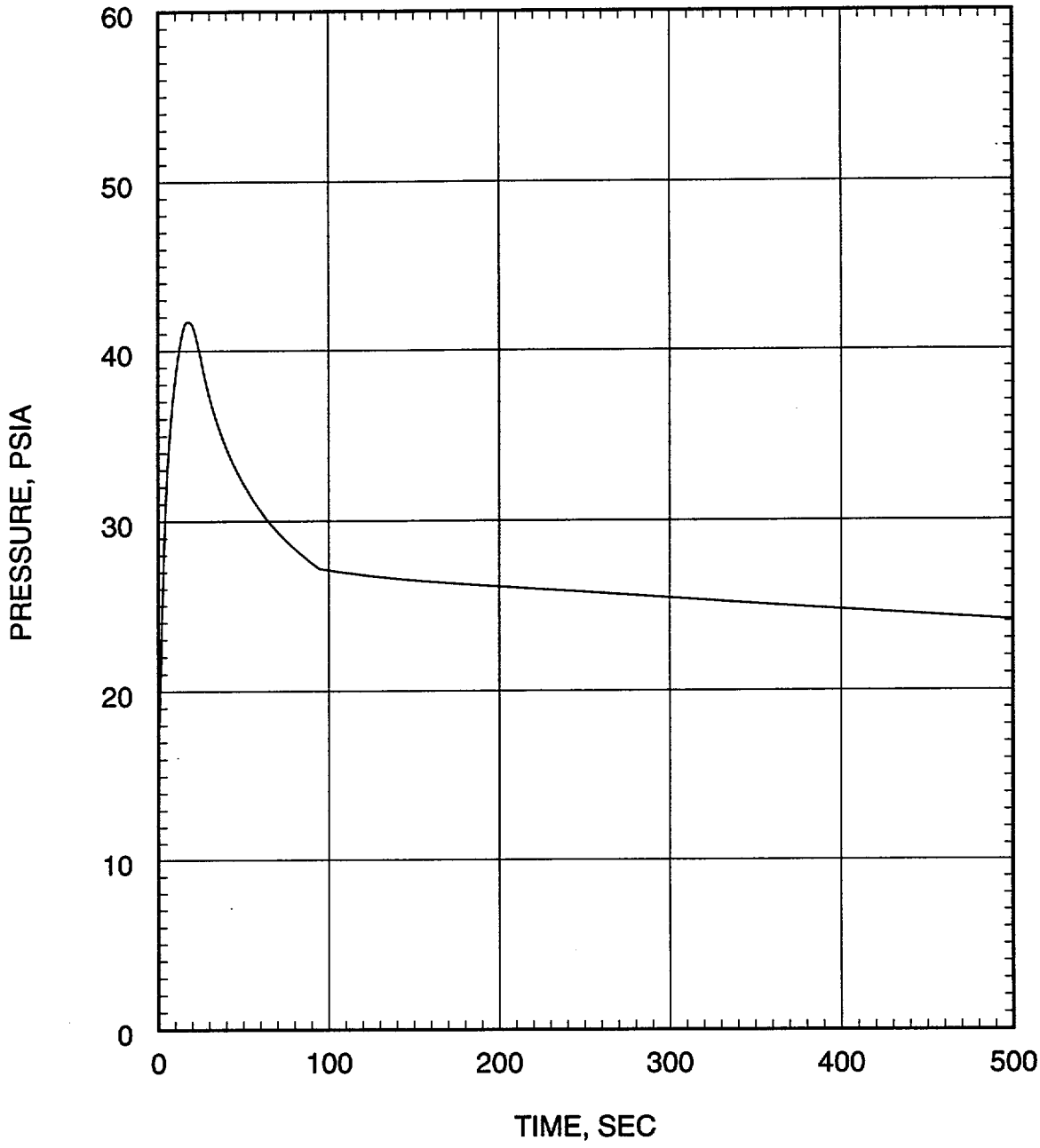

Figure 7.1.3-35
Large Break LOCA ECCS Performance Analysis
0.4 DEG/PD Break
Mass Added to Core During Reflood

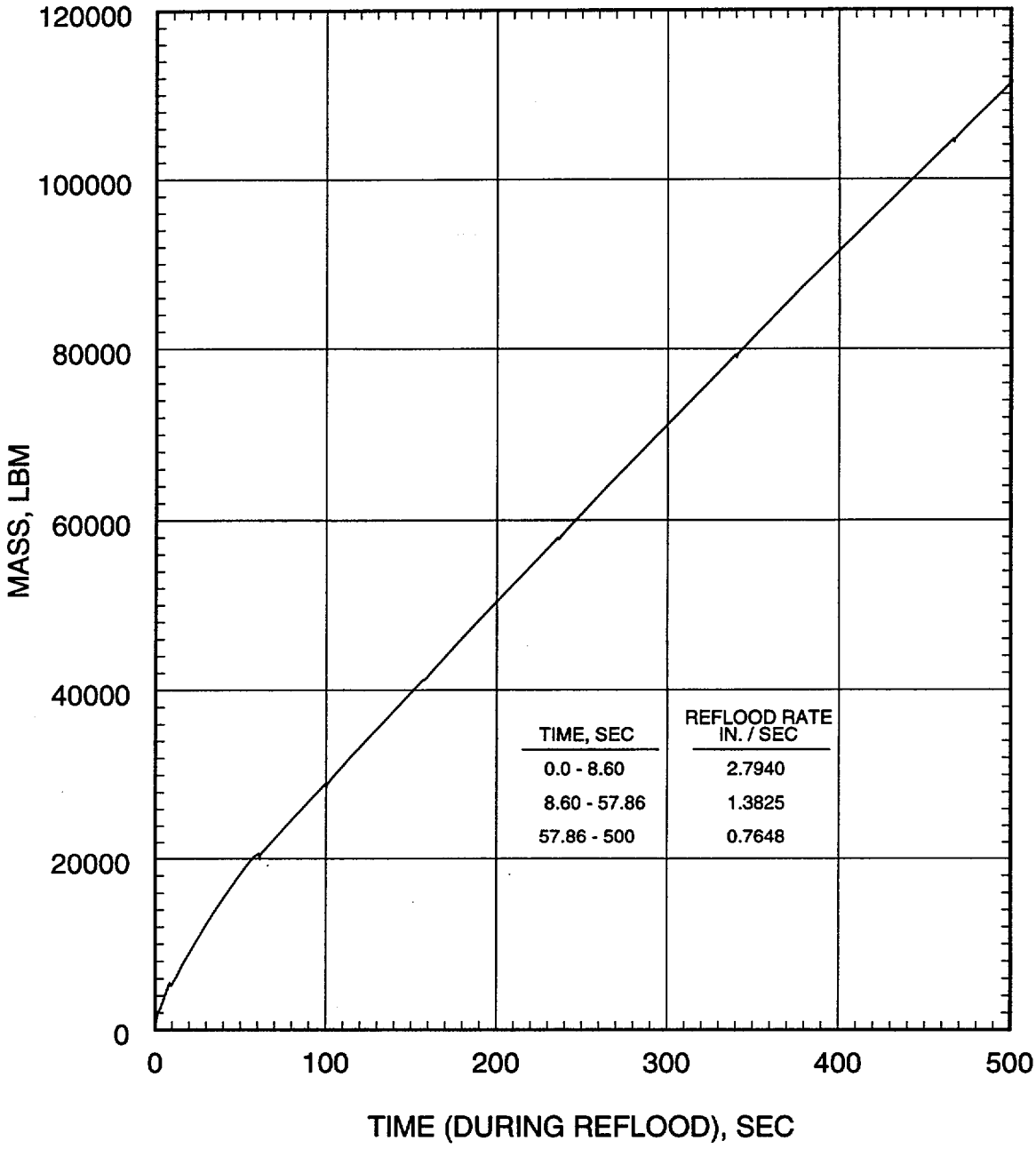

Figure 7.1.3-36
Large Break LOCA ECCS Performance Analysis
0.4 DEG/PD Break
Peak Cladding Temperature

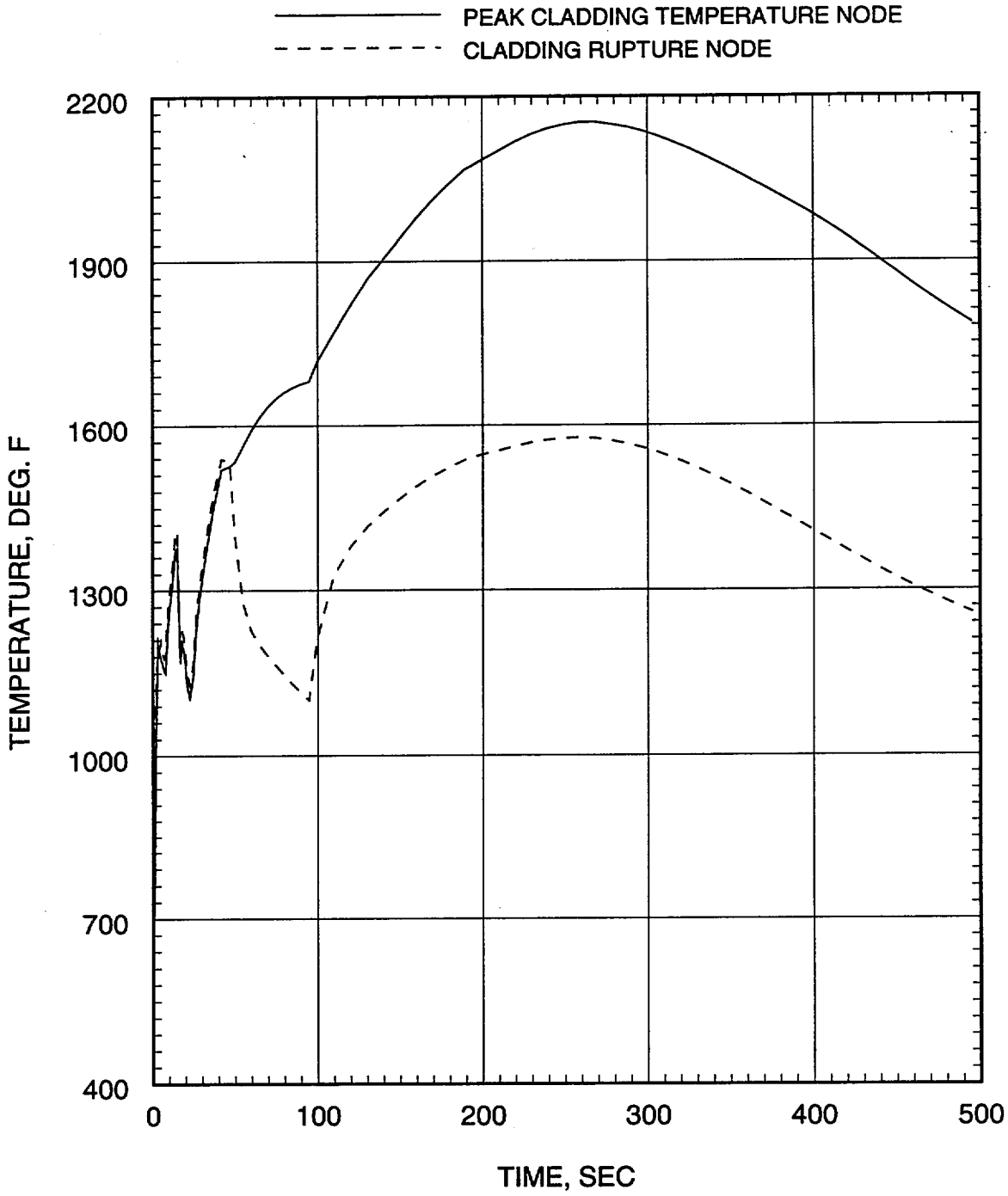

Figure 7.1.3-37
Large Break LOCA ECCS Performance Analysis
0.4 DEG/PD Break
Mid Annulus Flow Rate

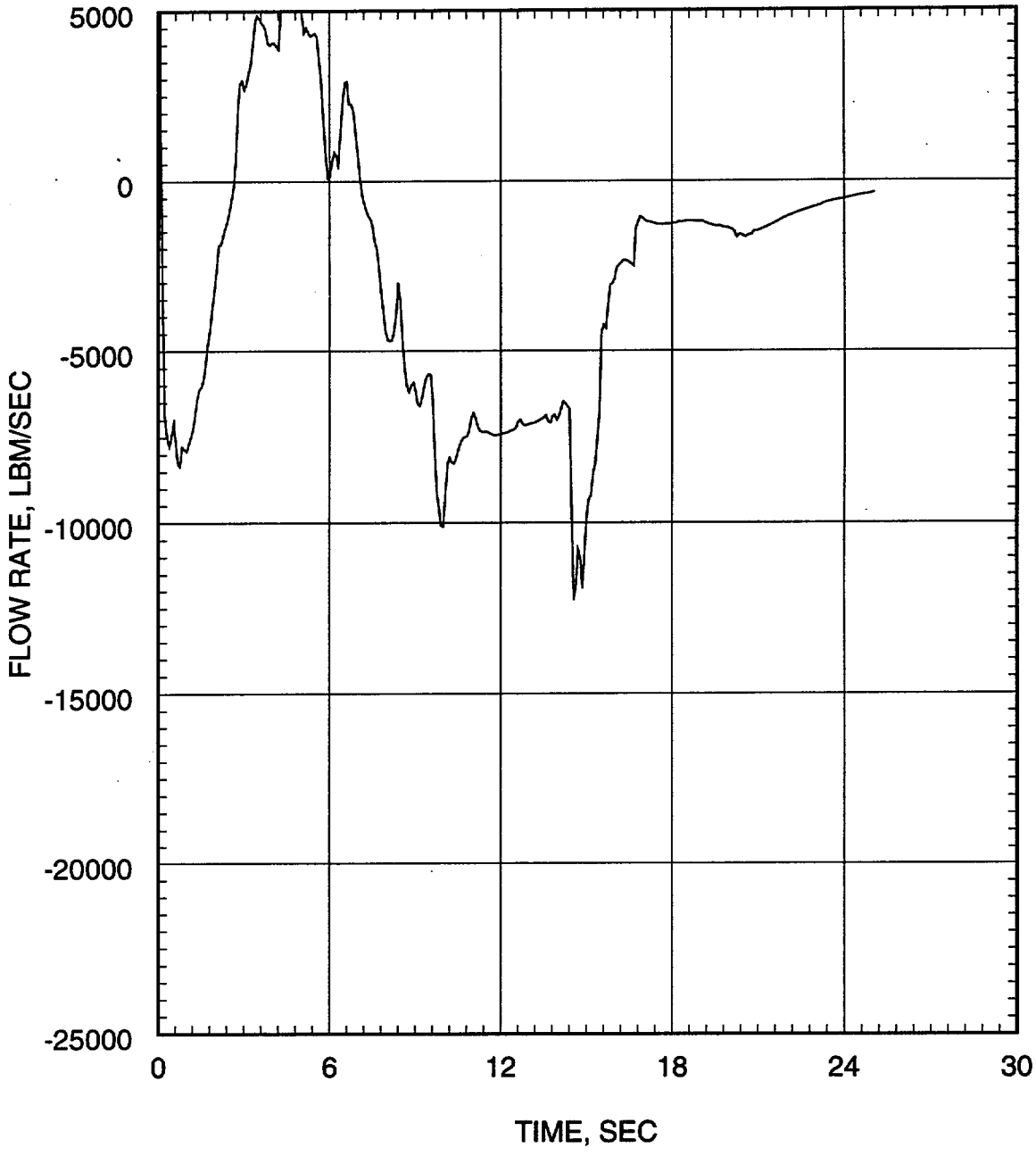

Figure 7.1.3-38
Large Break LOCA ECCS Performance Analysis
0.4 DEG/PD Break
Quality Above and Below the Core

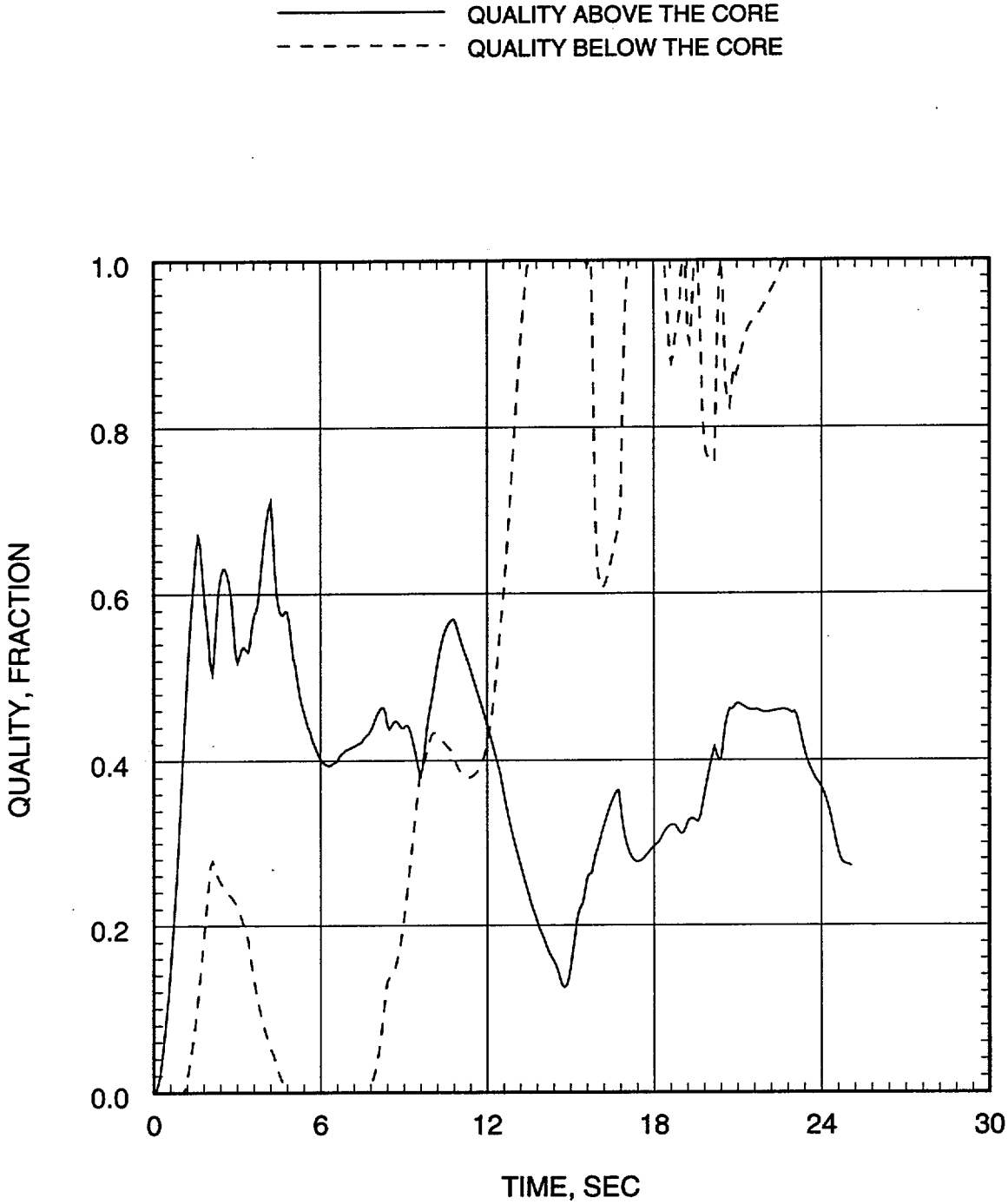

Figure 7.1.3-39
Large Break LOCA ECCS Performance Analysis
0.4 DEG/PD Break
Core Pressure Drop

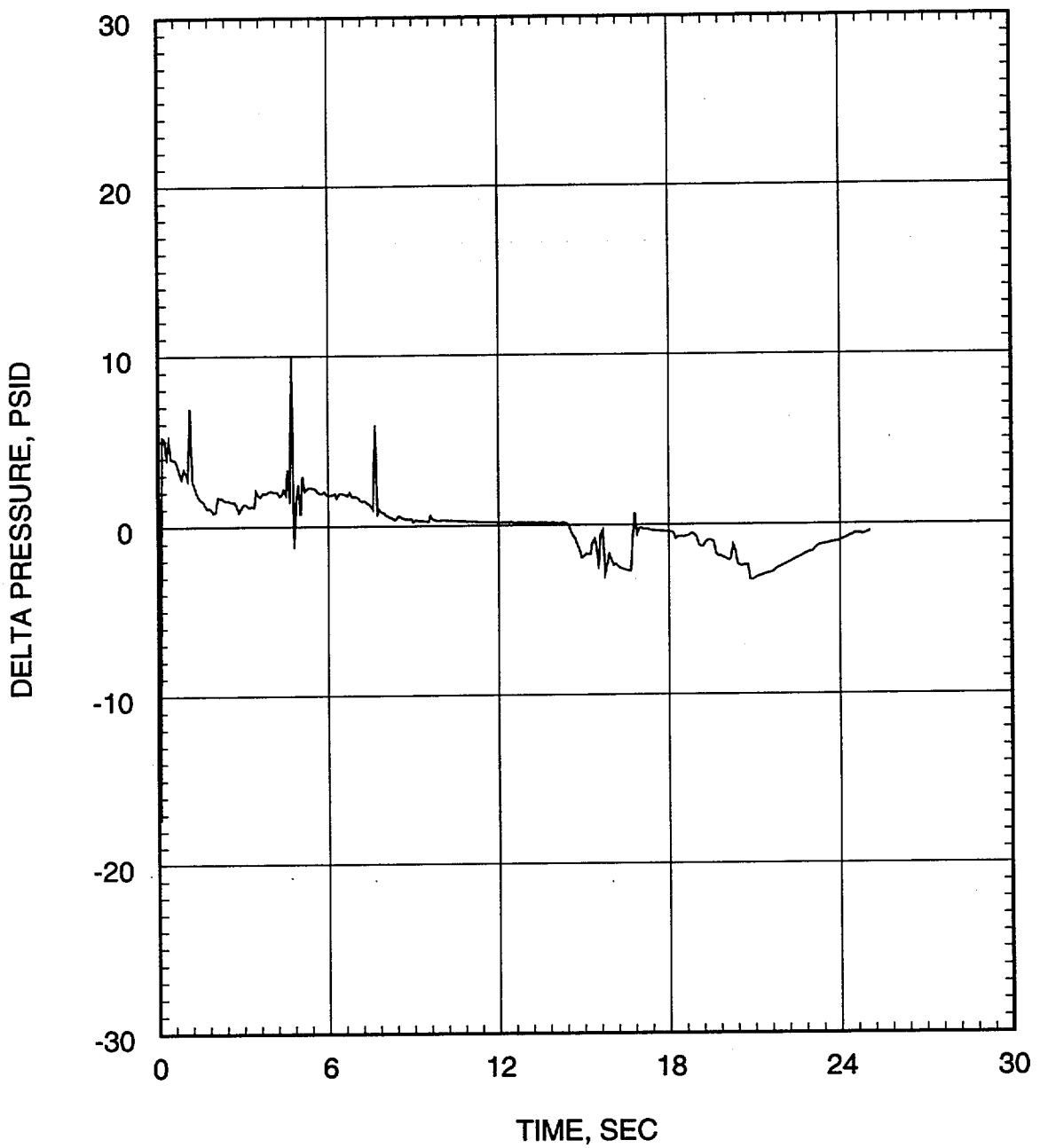

Figure 7.1.3-40
Large Break LOCA ECCS Performance Analysis
0.4 DEG/PD Break
Safety Injection Flow Rate into Intact Discharge Legs

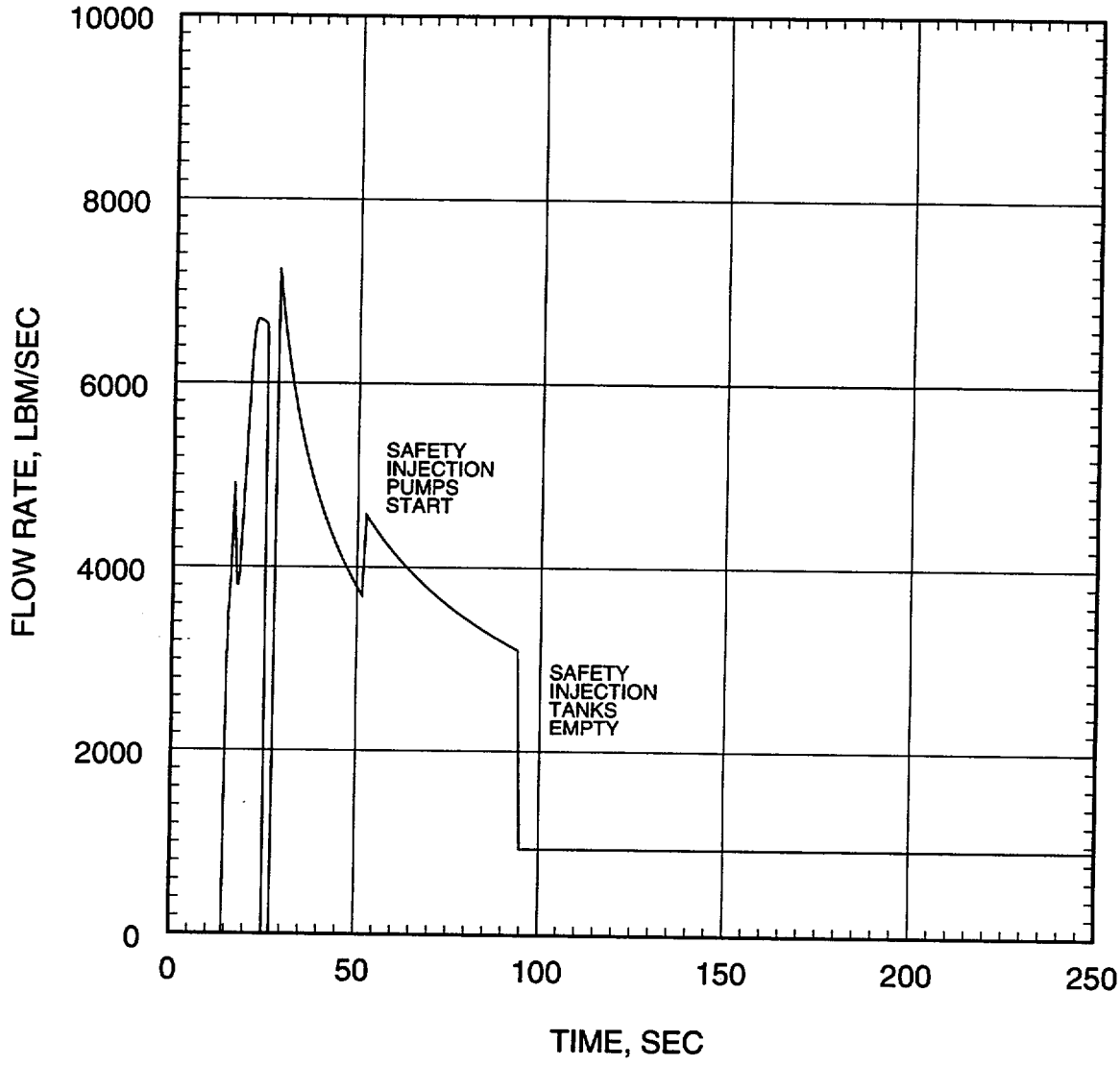

Figure 7.1.3-41
Large Break LOCA ECCS Performance Analysis
0.4 DEG/PD Break
Water Level in Downcomer During Reflood

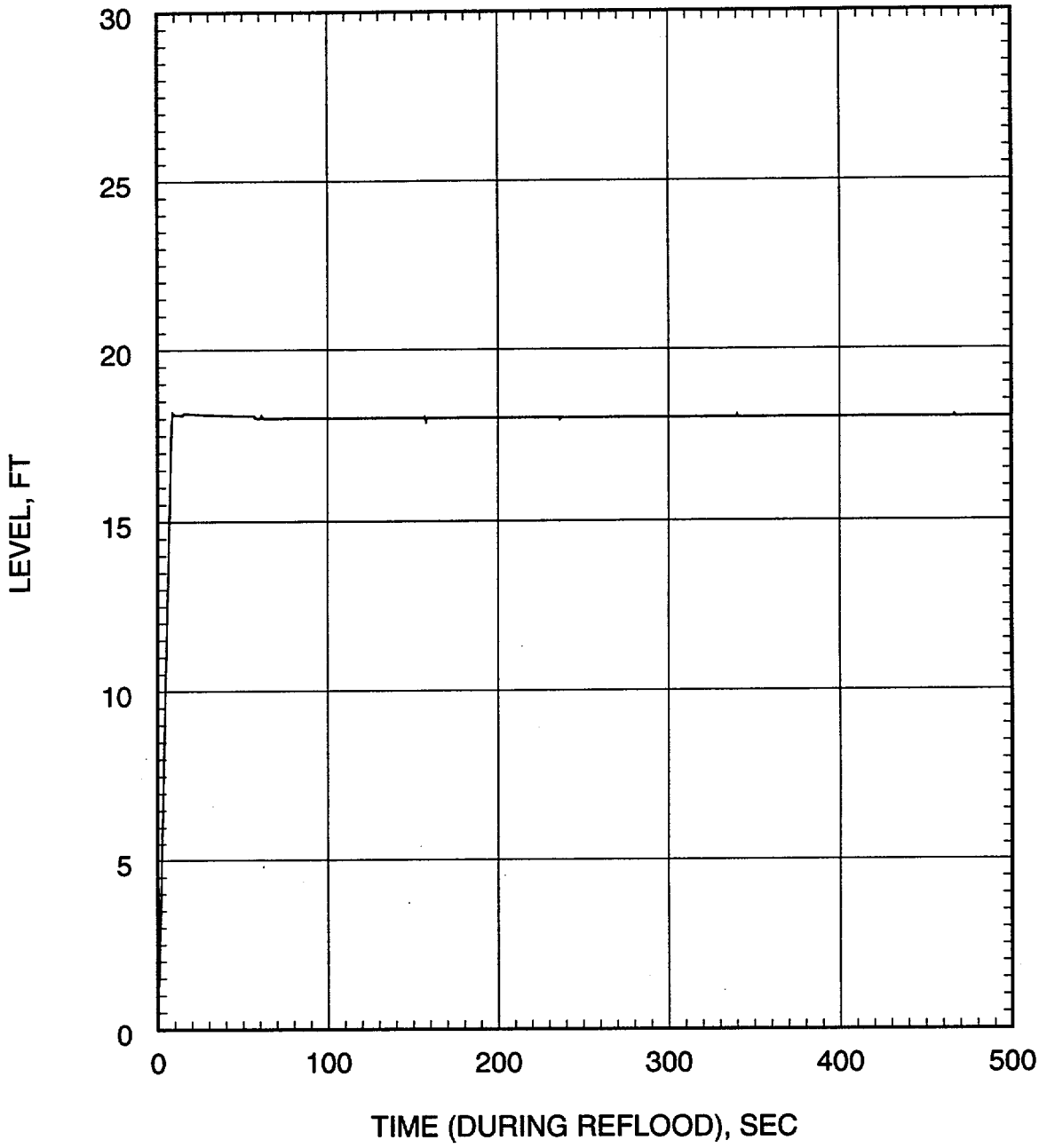

Figure 7.1.3-42
Large Break LOCA ECCS Performance Analysis
0.4 DEG/PD Break
Hot Spot Gap Conductance

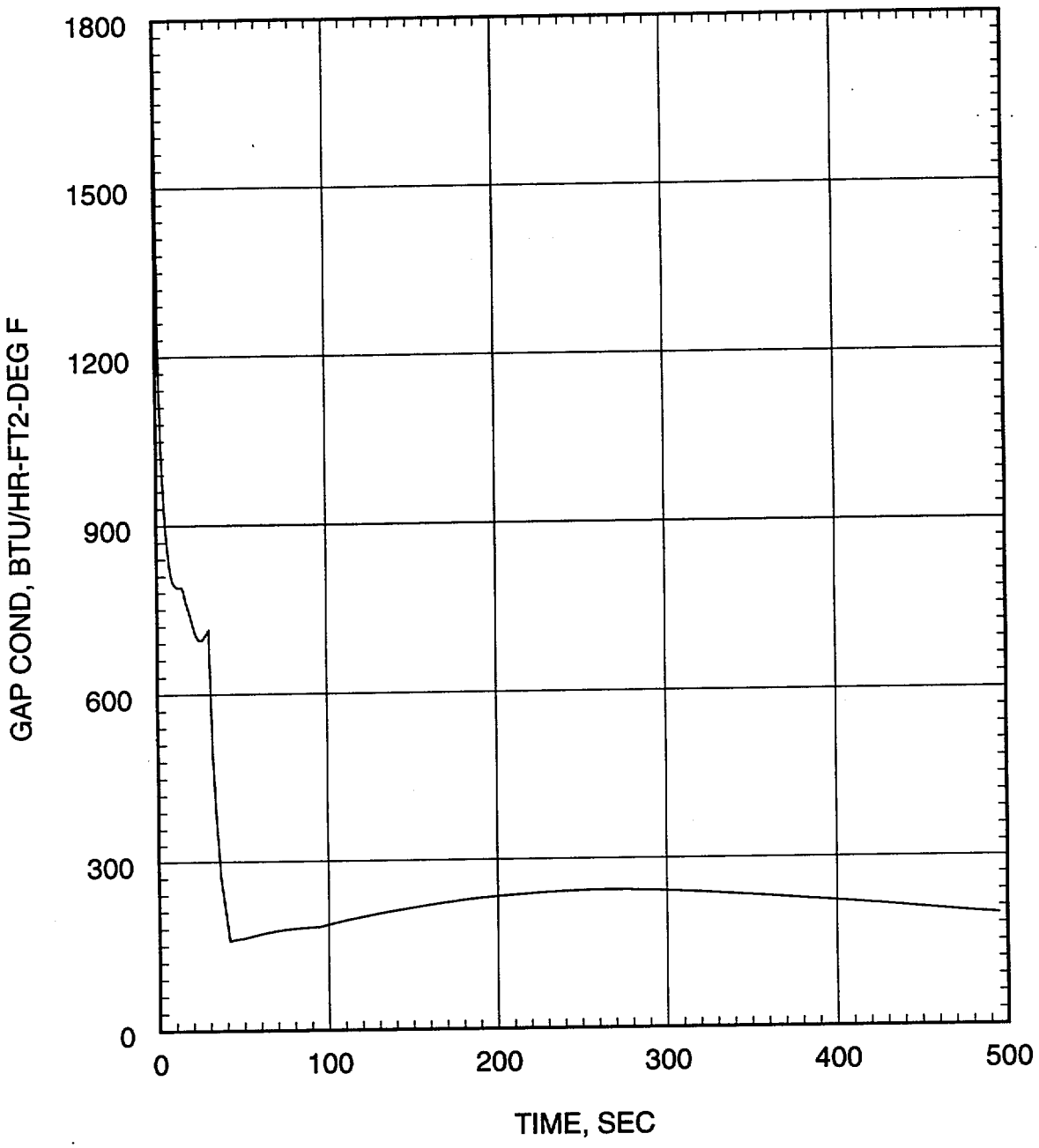

Figure 7.1.3-43
Large Break LOCA ECCS Performance Analysis
0.4 DEG/PD Break
Maximum Local Cladding Oxidation Percentage

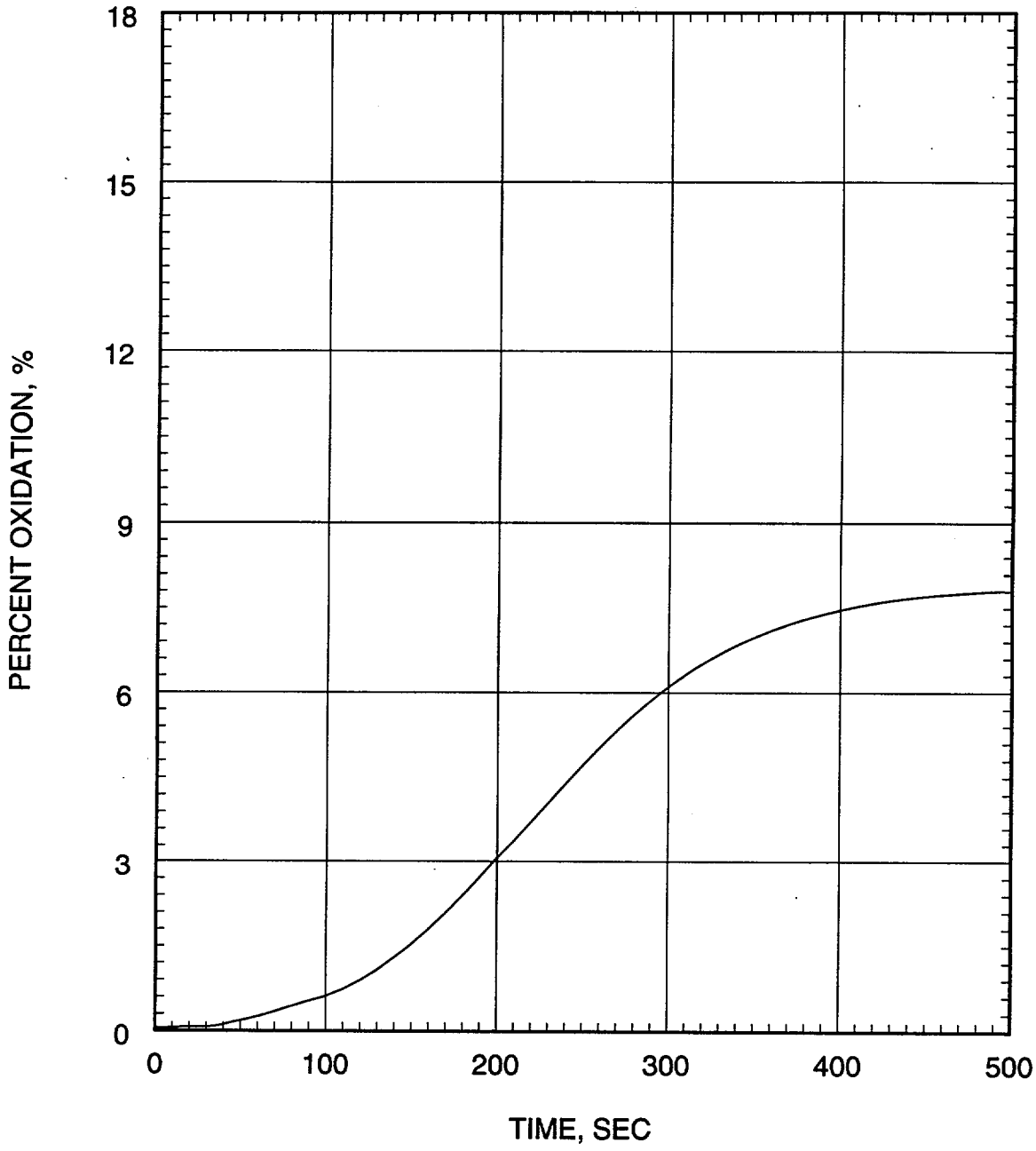

Figure 7.1.3-44
Large Break LOCA ECCS Performance Analysis
0.4 DEG/PD Break
Fuel Centerline, Fuel Average, Cladding, and Coolant Temperature at the Hot Spot

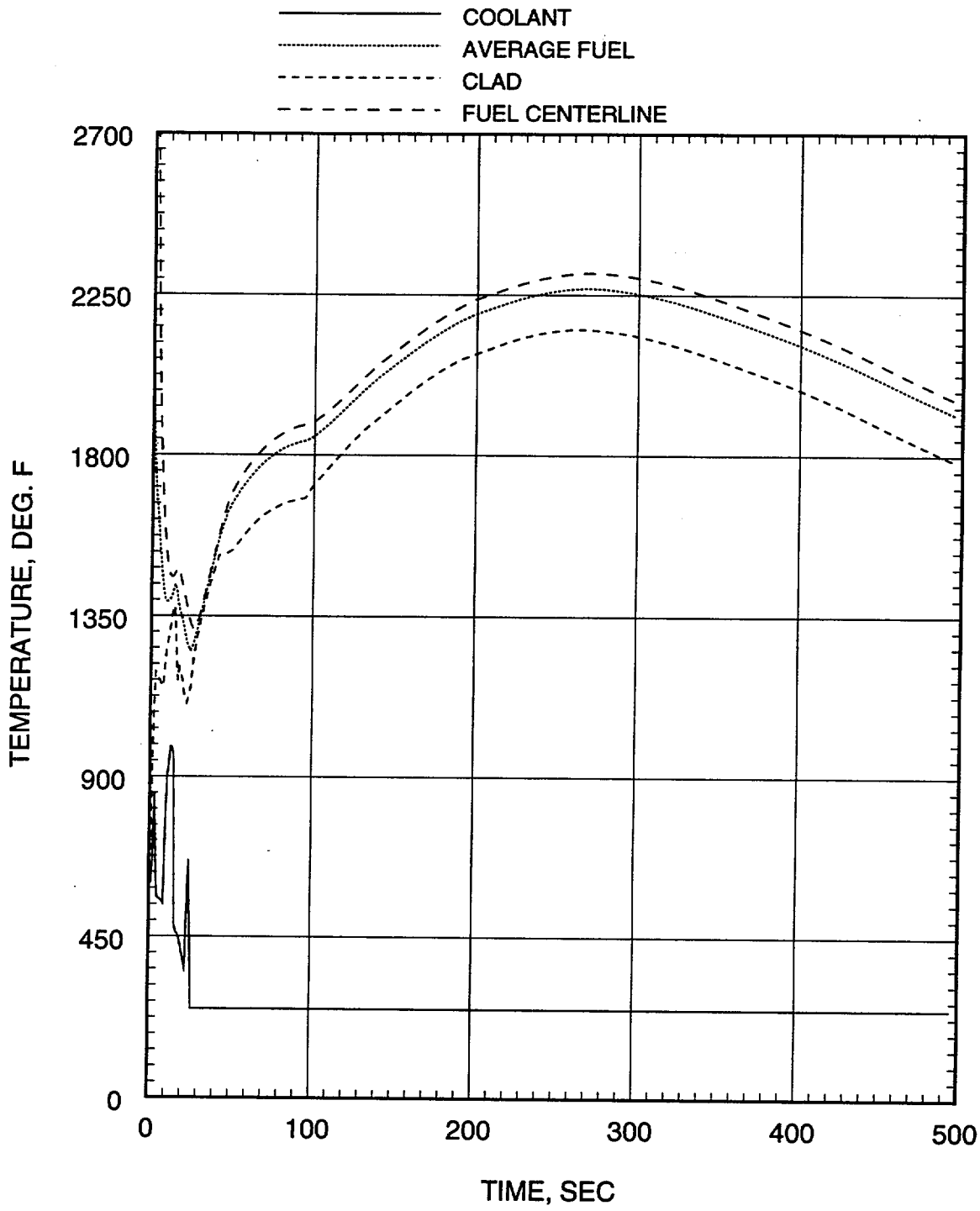

Figure 7.1.3-45
Large Break LOCA ECCS Performance Analysis
0.4 DEG/PD Break
Hot Spot Heat Transfer Coefficient

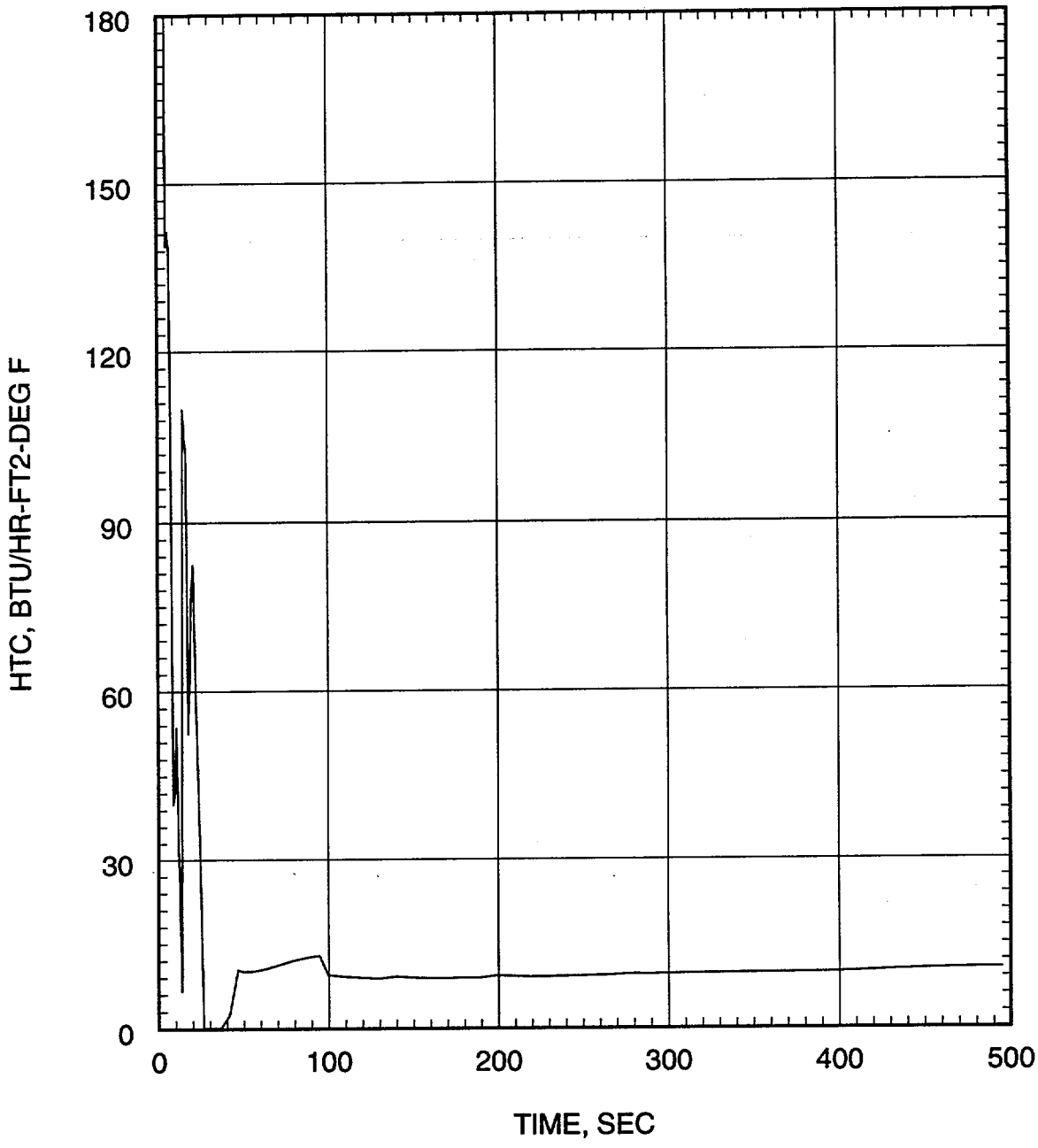

Figure 7.1.3-46
Large Break LOCA ECCS Performance Analysis
0.4 DEG/PD Break
Hot Pin Pressure

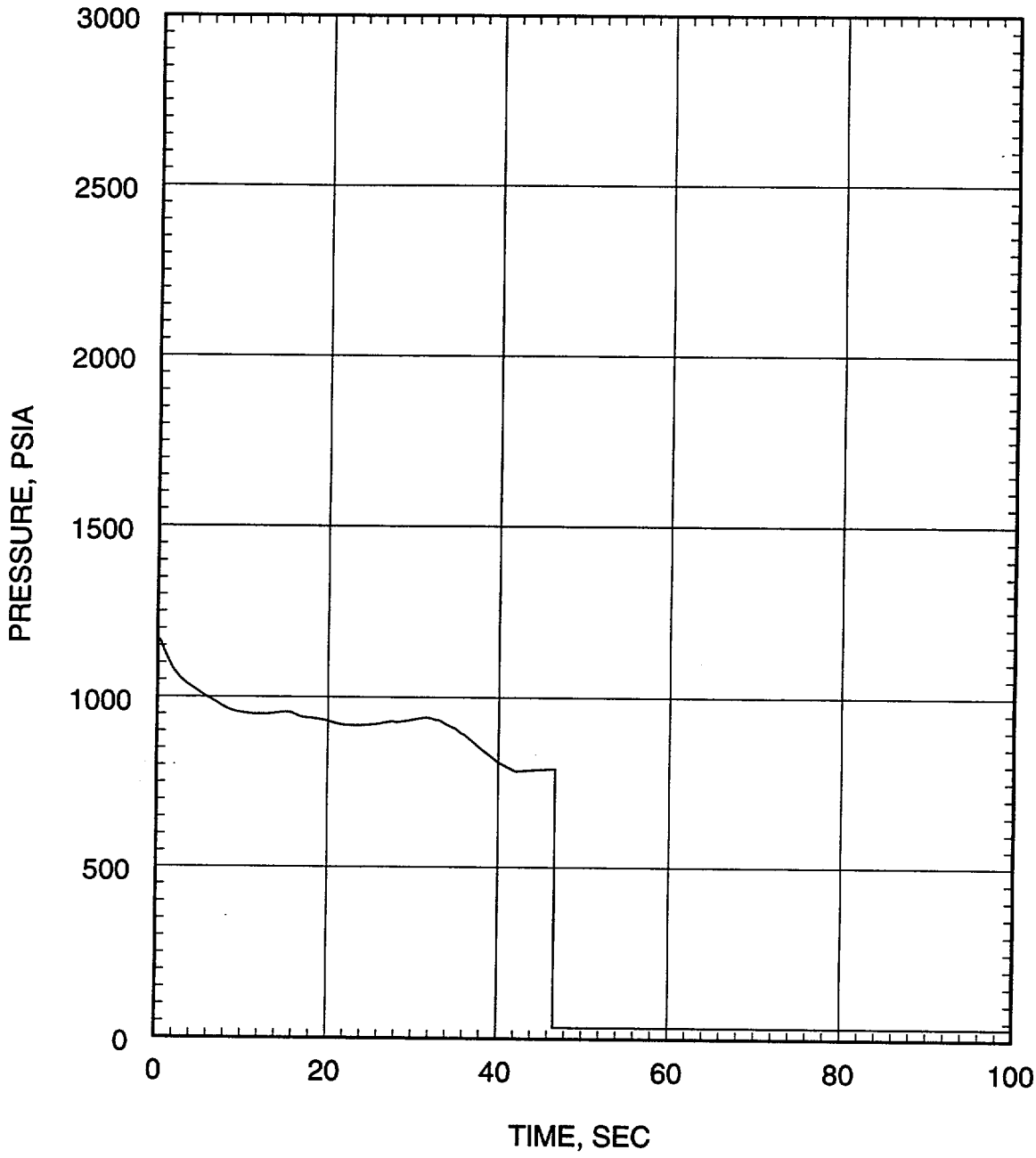

Figure 7.1.3-47
Large Break LOCA ECCS Performance Analysis
0.3 DEG/PD Break
Core Power

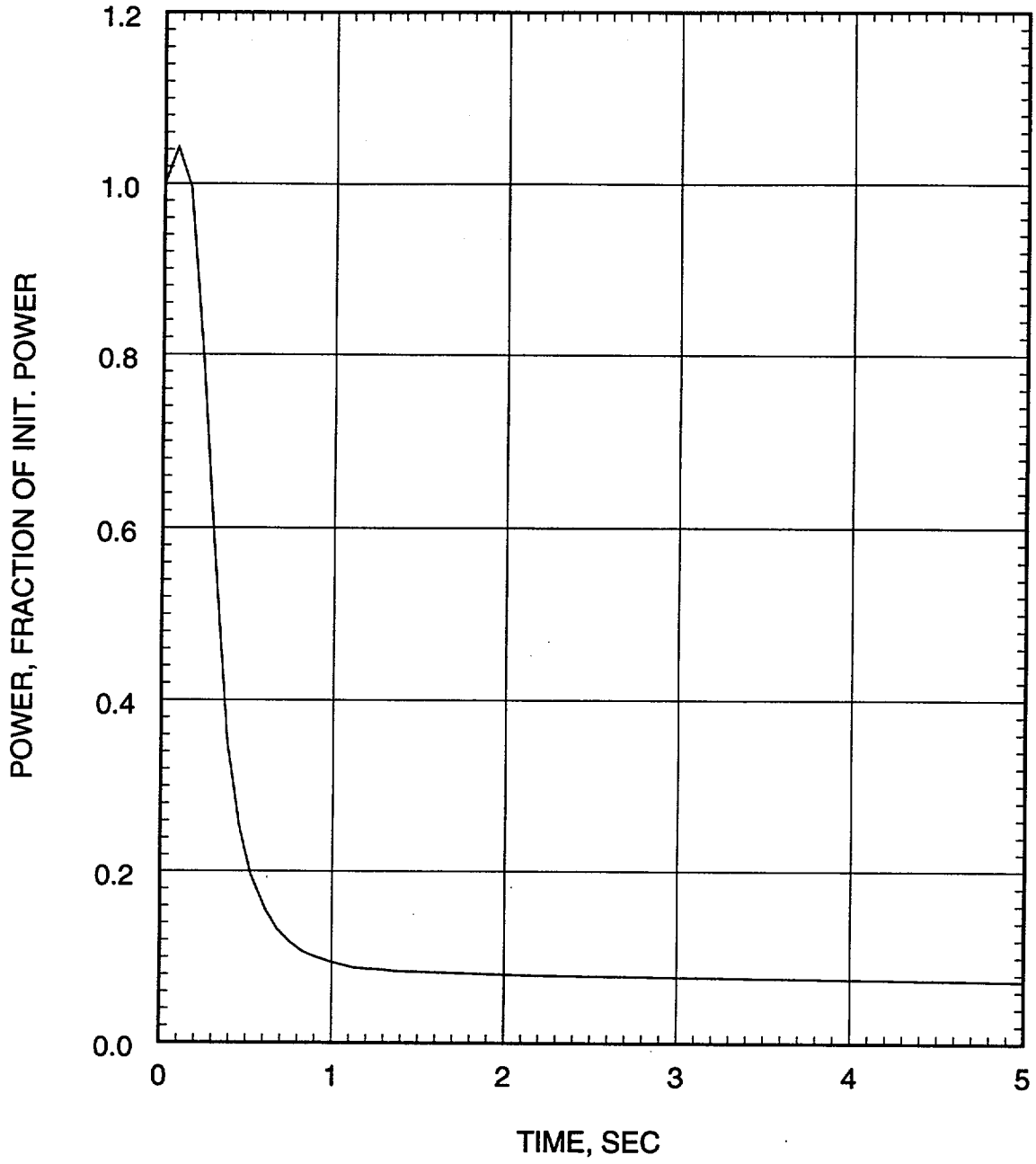

Figure 7.1.3-48
Large Break LOCA ECCS Performance Analysis
0.3 DEG/PD Break
Pressure in Center Hot Assembly Node

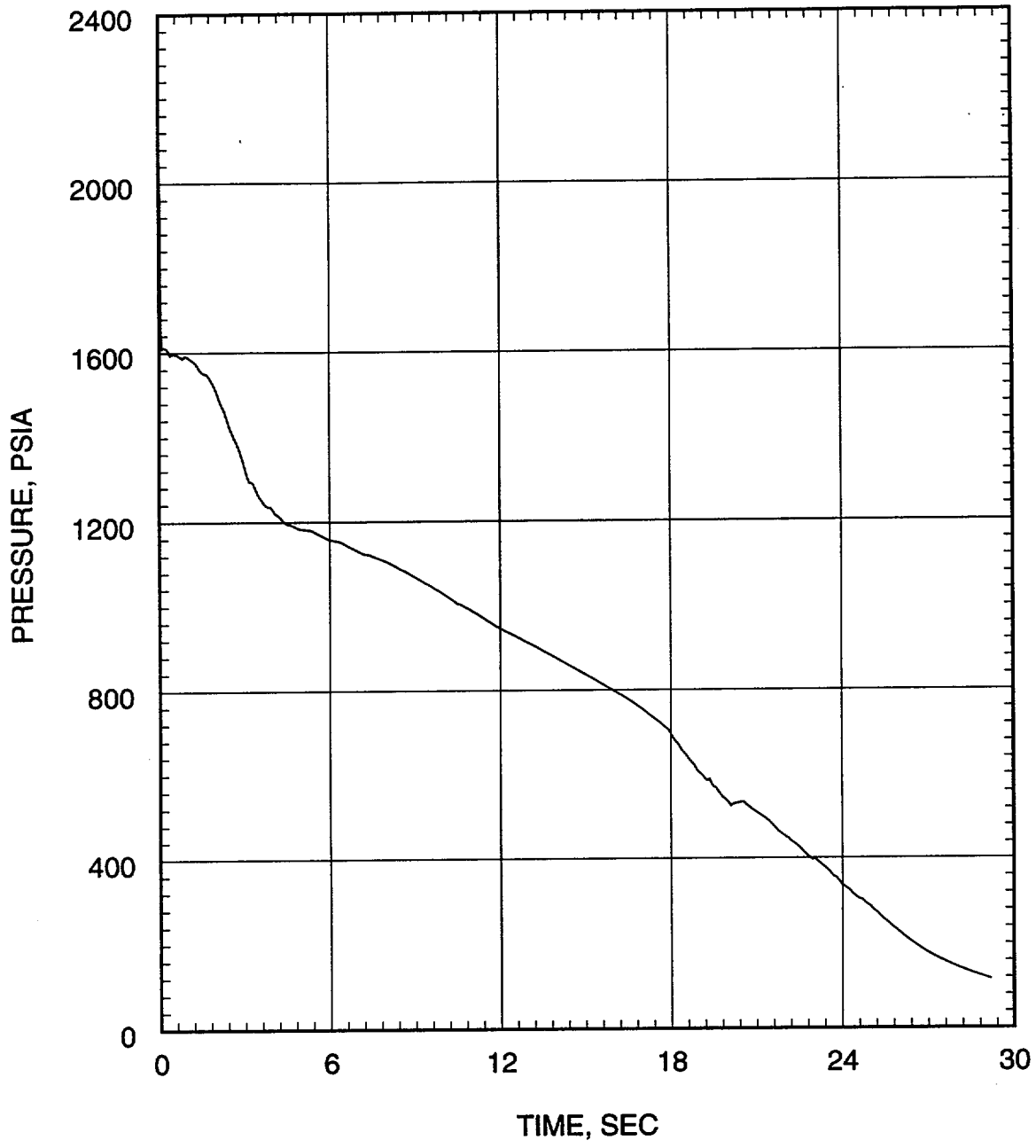

Figure 7.1.3-49
Large Break LOCA ECCS Performance Analysis
0.3 DEG/PD Break
Leak Flow Rate

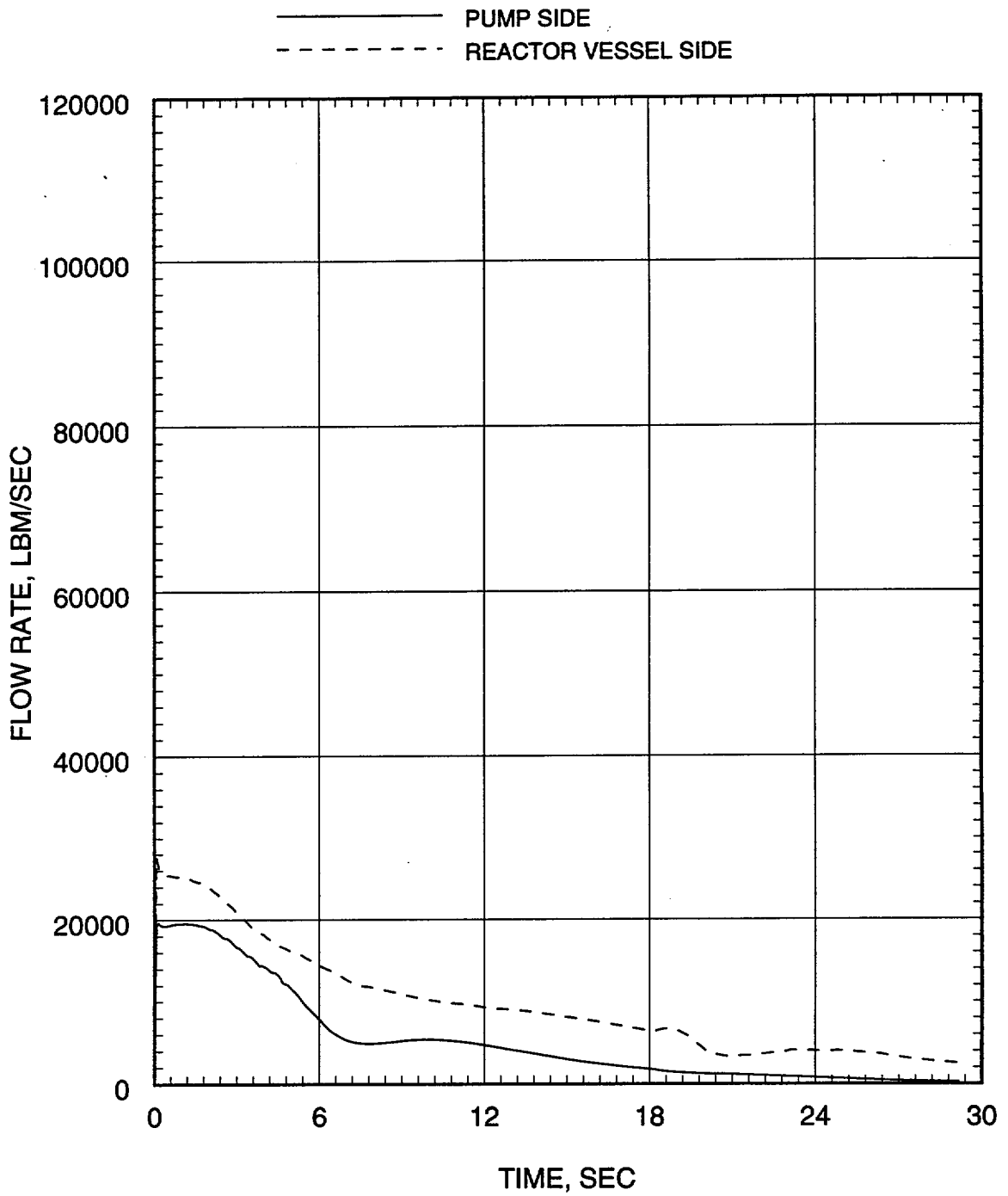

Figure 7.1.3-50
Large Break LOCA ECCS Performance Analysis
0.3 DEG/PD Break
Hot Assembly Flow Rate (Below Hot Spot)

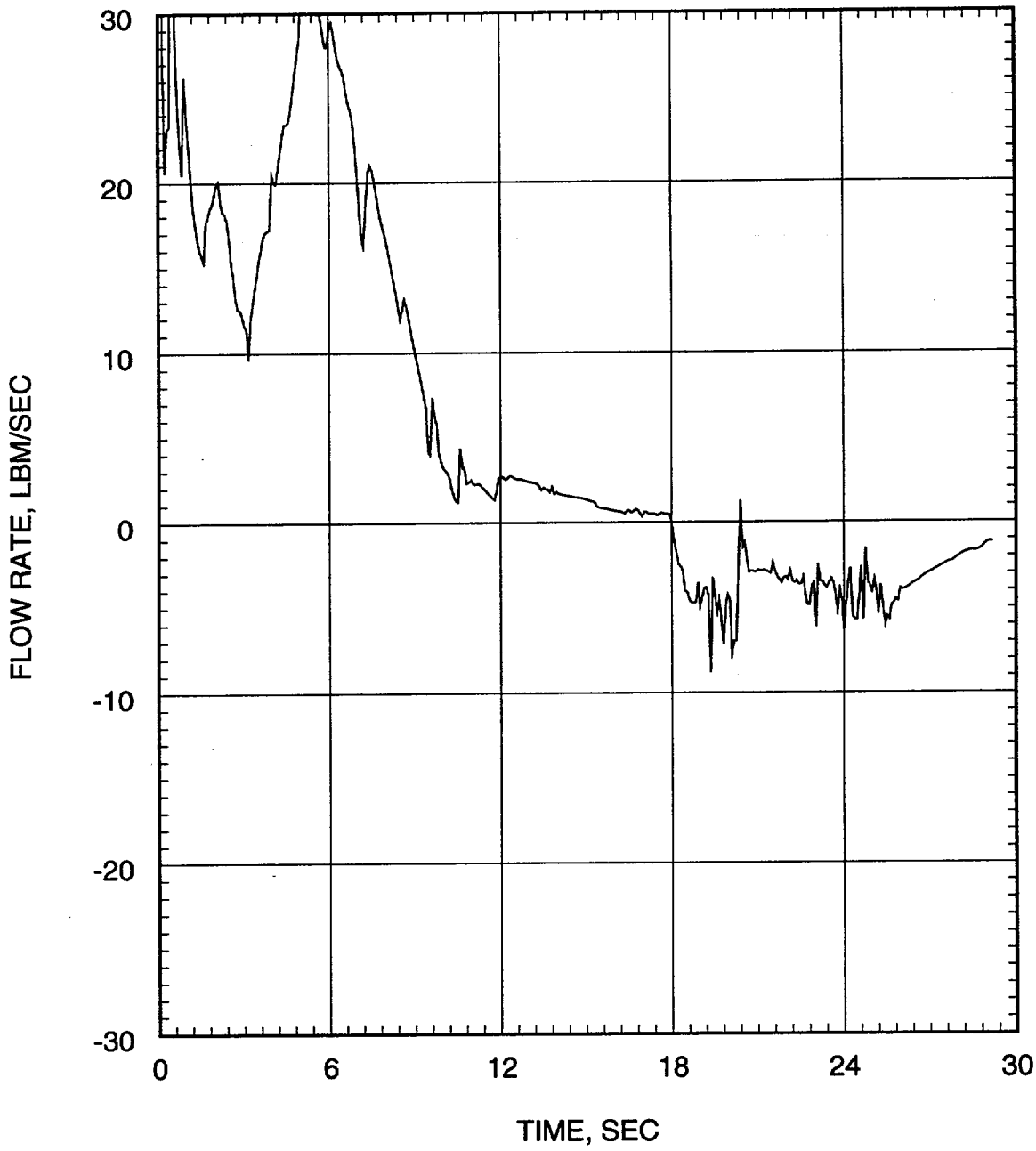

Figure 7.1.3-51
Large Break LOCA ECCS Performance Analysis
0.3 DEG/PD Break
Hot Assembly Flow Rate (Above Hot Spot)

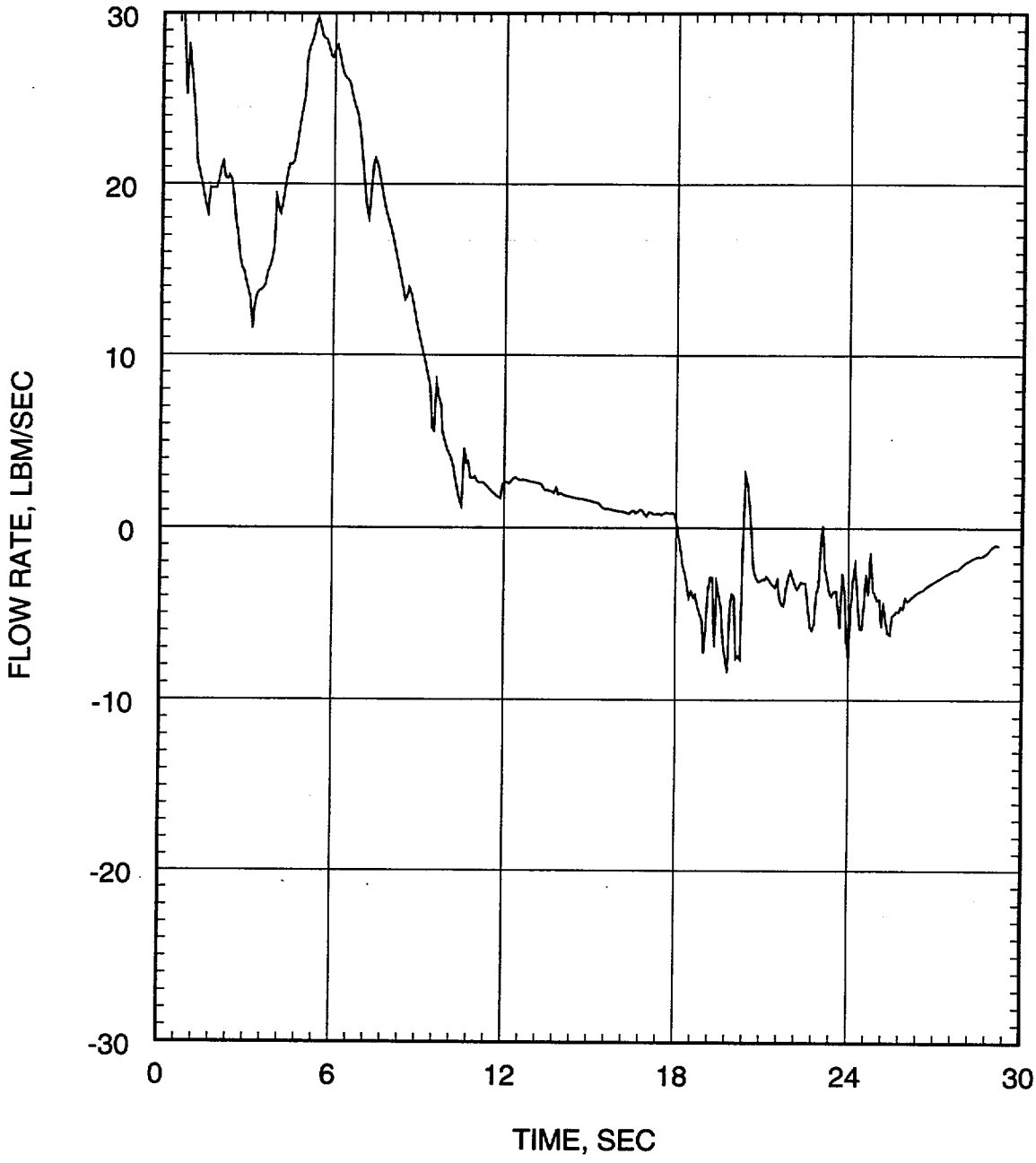

Figure 7.1.3-52
Large Break LOCA ECCS Performance Analysis
0.3 DEG/PD Break
Hot Assembly Quality

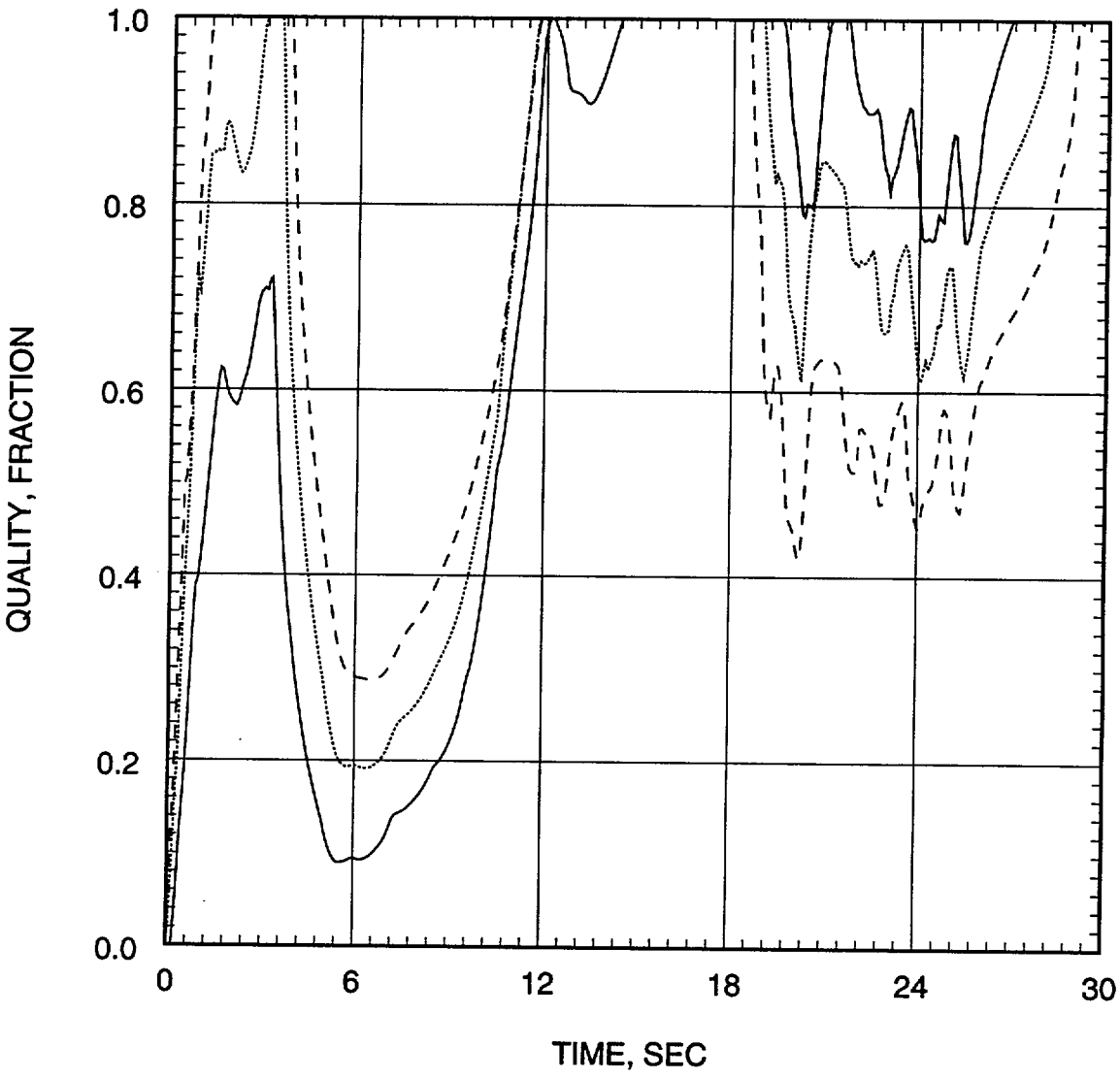

Figure 7.1.3-53
Large Break LOCA ECCS Performance Analysis
0.3 DEG/PD Break
Containment Pressure

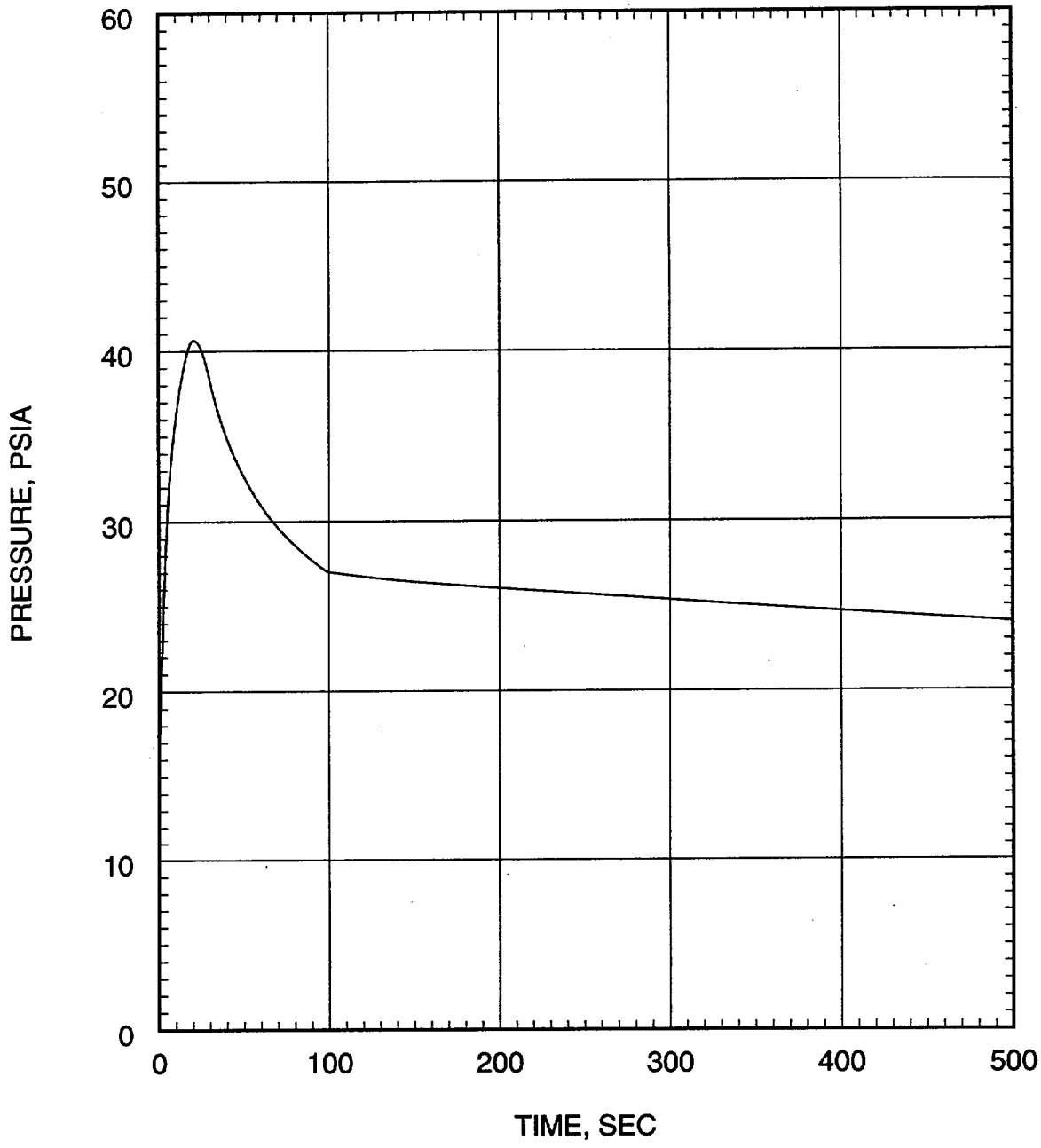

Figure 7.1.3-54
Large Break LOCA ECCS Performance Analysis
0.3 DEG/PD Break
Mass Added to Core During Reflood

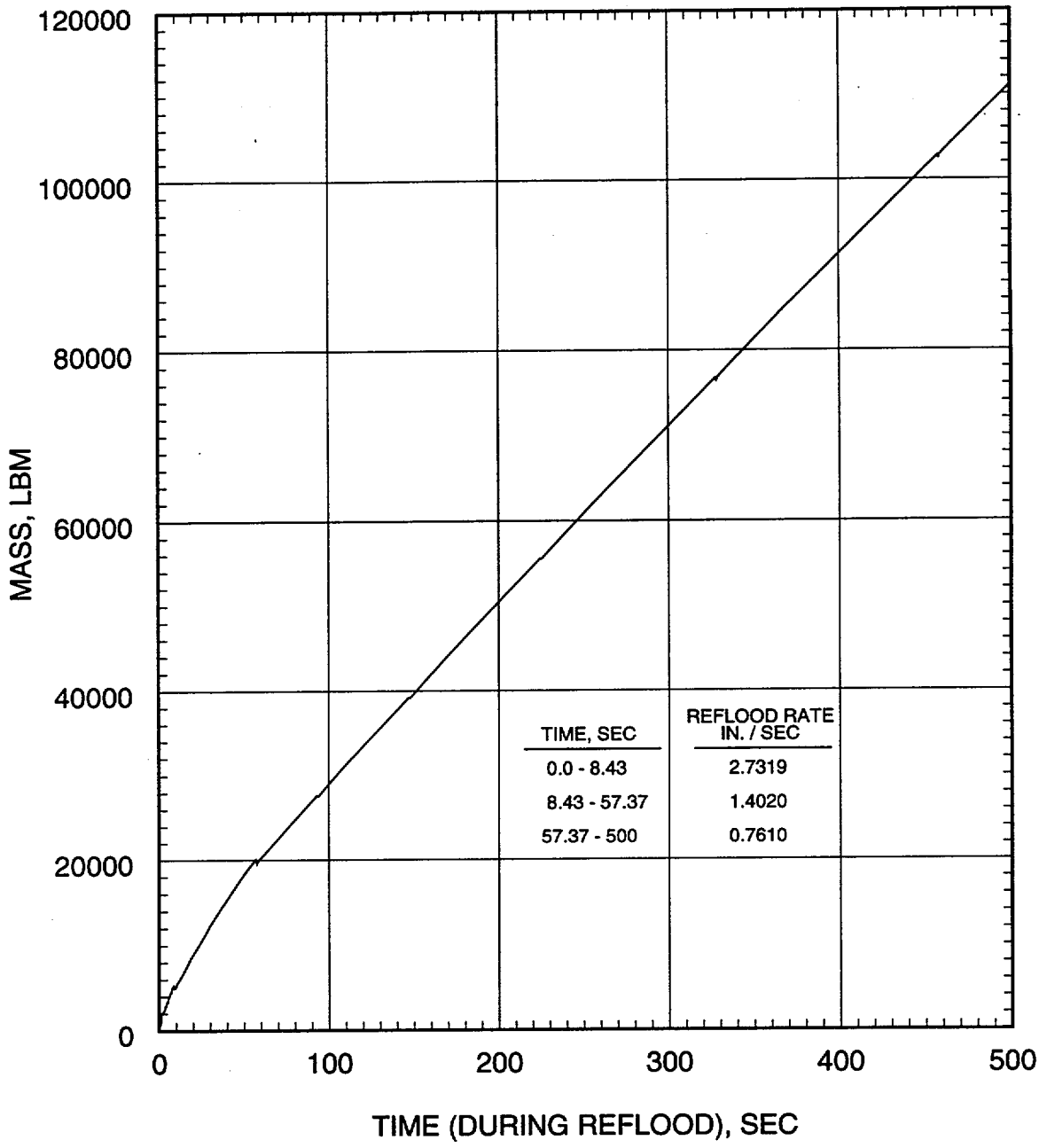

Figure 7.1.3-55
Large Break LOCA ECCS Performance Analysis
0.3 DEG/PD Break
Peak Cladding Temperature

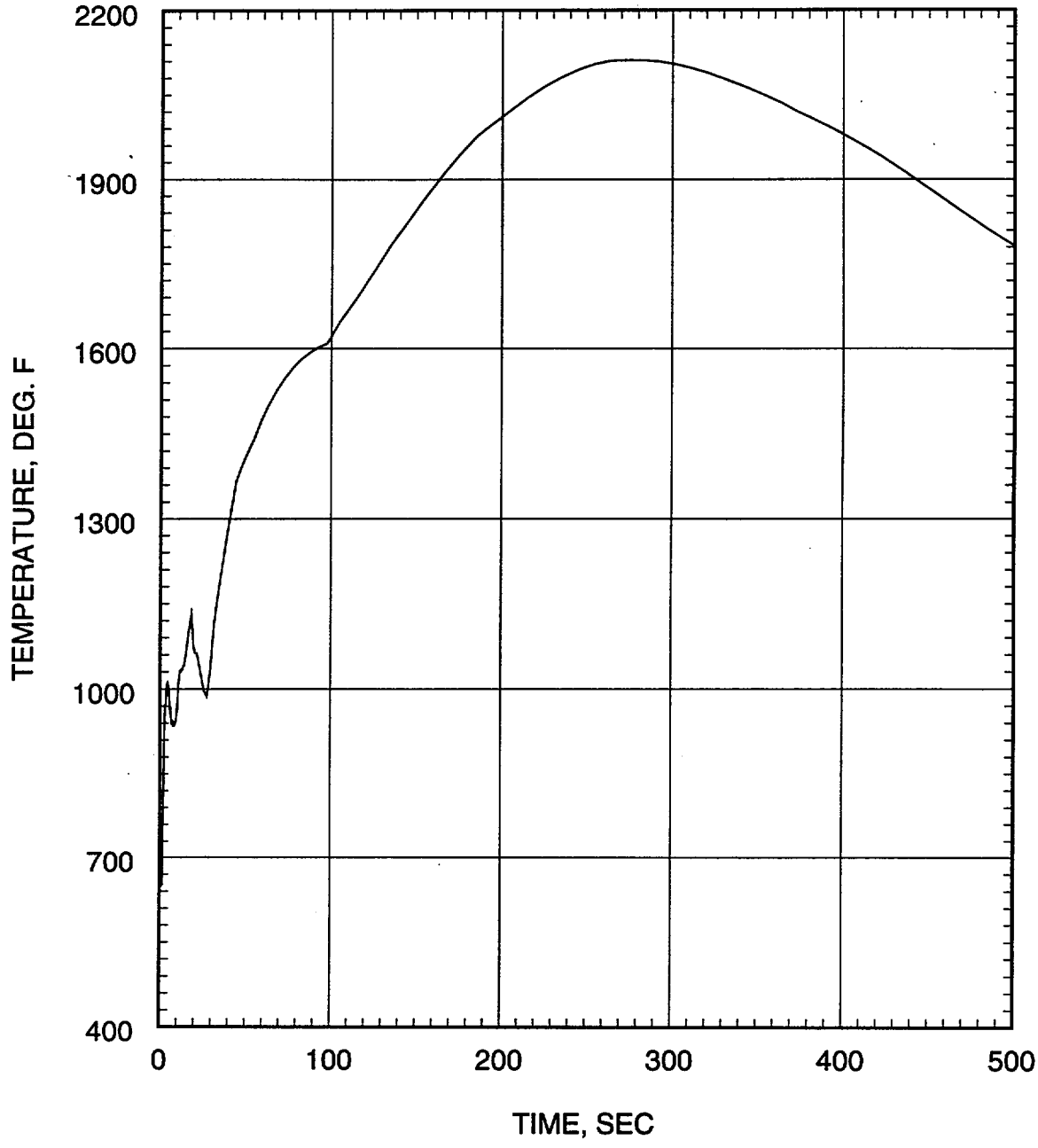

Figure 7.1.4-1
Small Break LOCA ECCS Performance Analysis
0.03 ft^2/PD Break
Core Power

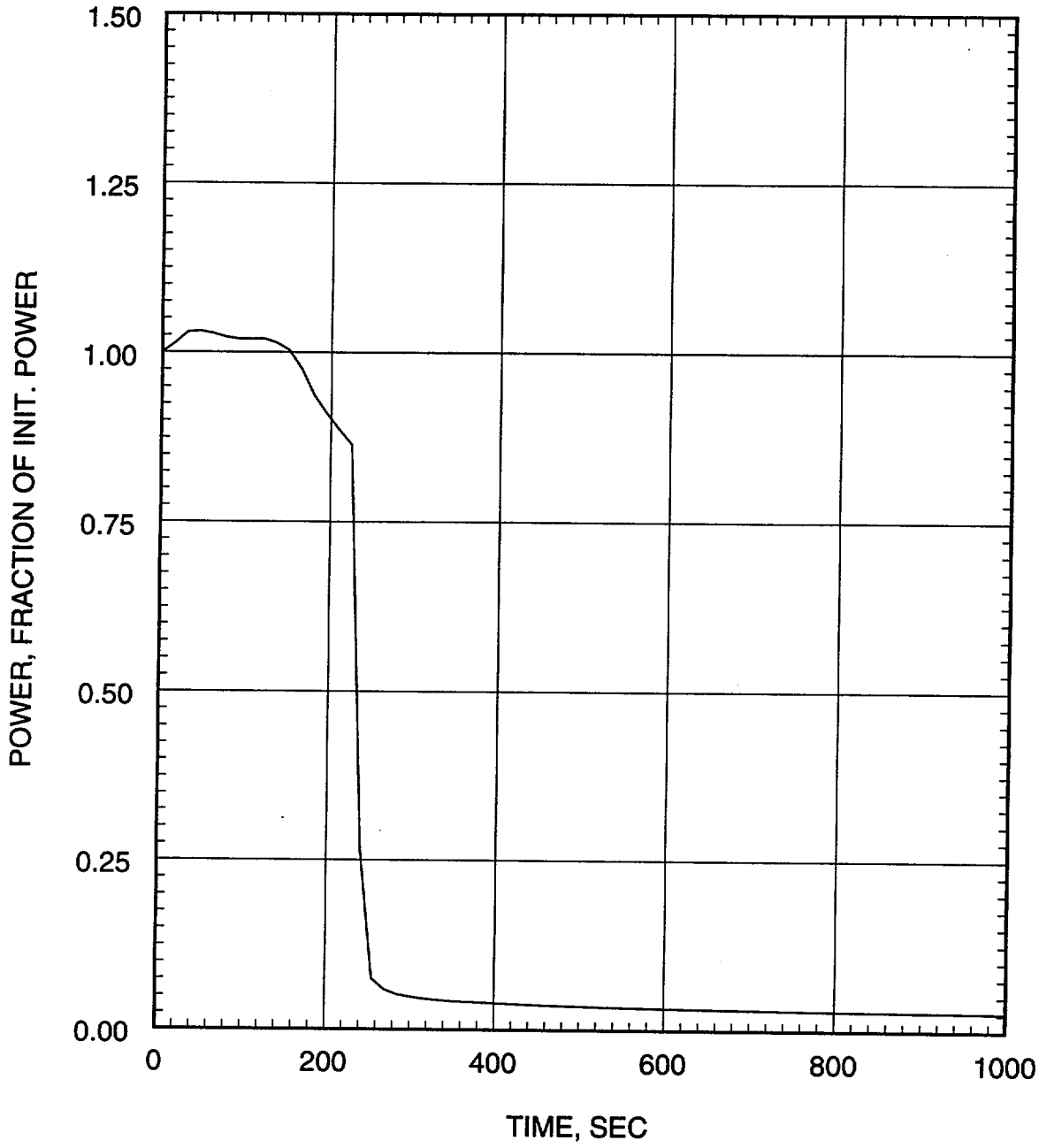

Figure 7.1.4-2
Small Break LOCA ECCS Performance Analysis
0.03 ft^2/PD Break
Inner Vessel Pressure

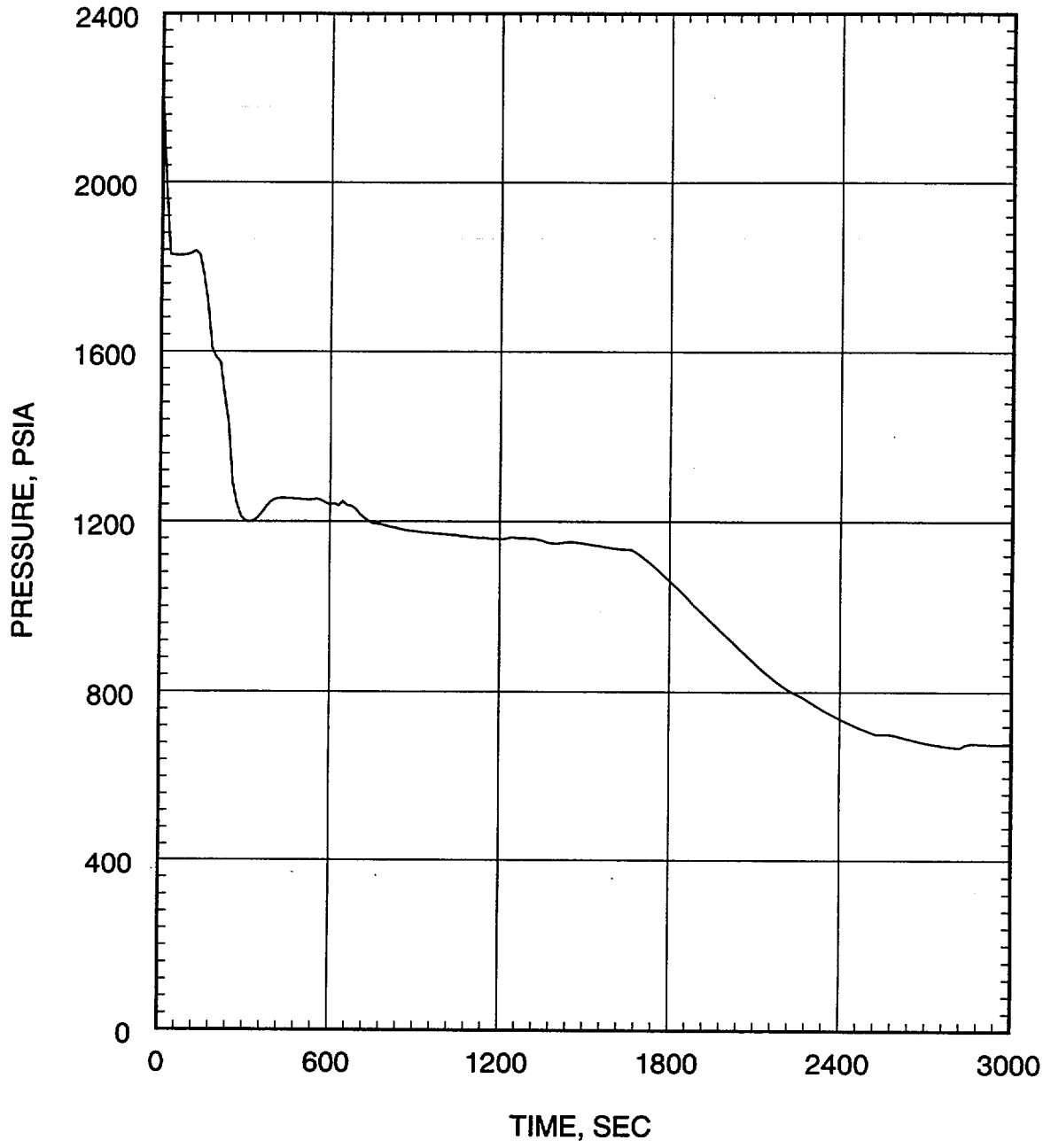

Figure 7.1.4-3
Small Break LOCA ECCS Performance Analysis
0.03 ft^2/PD Break
Break Flow Rate

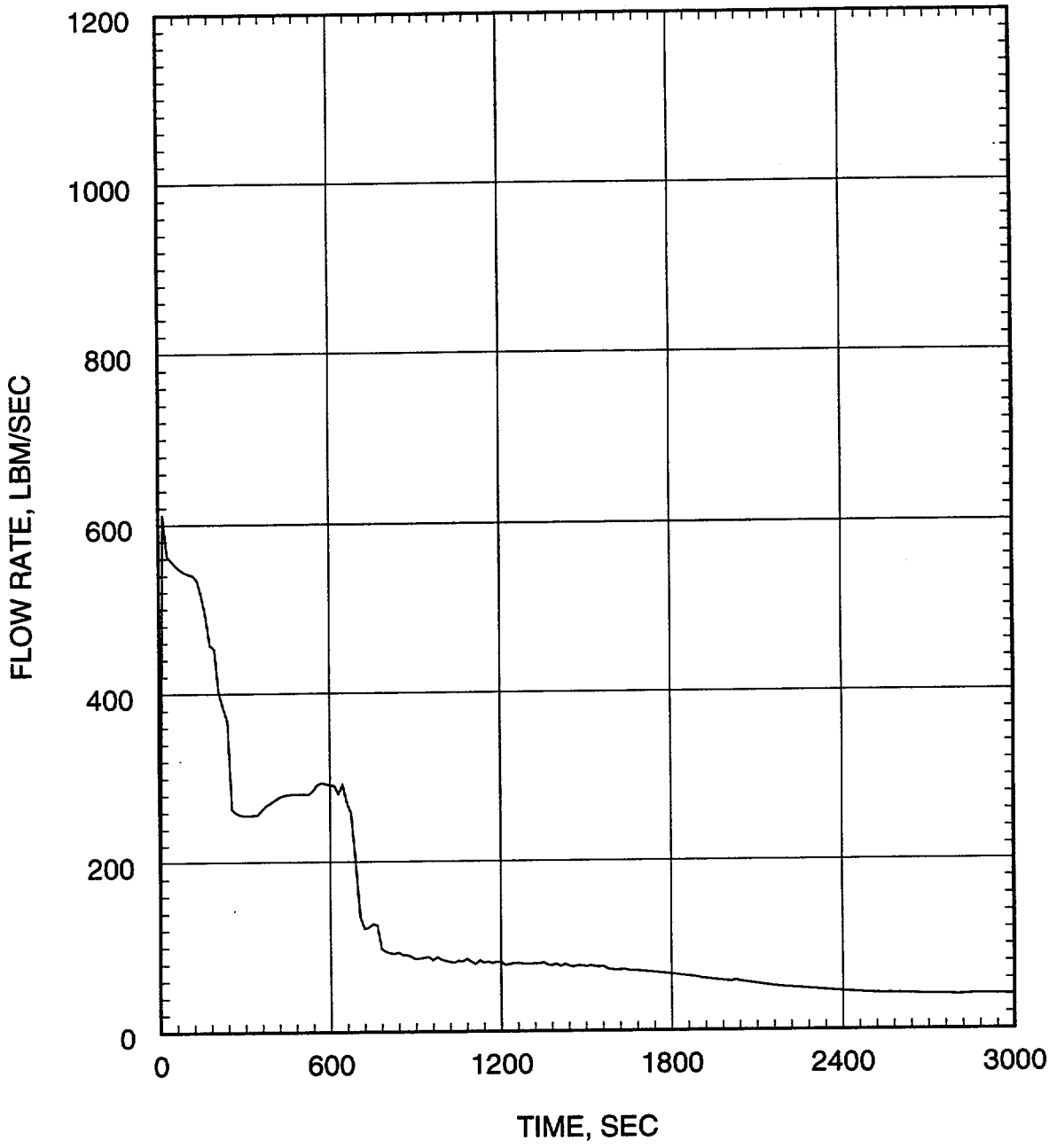

Figure 7.1.4-4
Small Break LOCA ECCS Performance Analysis
0.03 ft^2/PD Break
Inner Vessel Inlet Flow Rate

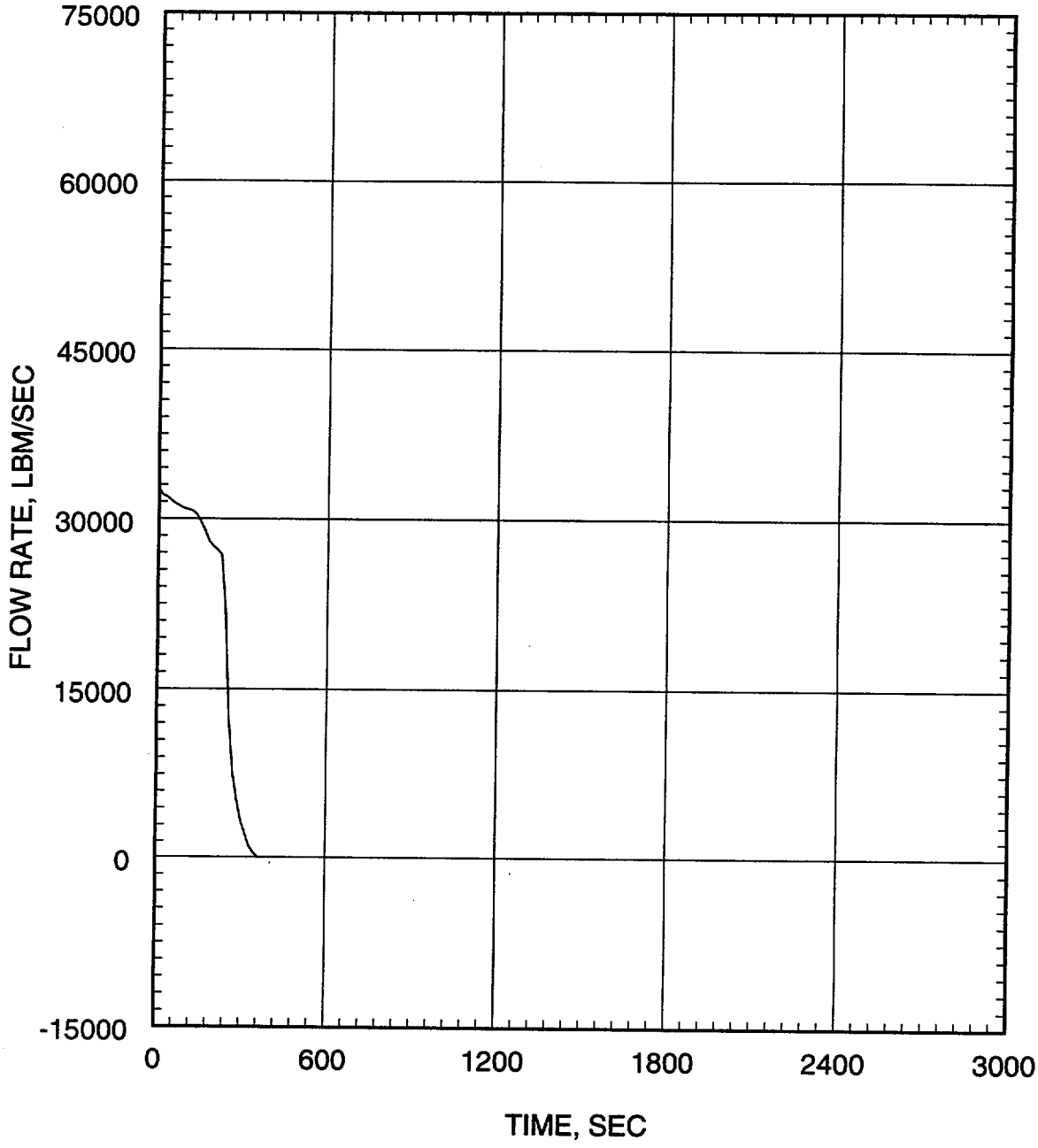

Figure 7.1.4-5
Small Break LOCA ECCS Performance Analysis
0.03 ft^2/PD Break
Inner Vessel Two-Phase Mixture Level

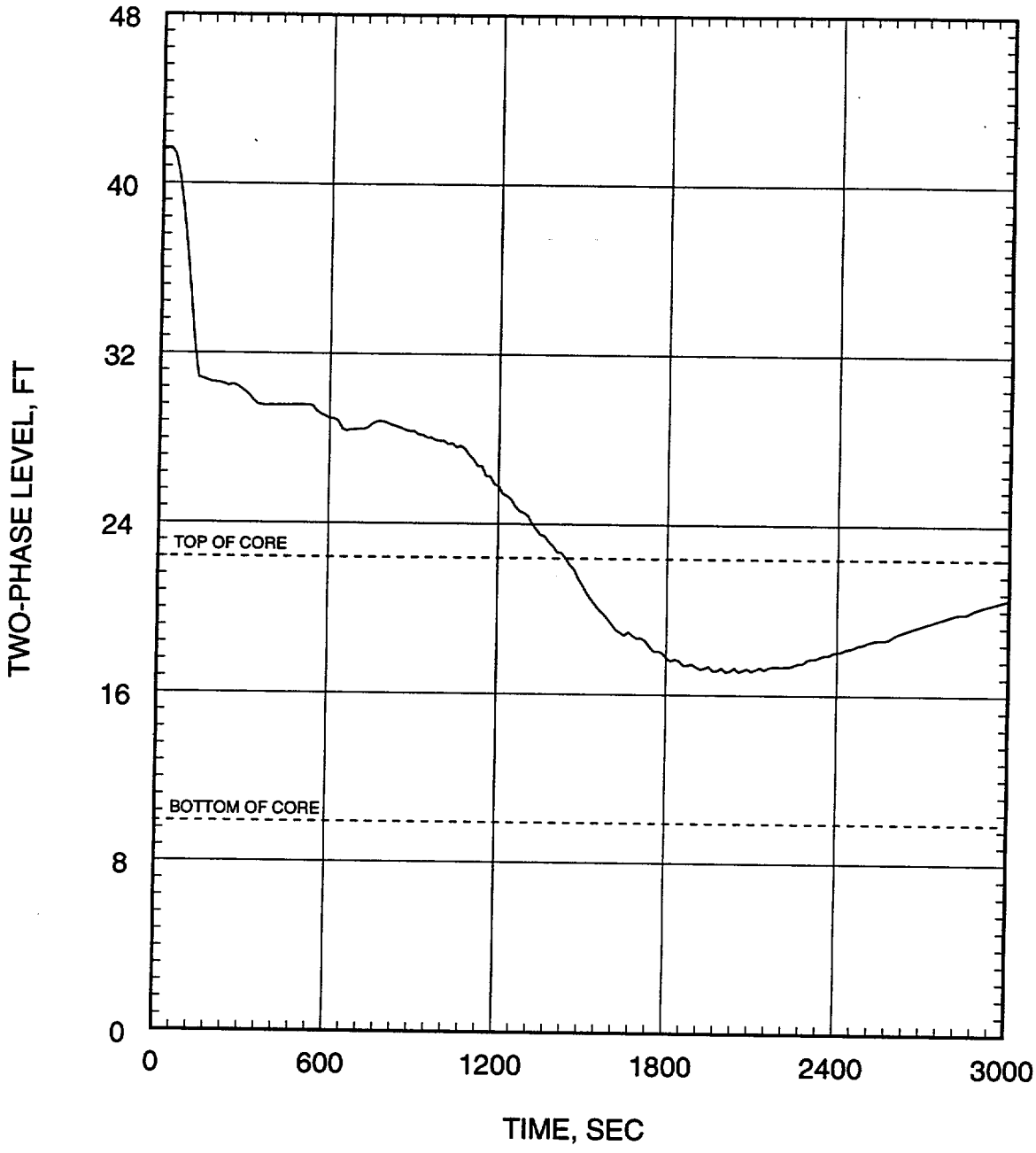

Figure 7.1.4-6
Small Break LOCA ECCS Performance Analysis
0.03 ft^2/PD Break
Heat Transfer Coefficient at Hot Spot

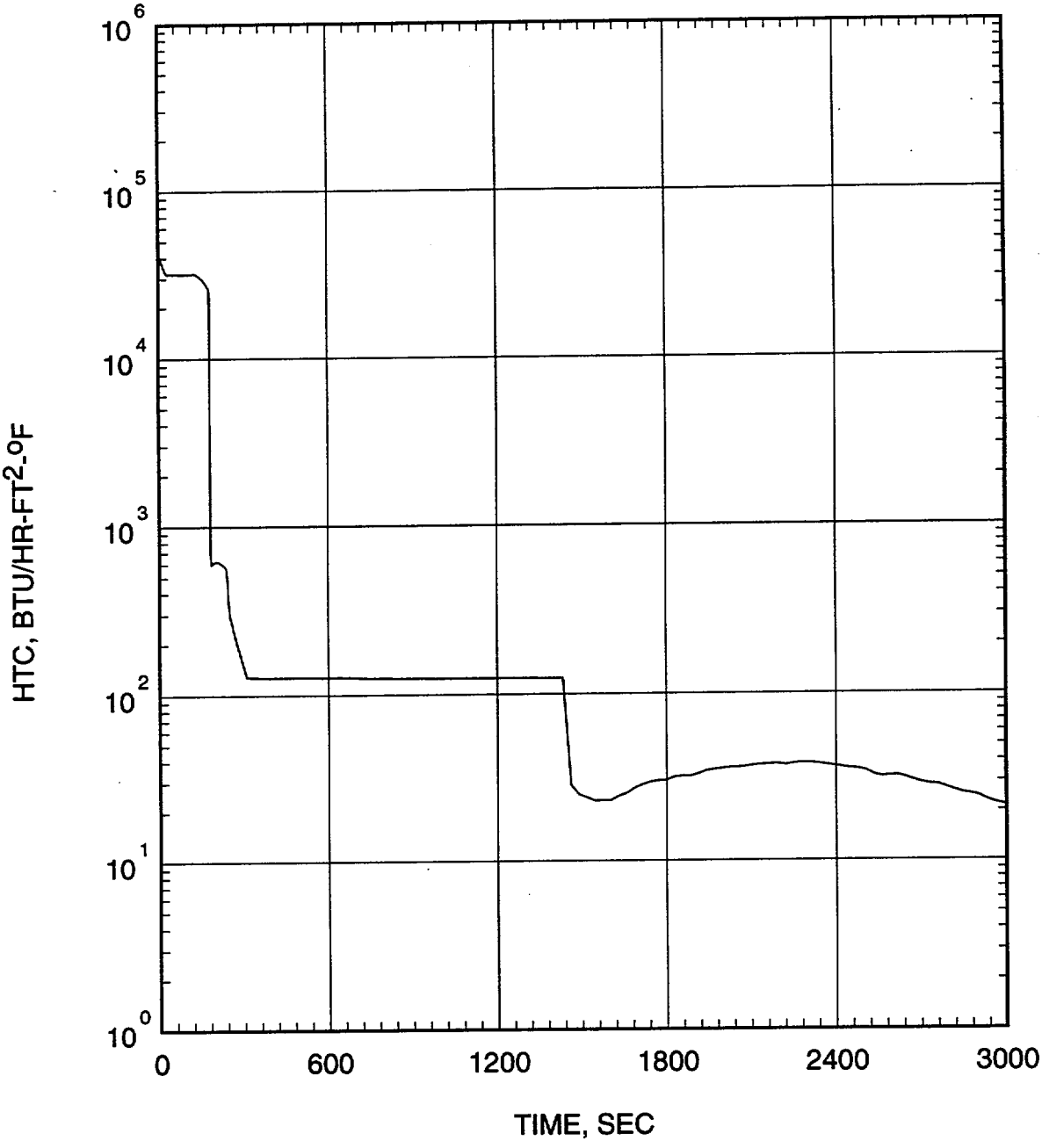

Figure 7.1.4-7
Small Break LOCA ECCS Performance Analysis
0.03 ft^2/PD Break
Coolant Temperature at Hot Spot

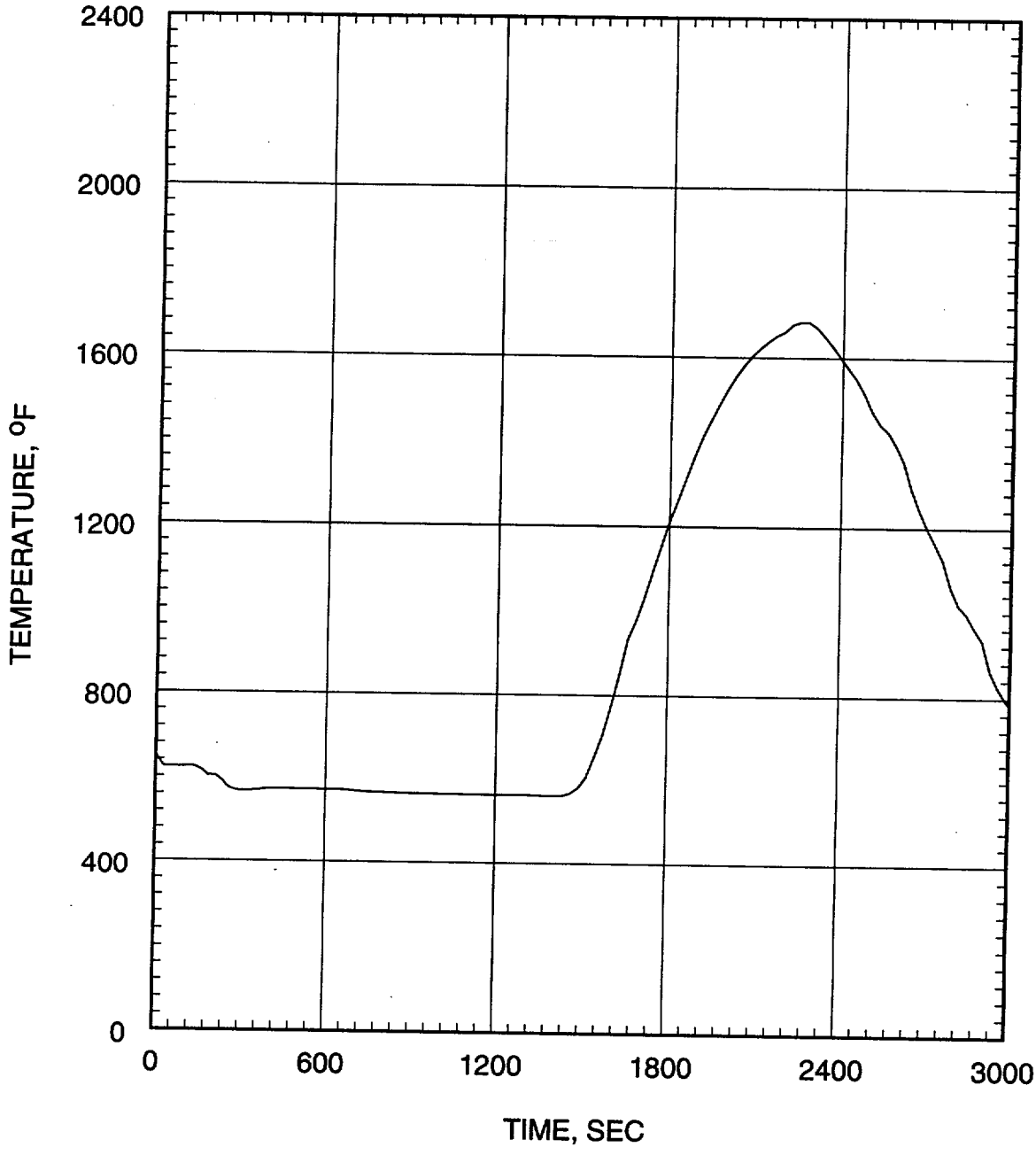

Figure 7.1.4-8
Small Break LOCA ECCS Performance Analysis
0.03 ft^2/PD Break
Cladding Temperature at Hot Spot

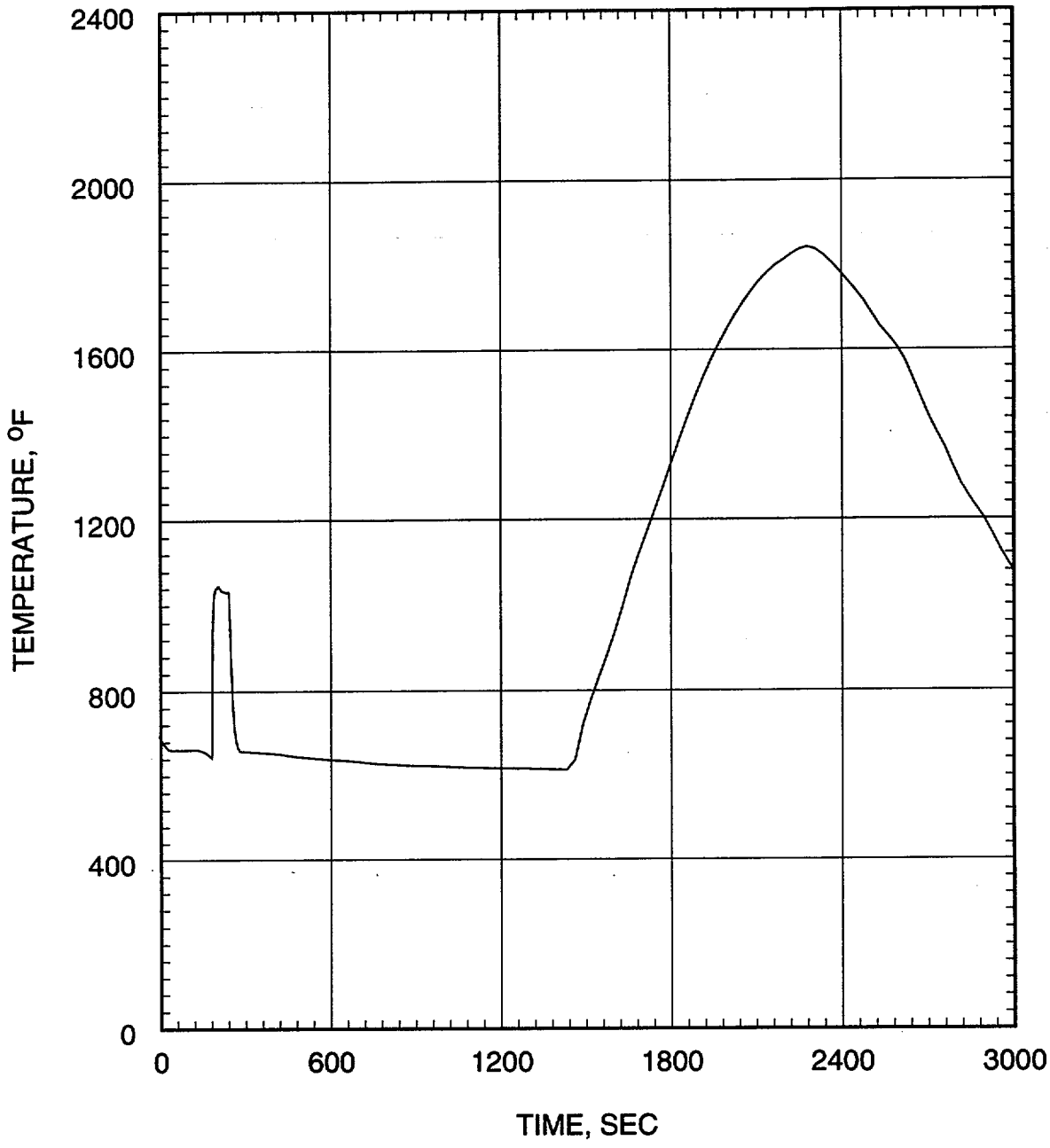

Figure 7.1.4-9
Small Break LOCA ECCS Performance Analysis
0.04 ft^2/PD Break
Core Power

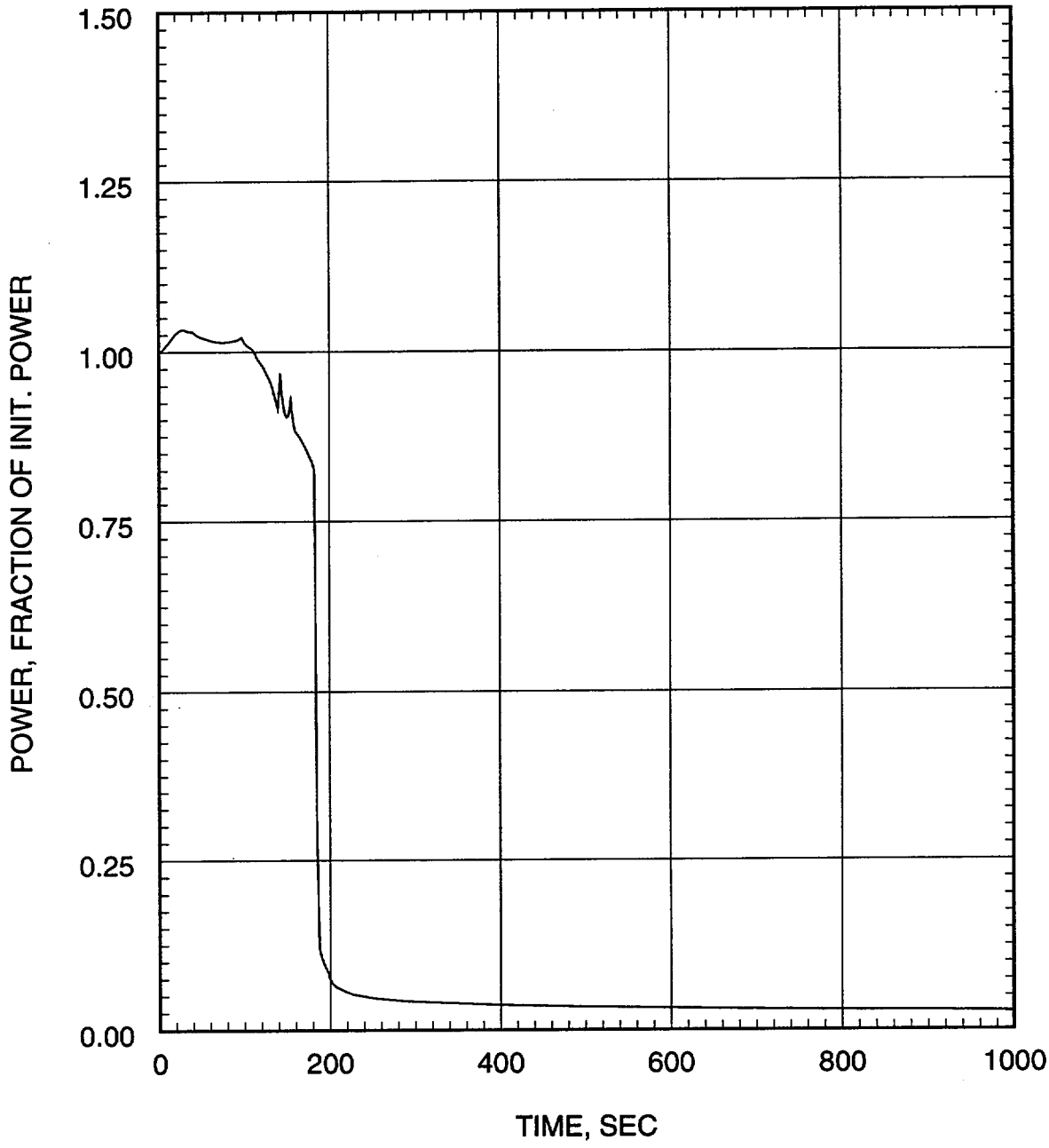

Figure 7.1.4-10
Small Break LOCA ECCS Performance Analysis
0.04 ft^2/PD Break
Inner Vessel Pressure

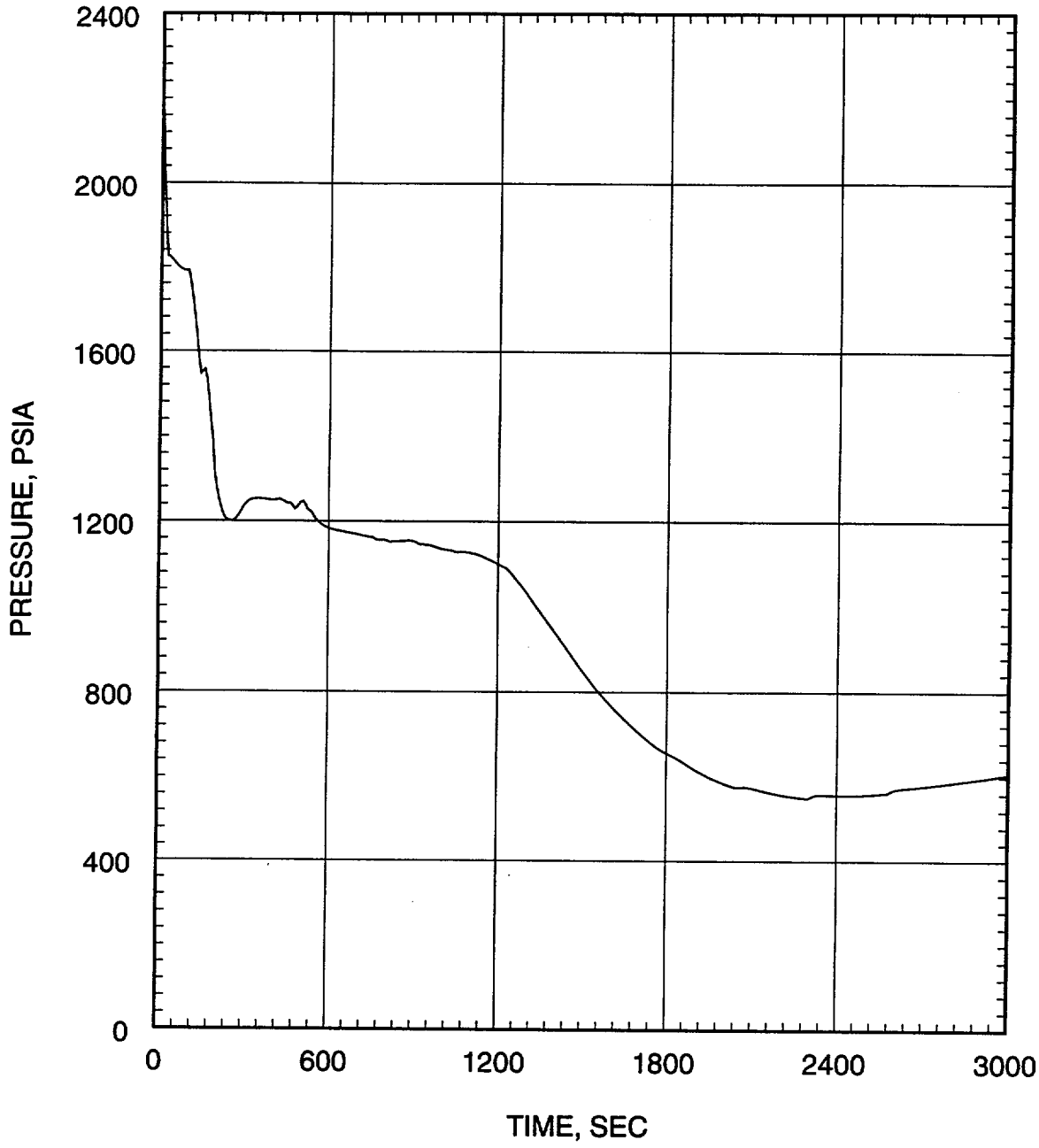

Figure 7.1.4-11
Small Break LOCA ECCS Performance Analysis
0.04 ft^2/PD Break
Break Flow Rate

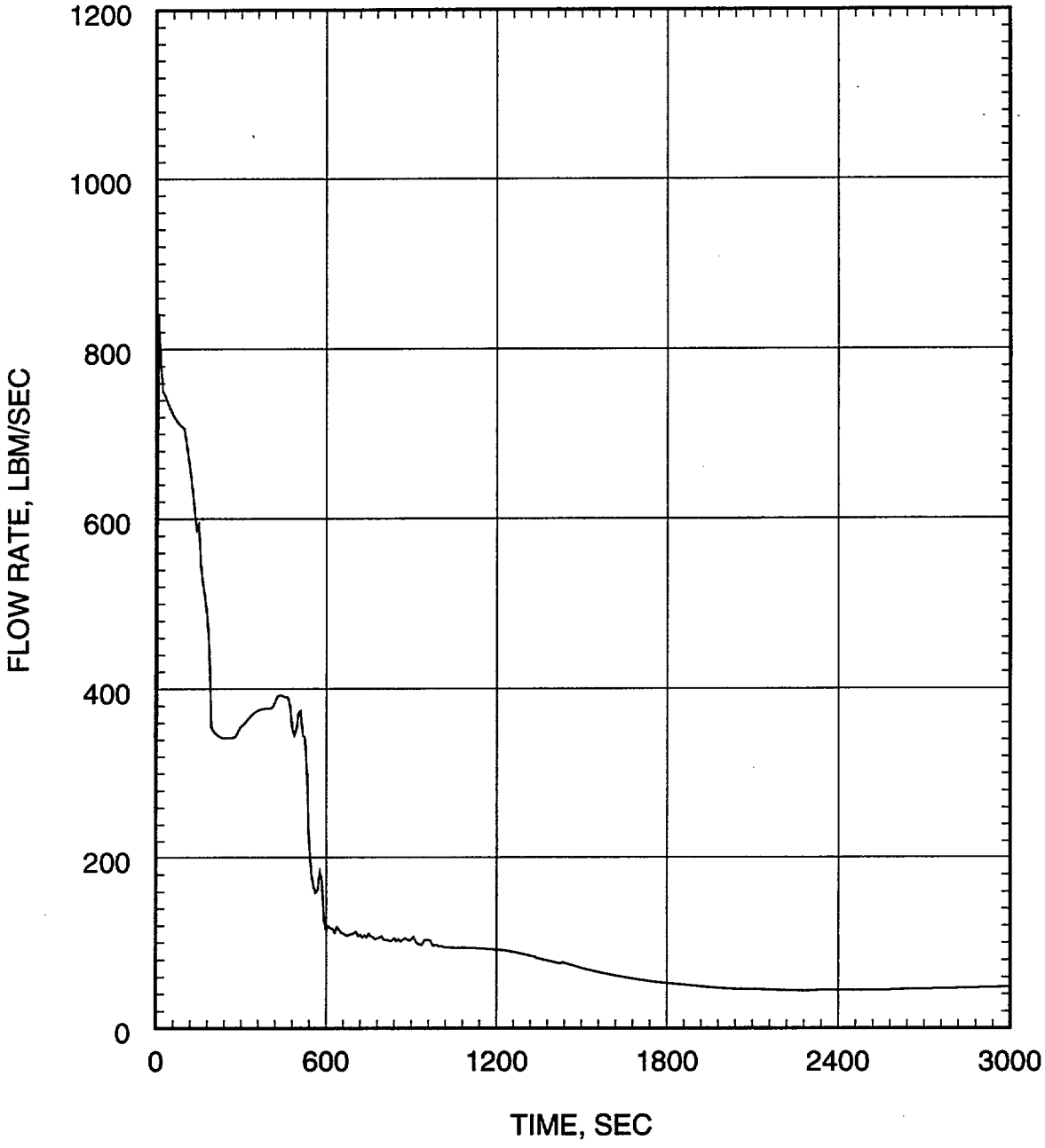

Figure 7.1.4-12
Small Break LOCA ECCS Performance Analysis
0.04 ft^2/PD Break
Inner Vessel Inlet Flow Rate

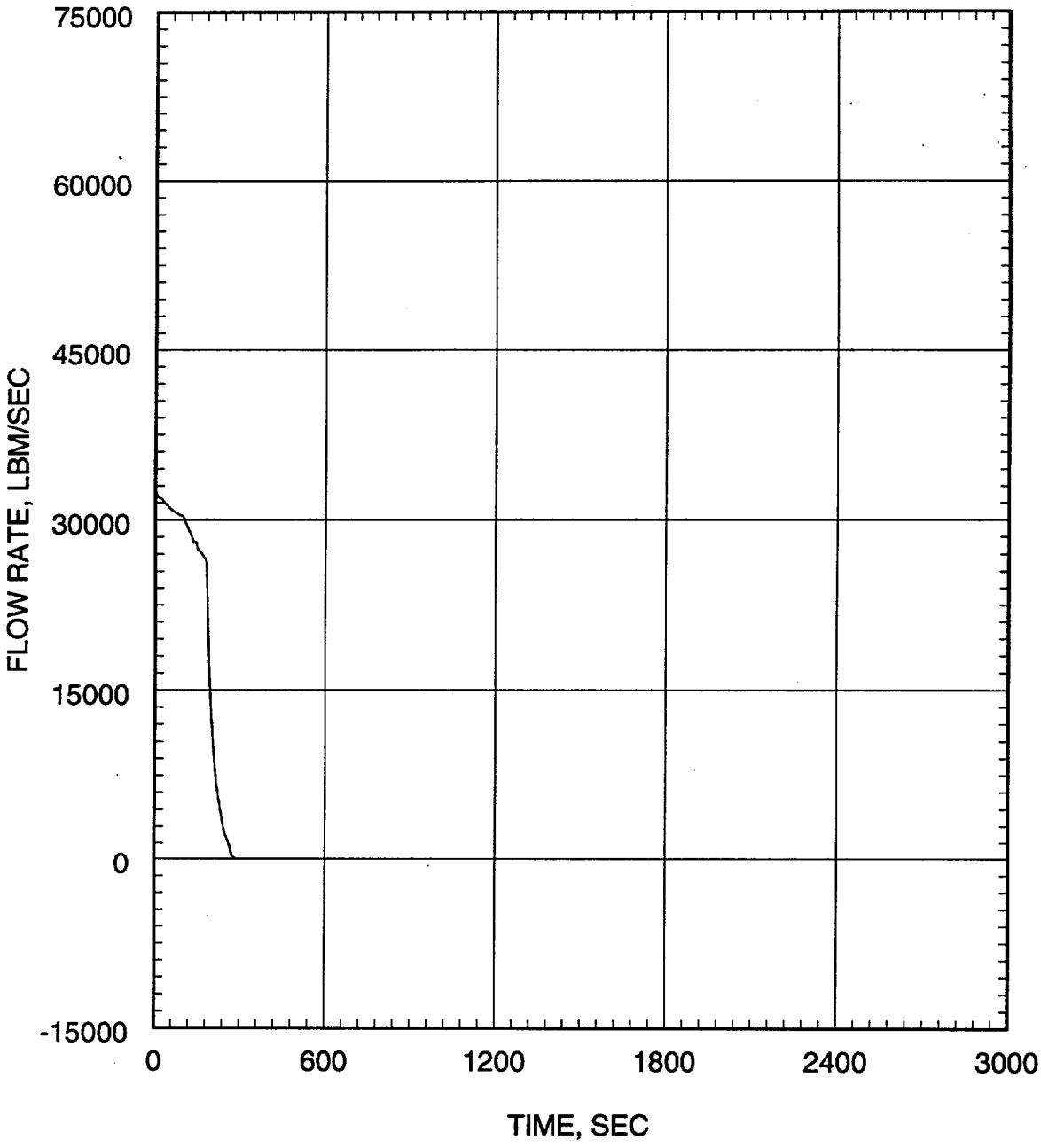

Figure 7.1.4-13
Small Break LOCA ECCS Performance Analysis
0.04 ft^2/PD Break
Inner Vessel Two-Phase Mixture Level

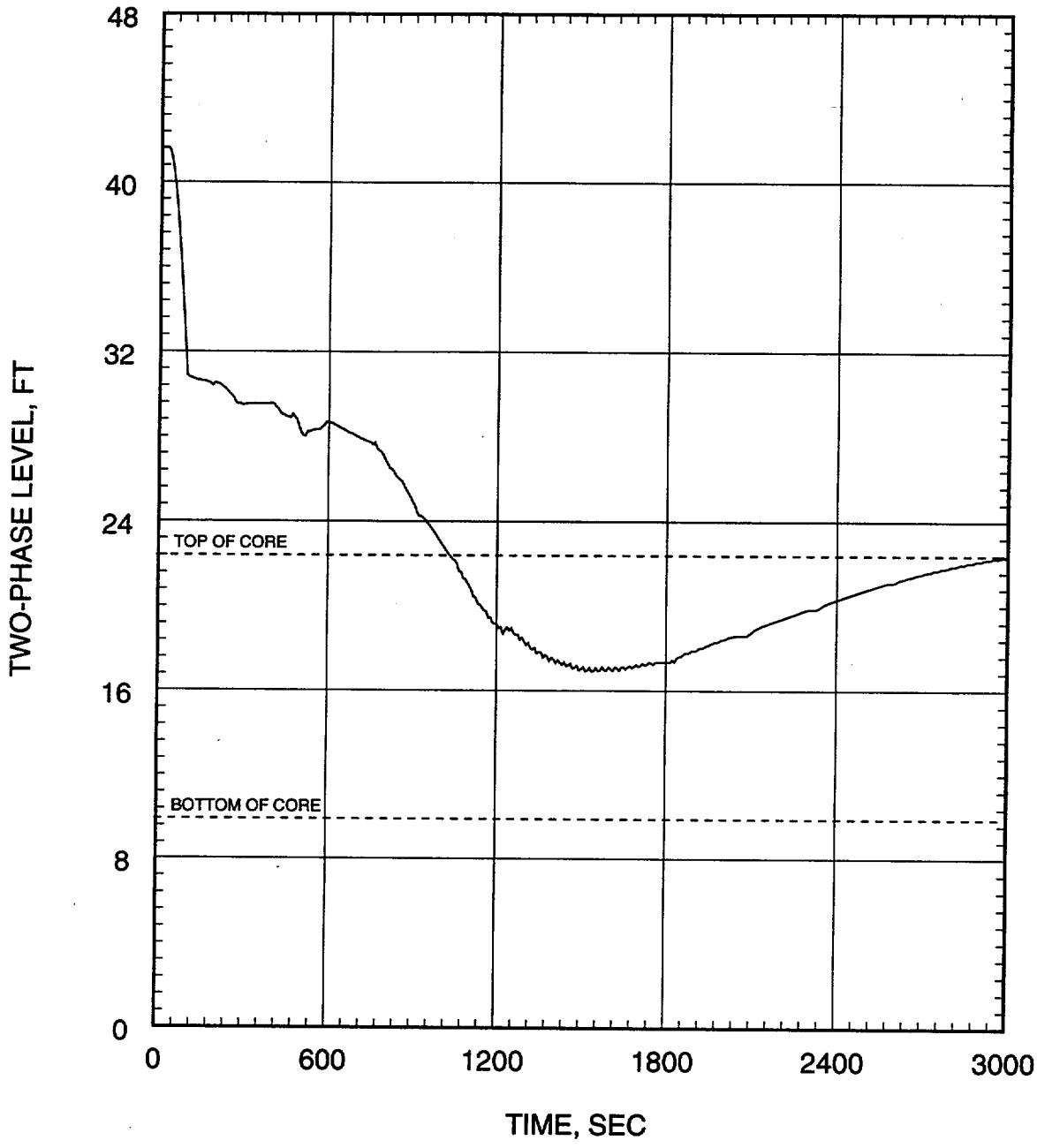

Figure 7.1.4-14
Small Break LOCA ECCS Performance Analysis
0.04 ft^2/PD Break
Heat Transfer Coefficient at Hot Spot

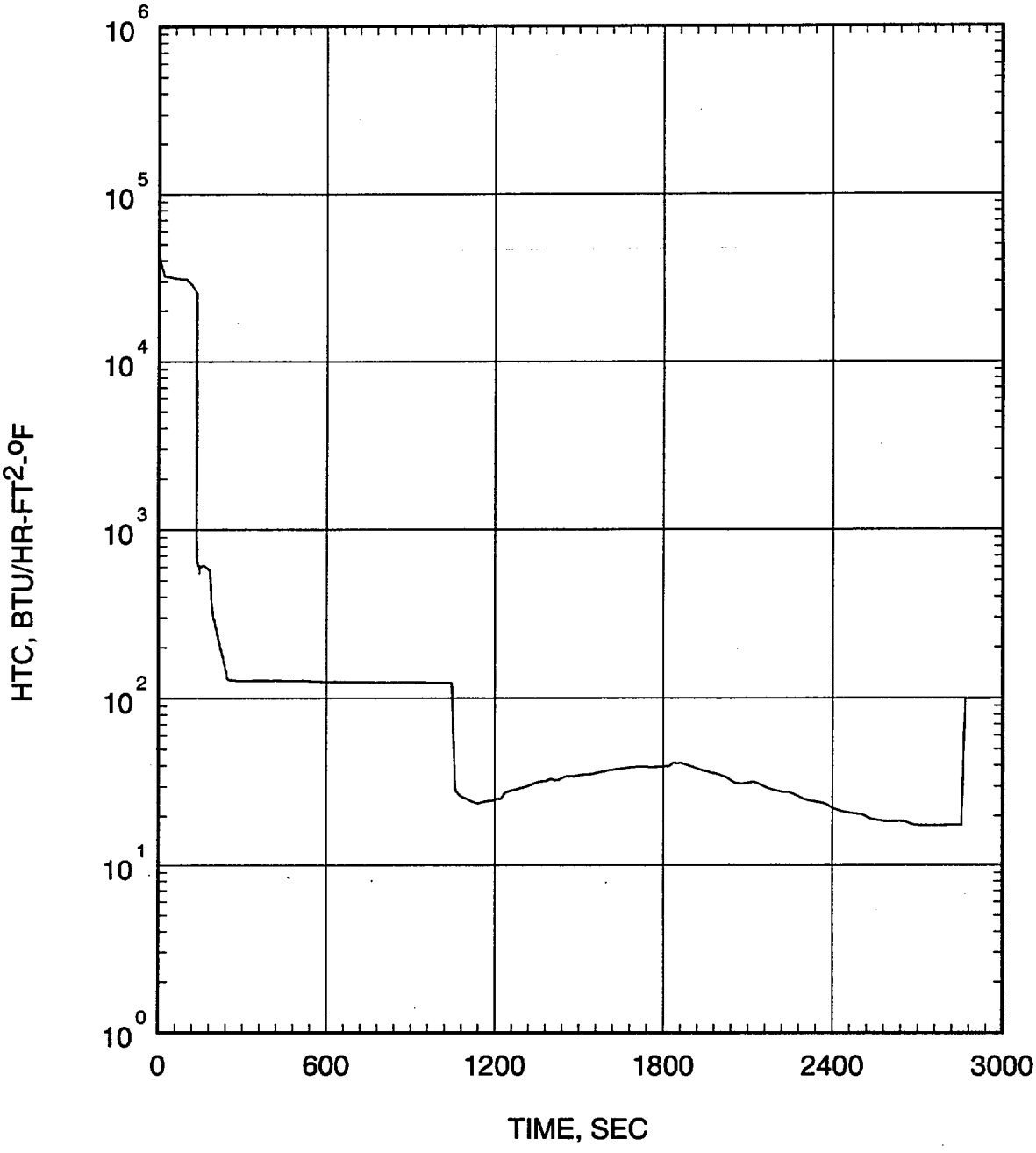

Figure 7.1.4-15
Small Break LOCA ECCS Performance Analysis
0.04 ft^2/PD Break
Coolant Temperature at Hot Spot

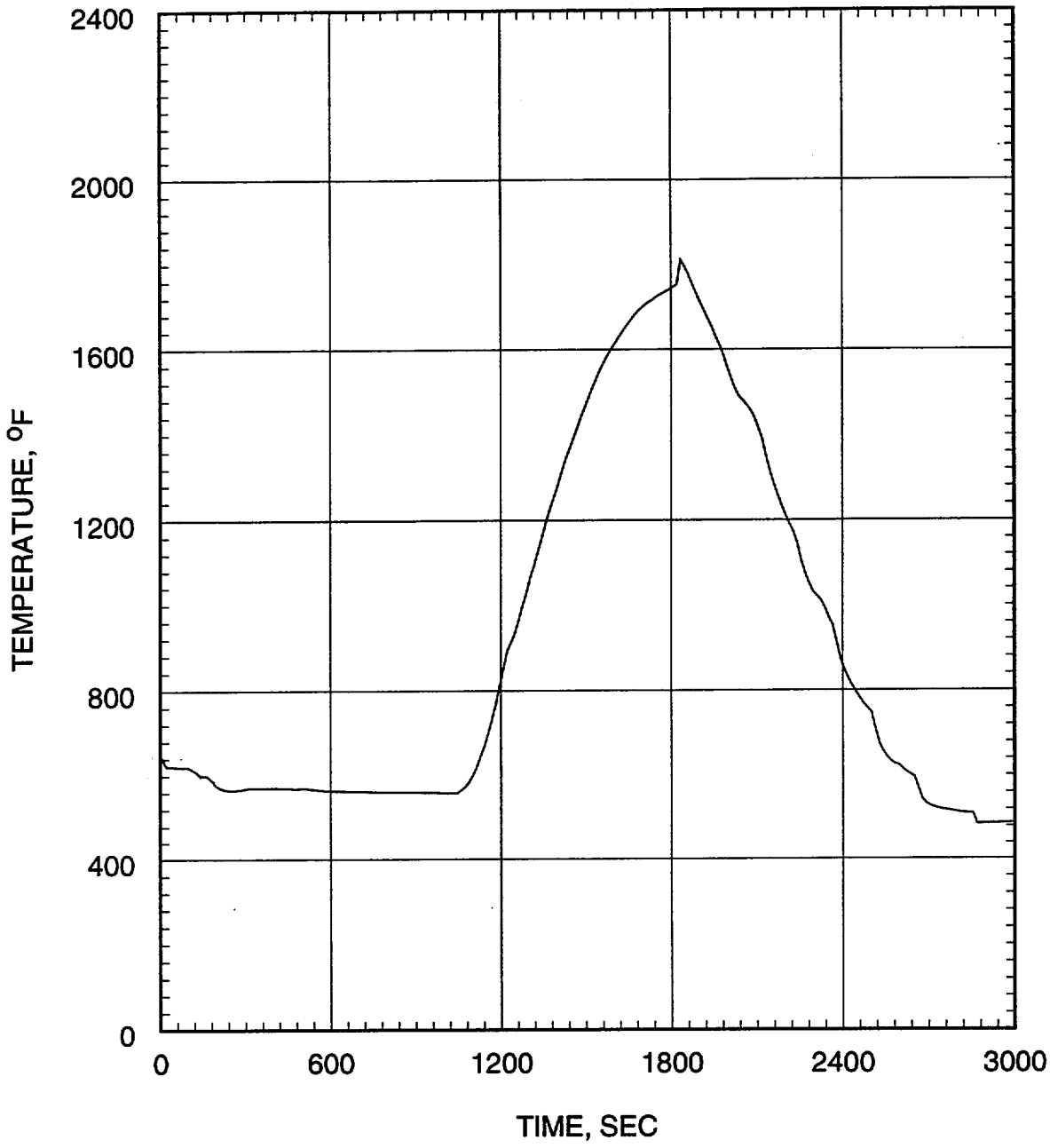

Figure 7.1.4-16
Small Break LOCA ECCS Performance Analysis
0.04 ft^2/PD Break
Cladding Temperature at Hot Spot

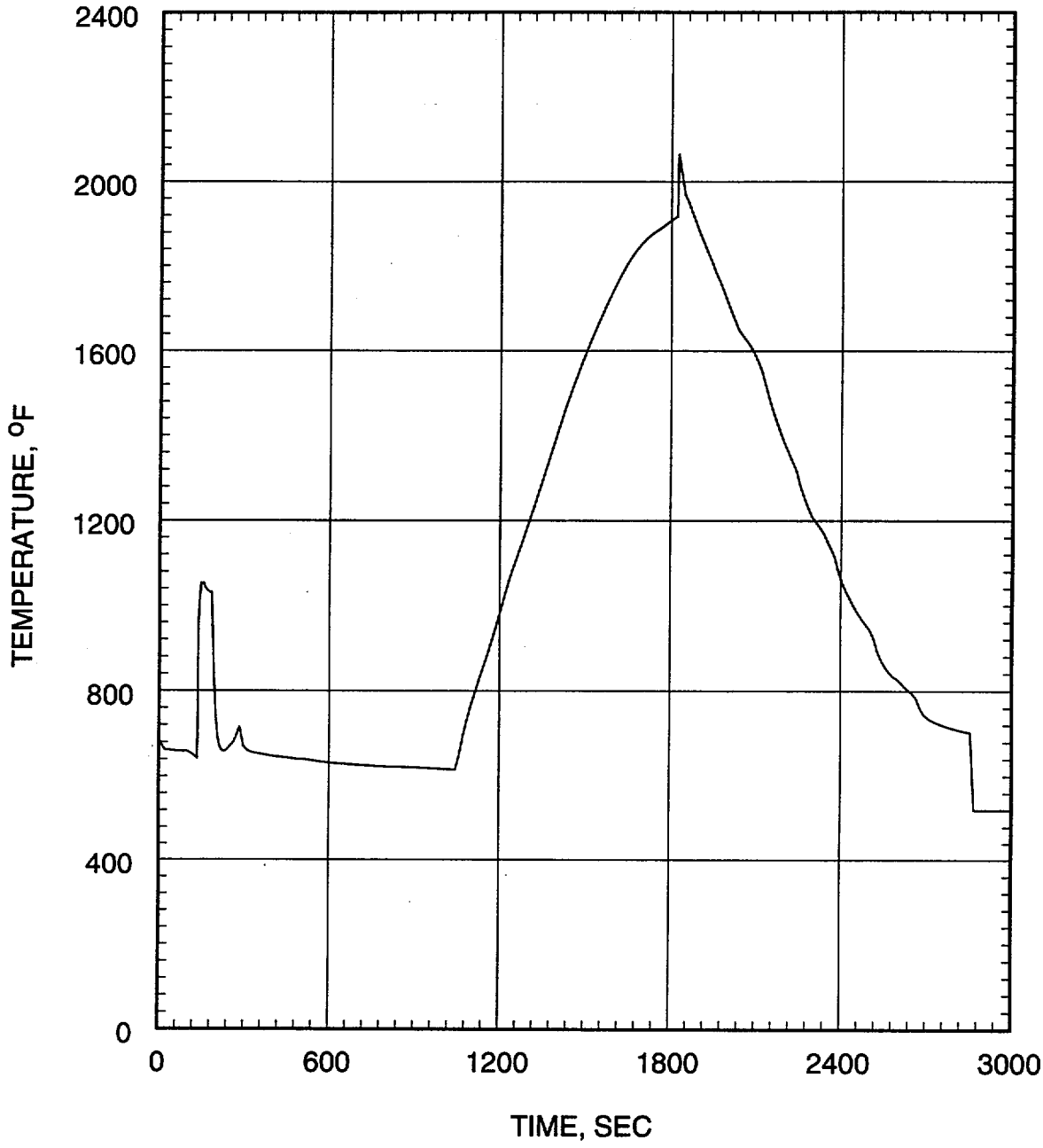

Figure 7.1.4-17
Small Break LOCA ECCS Performance Analysis
0.05 ft^2/PD Break
Core Power

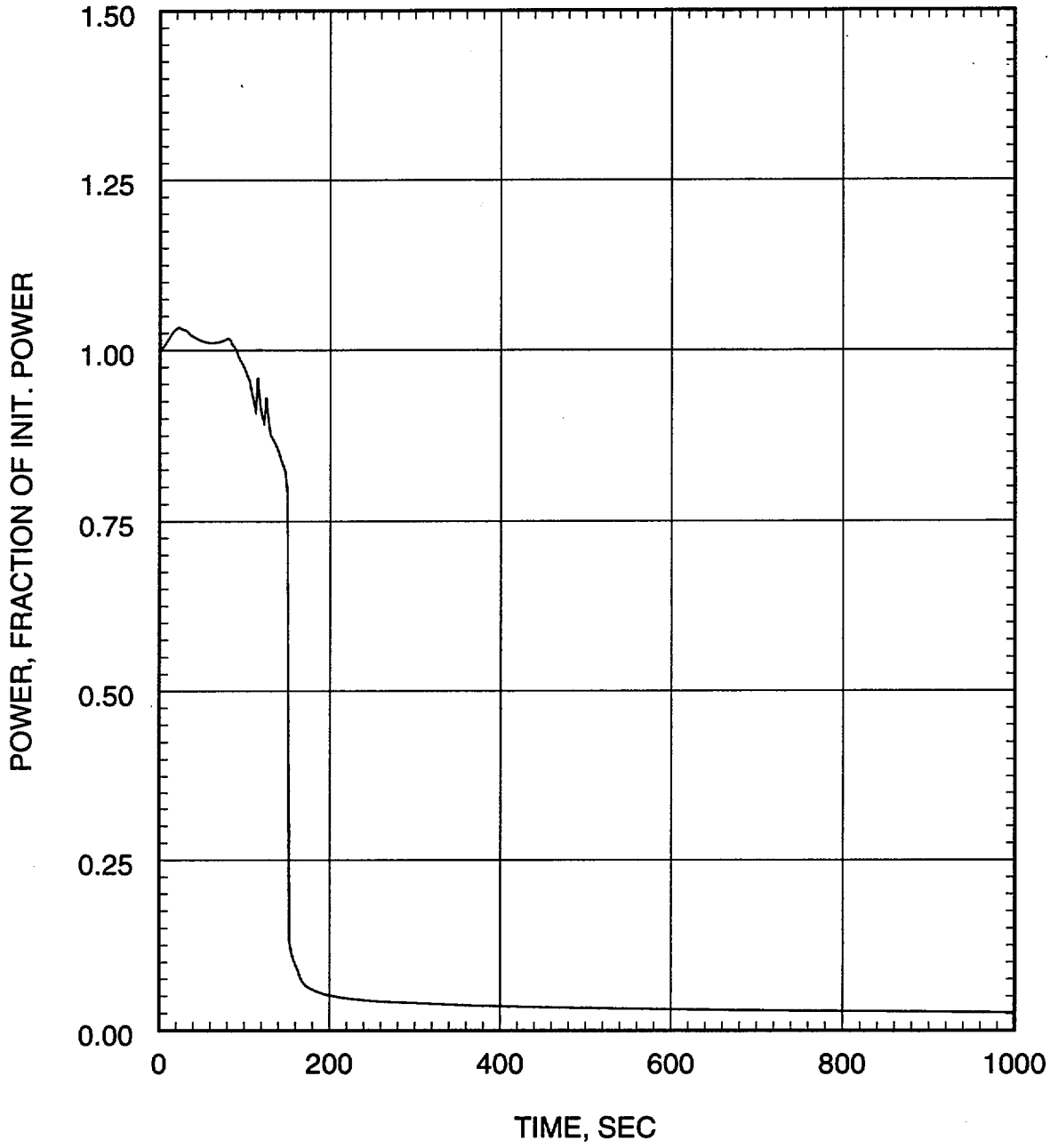

Figure 7.1.4-18
Small Break LOCA ECCS Performance Analysis
0.05 ft^2/PD Break
Inner Vessel Pressure

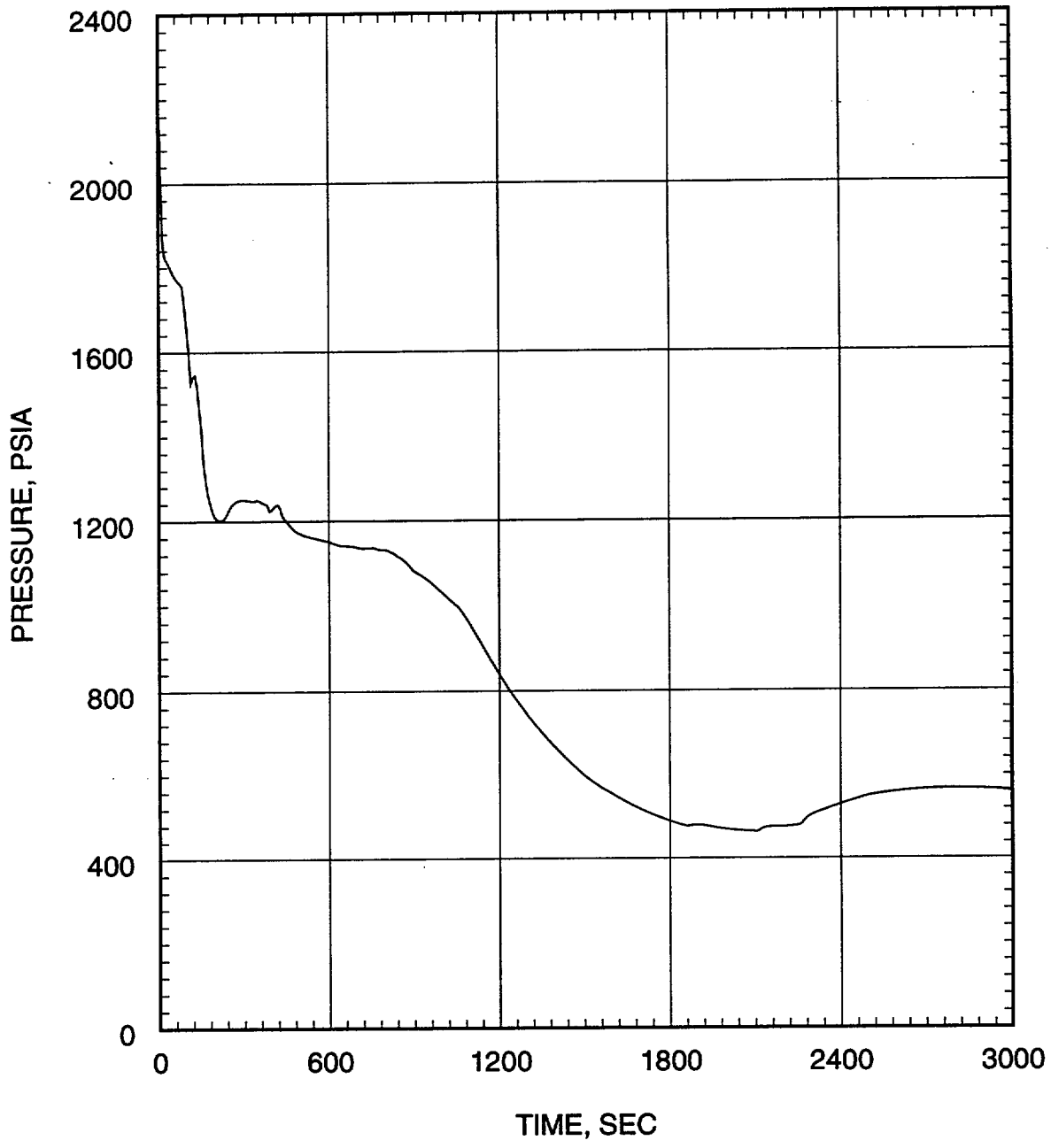

Figure 7.1.4-19
Small Break LOCA ECCS Performance Analysis
0.05 ft^2/PD Break
Break Flow Rate

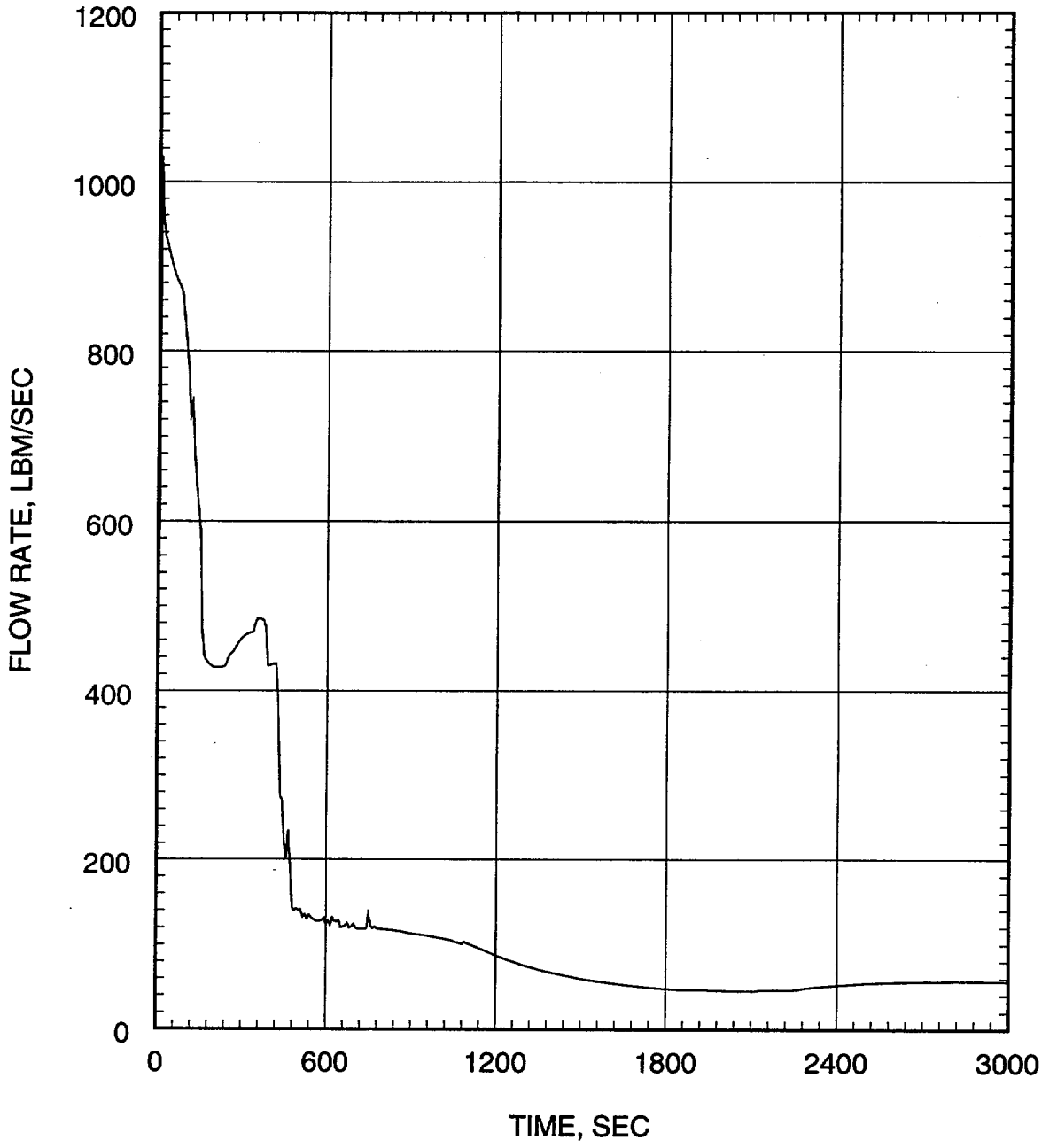

Figure 7.1.4-20
Small Break LOCA ECCS Performance Analysis
0.05 ft^2/PD Break
Inner Vessel Inlet Flow Rate

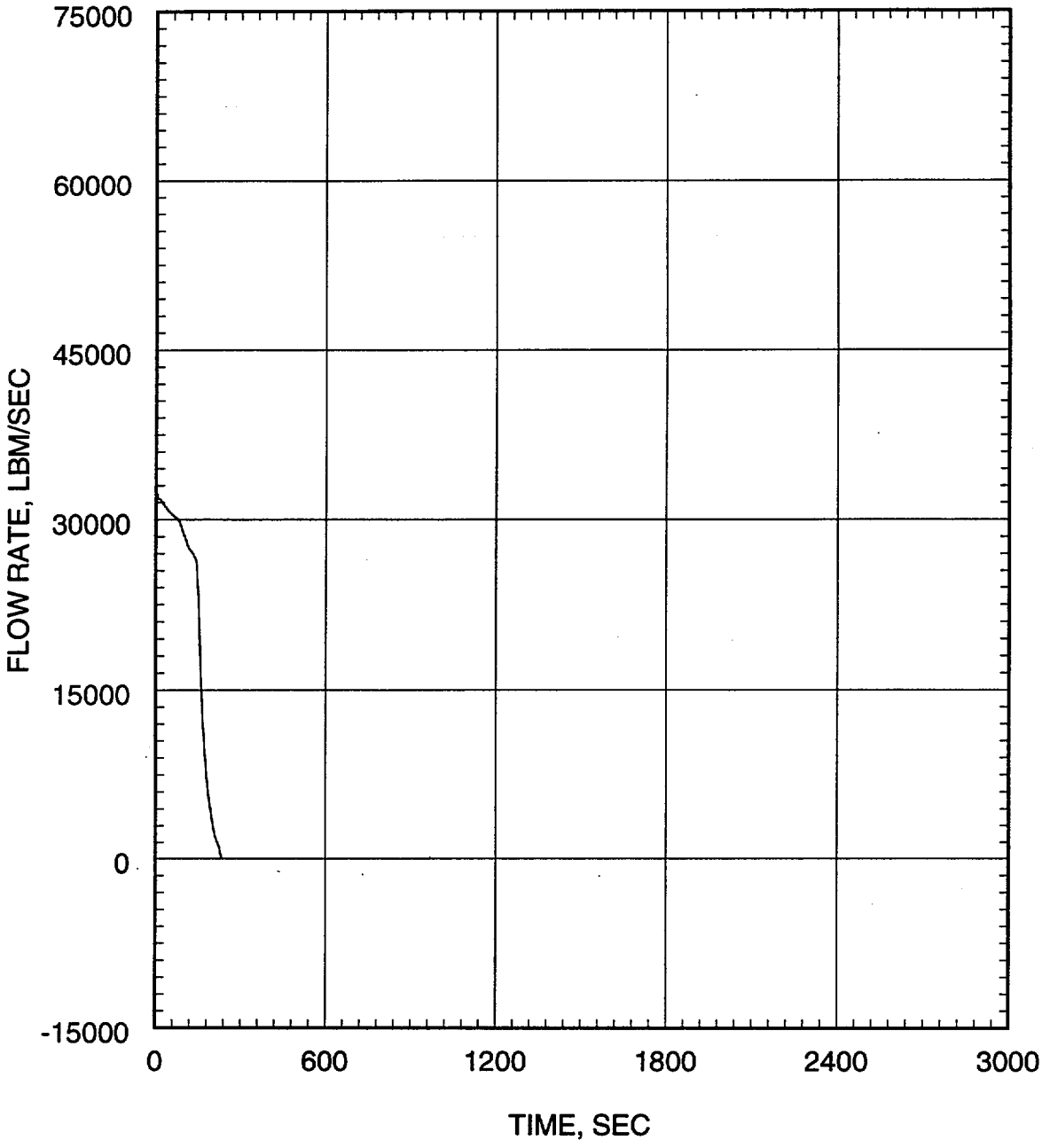

Figure 7.1.4-21
Small Break LOCA ECCS Performance Analysis
0.05 ft^2/PD Break
Inner Vessel Two-Phase Mixture Level

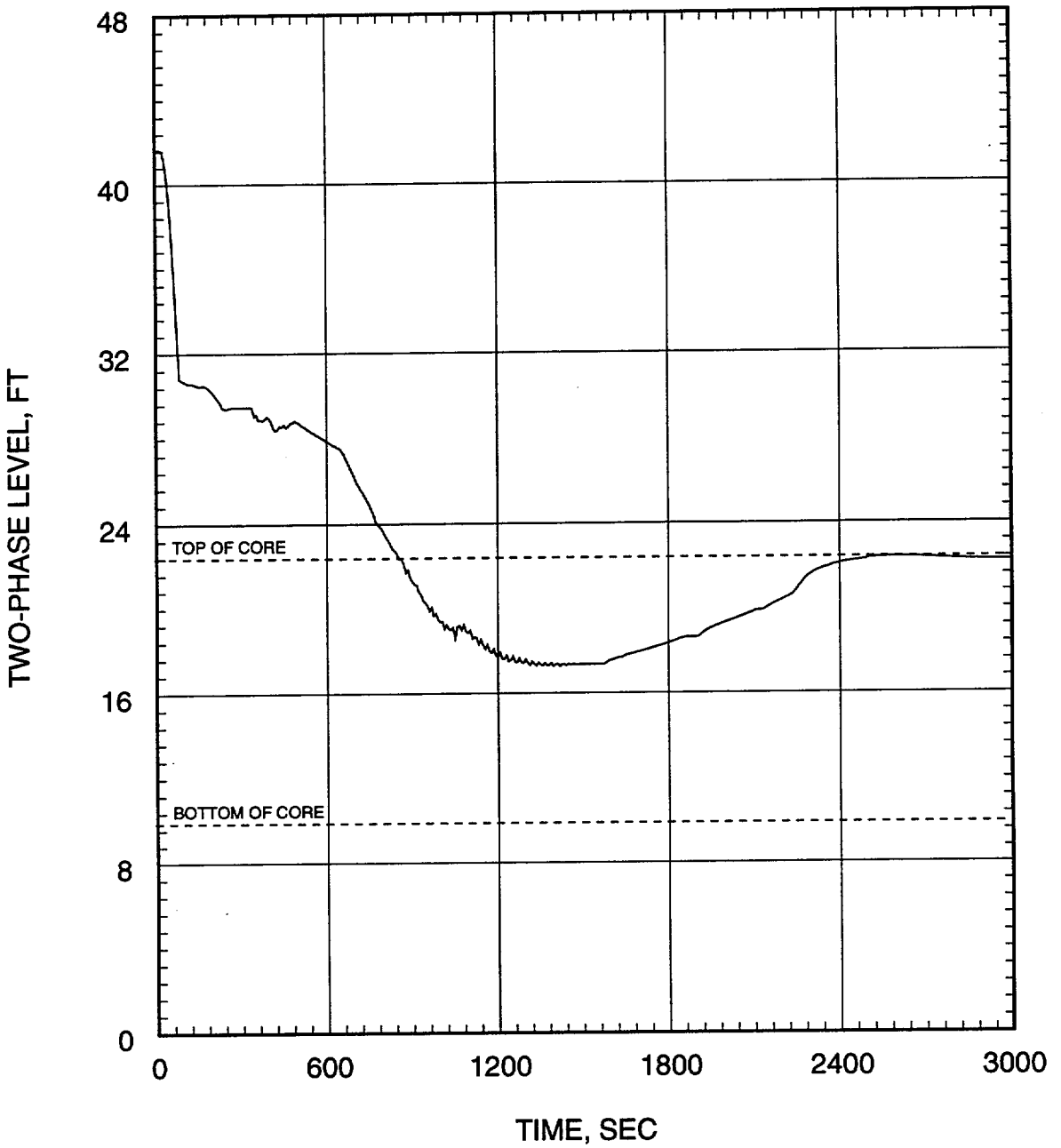

Figure 7.1.4-22
Small Break LOCA ECCS Performance Analysis
0.05 ft^2/PD Break
Heat Transfer Coefficient at Hot Spot

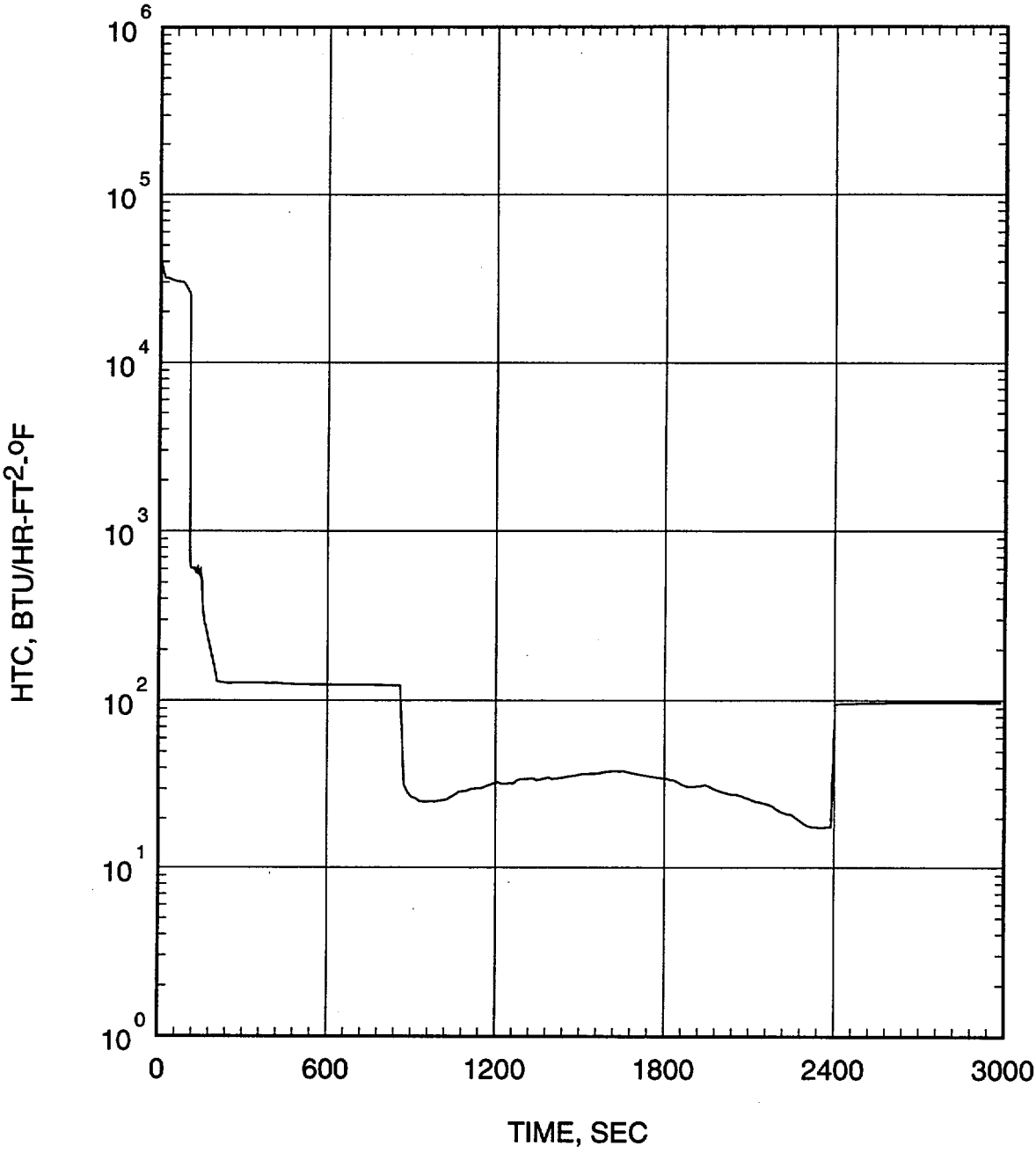

Figure 7.1.4-23
Small Break LOCA ECCS Performance Analysis
0.05 ft^2/PD Break
Coolant Temperature at Hot Spot

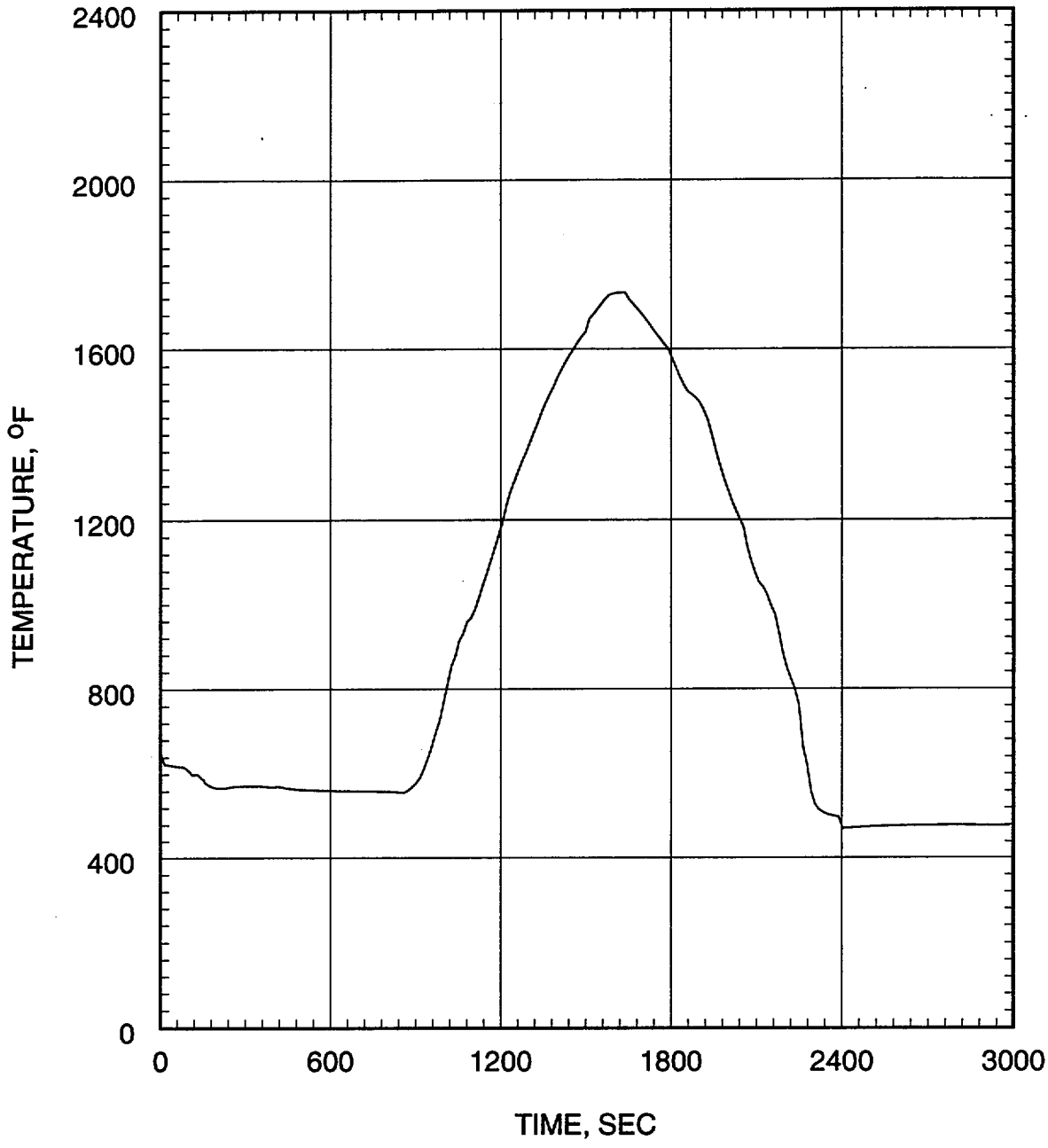

Figure 7.1.4-24
Small Break LOCA ECCS Performance Analysis
0.05 ft^2/PD Break
Cladding Temperature at Hot Spot

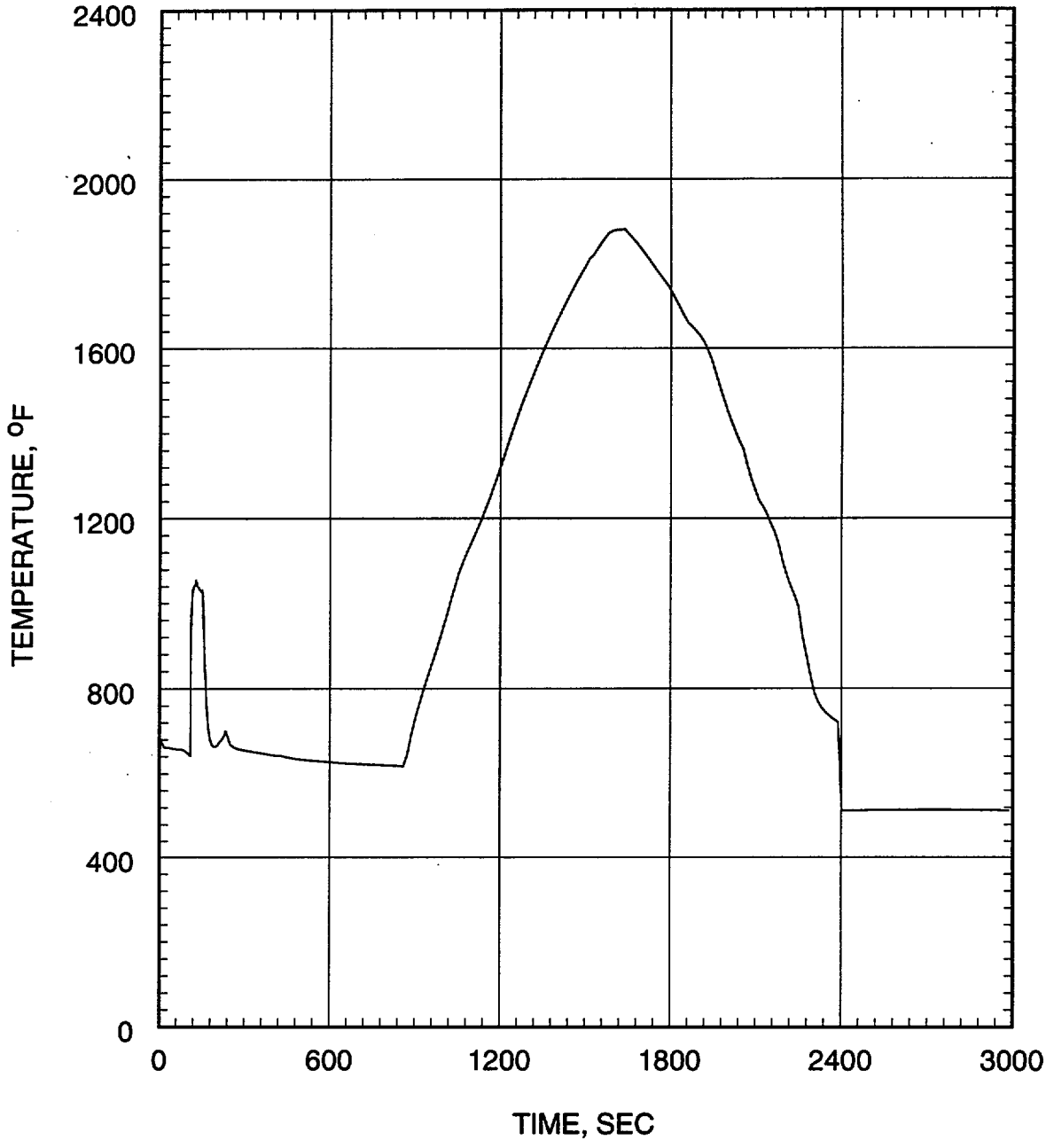

Figure 7.1.5-1
Long Term Cooling Analysis
Comparison of Core Boiloff Rate and the Minimum
Simultaneous Hot and Cold Side Injection Flow Rate

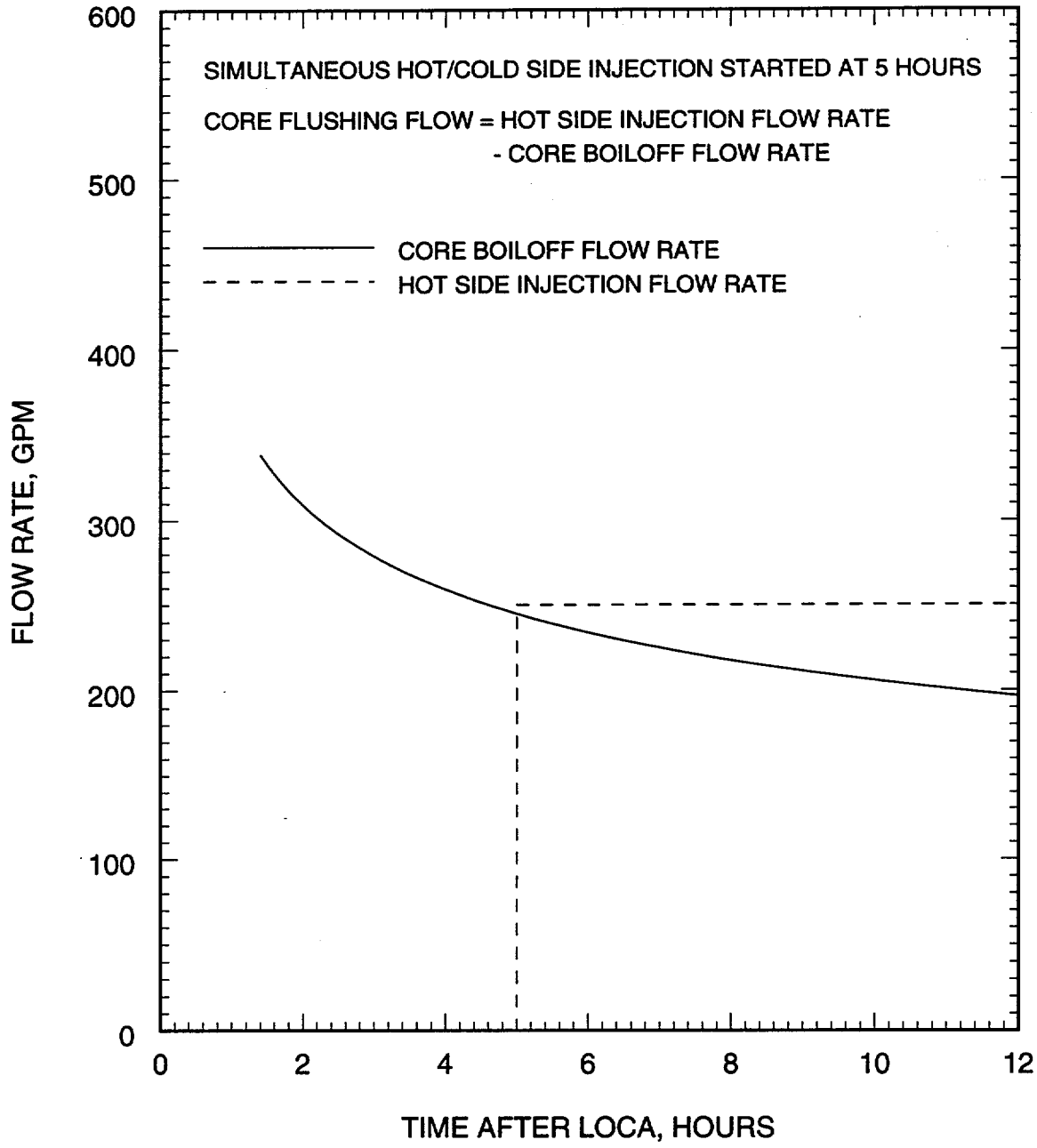

Figure 7.1.5-2
Long Term Cooling Analysis
Boric Acid Concentration in the Core Versus Time

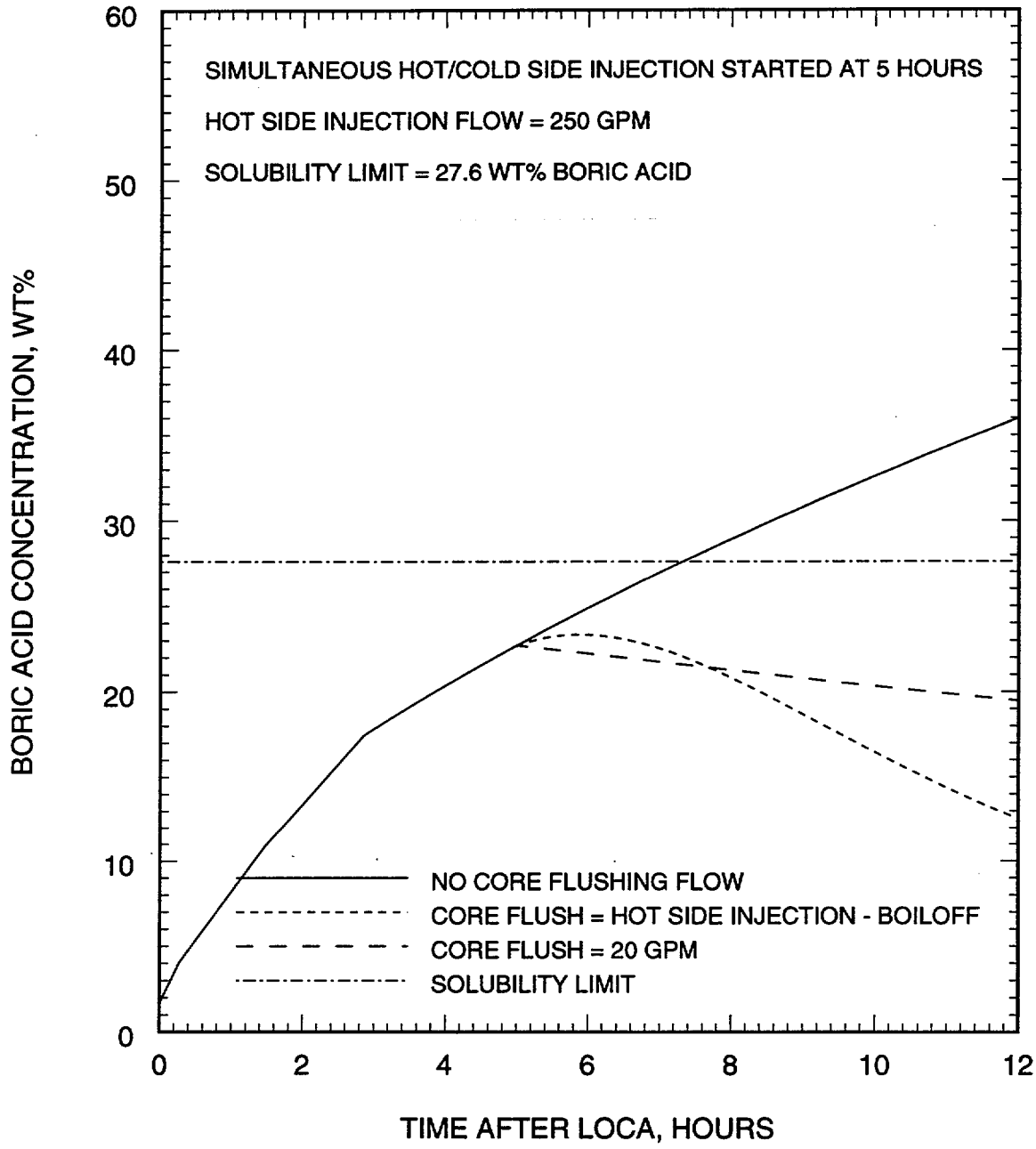

7.2 CONTAINMENT RESPONSE ANALYSIS

SAR Section 6.2 discusses the containment response to design basis accidents. Both the loss of coolant accident (LOCA) and the main steam line break (MSLB) result in the addition of mass and energy to the containment building. These accidents have been analyzed at power uprate conditions to ensure continued acceptability of the response of the containment structure. This analysis was performed in conjunction with the analysis to support the installation of the replacement steam generators (RSGs) and resulted in the submittal of the Containment Uprate License Amendment (2CAN119903) dated November 3, 1999, as supplemented by letters dated April 4 (2CAN040004), June 9 (2CAN060007), June 29 (2CAN060014), August 2 (2CAN080005), and August 16, 2000 (2CAN080010) as approved by the NRC in a safety evaluation dated November 13, 2000 (2CNA110002). The containment uprate increased the design pressure of the containment building from 54 psig to 59 psig The design temperature for the containment building remains unchanged at 300° F. No additional analyses of containment peak pressure and temperature are required for power uprate.

Associated with the containment uprate was a second submittal, the Containment Cooling License Amendment (2CAN060003) dated June 29, 2000, as supplemented by letter dated October 4, 2000 (2CAN100004) as approved by the NRC in the safety evaluation dated November 13, 2000 (2CNA110003). Because the pitch of the fan blades was reduced to accommodate the motor horsepower rating, the requirement for an operable cooling group was changed from one operational cooling unit to two operational cooling units. With this change, the containment cooling system is adequate for power uprate conditions. No changes were necessary for the containment spray system.

The effect of the higher radiological doses in containment after a LOCA under power uprate conditions is evaluated in Section 7.3.10 of this report, which discusses the dose rates for the maximum hypothetical accident, and in Section 9.4, which discusses the impact of doses on the environmental qualification of electrical equipment inside containment.

The effect of the power uprate on post-LOCA hydrogen generation is discussed in Section 9.1 of this report.

7.3 ACCIDENT ANALYSES

7.3.0 Introduction

This section reviews the accident analyses presented in Chapter 15 of the ANO-2 Safety Analysis Report. Table 7.3.0-1 is a listing of the events in Chapter 15 cross-referenced to the appropriate section in the power uprate report. In the right-hand column a note states how the power uprate was addressed for each design basis event (DBE). Events which were reanalyzed for power uprate are indicated as "reanalyzed." "Reanalyzed with RSG" indicates events that were previously reanalyzed as part of the steam generator replacement (see Reference 7.3-5 and SER Amendment 222, Reference 7.3-6). "Not affected" means that these events are not impacted by the power uprate. "Not applicable" denotes events identified in the ANO-2 SAR as not applicable to ANO-2.

The following sections provide a summary of the analysis or evaluation performed for each event affected by the increase in rated power.

7.3.0.1 Input Parameters and Analysis Assumptions

The power uprate necessitates the following changes in analyses or evaluations:

1. The initial power levels are based on a rated power 3026 MWt versus 2815 MWt.
2. The power measurement uncertainty is decreased from 3% to 2%.
3. The target limiting heat rate limit (including all uncertainties) of the hot rod at hot full power has been increased from 13.5 kW/ft to 13.7 kW/ft.
4. The most negative moderator temperature coefficient (MTC) has been increased from $-3.4*10^{-4}\ \Delta\rho/°F$ to $-3.8 * 10^{-4}\ \Delta\rho/°F$.
5. The feedwater line break event has incorporated a change of methodology. This event assumes a reactor trip on low steam generator water level in the ruptured steam generator.
6. The MTC values versus maximum high linear power level and trip setpoints have changed due to the increase in power level for the loss of load event with one main steam safety valve inoperable and one MSSV inoperable on each steam header.

In addition to power uprate related changes, other plant parameter changes have been incorporated into the following analyses and evaluations. The following changes have been incorporated in the analyses:

1. The time to re-align a rod during the CEA misalignment event for inward deviations has been increased to 2-hours.
2. The main steam line break hot full power scram worth trade-off has been extended to include hot zero power also.
3. A maximum charging flow of 46 gpm per pump was assumed versus 44 gpm.

4. The CPC low reactor coolant pump shaft speed trip response time was increased to 0.4 seconds versus 0.3 seconds.
5. Replacement steam generators and the effects such as increased secondary mass, increased primary mass, small tube diameter, and increased RCS flow rates were accounted for in the following analyses.
6. The analytical High Pressurizer Pressure Trip response time was increased from 0.65 seconds to 0.9 seconds for the FWLB.
7. The MSSV analytical setpoints in the FWLB analysis have accounted for an extra 0.5% margin.
8. The dose methodology defined in Reference 7.3-5 for Amendment 222 was applied to the CEA ejection and steam generator tube rupture analyses.

Table 7.3.0.1-1 presents the key parameters assumed in the transient analyses. Specific initial conditions for each event are listed in that event's section. Events were evaluated to determine the effect of power uprate and bounding parameters. For those events for which a detailed analysis was performed (see Table 7.3.0-1), the initial core power was assumed based on a rated core power of 3026 MWt. Examples of input parameter changes from the current analyses of record include RPS response time changes, more negative moderator temperature coefficients, and higher reactor coolant system flow ranges.

Table 7.3.0.1-2 presents the reactor protection system (RPS) and the engineered safety features actuation system (ESFAS) instrumentation trip setpoints and delay times. The analysis setpoints in the table include instrument response times and total response time for the actuation of the ESFAS functions such as main steam isolation valves, feedwater isolation valves, and emergency feedwater system.

7.3.0.2 Bounding Physics Data

Many of the analyses discussed below were performed using core physics data that is anticipated to bound future core designs. Moderator temperature coefficient, fuel temperature coefficient (Doppler curve), delayed neutron fractions, effective neutron lifetime, and control element assembly (CEA) reactivity insertion curves are core physics parameters that are typically considered on a cycle-specific basis and are inputs to many of the analyses discussed below. A set of core physics data will be presented here, so that the respective analyses can refer to this data as it is applied. The core physics data is unchanged from Cycle 15 with the exception of the most negative MTC value. Detailed core physics data that affects a particular analysis will be discussed below with the respective analysis.

A moderator temperature coefficient within the ranges defined in Figure 7.3.0.2-1 was assumed in the non-LOCA safety analyses. This figure is consistent with the current COLR Figure 1 except for an expanded MTC range from -3.4×10^{-4} $\Delta\rho/°F$ to -3.8×10^{-4} $\Delta\rho/°F$.

Figure 7.3.0.2-2 represents the bounding fuel temperature reactivity curves for Beginning of Cycle (BOC) and End of Cycle (EOC). These curves, which include uncertainty, have been used as noted in the specific analyses.

The CEA reactivity insertion curve assumed for the analyses (Figure 7.3.0.2-3) remains the same as for previous cycles. The scram curve is based on an axial shape index (ASI) of + 0.3. A CEA insertion curve consistent with Figure 7.3.0.2-4 was assumed utilizing a 0.6-second holding coil delay time and a 3.2-second arithmetic average drop time to 90% inserted. A shutdown worth of 5% $\Delta\rho$ was incorporated into Figure 7.3.0.2-3.

The following effective neutron lifetime and delayed neutron fraction were established for the following analyses. These parameters were used as indicated in the respective analyses.

	Neutron Lifetime, 10^{-6} seconds	Delayed Neutron Fraction
Beginning of Cycle	13	0.007252
End of Cycle	36	0.004341

7.3.0.3 COLSS and CPCS

One of the impacts that power uprate has on plant operation is a change in operating margin to the DNBR and LHR limits. ANO-2 uses the core operating limits supervisory system (COLSS) and the core protection calculator system (CPCS) to monitor the DNBR and LHR margins. The fuel reload core design will be modified if additional margin is needed to account for the changes due to the power uprate. The fuel peaking factors can be controlled in the fuel reload core design to ensure that adequate operating margin is maintained in the future.

7.3.0.4 Computer Codes

The transient analysis methodologies used for the replacement steam generator and power uprate analysis are similar to the methodologies documented in the SAR, except when noted. For explicit transient analyses, the CENTS code from Reference 7.3-2 was employed.

The minimum DNBR and the DNB thermal margin analyses were determined using the CETOP code described in Reference 7.3-3. This was approved in Reference 7.3-10. The minimum DNBR values for loss of reactor coolant flow resulting from a pump shaft seizure were determined with the TORC code described in Reference 7.3-7.

The HERMITE code, described in Reference 7.3-4, was used for the 4-pump loss of flow analysis in Section 7.3.5.

The STRIKIN II code, described in Reference 7.3-9, was used for the CEA ejection analysis in Section 7.3.14.

7.3.0.5 Radiological Dose Input Parameters

The steam generator tube rupture and CEA ejection events radiological analyses performed to support the power uprate utilized the same inputs, methods, and assumptions as presented in Reference 7.3-5 for replacement steam generator and power uprate work for Amendment 222. An increase in rated power produces an increase in core average temperature, and an increase in post-trip decay heat. This results in larger steam releases during plant cooldown after reactor trip. All event radiological doses previously presented in Reference 7.3-5 and approved in Amendment 222 were performed at a rated power of 3026 MWt and remain valid. This also includes the feedwater line break event that was presented in Reference 7.3-5.

For the steam generator tube rupture (SGTR) event, a generated induced iodine, a preexisting iodine and no iodine spiking cases were performed. These calculations and the noted method used in Reference 7.3-5 are conservative methods with respect to the ANO-2 licensing basis. The licensing basis analyses used the radiological information presented in Section 15.1.0 of the SAR. A dose calculation was presented based only on the initial primary and secondary concentrations without assuming a preaccident iodine spike or an induced iodine spike. Given this, the SGTR no iodine spiking case presented in Section 7.3.1.3 is most consistent with the methods used for the dose calculations presented in the SAR except for the following significant differences:

1. A decontamination factor of 100 was assumed in this assessment. This is more conservative than the value of 400 presented in Section 15.1.0.5.1 which was assumed for the iodine concentration released in the steam from the steam generator liquid.
2. The secondary side initial steady state radiological concentration was assumed to be 0.1 μCi/gm dose equivalent I-131, and the primary side initial specific activity was assumed to be 1 μCi/gm dose equivalent I-131 and 100 / E μCi/gm. This deviates from the SAR Section 15.1.0.5.1 assumptions based on 1% failed fuel concentrations.
3. An unaffected steam generator primary to secondary leak of 1 gpm was assumed rather than SAR assumption of 100 gpd.

The noted exceptions above delineate conservative assumptions used in the no iodine spiking case presented in Section 7.3.1.3 with respect to the licensing basis analysis requirements.

7.3.1 Uncontrolled CEA Withdrawal from Subcritical Conditions

The objective of the subcritical CEA bank withdrawal event analysis is to document the impact of the following changes:

1. the increase in rated power from 2815 MWt to 3026 MWt and the change in the initial power assumption,
2. an increase in RCS flow, and

3. the RSGs.

The impact of the above changes results in no violation of the Specified Acceptable Fuel Design Limits (SAFDLs).

7.3.1.1 General Description of the Event

The withdrawal of CEAs from subcritical conditions (less than 10^{-4} percent power) adds reactivity to the reactor core, causing both the core power level and the core heat flux to increase. Since the transient is initiated at low power levels, the normal reactor feedback mechanisms (moderator feedback and Doppler feedback) do not occur until power generation in the core is large enough to cause changes in the fuel and moderator temperatures. The reactor protection system (RPS) is designed to prevent such a transient from resulting in a minimum DNBR less than 1.25 by initiating a high logarithmic power level reactor trip. The high linear power level trip and the Core Protection Calculator System (CPCS) variable overpower trip (VOPT), high local power density and low DNBR trips provide backup protection while the high pressurizer pressure trip provides protection for the reactor coolant pressure boundary.

A continuous withdrawal of CEAs could result from a malfunction in the control element drive mechanism control system (CEDMCS) or by operator error.

Startup of the reactor involves a planned sequence of events during which certain CEA groups are withdrawn, at a controlled rate and in a prescribed order, to increase the core reactivity gradually from subcritical to critical. To ensure that rapid shutdown by CEAs is always possible when the reactor is critical or near critical, technical specifications require that specified groups of CEAs be withdrawn before reaching criticality. These groups of assemblies combined with soluble boron concentration will have a total negative reactivity worth that is sufficient to provide at least the shutdown margin required by the technical specifications at the hot standby condition, with the most reactive CEA assumed to remain in the fully withdrawn position.

7.3.1.2 Purpose of Analysis and Acceptance Criteria

The purpose of the analysis is to determine that the SAFDLs are not violated and the peak RCS pressure remains below the upset pressure criterion.

The following criteria apply to the CEA bank withdrawal from subcritical event:

- DNBR $\geq$ DNB SAFDL
- Fuel centerline temperatures < fuel centerline melt limit
- Peak RCS pressure $\leq$ 2750 psia

The CEA bank withdrawal from subcritical event is described in Chapter 15.1.1 of the SAR (Reference 7.3-1).

7.3.1.3 Impact of Changes

The power uprate could result in a small degradation of the calculated thermal margin. The initial power, source power strength, and the high logarithmic power level trip setpoint are based on the rated power. The increase in minimum RCS flow has a small beneficial impact on the calculation of minimum DNBR. The RSGs do not have any impact on this event, as it is a core physics related event.

7.3.1.4 Analysis Overview

The methodology used in this analysis is the same as that used in the current analysis. This analysis has utilized the CENTS computer code for the transient analysis simulation. The minimum DNBR evaluation was determined using the CETOP code.

Two reactivity addition rates were considered for Cycle 16, 0.00025 $\Delta\rho$/sec and 0.0002 $\Delta\rho$/sec. These reactivity addition rates are consistent with the maximum addition rates expected for bank withdrawals near critical conditions. Only bank withdrawals that will result in critical conditions are considered for this event. Procedural controls on rod withdrawal sequences limits the potential inadvertent bank withdrawal that could result in critical core condition and ensure greater than critical boron concentration is maintained whenever the CEDMCS are energized.

Input parameters from Table 7.3.1-1 and the core physics data from Section 7.3.0.2 have been incorporated in this analysis with the following clarifications:

1. The BOC Doppler curve in Figure 7.3.0.2-2 was assumed.

2. An EOC delayed neutron fraction and neutron lifetime consistent with those defined in Section 7.3.0.2 were assumed.

3. CEA scram worth was not credited on trip; rather a CEA coil decay time of 0.6 seconds was assumed followed by negative reactivity proportionate to the CEA position post trip. Reactivity is held constant for the 0.6 second delay time. After the 0.6 second delay, negative reactivity is reinserted at the same rate of the positive reinsertion relative to the rod position, up to the total positive reactivity added. The CEA position versus time post-trip is consistent with Figure 7.3.0.2-4.

4. A high logarithmic power level trip setpoint of 4% and a response time of 0.4 seconds were assumed in the analysis.

5. An initial power of $9.63 * 10^{-7}$ MWt was assumed.

6. Installation of the RSGs was assumed.

7. Parametric analyses were performed on the number of plugged U-tubes per steam generator. It was determined that 10% plugged U-tubes per steam generator was slightly more limiting.

7.3.1.5 Analysis Results

A subcritical CEA bank withdrawal can result in a rapid core power increase. As core power increases both RCS temperatures and pressures also increase. The action of the high logarithmic power level trip terminates the transient.

The NSSS and RPS responses to a subcritical CEA bank withdrawal event are shown in Tables 7.3.1-2 and 7.3.1-3, and in Figures 7.3.1-1 through 7.3.1-4.

For the limiting subcritical CEA bank withdrawal event, the peak fuel temperature is well below centerline melt. The peak heat flux results in a minimum DNBR greater than 1.25. This is not a limiting peak RCS pressure event. Thus, there is no violation of the SAFDLs.

7.3.2 Uncontrolled CEA Withdrawal from Critical Conditions

The objective of the uncontrolled CEA bank withdrawal from critical condition event analysis is to document the impact of the following changes:

1. the increase in rated power,
2. a conservative decrease in the assumed initial power for HZP,
2. an increase in RCS flow,
3. the RSGs,
4. an increase in the CPCS excore response time,
5. a decrease in the CPCS VOPT setpoint, and
6. an increase in the HZP heat flux factor.

The impact of the above changes results in no violation of the SAFDLs.

7.3.2.1 General Description of the Event

The sequential withdrawal of CEAs from a critical condition (greater than 10^{-4} percent power) adds reactivity to the reactor core, causing the core power level to increase. A continuous withdrawal of CEAs could result from a malfunction in the CEDMCS, or by operator error. No failure that can cause a CEA withdrawal or insertion can prevent the insertion of CEA banks upon receipt of any reactor protection system trip signal.

Analyses have shown that the most adverse results for the CEA withdrawal events occur with the maximum reactivity addition rates. The analysis of the CEA withdrawal from critical conditions therefore utilizes the maximum reactivity addition rate with the CEA withdrawal speed of 30 in/minute.

The sequential CEA withdrawal events from critical conditions are considered from hot zero power (HZP) and hot full power (HFP) conditions.

A CPCS low DNBR trip, CPCS high local power density (LPD) trip or a CPCS VOPT terminates the sequential CEA withdrawal events. The CPCS has dynamic compensation lead-lag filters that project increases in core heat flux and core power. These dynamic compensation filters in conjunction with static power correction factors ensure that the CEA withdrawal transients are terminated before the SAFDLs are violated.

7.3.2.2 Purpose of Analysis and Acceptance Criteria

The purpose of the analysis was to determine that the SAFDLs are not violated, the peak RCS pressure is less than 2750 psia, and a secondary heat sink is maintained.

The following criteria apply to the CEA bank withdrawal from critical event:

- DNBR ≥ DNB SAFDL
- Peak LHR ≤ 21 kW/ft, or
  fuel centerline temperatures < fuel centerline melt limit
- Peak RCS pressure ≤ 2750 psia
- No loss of secondary heat sink

For sequential CEA bank withdrawals initiated at power for critical conditions, SAFDL protection (DNBR and LHR) is provided by the CPCS. Transient analysis provides verification that the lead-lag dynamic compensation filters respond conservatively. See Section 7.3.18 of this report for this analysis. This safety analysis verification along with other conservative CPCS inputs ensures the overall conservatism of the CPCS.

The CEA bank withdrawal from critical condition events are described in Chapter 15.1.2 of the SAR (Reference 7.3-1).

7.3.2.3 Impact of Changes

The RSGs do not result in any changes to key input data for the HFP and HZP sequential CEA bank withdrawal events from critical conditions. The core physics, reactivity insertion rate of the CEA bank withdrawals, 3-D power peaks, kinetics parameters, Doppler coefficient and moderator temperature coefficient dominate these events.

a. Hot Full Power

The increase in rated power results in a small decrease in thermal margin at HFP. The impact on HFP is negligible since the CPCS increasing power filters provide conservative neutron and thermal power input into the CPCS Low DNBR and High Local Power Density (LPD) trips.

A very small increase in the neutron flux power from the excore detectors results from the slightly longer delay CPCS delay. This has a very small impact on the analysis.

The increase in flow has a small effect and is discussed in Reference 7.3-5 Section 1.1.2.

b. Hot Zero Power

The decrease in initial power in conjunction with the increase in CPCS response time results in a larger power increase prior to mitigation of the event. These changes in conjunction with the increase in nuclear heat flux factor result in a small decrease in thermal margin. The increase in RCS flow results in a small increase in thermal margin, which offsets some of the previously discussed margin degradation.

7.3.2.4 Analysis Overview

The methodology used in this analysis is the same as that used in the analysis of record. This analysis has utilized the CENTS computer code for the transient analysis simulation. The minimum DNBR was determined using the CETOP code.

a. Hot Full Power

Input parameters from Table 7.3.2-1 and the bounding physics data from Section 7.3.0.2 have been incorporated in this analysis with the following clarifications:

1. The BOC Doppler curve in Figure 7.3.0.2-2 was assumed.

2. A delayed neutron fraction and neutron lifetime consistent with those defined in Section 7.3.0.2 were assumed.

3. The CEA insertion curve in Figure 7.3.0.2-4 was assumed. A 0.6 second CEA holding coil delay after the trip breakers open is assumed prior to the CEA Bank beginning to drop into the core. After the 0.6 second delay, negative reactivity is reinserted at the same rate of positive insertion caused by the CEA Bank withdrawal. A CEA worth of -5.0% $\Delta\rho$ was assumed for HFP.

4. An initial core power of 3087 MWt was assumed based on a rated power of 3026 MWt and a 2% measurement uncertainty.

5. A MTC of $0.0 * 10^{-4}$ $\Delta\rho$/°F was assumed. This is conservative to the BOC MTC of $-0.2 * 10^{-4}$ $\Delta\rho$/°F in Figure 7.3.0.2-1.

6. The response time for the neutron flux power from the ex-core neutron detectors was increased to 0.40 seconds.

7. A Reactivity Insertion Rate (RIR) of 1×10^{-4} $\Delta\rho$/sec was assumed.

8. The Core Protection Calculator System (CPCS) Variable Overpower Trip (VOPT) ceiling was not credited. The CPCS VOPT follow trip of 10.2% was assumed resulting in a power trip at 112.4% of full power.

9. Installation of the RSGs was assumed with a tube plugging limit of 10%.

b. Hot Zero Power

Input parameters from Table 7.3.2-2 and the bounding physics data from Section 7.3.0.2 have been incorporated in this analysis with the following clarifications:

1. The BOC Doppler curve in Figure 7.3.0.2-2 was assumed.
2. A delayed neutron fraction and neutron lifetime consistent with those defined in Section 7.3.0.2 were assumed.
3. The CEA insertion curve (scram curve) is based on an ASI of +0.6. A CEA insertion curve consistent with Figure 7.3.0.2-4 was assumed utilizing a 0.6-second holding coil. A CEA worth of 2.0% $\Delta\rho$ was conservatively assumed.
4. A positive MTC of $0.5 * 10^{-4}$ $\Delta\rho$/°F was assumed.
5. A conservative VOPT setpoint of 36% of rated power and a response time of 0.6 seconds were assumed. The response time for the neutron flux power from the neutron excore detectors was increased to 0.40 seconds and is included in the 0.6 seconds.
6. An initial core power of 0.0003026 MWt (10^{-5} % initial power) was assumed. This is conservative to the high log power trip bypass permissive setpoint of 10^{-4} % initial power. The use of a lower initial power results in the largest power spike.
7. Installation of the RSGs was assumed with 10% plugged U-tubes per steam generator.
8. A minimum initial RCS flow rate 315,560 gpm was assumed.
9. An RIR of 1.8×10^{-4} $\Delta\rho$/sec was assumed
10. A nuclear heat flux factor of 7.7 was assumed.

7.3.2.5 Analysis Results

a. Hot Full Power

A CEA bank withdrawal at HFP can result in a core power increase. As core power increases, both RCS temperatures and pressures also increase. The action of the CPCS terminates the transient.

The NSSS and RPS responses for the HFP CEA bank withdrawal event are shown in Table 7.3.2-3 and in Figures 7.3.2-1 through 7.3.2-5.

For the limiting HFP CEA bank withdrawal event, the peak core power results in a peak linear heat rate of less than 21 kW/ft. The peak heat flux results in a minimum DNBR greater than

1.25. This is not a limiting peak RCS pressure event. Thus, there is no violation of the SAFDLs for HFP.

b. Hot Zero Power

A CEA bank withdrawal at HZP can result in a core power increase. As core power increases, both RCS temperatures and pressures also increase. The action of the CPCS terminates the transient.

The NSSS and RPS responses to the HZP CEA bank withdrawal event are shown in Table 7.3.2-4 and in Figures 7.3.2-6 through 7.3.2-9.

For the limiting HZP CEA bank withdrawal event, the peak core power results in fuel temperatures well below centerline melt. The peak heat flux results in a minimum DNBR greater than 1.25. This is not a limiting peak RCS pressure event. Thus, there is no violation of the SAFDLs for HZP.

7.3.3 CEA Misoperation

The objective of the control element assembly (CEA) misoperation event analysis is to document the impact of the following changes:

1. increase in rated power,
2. change in the COLR limit (Required Power Reduction after CEA Inward Deviation, Figure 2), and
3. initial conditions for core power, temperature, pressure and RCS flow.

The impact of the above changes results in no violation of the SAFDLs.

7.3.3.1 General Description of the Event

A CEA misoperation is defined as any event that could result from a single malfunction in the reactivity control system with the exception of sequential group withdrawals, which are considered in Sections 7.3.1 and 7.3.2. A list of the events that could be caused by a single malfunction in the reactivity control system is included in Reference 7.3-1, Chapter 7.

Protection for CEA misoperation events is provided either by a core protection calculator system (CPCS) trip or, for events which do not require a trip, by providing adequate initial DNBR and local power density margin to preclude violation of the SAFDLs before the reactor operator takes action to restore plant conditions and CEA alignment.

The core protection calculator (CPC) and core element assembly calculator (CEAC) algorithms detect and compensate for the effect of CEA misoperation on the core power distribution by

providing heat flux and radial peaking factor penalties to the on-line DNBR and linear heat rate calculations..

The single CEA drop event will not generate and does not require a reactor trip. Adequate initial DNBR and local power density margin provides protection against this CEA misoperation event.

A single CEA drop is defined as the inadvertent release of a CEA causing it to drop into the core. After the drop of a single CEA, a rapid decrease in power follows. This is accompanied by a decrease in reactor coolant temperatures and pressure. In the presence of a negative moderator temperature coefficient (MTC), positive reactivity is added. Since there is a power mismatch between the secondary side and the primary side, the primary side responds and attempts to restore itself to the initial power level.

7.3.3.2 Purpose of Analysis and Acceptance Criteria

The purpose of the analysis is to review the CEA misoperation DNB thermal margin requirements that must be reserved in the technical specification LCOs. This assures that the minimum DNBR for these events does not exceed the DNB SAFDL.

The following criterion applies to the CEA misoperation event:

$$\text{DNBR} \geq \text{DNB SAFDL}$$

The CEA misoperation events are described in Chapter 15.1.3 of the SAR (Reference 7.3-1).

7.3.3.3 Impact of Changes

The methodology employed for the single CEA drop event is to "back-calculate" the maximum radial distortion factor (Fr) allowed assuming the minimum required thermal margin reserved by the limiting conditions for operation (LCOs). This maximum sensitivity of DNBR to Fr is calculated based on the range of initial conditions possible for the event. For Cycle 16 and beyond, the reload analysis process will confirm that these radial distortion factors are not exceeded for the as-built core.

The increase in rated power, the range of initial conditions (temperature, pressure and RCS flow), and the "Required Power Reduction After CEA Inward Deviation" figure increase from 1 hour to 2 hours have been accounted for in the DNBR to Fr sensitivity.

7.3.3.4 Analysis Overview

In the analysis of the CEA drop event, power is assumed to return to the original power level driven by turbine demand, with negligible changes in temperature, pressure, or RCS flow. This is the most adverse possible outcome of a CEA drop that changes the power distortion without any accompanying power or temperature reduction. This conservative modelling assumption eliminates the need for explicit transient analysis with CENTS. The change in margin to DNB is

evaluated using the maximum sensitivity of DNBR to Fr for the range of the conditions of the event.

DNBR margin degradation for the single CEA drop event is determined crediting the operator response requirements of Technical Specification 3.1.3.1, "CEA Position," and Figure 7.3.3-1 (COLR Figure 2), "Required Power Reduction After CEA Inward Deviation." This technical specification requires that the operator initiate a power reduction as specified in the Figure 7.3.3-1 shortly after the occurrence of a CEA drop.

For the single CEA drop event, the change in margin to the linear heat rate limit is smaller than the change in margin to the DNBR limit.

The margin requirements for CEA drop events (which do not result in a reactor trip) clearly bound the margin requirements for CEA misoperation events that result in reactor trip.

The change in sensitivity of DNBR to Fr is based on the input parameter ranges from Table 7.3.3-1.

7.3.3.5 Analysis Results

The single CEA drop event is a subset of the anticipated operational occurrences (AOOs) that are analyzed to determine the minimum required thermal margin that must be maintained by the LCOs such that, in conjunction with the reactor protection system, the DNB and centerline-to-melt SAFDLs are not violated. The required thermal margin is monitored by COLSS when it is in service and by the operators using the CPCS and COLR specified limits when COLSS is out of service.

Single CEA drop event radial power peaking distortion factor limits have been determined to assure that the DNBR and LHR SAFDLs are not exceeded. For Cycle 16 and beyond, the reload analysis process will confirm that these radial distortion factor limits are not exceeded for the as-built core based on the "CEA Positions" (Tech Spec 3.1.3.1), "Required Power Reduction After CEA Inward Deviation" figure (Figure 7.3.3-1 / COLR Figure 2).

7.3.4 Uncontrolled Boron Dilution Incident

The objective of the uncontrolled boron dilution incident (UBDI) analysis is to document the impact of the following changes:

1. the increase in rated power,
2. the RSGs,
3. an increase in the analytical assumption for charging flow, and
4. a more detailed individual mode analysis (separate Hot Standby and Hot Shutdown mode analyses).

The impact of the above changes result in no violation of the SAFDLs for Cycle 16. The increase in charging flow is a conservative increase in the analytically assumed charging flow. The increased flow does not reduce the time required for operator action below acceptable limits.

7.3.4.1 General Description of the Event

The uncontrolled boron dilution event could be caused by improper operator action or by a failure in the boric acid make-up flow path that reduces the flow of borated water to the charging pump suction. Either can produce a charging flow boron concentration that is lower than the reactor coolant system (RCS) boron concentration. During operation at power (Modes 1 and 2), an uncontrolled boron dilution adds positive reactivity and can cause an approach to the DNBR and centerline-to-melt (CTM) limits. The core protection calculator system (CPCS) monitors the transient behavior of pertinent safety parameters and will generate a reactor trip if necessary to prevent the DNB and CTM limits from being exceeded. The high pressurizer pressure trip will prevent primary pressure from reaching the RCS pressure upset limit. The reactor protection system trip that is actuated depends of the rate of reactivity addition.

For the subcritical modes (Modes 3 through 6), various alarms and indicators are available to the operator (depending on the mode of operation and plant configuration) to ensure sufficient time to respond to an uncontrolled boron dilution event before shutdown margin (SDM) is lost. The time required to achieve criticality due to boron dilution is dependent on the initial and critical boron concentrations, the boron reactivity worth, and the rate of dilution.

7.3.4.2 Purpose of Analysis and Acceptance Criteria

The purpose of this analysis is to demonstrate that the SAFDLs are not violated. This is indirectly demonstrated by ensuring that an uncontrolled criticality does not occur within the specified times for operator corrective action.

To evaluate the results of the analyzed events, the time between the beginning of the event and the loss of shutdown margin is determined for events initiated from critical conditions. The consequences of a UBDI initiating from Mode 1 conditions are demonstrated to be bounded by the CEA bank withdrawal event as described in Section 7.3.2 of this report. For events initiated in other modes of operation, the time from a control room alarm or other indication of the event to the loss of shutdown margin is determined. For those events initiated from subcritical conditions, the time from an alarm until the loss of shutdown margin must exceed 15 minutes or 30 minutes for events during refueling.

The uncontrolled boron dilution event is described in Chapter 15.1.4 of the SAR (Reference 7.3-1).

7.3.4.3 Impact of Changes

The increase in rated power from 2815 to 3026 MWt has a negligible impact on the results of the uncontrolled boron dilution event. The increase in charging flow from 132 gpm to 138 gpm results in a faster dilution and less time from the time of alarm to the time of criticality.

The replacement steam generators result in an increase in RCS mass. A larger RCS mass results in a slower dilution and increases the time that the operator has to perform corrective action.

A more detailed mode analysis was performed for Hot Standby versus Hot Shutdown conditions in which RCS temperature differences were accounted for in the analysis. The colder temperature of the Hot Shutdown conditions improve the results.

7.3.4.4 Analysis Overview

The time required to achieve criticality from a subcritical condition due to boron dilution is based on the initial and critical boron concentrations, the boron reactivity worth, and the rate of dilution. Reactivity increase rates due to boron dilution are based on the boron worth and the dilution rate.

Six different general operational modes were analyzed for the boron dilution incident: refueling, cold shutdown, hot shutdown, hot standby, and low and full power operation. During normal plant operation, operation of more than one charging pump is not the normal mode. However, operation of more than one charging pump may result from a system transient or direct operator control. Nevertheless, in each case it is assumed that the boron dilution results from pumping unborated demineralized water into the RCS at the maximum possible rate of 138 gpm (the revised combined capacity of three charging pumps).

The boron concentration within the minimum volume considered in each analyzed mode is uniform at all times since sufficient circulation exists to maintain a uniform mixture. During refueling, cold shutdown, and occasionally during hot shutdown conditions this circulation is provided by the operation of the shutdown cooling system. Operation of the shutdown cooling system does not assure complete mixing of the RCS under all conditions. Consequently, a reduced RCS volume is assumed in these conditions. During hot shutdown, hot standby, and power conditions, the reactor coolant pumps are normally operating. If both pumps are off in one loop, there is sufficient reverse flow through the idle loop to ensure a uniform concentration throughout the system.

The method of analysis used to determine the rate of change in core reactivity due to uncontrolled boron dilution is dependent on the boron reactivity and the dilution time constant τ, which is defined by the ratio of the reactor coolant mass inventory to the maximum charging rate. The reactivity held down by soluble boron is determined by the time in core life and the degree of subcriticality at shutdown. For any shutdown condition, the maximum negative reactivity contributed by soluble boron and, therefore, the maximum boron concentration, occurs at the BOC. Therefore, BOC conditions are assumed in these analyses. This assumption results in minimum calculated times to loss of shutdown.

In the evaluation of the UBDI, the dilution equations were rearranged to solve for relationships between inverse boron worth (IBW) and critical boron concentration (CBC). That is, for a given dilution time constant (τ), subcriticality at time of alarm ($\%\Delta\rho$), and time from alarm to criticality (t_{crit}), various values of CBC were input into the equations and the corresponding

IBWs were calculated. The resulting CBC/IBW "limit lines" are used to determine the acceptability of a cycle's core design with respect to a UBDI by verifying that the cycle specific CBC and IBW values fall within the acceptable region.

The methodology used in this analysis is the same as that used in the SAR, Reference 7.3-1, Section 15.1.4. Changes from the SAR analyses are presented below for the respective operating modes.

Dilution During Refueling

Input parameters from Table 7.3.4-1 have been incorporated in this analysis with the following clarifications and changes from the SAR analysis:

A. The initial shutdown reactivity is determined by the difference between the minimum refueling water boron concentration allowed by technical specifications and a bounding beginning of cycle critical boron concentration for refueling conditions. The initial boron concentration was chosen to be consistent with a Keff = 0.95, with the physics calculations accounting for the 1% $\Delta k/k$ uncertainty. That is, the physics calculated refueling boron concentration is based upon a Keff = 0.94.

B. A charging and corresponding letdown flow of 138 gpm was assumed.

Dilution During Cold Shutdown with the RCS Filled

Input parameters from Tables 7.3.4-3a and 7.3.4-3b have been incorporated in this analysis and the following change from the SAR analysis:

A. A charging pump flow of 138 gpm was assumed.

Dilution During Cold Shutdown with the RCS Partially Drained

Input parameters from Tables 7.3.4-2 have been incorporated in this analysis with the following clarifications and changes from the SAR analysis:

A. A charging pump flow of 138 gpm was assumed.

B. To provide indication of the UBDI, an alarm on initial operation of a charging pump or an alarm when the startup range excore neutron detectors indicate an increasing count rate is available. The monitors are set to provide the alarm when the count rate reaches 1.5 times the background count rate.

Dilution During Hot Shutdown and Hot Standby

Input parameters from Tables 7.3.4-4a, 7.3.4-4b, 7.3.4-5a and 7.3.4-5b have been incorporated in this analysis with the following changes from the SAR analysis:

A. A charging pump flow of 138 gpm was assumed.

B. Hot Shutdown was separated from Hot Standby by taking credit for the temperature difference between the modes.

Dilution During Critical Operation

The mode 1 analysis has been determined to be bounded by the CEAW event as discussed below.

Input parameters from Table 7.3.4–6 have been incorporated in the mode 2 analysis with the following clarifications and changes from the SAR analysis:

A. The RCS inventory was increased consistent with the new steam generators.

B. A charging pump flow of 138 gpm was assumed.

C. An initial shutdown reactivity of 5 %$\Delta\rho$ was assumed.

7.3.4.5 Analysis Results

Dilution During Refueling

Alarms and indications would alert the operator to the starting of the first charging pump coincident with the start of the dilution event. Since the alarms are coincident with the start of the event, the operator will have more than the minimum 30 minutes to respond prior to losing shutdown margin. For conservatism, the initial boron concentration was chosen to be consistent with the technical specification limit, Keff = 0.95 and the CBC / IBW limit line as presented in Figure 7.3.4-1 was based on 31 minutes from alarms to loss of shutdown margin.

Dilution During Cold Shutdown

Dilution During Cold Shutdown with the RCS Filled

If the boron dilution count rate monitors are operable and no CEAs are withdrawn, the operator will receive an alarm from the count rate monitors more than 15 minutes before the loss of all shutdown margin. If the count rate monitors are not operating and assuming the withdrawn CEAs are worth a minimum of 2.0% $\Delta k/k$, the high logarithmic power trip will alert the operator more than 15 minutes before the loss of all shutdown margin. In both of these conditions, the operator will be alerted to the event with more than the minimum 15 minutes of response time

available. The CBC / IBW limit lines presented in Figures 7.3.4-3 and 7.3.4-4, for alarms inoperable and operable, respectively, were based on 16 minutes from alarms to loss of shutdown margin.

Dilution During Cold Shutdown with the RCS Partially Drained

For the partially drained condition, the operator will receive an alarm from the count rate monitors or charging pump start more than 15 minutes before the loss of all shutdown margin. The operator will be alerted to the event with more than the minimum 15 minutes response time available. The CBC / IBW limit line presented in Figure 7.3.4-2 was based on 16 minutes from alarms to loss of shutdown margin.

Dilution During Hot Shutdown

If the boron dilution count rate monitors are operable and no CEAs are withdrawn, the operator will receive an alarm more than 15 minutes before the loss of all shutdown margin. If the monitors are not operating and assuming the withdrawn CEAs are worth a minimum of 2.0 % $\Delta k/k$, the high logarithmic power trip will alert the operator more than 15 minutes before the loss of all shutdown margin. In both of these conditions, the operator will be alerted to the event with more than the minimum 15 minutes response time available. The CBC / IBW limit lines for Mode 4 are presented in Figures 7.3.4-5 and 7.3.4-6, for alarms inoperable and operable, respectively. The limit lines associated with Mode 4 were based on 16 minutes from alarms to loss of shutdown margin.

Dilution During Hot Standby

If the boron dilution count rate monitors are operable and no CEAs are withdrawn, the operator will receive an alarm more than 15 minutes before the loss of all shutdown margin. If the monitors are not operating and assuming the withdrawn CEAs are worth a minimum of 2.0 % $\Delta k/k$, the high logarithmic power trip will alert the operator more than 15 minutes prior to the loss of all shutdown margin. In both of these conditions, the operator will be alerted to the event with more than the minimum 15 minutes response time available. The CBC / IBW limit lines for Mode 3 are presented in Figures 7.3.4-7 and 7.3.4-8, for alarms inoperable and operable, respectively. The limit lines associated with Mode 3 were based on 16 minutes from alarms to loss of shutdown margin.

Dilution During Critical Operation

When considering an UBDI in Modes 1 and 2, care needs to be taken to ensure that the DNBR and CTM limits are not exceeded. The concern is the rate of power increase. For example, inadvertent charging of unborated water into the RCS while the reactor is at full power could result in a maximum rate of reactivity addition of $\sim 1.5 \times 10^{-5}$ $\Delta\rho$/sec. If boron dilution occurs at this rate, and the operator fails to take corrective action, then reactor power, coolant temperature, and coolant pressure would increase. These changes are such that a low minimum DNBR or variable overpower trip would occur. During a CEA bank withdrawal event, the reactivity insertion rate at full power is $\sim 1.0 \times 10^{-4}$ $\Delta\rho$/sec (0% power is $\sim 1.8 \times 10^{-4}$ $\Delta\rho$/sec). Hence, the

rate of reactivity addition (and corresponding power increase) during a UBDI as compared to that of a full power CEA bank withdrawal event would result in a less limiting event. Therefore, the concern of violating the peak LHR and DNBR criteria, which would be present for Modes 1 and 2, are bounded by the CEAW event.

The CBC / IBW limit line for critical operation is presented in Figure 7.3.4-9 and is based on 86 minutes from trip to loss of shutdown margin.

7.3.5 Loss of Flow Events

7.3.5.1 Loss of Reactor Coolant Flow Resulting from an Electrical Failure

The objective of the loss of reactor coolant flow (LOF) event analysis is to document the impact of the following changes:

1. an increase in rated power,
2. the RSG's,
3. an increase in RCS flow,
4. a decrease in Doppler coefficient,
5. a change to the 4-pump flow coastdown curve, and
6. an increase in CPCS response time.

The above changes result in no violation of the minimum DNBR and small increase in required DNB thermal margin.

7.3.5.1.1 General Description of the Event

The LOF event may result from a loss of electrical power to one or more of the four RCPs. The RCS flow begins to coast down and the RCS temperature and pressure increase simultaneously. This event is mitigated by the CPCS when any one of the four RCP's shaft speed drops below 95% of its nominal speed.

The LOF is analyzed to determine the minimum initial thermal margin that must be maintained by the limiting conditions for operation (LCOs) such that, in conjunction with the reactor protection system (RPS), the DNB SAFDL is not violated during the event. This initial margin is monitored by the core operational limit supervisory system (COLSS) when in service and by the operators using the CPCS and a DNBR limit line when COLSS is out of service.

The principal process variables that determine thermal margin to DNB in the core are monitored by the COLSS. The COLSS computes a power operating limit that ensures that the thermal margin available in the core is equal to or greater than that needed to maintain the minimum DNBR greater than the DNBR limit during anticipated operational occurrences.

The action of the RPS and insertion of the CEAs mitigate the decrease in DNB thermal margin due to the four RCP flow coastdown. The minimum DNBR occurs in less than four seconds after the initiation of the event.

7.3.5.1.2 Purpose of Analysis and Acceptance Criteria

The purpose of the analysis is to calculate the LOF DNB thermal margin requirements that must be reserved in the technical specification LCOs. This assures that the minimum DNBR for the event does not exceed the DNB SAFDL.

The criterion for the LOF event is the following:

$$DNBR \geq DNB\ SAFDL$$

The loss of reactor coolant flow resulting from an electrical failure event is described in Chapter 15.1.5 of the SAR (Reference 7.3-1).

7.3.5.1.3 Impact of Changes

The increase in rated thermal power results in a higher DNB margin degradation with the onset of the loss of RCS flow when the reactor coolant pumps lose power and coast down.

The RSGs result in a higher maximum initial RCS flow limit and lower steam generator primary side flow resistance. The lower steam generator primary side flow resistance results in essentially the same RCP flow coastdown upon electrical failure; however, more conservative initial conditions have been assumed which results in a slightly more rapid coastdown. Hence, a bounding four reactor coolant pump flow coastdown is employed.

The small increase in the CPC response time delays the time that the CEAs enter the core to mitigate the thermal margin degradation.

The decrease in least negative Doppler coefficient results in a higher power/heat flux increase during the event.

The above changes result in slightly higher DNB thermal margin requirements (or lower event DNBR values in the absence of increased thermal margin). This margin degradation is slightly offset by the increase in initial RCS flow.

As part of this analysis the limiting conditions are presented for the minimum subcooled case as well as the maximum subcooled case to re-verify that the maximum subcooled case is still limiting. Hence, both limits of the LCO ranges for RCS flow, pressure, temperature and Fr are used in this re-verification of the limiting case.

7.3.5.1.4 Analysis Overview

For a loss of flow at any power operating condition, a reactor trip will be initiated when any one of four reactor coolant pump (RCP) shaft speeds drops to 95 percent of its nominal speed. Crediting this trip, the partial loss of flow resulting from a loss of electrical power to three or fewer RCPs is less limiting than a four pump loss of flow. This is because the reactor will trip at the same time for both cases but the partial loss of flow has a slower flow coastdown. Therefore, only the four pump loss of flow event is presented herein.

The method used in this analysis employs the HERMITE (Reference 7.3-4), CENTS and CETOP codes which are consistent with the analysis of record.

The analysis was carried out in the following steps:

A. The RCP coastdown data for the loss of flow event was generated using the CENTS code. Coastdown data to account for up to 10% steam generator tube plugging was determined. The CENTS coastdown analysis considered the affects of both symmetric and asymmetric steam generator tube plugging (up to 10% tube asymmetry). The coastdown analysis also considered the effects of initial RCS pressure, temperature, and flow. The resulting coastdown data generated from CENTS was used as input to the HERMITE code.

B. The HERMITE code is used to determine the reactor core response during the postulated loss of flow event. The HERMITE code solves the few-group, space and time dependent neutron diffusion equation including the feedback effects of fuel temperature, coolant temperature, coolant density, and control rod motion for a one-dimensional average fuel bundle.

C. The time dependent thermal hydraulic information generated from the HERMITE code is transferred directly to the CETOP computer code for thermal margin and DNBR evaluation. The CETOP method was used to calculate both the time of occurrence and value of the minimum DNBR during the transient.

Input parameters from Tables 7.3.5.1-1 and 7.3.5.1-2 and the bounding physics data from Section 7.3.0.2 have been incorporated in this analysis with the following clarifications:

1. The least negative Doppler coefficient of -0.00128 $\Delta\rho/\sqrt{°K}$ was assumed.

2. A BOC delayed neutron fraction consistent with those defined in Section 7.3.0.2 was assumed.

3. The CEA insertion curve in Figure 7.3.0.2-4 was assumed. This curve accounts for a 0.6-second holding coil delay. A CEA worth of -5.0% $\Delta\rho$ was conservatively assumed.

4. An initial core power of 3087 MWt was assumed, based on a rated power of 3026 MWt and a 2% uncertainty.

5. A MTC of $0.0 * 10^{-4}$ $\Delta\rho/°F$ was assumed.

6. The following RCS flow, temperature, and pressure ranges in conjunction with a radial peaking factor range are assumed as the basis for input into the maximum and minimum subcooled cases.

   - 118×10^6 lbm/hr $\leq$ RCS flow $\leq 142.1 \times 10^6$ lbm/hr
   - 540 °F $\leq$ core inlet temperature $\leq$ 556.7 °F
   - 2000 psia $\leq$ RCS pressure $\leq$ 2300 psia
   - 1.28 $\leq$ radial peak factor $\leq$ 1.71

7. A CPCS low reactor coolant pump shaft speed trip setpoint of 95% and a total delay time of 0.4 seconds were assumed. CPCS initiates a reactor trip when the reactor coolant pump shaft speed drops below 95% of its nominal speed.

8. The four reactor coolant pump flow coastdown in Table 7.3.5.1-1 was assumed.

7.3.5.1.5 Analysis Results

The four pump loss of coolant flow produces an approach to the DNB limit due to the decrease in the core coolant flow. Protection against the DNB limit for this transient is provided by the initial steady state thermal margin which is maintained by adhering to the technical specification LCOs on DNBR margin and by the response of the RPS, which provides an automatic reactor trip as calculated by the CPCS.

The COLSS monitors the principal process variables that determine thermal margin to DNB in the core. The COLSS computes a power operating limit, which ensures that the thermal margin available in the core is equal to or greater than that needed to cause the minimum DNBR to remain greater than the DNB limit.

The initial conditions are typically selected such that the system is at a very subcooled state. Initiating the event from such a state results in the least amount of negative reactivity inserted due to generation of voids in the core. In this manner, the system undergoes the greatest amount of thermal margin degradation due to the RCP coastdown.

To demonstrate explicitly that the DNB SAFDL is not violated during a loss of flow event, two sample cases have been provided in which the initial conditions are chosen such that at the onset of the event, the minimum thermal margin required by the COLSS power operating limit is preserved.

The results of these analyses are the calculation of minimum thermal margins required to be reserved in COLSS to prevent the violation of the DNB SAFDL during a loss of flow event. With a minimum thermal margin reserved in COLSS, the minimum DNBR observed during this event is greater than 1.25 for the maximum subcooled case. The sequence of events for the four pump loss of flow is provided in Table 7.3.5.1-3. Figures 7.3.5.1-2 and 7.3.5.1-3 plot DNBR versus time for the maximum and minimum subcooled cases, respectively.

For the loss of flow event, the CPC trip on low pump speed in conjunction with the initial margin reserved in COLSS is sufficient to prevent the violation of the DNBR SAFDL from any set of initial conditions.

7.3.5.2 Loss of Reactor Coolant Flow Resulting from a Pump Shaft Seizure

The objective of the loss of reactor coolant flow from a pump shaft seizure event analysis is to document the impact of:

1. an increase in rated power,
2. the RSG's,
3. an increase in RCS flow,
4. a change in RCS pressure,
5. decrease in MTC,
6. a bounding one-pump seized rotor flow coastdown curve / 3-pump asymptotic flow fraction, and
7. the application of a different CPCS trip.

The impact of many of the above changes on the exclusion area boundary (EAB) and low population zone (LPZ) radiological doses were considered in the bounding Reference 7.3-5 evaluation for Amendment 222. The results of Reference 7.3-5 remain bounding for this power uprate assessment.

7.3.5.2.1 General Description of the Events

The RCP seized shaft event is analyzed to determine the expected number of fuel pins in DNB due to a reduction from four-pump to three-pump flow. The event is initiated from the minimum initial thermal margin that must be maintained by the technical specifications limiting conditions for operation (LCOs). Assuming all fuel pins in DNB fail, the radiological dose values can be determined.

The seized shaft event may result from a seizure of one of the reactor coolant pump (RCP) shafts. Following the shaft seizure, the core flowrate rapidly decreases to the asymptotic three RCP flowrate. The reduction in reactor coolant system (RCS) flow may result in some fuel pins experiencing DNB.

This event is mitigated either by the core protection calculator system (CPCS) low DNBR trip or by a CPCS RCP shaft speed trip.

7.3.5.2.2 Purpose of Analysis and Acceptance Criteria

The purpose of the analysis is to determine the seized shaft calculated fuel failures and the corresponding EAB (2 hour) and LPZ (8 hour) radiological doses.

The only criterion for the seized shaft event is to keep radiological doses less than or equal to 10CFR100 limits.

The loss of reactor coolant flow resulting from a pump shaft seizure event is described in Chapter 15.1.5 of the SAR (Reference 7.3-1).

Calculated fuel failure below 14% assures no violation of the above criteria. This limit was established in Reference 7.3-5 for Amendment 222.

7.3.5.2.3 Impact of Changes

The impact of the replacement steam generators results in a higher maximum initial RCS flow limit, lower steam generator primary side flow resistance, and larger primary and steam generator fluid masses. The lower steam generator primary side flow resistance results in a lower three pump asymptotic flow fraction. The RSG increase in RCS and steam generator masses requires slightly larger steam releases. The increase in core power and the larger replacement steam generator mass were analyzed in Reference 7.3-5 for Amendment 222.

The increase in RCS flow and the higher RCS pressure result in larger DNB thermal margin requirements (or, lower event DNBR values in the absence of increased required thermal margin) when combined with the larger RCS flow reduction from the lower 3-pump asymptotic flow fraction. These factors ultimately affect the amount of fuel failure.

The change in the CPCS trip and MTC coefficient have a negligible impact on both the thermal margin degradation and radiological doses due to the conservative methods employed.

7.3.5.2.4 Analysis Overview

The analytical basis for the seized rotor simulation are discussed below.

1. Upon initiation of this transient, the core flow rate reduces rapidly to the asymptotic (steady state) 3-pump flow fraction. The RCP coastdown data for the seized rotor event was generated using the CENTS code.
2. The method of the analysis for the seized rotor conservatively assumes an instantaneous drop from the initial flow rate to the reduced 3-pump "steady state" flow fraction calculated previously. Only the final asymptotic 3-pump flow fraction is important to calculation of potential fuel failure and not the actual RCS flow coastdown.
3. A minimum thermal margin power operating limit is modeled using the CETOP code. Then the mass flow is conservatively reduced to the 3-pump asymptotic flow fraction value while maintaining all the other initial conditions. Therefore, no transient response is required and the only physics data is the pin census.
4. The analysis is repeated with the above assumptions, using the TORC computer code to determine the minimum DNBR for fuel pins of various radial peaks. An integral fuel damage calculation is then performed by combining the results from the TORC code with the

number of fuel rods having a given radial peaking factor. The number of fuel rods versus radial peaking factor is taken from the "cumulative distribution of the fraction of fuel rods versus nuclear radial peaking factor." Figure 7.3.5.2-6 presents the results of the TORC computer code determined minimum DNBR for fuel pins of various radial peaks. The total number of calculated fuel failures is compared to the 14% fuel failure limit that assures dose limits are met.

Although no transient response is required, a representative pump shaft seizure was performed from the limiting thermal margin conditions to provide the NSSS response to the event and determine the time of minimum DNBR. The results from the typical NSSS response have no impact on the calculated fuel failure due to the conservative methods discussed above. The CENTS digital computer code is used to simulate the NSSS response and calculate the time of minimum DNBR assuming a CPCS low reactor coolant pump shaft speed trip and response time to mitigate the event. The minimum DNBR condition exists for only a short period of time below the DNB SAFDL. The parameters from Table 7.3.5.2-1 and the bounding physics data from Section 7.3.0.2 have been incorporated into the NSSS system response with the following clarifications:

1. The BOC Doppler curve in Figure 7.3.0.2-2 was assumed.

2. A BOC delayed neutron fraction consistent with that defined in Section 7.3.0.2 was assumed.

3. The CEA insertion curve in Figure 7.3.0.2-3 was assumed. This curve accounts for a 0.6-second holding coil delay. A CEA worth of -5.0% $\Delta\rho$ was conservatively assumed.

4. An initial core power of 3087 MWt was assumed, based on a rated power of 3026 MWt and a 2% uncertainty.

5. A MTC of $-0.2 * 10^{-4}$ $\Delta\rho$/°F was assumed.

6. A maximum RCS flow of 386,400 gpm was assumed.

7. A maximum RCS pressure of 2300 psia was assumed.

8. A CPCS low reactor coolant pump shaft speed trip setpoint of 95% and a conservative total delay time of 0.5 seconds were assumed. CPCS initiates a reactor trip when the reactor coolant pump shaft speed drops below 95% of its nominal speed.

9. The asymptotic flow for the one-pump reactor coolant pump flow coastdown was assumed to be 73%. A representative one-pump flow coastdown can be found in Figure 7.3.5.2-1.

The analysis input and assumptions used in the calculation of the radiological dose releases for the seized rotor event are discussed in Section 3.6.3.2 of Reference 7.3-5.

7.3.5.2.5 Analysis Results

The offsite releases considered in Reference 7.3-5 included considerations for the increased thermal power. Hence, as long as the calculated fuel failure remains less than or equal to 14%, the radiological dose results for the EAB and LPZ will be less than a small fraction of the 10CFR100 limits of 30 Rem for the thyroid and 2.5 Rem for whole body. The calculated fuel failure is determined explicitly for each reload fuel cycle and compared to the 14% limit.

Table 7.3.5.2-2 and Figures 7.3.5.2-1 through 7.3.5.2-5 show the NSSS and RPS responses for a typical loss of reactor coolant flow from a pump shaft seizure event.

7.3.6 Loss Of External Load and/or Turbine Trip

The loss of external load and/or turbine trip event was analyzed as a part of the replacement steam generator project in Reference 7.3-5 at a rated power of 3026 MWt for Amendment 222. There are no other changes that impact this analysis. However, the Technical Specification limits in Table 3.7.1 / Figure 3.7-1 on maximum power levels, MTC, and high linear power trip setpoints (specified as percent of rated thermal power) that apply when one or more main steam safety valves (MSSVs) are inoperable have been modified. New maximum power levels versus MTC for one MSSV inoperable and one MSSV inoperable per steam line are proposed. These new limits are provided in Table 7.3.6-1. The change in the Maximum Allowable Linear Power Level – High Trip Setpoint was determined based on a ratio of the old versus new rated thermal power levels. For several of the data points, the change is not exactly related to the ratio of rated thermal power levels. This slight difference is due to the Cycle 15 values currently provided in the Technical Specifications were conservatively rounded down. Whereas, the values presented for the submittal were used explicitly in the Reference 7.3-5 analysis.

The power level versus two MSSVs inoperable per steam line and three MSSVs inoperable per steam line remain unchanged from the values presented in Reference 7.3-5. These values were calculated based on a rated power of 3026 MWt.

The values in Table 7.3.6-1 will be incorporated in Table 3.7.1 / Figure 3.7-1 of Technical Specification 3/4.7.1.

7.3.7 Loss of Normal Feedwater Flow

The loss of normal feedwater flow event was analyzed as a part of the replacement steam generator project in Reference 7.3-5 at a rated power of 3026 MWt for Amendment 222. There are no other power uprate changes that impact this event.

7.3.8 Loss of all Normal and Preferred AC Power to the Station Auxiliaries

The loss of all normal and preferred AC power to the station auxiliaries event was analyzed as a part of the replacement steam generator project in Reference 7.3-5. This event has been determined to be bounded by other events. There are no other power uprate changes that impact this event.

7.3.9 Excess Heat Removal

7.3.9.1 Feedwater System Malfunction

The excess heat removal due to feedwater system malfunction event was analyzed as a part of the replacement steam generator project in Reference 7.3-5 at a rated power of 3026 MWt for Amendment 222. There are no other power uprate changes that impact this event.

7.3.9.2 Main Steam System Valve Malfunction

The excess heat removal due to main steam system malfunction event was analyzed as a part of the replacement steam generator project in Reference 7.3-5 at a rated power of 3026 MWt for Amendment 222. There are no other power uprate changes that impact this event.

7.3.10 LOCA Dose Analysis

The objective of the LOCA dose analysis is to document the impact of:

1. an increase in rated power,
2. the RSG's effect on containment volume,
3. updated sump volume,
4. updated containment mixing rates between sprayed and unsprayed regions,
5. updated particulate spray removal rates, and
6. new control room χ/Q values.

The impact of the above changes on the exclusion area boundary, low population zone and control room radiological doses did not result in the acceptance criteria being exceeded.

7.3.10.1 General Description of the Event

The design basis LOCA is postulated as a break in the reactor coolant pressure boundary piping. An immediate release of the core's radioactive inventory to the containment is assumed. The following fractions of the core's radioactive inventory are assumed to be airborne within the containment and available for release by leakage to the environment:

A. 100 percent of the noble gases; and

B. 25 percent of the iodines.

For iodines, of the 25 percent which becomes available, it is assumed that 91 percent is elemental iodine, five percent is particulate iodine, and four percent are organic iodines.

7.3.10.2 Purpose of Analysis and Acceptance Criteria

The purpose of the analysis is to determine the impact of the above changes on the exclusion area boundary (EAB), low population zone (LPZ) and control room radiological doses.

The acceptance criterion for the LOCA dose analysis is to keep the EAB and LPZ radiological doses within 10CFR100 limits and the control room radiological doses with 10CFR20 limits.

7.3.10.3 Impact of Changes

The increase in rated thermal power will result in an increase in the radiological releases. A small reduction in the containment net free volume (1.778E6 ft^3 versus 1.78E6 ft^3) was assumed to accommodate the effects of the replacement steam generators. A smaller sump volume (62, 898 ft^3 versus 64, 552 ft^3) was also assumed. These slightly smaller volumes result in slightly higher doses due to the increased concentrations in the sump and the vapor.

Smaller particulate iodine spray removal constants (3.97 hr^{-1} prior to recirculation and 4.24 hr^{-1} during recirculation until DF = 50 then 0.424 hr^{-1} versus 4.3 hr^{-1} until DF = 50 then 0.43 hr^{-1}) were assumed due to reduced spray flow considerations. Containment mixing rates were also reduced (11, 880 cfm versus 13,200 cfm). These small changes in parameters resulted in slightly higher doses.

Improved control room dispersion factors resulted in reductions in the control room doses.

7.3.10.4 Analysis Overview

The evaluation included the dose from reactor building leakage, ESF valve leakage, and a passive component failure in compliance with the current ANO design basis. The TACT5 radiological isotope library was used in this analysis (Reference 7.3-12). The ANO-2 containment was modeled as two regions, a sprayed and an unsprayed region, both of which release 0.1%/day of their volume directly to the environment. An instantaneous uniform distribution of the core release is assumed in the sprayed and unsprayed regions that consist of 78% and 22% of the containment volume respectively. The parameters used in the LOCA evaluation are shown in Table 7.3.10-1.

New control room dispersion factors have been developed using ARCON96. The development of the new dispersion factors listed in Table 7.3.10-1 were generated consistent with the approach delineated in Reference 7.3-8 with the following clarifications:

a. Two release locations were considered, the surface of containment and the penetration room ventilation system discharge to the containment flute. The atmospheric dispersion values from the limiting location were used.
b. The auxiliary building roof level is assumed to be 450'6".
c. The distance to the control room intake from containment is the shortest distance possible (rather than an average), the release has no vertical velocity, and the release occurs at the level of the auxiliary building roof.
d. Release data:

Release Source	Release Height above Grade (m)	Horizontal Distance to Intake (m)		Direction from Intake to Release Source (north is 0°)	
		VPH-1*	VPH-2*	VPH-1*	VPH-2*
Flute	55.6	59.5	71.7	341	345
Containment	29.4	56.5	67.9	331	335

*Control room intake dampers

e. For the containment source, an initial horizontal diffusion coefficient of 6.27 meters and an initial vertical diffusion coefficient of 4.22 meters was assumed.

7.3.10.5 Analysis Results

The results are shown below:

	Thyroid Dose (Rem)			Whole Body Dose (Rem)			Skin Dose[1] (Rem)
	EAB	LPZ	Control Room	EAB	LPZ	Control Room	Control Room
LOCA Doses	83	19	7	3	0.3	0.2	5
Acceptance Criteria (Rem)	300	300	30	25	25	5	75

[1]The "total" skin dose is reported, that is, the skin dose resulting from gamma radiation plus that resulting from beta radiation.

7.3.11 Major Secondary System Pipe Break

7.3.11.1 Steam Line Break Accident with or without Concurrent Loss of AC Power Evaluated for Post-Trip Return to Power

The steam line break accident with or without concurrent loss of AC power evaluated for post-trip return to power event was analyzed as a part of the replacement steam generator project in

Reference 7.3-5 at a rated power of 3026 MWt with an MTC of -3.8×10^{-4} $\Delta k/k/°F$ for Amendment 222. There are no other power uprate changes that impact this event.

A sensitivity study was presented in Reference 7.3-5 on CEA worth at trip to determine the lowest CEA worth value that would produce either a DNBR of 1.30 (MacBeth) or a peak linear heat rate of 21 kW/ft. The method used was to hold all input parameters, both physics input and plant values constant, and lower the CEA worth at trip until one of the above limits was reached.

The purpose of this sensitivity study was to determine the amount of CEA worth that could be utilized in future reload efforts to offset other physics parameters. Thus, the incremental CEA worth at trip of 0.09 $\%\Delta\rho$ can be credited in future reload efforts for HFP cases. Similarly, an incremental shutdown margin of 1.29 $\%\Delta\rho$ can be credited in future HZP analyses.

7.3.11.2 Feedwater Line Break Accident

The objective of the feedwater line break event analysis is to document the impact of the following changes:

1. an increase in rated power,
2. a change in FWLB method – assume RPS trip on ruptured SG low water level,
3. a change in initial pressurizer pressure,
4. a change in feedwater line break area,
5. an increase in MSSV tolerance,
6. a change in SG liquid mass, and
7. a change in the MSIS setpoint and MSIV response time.

The above changes result in no violation of RCS and steam generator pressure criteria and no pressurizer overfill condition.

7.3.11.2.1 General Description of the Event

A feedwater line break (FWLB) event is defined as the rupture of a main feedwater pipe during plant operation. If the feedwater line breaks upstream of the feedwater check valves, steam generator blowdown is prevented by the closure of the check valves. If the break occurs between the steam generator and the check valves, blowdown of that steam generator continues until it empties. Blowdown of the unaffected steam generator is prevented by the action of the feed line check valves and, after main steam isolation signal (MSIS) actuation, by closure of the main steam isolation valves.

In a postulated FWLB accident, a reactor trip occurs due to one of the following reactor protection system (RPS) signals:

1. Low steam generator level (LSGL)

2. High pressurizer pressure (HPP)
3. Low steam generator pressure (LSGP).

Additional reactor trip signals that may respond to the transient are the CPCS low DNBR trip or the high containment pressure trip.

A loss of normal AC power is postulated for this transient.

The engineered safety feature actuation system (ESFAS) logic initiates emergency feedwater (EFW) to the intact steam generator upon receiving an emergency feedwater actuation signal (EFAS) after the appropriate time delay has been satisfied. Prior to the MSIS condition, EFW flow to the ruptured steam generator is assumed to flow directly out of the break. Because the EFW header is cross-tied to the steam generators, flow to the intact steam generator may not begin until the ruptured steam generator is isolated. The steam generators are isolated after actuation by the MSIS signal. After the MSIS signal, EFW flow to the ruptured steam generator ceases and all available EFW flow is directed to the intact steam generator.

The opening of the pressurizer safety valves (PSVs) and the main steam safety valves (MSSVs) mitigates overpressurization of the reactor coolant system (RCS) and steam generators.

7.3.11.2.2 Purpose of Analysis and Acceptance Criteria

The purpose of the analysis is to determine that for the limiting FWLB event, the peak RCS pressure remains below its criterion and that the pressurizer does not overfill.

The following criteria apply to the FWLB event:

- Peak RCS pressure $\leq$ 2750 psia;
- Peak secondary system generator pressure $\leq$ 1210 psia;
- Pressurizer does not go solid;
- Radiological doses $\leq$ small fraction (10%) of 10CFR100 limits.

The feedwater line break event is described in Chapter 15.1.14.2 of the SAR (Reference 7.3-1).

7.3.11.2.3 Impact of Changes

The methodology used in this analysis has changed slightly from that used in the previous analysis. The previous method determined the limiting FWLB area by combining a simultaneous High Pressurizer Pressure Trip and Low Steam Generator Level Trip on the intact steam generator. The new method credits a Low Steam Generator Level Trip on the affected steam generator will occur with at least 40,000 lbm liquid inventory remaining in the steam generator. The limiting FWLB area is calculated based on a simultaneous High Pressurizer Pressure Trip and Low Steam Generator Level Trip on the affected steam generator at 40,000

lbm. This is still considered a very conservative approach as the fluid discharge through the break was assumed to be saturated liquid until the affected generator empties.

A parametric analysis was performed to determine the FWLB area such that a simultaneous trip occurred on High Pressurizer Pressure and Low Steam Generator Level of the affected steam generator at both the maximum and minimum allowed initial pressurizer limits. This is different than the previous analysis, which assumed a Low Steam Generator Level Trip on the intact steam generator.

Due to the change in the above methodology, the initial pressurizer pressure which allows simultaneous trips with ruptured low steam generator level was determined to be the maximum allowable initial value. This is different from previous analyses where the lowest allowable initial pressurizer pressure provided the limiting transient RCS pressure.

A maximum MSIS analytical setpoint was assumed with no delay in response time and instantaneous MSIV closure time. This is a modification to the previous analysis that assumed a minimum MSIS analytical setpoint and a maximum response time delay and MSIV valve closure time. For this analysis, a maximum MSIS setpoint minimizes the cooldown of the RCS. In the previous analysis, a minimum setpoint was used to provide maximum depletion of the intact steam generator inventory. For this analysis, intact steam generator inventory depletion is mitigated by the affected steam generator low level trip.

The increase in rated thermal power produces a higher performance regime which requires re-analysis to determine if RCS peak pressure (and long-term pressurizer fill) is adversely affected during the FWLB event.

The tolerance on the MSSVs has been increased for conservatism. This results in a slightly more adverse heat-up event, but is offset by the change in methodology described above.

The initial steam generator liquid mass decreases with an increase in rated power level. The smaller mass has a negligible, if any, impact since this change is a relative change.

7.3.11.2.4 Analysis Overview

The methodology used in this analysis has changed slightly from that used in the previous analysis. The previous method determined the limiting FWLB area by combining a simultaneous High Pressurizer Pressure Trip and Low Steam Generator Level Trip on the intact steam generator. The new method assumes that a Low Steam Generator Level Trip on the affected steam generator will occur with 40,000 lbm liquid inventory remaining in the steam generator. The limiting FWLB area is calculated based on a simultaneous High Pressurizer Pressure Trip and Low Steam Generator Level Trip on the affected steam generator at 40,000 lbm. This is still considered a very conservative approach as the fluid discharge through the break was assumed to be saturated liquid until the affected generator empties.

The initial pressurizer pressure which allows simultaneous trips with ruptured steam generator low level, as discussed above, is 2300 psia. This is different from previous analyses where the

lowest allowable initial pressurizer pressure, 2000 psia, provided the limiting transient RCS pressure.

This analysis has utilized the CENTS computer code for the transient analysis simulation.

Input parameters from Table 7.3.11.2-1 and the bounding physics data from Section 7.3.0.2 have been incorporated in this analysis with the following clarifications (inputs marked at the end by "***" are changes from the previous analysis):

1. The BOC Doppler curve in Figure 7.3.0.2-2 was assumed.

2. A BOC delayed neutron fraction and neutron lifetime consistent with those defined in Section 7.3.0.2 were assumed.

3. The CEA insertion curve in Figure 7.3.0.2-3 was assumed. This curve accounts for a 0.6 second holding coil delay. A CEA worth of -5.0% $\Delta\rho$ was conservatively assumed.

4. The feedwater line break analyzed was assumed to occur during hot full power operation with a loss of offsite power at the time that the trip breakers opened. With a loss of offsite power the turbine stop valves are assumed to close, reactor coolant pumps begin to coast down, and the pressurizer control systems are lost.

5. The initial steam generator liquid inventory for both steam generators was assumed to be 164,400 lbm. ***

6. A parametric analysis was performed to determine the FWLB area (0.1492 ft^2) such that a simultaneous trip occurred on High Pressurizer Pressure and Low Steam Generator Level of the affected steam generator at 40,000 lbm liquid inventory. A High Pressurizer Pressure Trip analytical setpoint of 2415 psia with a delay time of 0.90 seconds was assumed. A Low Steam Generator Level Trip response time of 1.3 seconds was assumed. This is different than the previous analysis, which assumed a Low Steam Generator Level Trip at 6% narrow range level on the intact steam generator. The analytical trip setpoints for the High Pressurizer Pressure Trip conservatively assumes a harsh environment uncertainty. ***

7. Only EFW flow from one EFW pump was credited to the steam generator with the intact feedwater line. A conservative EFW flow actuation setpoint of 0% of narrow range was assumed with the delay time of 112.4 seconds. The uncertainty assumed on the EFW flow actuation setpoint is based on a harsh environment uncertainty. The time of EFW flow delivery to this generator was based on the maximum of:

   a) the time to receive an EFAS with a delay period that allows the EFW pump to accelerate, or

   b) the time to receive a MSIS with a delay period that allows EFW flow to the affected steam generator to be isolated, or

c) the time the steam generator ΔP setpoint is reached with a delay period that allows EFW flow to the intact steam generator to be re-initiated. Isolation of EFW to the affected steam generator is based on the EFW valve isolation time of 36.4 seconds. EFW flow rate to the intact steam generator is dependent on steam generator pressure.

8. An MSIS analytical setpoint of 905 psia was assumed with no delay in response time, instantaneous MSIV closure time, and a 35 second EFW isolation valve stroke time. A high ΔP analytical setpoint of 220 psid was assumed with a 1.4-second response time and a 35-second EFW isolation valve stroke time. This is a modification to the previous analysis that assumed a minimum MSIS analytical setpoint pressure of 658 psia and a maximum response time delay and MSIV valve closure time. For the current analysis, a maximum MSIS setpoint minimizes the cooldown of the RCS. In the previous analysis, a minimum setpoint was used to provide maximum depletion of the intact steam generator inventory. For this analysis, intact steam generator inventory depletion is mitigated by the affected steam generator low level trip. ***

9. A conservatively small value for the fuel gap heat transfer coefficient was assumed corresponding to BOC.

10. An MSSV lift tolerance of +3.5% and PSV lift tolerance of +3.2% were assumed. ***

11. An initial core power of 3087 MWt was assumed, based on a rated power of 3026 MWt and a 2% uncertainty.

12. The BOC MTC of -0.2×10^{-4} Δρ/°F was assumed.

13. Assuming equilibrium core conditions maximized decay heat.

14. The analysis considered plugged U-tubes between zero and 10% plugged range per steam generator, with zero percent being conservative.

15. Installation of the RSGs was assumed.

16. A minimum RCS flow of 315,560 gpm.

17. An initial steam generator pressure of 999 psia was assumed. ***

18. The primary safety valve flow was adjusted by the Napier correction.

19. Steam generator full heat transfer area is conservatively assumed down to 19,000 lbm liquid mass. At 19,000 lbm liquid mass, the steam generator heat transfer is assumed to ramp linearly to zero at 2000 lbm.

20. An initial pressurizer pressure of 2300 psia was assumed. ***

The analysis input and assumptions used in the calculation of the radiological dose releases for the feedwater line break have not changed from those reported in Reference 7.3-5, Enclosure 4,

Section 1.0.4 for Amendment 222. The doses presented for Amendment 222 assumed an initial power of 3087 MWt, which is consistent with 102% of the new rated power of 3026 MWt.

7.3.11.2.5 Analysis Results

Figure 7.3.11.2-1 documents the parametric analysis on feedwater line break area versus peak RCS pressure based upon a HPP trip and a LSGL trip at 40,000 lbm on the affected steam generator. As can be seen from the figure, the limiting feedwater line break size was calculated to be 0.1492 ft^2.

The peak RCS and secondary system pressures remained below their respective criteria of 2750 psia and 1210 psia. The cooling provided by the EFW system and MSSV operation was sufficient to prevent the pressurizer overfill condition.

The NSSS, RPS, and EFW system responses for the FWLB with loss of AC power on turbine trip event are shown in Table 7.3.11.2-2 and in Figures 7.3.11.2-2 through 7.3.11.2-6.

The combination of the increased core power, the change in the analytical Low Steam Generator Level Trip methodology, and the change in the analytical MSIS setpoint and MSIV response time did not result in the RCS and secondary system pressures exceeding criteria and a pressurizer overfill condition did not occur.

The radiological doses for the two-hour exclusion area boundary and eight-hour low population zone are less than a small fraction of the 10CFR100 limits of 30 Rem for the thyroid and 2.5 Rem for whole body. The calculated results for all doses were previously performed at a power of 3087 MWt and have not changed from those presented in Reference 7.3-5 for Amendment 222.

7.3.12 Inadvertent Loading of a Fuel Assembly into the Improper Position

The objective of this analysis is to document that undetectable assembly misloadings are no more adverse than those for the previous ANO-2 cores. Relative to the previous analysis, changes addressed by this analysis include the following:

1. an increase in rated power, and
2. changes in core design (feed enrichments, number of feed assemblies, burnable absorber, assembly loading patterns) driven by increased fuel cycle length and low leakage fuel management.

The ability to detect core assembly misloadings is not degraded due to the power uprate.

7.3.12.1 General Description of the Event

For this analysis , it is assumed that an assembly is placed in the wrong core position. The worst situation would be the interchange of two assemblies of different reactivities.

7.3.12.2 Purpose of Analysis and Acceptance Criteria

The purpose of this analysis is to demonstrate that the implementation of power uprate will not result in undetectable assembly misloadings that are more adverse than those for the previous ANO-2 core designs.

The inadvertent loading of a fuel assembly into the improper position event is described in Chapter 15.1.15 of the SAR (Reference 7.3-1).

7.3.12.3 Impact of Changes

Power uprate and associated core design changes potentially limit the ability to detect significant fuel misloadings during startup testing. The relative change in power distributions caused by an assembly misloading will be affected by any or all of the following:

1. an increase in rated power, and
2. core design (feed enrichments, number of feed assemblies, burnable absorber, assembly loading patterns).

7.3.12.4 Analysis Overview

A method for determining if an assembly misloading is detectable was developed based on the tests used to identify assembly misloading during startups. Representative (worst case) assembly misloadings (interchange of two assemblies and misrotation of one assembly) were evaluated for the ANO-2 Power Uprate using the ROCS model for the Cycle 16 core design.

This analysis made the following input assumptions:

1. an increase in rated power to 3026 MWt, and
2. the Cycle 16 core design.

7.3.12.5 Analysis Results

The relative changes in core power distribution at the current and uprated power levels were similar for the Cycle 16 core design. Therefore, the ability to detect core misloadings using in-core detectors is not degraded due to the power uprate.

The minimum required over-power margin (ROPM) set aside in the setpoint analysis to protect the linear heat generation rate (LHGR) and DNB SAFDLs for the non-LOCA safety analysis AOOs (rod drop, loss of flow, CEAW, etc.) is available to offset the increase in peaking associated with assembly misloadings. Since the maximum increase in peaking associated with

the representative (worst case) assembly misloading (a detectable assembly misloading) is bounded by the minimum ROPM, the LHGR and DNB SAFDLs will not be violated.

7.3.13 Steam Generator Tube Rupture with or without a Concurrent Loss of AC Power

The objective of the steam generator tube rupture with and without concurrent loss of AC power (LOAC) event analysis is to document the impact of the following changes:

1. an increase in rated power,
2. the RSGs,
3. a change in RCS flow,
4. a change in actuation of emergency feedwater,
5. a change in initial SG pressure,
6. an increase in initial pressurizer pressure,
7. a change to the CENTS code,
8. an increase in SIAS setpoint and associated time delays to accurate the HPSI pumps,
9. a different HPSI pump response,
10. a change in CPCS trip setpoint and response time,
11. an increase in holding coil delay time,
12. application of a more negative MTC,
13. application of EOC fuel temperature coefficient,
14. application of BOC kinetics,
15. a change in CEA insertion curve and a decrease in CEA worth at trip,
16. a change in MSSV opening setpoints and tolerances,
17. a change in radiological dose methods (consistent with that used for Amendment 222).

The impact of the above changes results in an increase in the exclusion area boundary (EAB) and low population zone (LPZ) radiological doses. Additionally the changes in methods presented in Section 7.3.0.5 contribute to larger doses than those currently in the SAR.

7.3.13.1 General Description of the Event

The steam generator tube rupture (SGTR) event with or without a loss of AC (LOAC) power is a penetration of the barrier between the RCS and the main steam system. Integrity of this barrier is significant from a radiological standpoint. A leaking steam generator tube would allow transport of reactor coolant into the main steam system. Radioactivity contained in the reactor coolant would mix with the shell side water in the affected steam generator.

The initiating event is the double-ended rupture of one U-tube with either a concurrent loss of AC power or no loss of AC power. For the concurrent LOAC power event, a core protection calculator system (CPCS) low reactor coolant pump shaft speed trip occurs when any one of the four RCP shaft speeds drops below 95% of its nominal speed. For the no LOAC power event, the CPCS low DNBR trip will provide a reactor trip and prevent the DNB safety limit from being exceeded.

For the transient with AC power available, station auxiliaries would be available after the trip to mitigate the results of the event. The SDBCS valves are available and the secondary steam release would occur directly to the condenser. Operator action is taken at 30 minutes. At this time, the operator isolates the affected steam generator and initiates a controlled cooldown to shutdown cooling using either the SDBCS valves or the atmospheric dump valve of the intact steam generator. After the RCS temperature reaches the shutdown cooling temperature, the operator engages the shutdown cooling system. RCS heat removal via the steam generators is terminated at this time.

The initial RCS pressure spike on reactor trip is small and there is no challenge to the pressurizer safety valves. The actuation of main steam safety valves will prevent the secondary system pressure from exceeding 110% of its design limit.

The SGTR with concurrent LOAC event is analyzed to determine the radiological doses for the 2-hour exclusion area boundary (EAB) and the 8-hour low population zone doses. Since the steam releases for this event are directly to the atmosphere via the MSSVs and the intact steam generator atmospheric dump valve, it bounds the radiological doses for the SGTR event with AC power available. Hence, only the SGTR event with concurrent LOAC is analyzed.

7.3.13.2 Purpose of Analysis and Acceptance Criteria

The purpose of this analysis is to determine that the SGTR event EAB and LPZ radiological dose results are less than 10CFR100 limits.

The following criteria apply to the SGTR event with and without concurrent LOAC:

- DNBR ≥ DNB SAFDL
- Peak RCS pressure ≤ 2750 psia
- Peak secondary pressure ≤ 1210 psia
- Radiological doses are within 10CFR100 limits

The SGTR event with and without concurrent LOAC is described in Chapter 15.1.18 of the SAR (Reference 7.3-1).

7.3.13.3 Impact of Changes

The increase in rated power along with minimum RCS flow results in an increase in core outlet temperature, which results in an increase in flashing of the affected steam generator. A larger

flashing fraction results in higher iodine concentrations in the steam from the primary fluid flowing through the ruptured U-tube.

The RSGs have a larger steam generator volume and steam generator liquid mass, a higher steam generator pressure, a smaller steam generator primary side flow resistance, and a larger number of U-tubes that have a longer length and a smaller diameter. The larger steam generator volume results in larger steam generator liquid and steam inventories, which impact radiological dose results slightly. Higher steam generator pressures result in a lower pressure difference between primary and secondary systems, which results in a slower primary mass leak rate into the affected steam generator. Although the overall primary side flow resistance is lower due to the increase in the number of U-tubes, the flow resistance for an individual U-tube is higher due to the longer length and smaller diameter. This also results in a smaller leak rate into the affected steam generator. A smaller leak rate results in lower total primary mass release to the affected steam generator, which results in lower steam generator activity and lower radiological doses.

The increase in initial pressurizer pressure results in an increase in RCS pressure, which results in a larger primary-to-secondary pressure difference (ΔP). This is slightly offset by the increase in steam generator pressure, which reduces the primary-to-secondary ΔP.

In addition to the above changes, the following changes are used to maximize RCS pressure and the primary-to-secondary ΔP. The SIAS actuation setpoint was conservatively increased to actuate the HPSI pumps and charging pumps sooner. After the associated delays to start and load the HPSI pump after loss of normal AC power (LOAC), the HPSI pumps provide water to maintain RCS pressure. It is conservatively assumed that the charging pumps are loaded instantaneously on SIAS and provide water at the maximum flow rate.

To minimize steam generator pressure and maximize the primary-to-secondary ΔP, the emergency feedwater system is assumed to actuate on a high setpoint signal and provide the maximum flow from both emergency feedwater pumps at their maximum flow rate to minimize the steam generator pressure. The MSSV tolerance has increased, which results in the MSSV cycling open and close at lower steam generator pressure.

The CPCS have been modified since this analysis was last performed and the first reactor trip to occur is the CPCS low reactor coolant pump shaft speed trip. A very conservative response time is assumed to delay the reactor trip and subsequent power decrease. Delaying the rate of post-trip power reduction results in a slower decrease in the RCS energy and pressure, which maximizes the primary-to-secondary ΔP. The increase in holding coil delay time has the same impact as the increase in CPCS response time of extending the core power after reactor trip and post-trip RCS pressure decrease.

The decrease in CEA worth at trip, the application of the negative MTC and fuel temperature coefficients (Doppler) and the BOC kinetic parameters result in a slower decrease in core power after reactor trip. This has the same impact of the longer CPCS trip response and holding coil delay times.

This event is now analyzed with the CENTS code versus the CESEC and COAST codes.

The increase in core power also results in an increase in the radiological dose results. This change plus the change in radiological dose methodology results in an increase in the EAB and LPZ doses.

7.3.13.4 Analysis Overview

The methodology used in this analysis is similar to the methodology used in the current analysis of record, except that the CENTS code is used instead of the CESEC and COAST codes.

Input parameters from Table 7.3.13-1 and the bounding physics data from Section 7.3.0.2 have been incorporated in this analysis with these following clarifications (inputs marked at the end by "***" are changes from the previous analysis):

1. The EOC Doppler curve in Figure 7.3.0.2-2 was assumed. ***

2. An BOC delayed neutron fraction consistent with those defined in Section 7.3.0.2 were assumed. ***

3. The CEA insertion curve in Figure 7.3.0.2-3 was assumed. This curve accounts for a 0.6 second holding coil delay. A CEA worth of -5.0% $\Delta\rho$ was conservatively assumed. ***

4. The most negative MTC of -3.8 * 10-4 $\Delta\rho$/°F was assumed. ***

5. A loss of AC power concurrent with a guillotine rupture of a single U-tube was assumed.

6. For the analysis, at time zero, when all electrical power is lost to station auxiliaries, the following is assumed to occur:

    a. The turbine stop valves close and it is assumed that the area of the turbine admission valves is reduced to zero at the minimum closing rate.

    b. The steam generator feedwater flow to both steam generators is assumed to go to zero within ten seconds.

    c. The reactor coolant pumps begin to coastdown. Following the coastdown the coolant flow necessary to remove residual heat and to cool the reactor core is maintained by natural circulation.

    d. Charging and letdown flow are reduced to zero. Upon initiation of SIAS, the charging flow instantaneously resumes at maximum capacity. ***

    e. The steam dump and bypass control system is unavailable for post-trip steam releases.

7. A CPCS low reactor coolant pump shaft speed trip setpoint of 95% and a total delay time of 1.0 seconds were conservatively assumed. CPCS initiates a reactor trip when the reactor coolant pump shaft speed drops below 95% of its nominal speed. ***

8. An initial core power of 3087 MWt was assumed, based on a rated power of 3026 MWt and a 2% uncertainty. ***

9. An initial RCS flow of 315,560 gpm was assumed. ***

10. An initial maximum core inlet temperature of 556.7° F was assumed.

11. An initial pressurizer pressure of 2300 psia was assumed. ***

12. An initial steam generator pressure of 960 psia was assumed. ***

13. The emergency feedwater actuation signal setpoint is assumed at 41% narrow range. ***

14. An SIAS is actuated when the pressurizer pressure drops below 1800 psia. Time delays associated with the safety injection pump acceleration and valve opening are taken into account. A ten-second HPSI response time was assumed to account for these delays. ***

15. Installation of the replacement steam generators were assumed. ***

The analysis input and assumptions used in the calculation of the radiological dose releases for the SGTR event are discussed in Section 7.3.0.5 (which are the same as those in Reference 7.3-5, Enclosure 4, Section 1.0.4 for Amendment 222) and have been incorporated in this analysis with the following clarifications:

1. The condenser is assumed unavailable for cooldown. Thus, the entire cooldown was performed by dumping steam to the atmosphere from the intact steam generator.

2. An RCS primary to secondary leakage rate of 1 gpm for the intact steam generator was assumed. This is very conservative with respect to the Technical Specification limit of 150 gpd and the steam generators are not predicted to depressurize for this event.

3. Since the SGTR with concurrent loss of AC power event assumed no fuel failure, only the maximum initial RCS activity plus iodine spiking was analyzed.

4. A time dependent flashing fraction was assumed based on primary fluid and steam generator conditions.

5. An RCS liquid mass of 418,748 lbm is assumed.

A generated induced iodine, a preexisting iodine and no iodine spiking cases were performed for this analysis. These calculations and the noted method used in Reference 7.3-5 are conservative methods with respect to the ANO-2 licensing basis for the SGTR event. The licensing basis

analyses used the radiological information presented in Section 15.1.0 of the SAR. A dose calculation was presented based only on the initial primary and secondary concentrations without assuming a preaccident iodine spike or an induced iodine spike. Given this, the no iodine spiking case presented below is most consistent with the methods used for the dose calculations presented in the SAR except for the following significant differences:

1. A decontamination factor of 100 was assumed in this assessment. This is more conservative than the value of 400 presented in Section 15.1.0.5.1 which was assumed for the iodine concentration released in the steam from the steam generator liquid.
2. The secondary side initial steady state radiological concentration was assumed to be 0.1 μCi/gm dose equivalent I-131, and the primary side initial specific activity was assumed to be 1 μCi/gm dose equivalent I-131 and 100 / E μCi/gm. This deviates from the SAR Section 15.1.0.5.1 assumptions based on 1% failed fuel concentrations.
3. An unaffected steam generator primary to secondary leak of 1 gpm was assumed rather than SAR assumption of 100 gpd.

The noted exceptions above delineate conservative assumptions used in the no iodine spiking case presented below with respect to the licensing basis analysis requirements.

7.3.13.5 Analysis Results

Only the SGTR with concurrent LOAC power event is presented, as it bounds the SGTR with AC power available event EAB and LPZ doses.

The NSSS and RPS system responses for the SGTR with concurrent LOAC power event are shown in Table 7.3.13-2 and in Figures 7.3.13-1 through 7.3.13-8. The steam generator liquid inventory versus time is presented in Figure 7.3.13-7. Figure 7.3.13-8 provides the discharge rate out through the secondary safety valves. During the first 30 minutes following the initiation transient, < 70,000 lbm. of reactor coolant is transported to the main steam system. For this case, radioactivity can only be transported to the surrounding environment by the steam released through the main steam safety valves or atmospheric dump valves. During the first 30 minutes of the transient, approximately 250,000 lbm. of steam are released out the main steam safety valves.

Tables 7.3.13-3 and 7.3.13-4 presents the radiological doses associated with this event for the EAB and the LPZ. For these locations the dose received by the thyroid and whole body are shown for the event-generated iodine spiking (GIS), pre-existing iodine spiking (PIS) and no iodine spiking conditions.

The radiological doses for the 2-hour exclusion area boundary and 8-hour low population zone for a GIS and no iodine spike are less than a small fraction of the 10CFR100 limits, and for a PIS are within the 10CFR100 limits.

The radiological releases for a steam generator tube rupture with a concurrent loss of AC power event are less than the 10CFR100 guidelines.

7.3.14 Control Element Assembly Ejection

The objective of the control element assembly (CEA) ejection event analysis is to document the impact of the following changes:

1. the increase in rated power from 2815 MWt to 3026 MWt and the change in the initial power assumption,
2. an increase in RCS flow,
3. the RSGs,
4. an increase in excore detector uncertainty, and CPC VOPT trip setpoint
5. an increase in HZP core inlet temperature, and
6. an implementation of a radiological dose assessment (no SAR presentation currently exists).

The above changes result in lower acceptable ejected 3D peaks and a presentation of the exclusion area boundary (EAB) and low population zone (LPZ) radiological doses.

7.3.14.1 General Description of the Event

An ejected CEA is assumed to occur due to a complete circumferential break of either the control element drive mechanism (CEDM) housing or the CEDM nozzle on the reactor vessel. The ejection of the CEA results in positive reactivity insertion into the core, which causes local powers and fuel temperatures to increase. The increasing fuel temperature in conjunction with the Doppler fuel temperature coefficient causes negative reactivity to be inserted into the core. The negative reactivity mitigates the power rise due to the ejected CEA.

After ejection of a CEA, core power rises rapidly. The event proceeds until either a core protection calculator system (CPCS) variable overpower trip (VOPT) or a high linear power trip (HLPT) setpoint is reached. The event is terminated when negative reactivity is added due to the insertion of the CEAs.

7.3.14.2 Purpose of Analysis and Acceptance Criteria

The purpose of this analysis is to review the number of fuel rods that experience clad damage and contain hot fuel pellets that exceed an incipient centerline condition.

The analysis has the following acceptance criteria:

To preclude clad damage: total average enthalpy $\leq$ 200 cal/g, and
To preclude incipient centerline melting threshold: centerline (C_L) enthalpy $\leq$ 250 cal/g

In addition radiological doses are calculated assuming a certain number of fuel failure with clad damage and no fuel failures due to violation of the incipient C_L melting threshold. The analysis has the following acceptance criteria for radiological doses:

radiological doses < well within (25%) of 10CFR100 limits.

The CEA ejection events are described in Chapter 15.1.20 of the SAR (Reference 7.3-1).

7.3.14.3 Impact of Changes

The increase in power in conjunction with more conservative assumption of higher excore detector uncertainty and VOPT trip setpoint results in additional energy deposited in the fuel pin during the ejection. The larger deposited energy results in a lower allowed 3D peak threshold for determining calculated fuel failure for a given ejected worth. The increase in RCS flow results in a small benefit in the determination of the allowed 3D peak threshold.

The HZP core inlet temperature was conservatively assumed to be the HFP value. This results in a very small increase in deposited energy for the HZP event.

The RSGs have no impact on the allowed 3D peak, but they do impact the radiological doses. The impact of the replacement steam generators results in larger primary and steam generator fluid masses. The increase in RCS and steam generator masses results in slightly larger steam releases, which increase the radiological doses.

The increase in core power results in an increase in the radiological doses.

7.3.14.4 Analysis Overview

For Cycle 16, the CEA ejection events at HFP and HZP were assessed with regards to developing tables of acceptable ejected 3D peak (Fq's) versus ejected worths using the above acceptance criteria for total average enthalpy and incipient C_L melting threshold. Methods consistent with the analysis of record was employed in this analysis.

The key plant and physics input for the CEA ejection events are described in Reference 7.3-11 (C-E Method for CEA Ejection Analysis). This analysis has utilized the STRIKIN II computer code for the transient analysis simulation.

Input parameters from Tables 7.3.14-1 and 7.3.14-2 and the bounding physics data from Section 7.3.0.2 have been incorporated in this analysis with the following clarifications (inputs marked at the end by "***" are changes from the previous analysis):

1. The BOC Doppler curve in Figure 7.3.0.2-2 was assumed.

2. An EOC delayed neutron fraction consistent with that defined in Section 7.3.0.2 was assumed.

3. For HFP the CEA insertion curve in Figure 7.3.0.2-3 was assumed. This curve accounts for a 0.6 second holding coil delay. A CEA worth of -5.0% $\Delta\rho$ was conservatively assumed for HFP.

   For HZP the CEA insertion curve (scram curve) is based on an ASI of +0.6. A CEA insertion curve consistent with Figure 7.3.0.2-4 utilizing a 0.6 second holding coil delay was assumed. A CEA worth of –2.0% $\Delta\rho$ was conservatively assumed.

4. For MTC, zero and $+0.5 * 10^{-4}$ $\Delta\rho$/°F were assumed for HFP and HZP conditions, respectively.

5. The variable overpower trip (VOPT) of the core protection calculator system (CPCS) was employed in the analysis. A CPCS trip delay time of 0.60 seconds was assumed. The VOPT assumed an excore uncertainty of 40% from Table 7.3.14-3. For HFP and HZP, conservative VOPT setpoints of 153% and 98% were assumed. ***

6. For HFP an initial core power of 3087 MWt was assumed based on a rated power of 3026 MWt and a 2% uncertainty. For HZP an initial core power of 30.3 MWt was assumed based on one percent of the rated power value of 3026 MWt. ***

7. An axial power distribution in Table 7.3.14-2 was assumed.

8. The HFP core inlet temperature of 556.7 was conservatively assumed for HZP. ***

9. A RCS flow of 315,560 gpm was assumed for HFP and HZP conditions. ***

The analysis input and assumptions used in the calculation of the radiological dose releases for the CEA ejection event are discussed in Section 7.3.0.5 (which are the same as those in Reference 7.3-5, Enclosure 4, Section 1.0.4 for Amendment 222) and have been incorporated in this analysis with the following clarifications:

1. The condenser is assumed unavailable for cooldown. Thus, the entire cooldown was performed by dumping steam to the atmosphere from the steam generators.

2. An RCS primary to secondary leakage rate of 150 gpd per steam generator was assumed consistent with the technical specification limit on allowed leakage. No increase in leakage (to 720 gpd or 0.5 gpm) was considered for this event as the steam generators are not predicted to depressurize.

3. Releases from failed pins was based on 10% of the noble gases except Kr-85 in which 30% is assumed to escape, and 12% of iodine. These release fractions are used in combination with the maximum number of fuel pins of 41,772. A peaking factor of 1.65 was considered for the releases from the secondary side and an average pin activity was considered for the containment release contribution.

4. The containment release contribution was based on 15% fuel failure with all of the activity released to the RCS being released to containment. No credit was taken for activity left in the RCS or transported to the secondary system.

Potential fuel failures are calculated based on the 200 cal/gm for clad damage only. Failures due to violation of the incipient C_L melting threshold are calculated not to occur.

7.3.14.5 Analysis Results

Table 7.3.14-3 lists the 3D peaks versus ejected worths that were generated based on the acceptance criteria for total average enthalpy and incipient C_L melting threshold. The cycle specific physics data is compared to the limits presented in Table 7.2.14-3. If these limits are not exceeded, then no fuel failure is predicted to occur. To accommodate anticipated predicted fuel failure, radiological dose for up to 14% fuel failure due to clad damage has been considered.

The radiological dose results for the 2-hour Exclusion Area Boundary and 8-hour Low Population Zone are well within the 10CFR100 limits of 75 Rem for the thyroid and 6.25 Rem for whole body up to at least 14.0% calculated fuel failure-clad damage with no fuel exceeding incipient C_L melting threshold limits (see Table 7.3.14-4 for radiological dose results).

7.3.15 Fuel Handling Accident

The objective of the fuel handling accident analysis is to document the impact of the following:

- relaxation of auxiliary building fuel handling area integrity requirements during fuel handling;
- increased peaking factor of 1.7;
- increased iodine gas gap release fraction of 0.135;
- use of power uprate (3087 MWt) source terms obtained from the ORIGEN-II code; and
- updated Control Room χ/Q values.

The above changes resulted in an increase in the radiological doses that were within the acceptance criteria.

7.3.15.1 General Description of the Event

The analysis assumes that a fuel assembly is dropped during fuel handling. The worst case fuel assembly horizontal impact results from a vertical drop, followed by rotation of the fuel assembly to the horizontal position. During this rotation, it is postulated that the assembly strikes a protruding structure failing no more than four rows of fuel rods.

As part of the power uprate analyses, the exclusion area boundary (EAB) and control room dose consequences of a fuel handling accident (FHA) were reviewed. One bounding assessment was performed to cover both a fuel handling event in containment and the spent fuel building.

7.3.15.2 Purpose of Analysis and Acceptance Criteria

The purpose of this analysis is to assess the impact of pin failures due to a fuel assemble drop. The analysis acceptance criterion:

radiological doses < well within (25%) 10CFR100 limits.

The fuel handling accident is described in Chapter 15.1.23 of the SAR (Reference 7.3-1).

7.3.15.3 Impact of Changes

The use of one bounding analysis for both the containment location and the spent fuel building location simplifies the analysis approach, however, this results in higher radiological doses for the spent fuel building location as no credit is taken in the analysis for filtration.

The increase in core power, peaking factor, and iodine gas gap release fraction results in higher source terms.

Updated control room χ/Q values have been calculated which results in lower calculated operator doses.

7.3.15.4 Analysis Overview

EAB, LPZ, and control room personnel doses following a postulated accident were determined along with ICRP30 dose conversion factors.

Key assumptions employed in the analysis included the following (inputs marked at the end by "***" are changes from the previous analysis):

1. The accident occurs at least 100 hours after plant shutdown, allowing for natural decay.

2. Table 15.1.23-1 shows the gas gap activities for four rows of pins (60 pins). These activities are obtained from an ORIGIN2 analysis. A peaking factor of 1.7 was assumed with gas gap activities consisting of 13.5% iodines, and 10% of noble gases except for Kr-85 which is 30%. ***

3. Four rows of pins (60 pins) are damaged due to the dropped assembly.

4. A core power of 3087 MWt was assumed, which is the proposed rated power of 3026 MWt plus 2% for uncertainties. ***

5. No credit is taken for filtration. ***

6. The containment equipment hatch and personal airlock are assumed to be open.

7. The minimum water depth is 23 feet above the fuel.

8. A site boundary χ/Q of 6.5×10^{-4} seconds / cubic meter was assumed. A control room χ/Q of 1.2×10^{-3} seconds / cubic meter was used. The control room dispersion factor was calculated using ARCON96 consistent with the information provided in Reference 7.3-8,

except the spent fuel building exhaust fan location was used. The spent fuel building location dispersion factor was more limiting than the containment, hence was used in this assessment. ***

9. Refueling canal and spent fuel pool water decontamination factor for noble gases is assumed to be 1.0.

10. All releases to the environment are assumed to occur over a two hour time period.

11. The analysis assumes that the gap inventory is composed of 99.75% inorganic and 0.25% organic iodine. The refueling canal and spent fuel water total effective decontamination factor of iodine is assumed to be 100 (inorganic 133, organic 1).

12. A breathing rate of 3.47×10^{-4} cubic meter / sec was assumed.

7.3.15.5 Analysis Results

The offsite doses for an FHA in the fuel building without credit for the fuel pool ventilation and filtration system, or containment assuming the equipment hatch and personnel airlock are open, are given below.

ANO UNIT 2 FHA – 60 Rod Failure

Dose Category	EAB (2 hr.) Rem
Whole Body	1.0E-01
Skin (1)	3.8E-01
Thyroid	5.3E+01

(1) The "total" skin dose is reported, that is, the skin dose resulting from gamma radiation plus that resulting from beta radiation.

For the design basis FHA in which 60 rods are damaged, the EAB doses are within the regulatory limits without credit for filtration for the fuel building case and without credit for containment integrity for the containment building case. Control room doses were verified to be bounded by the MHA results.

7.3.16 Control Room Uninhabitability

As described in SAR Section 15.1.26, provisions have been made to allow operators to maintain the plant in a safe hot shutdown condition from outside the control room. Remote shutdown facilities allow for plant control after a control room evacuation that is not an Appendix R event. This event has been reviewed for power uprate conditions and verified not to be impacted.

7.3.17 Instantaneous Closure of a Single MSIV

The instantaneous closure of a single MSIV event was analyzed as a part of the replacement steam generator project in Reference 7.3-5 at a rated power of 3026 MWt. It was reviewed and approved in Reference 7.3-6. There are no other changes that impact this event.

7.3.18 CPC Dynamic Filters Analysis

The CPC dynamic filters were analyzed as a part of the replacement steam generator project in Reference 7.3-5 at a rated power of 3026 MWt. This was reviewed and approved in Reference 7.3-6. There are no other changes that impact this analysis.

7.3.19 References for Section 7.3

7.3-1 "Arkansas Nuclear One Unit 2 Safety Analysis Report," Amendment 15, Docket #50-368.

7.3-2 "Technical Manual for the CENTS Code," CENPD 282-P-A, February 1991.

7.3-3 "CETOP-D Code Structures and Modeling Methods for Arkansas Nuclear One – Unit 2," CEN-214(A)-P, July 1982.

7.3-4 "HERMITE, A Multi-Dimensional Space-Time Kinetics Code for PWR Transients," CENPD-188-A, March 1976.

7.3-5 Entergy Letter to NRC, "Arkansas Nuclear One – Unit 2, Docket No. 50-368, License No. NPF-6, Proposed Technical Specification Changes And Resolution of Unreviewed Safety Question Associated With Applicable Limits AND Setpoints Supporting Steam Generator Replacement," 2CAN119901, dated November 29,1999.

7.3-6 NRC Letter to Entergy, "Arkansas Nuclear One, Unit No. 2 – Issuance of Amendment Re: Technical Specification Changes and Unreviewed Safety Question Resolution Related to Applicable Limits and Setpoints for Steam Generator Replacement 9TAC No. MA7299)," 2CNA090002, dated September 29, 2000.

7.3-7 "TORC Code: A Computer Code for Determining the Thermal Margin of a Reactor Core," CENPD-161-P-A, April 1986.

7.3-8 Entergy Letter to NRC, "Arkansas Nuclear One – Unit 2, Docket No. 50-368, License No. NPF-6, Supplemental Information on Reactor Protection System Setpoint Changes – Probabilistic Safety Assessment Branch, " 2CAN080004, dated August 4, 2000.

7.3-9 "STRIKIN II, A Cylindrical Geometry Fuel Rod Heat Transfer Program," CENPD-135P, August 1974.

"STRIKIN II, A Cylindrical Geometry Fuel Rod Heat Transfer Program (Modification)," CENPD-135P, Supplement 2, February 1975.

"STRIKIN II, A Cylindrical Geometry Fuel Rod Heat Transfer Program," CENPD-135P, Supplement 4-P, August 1976.

7.3-10 "Safety Evaluation by the Office of Nuclear Reactor Regulation Supporting Amendment No. 24 to Facility Operating License No. NPF-6 Arkansas Power and Light Company, Arkansas Nuclear One, Unit No. 2, Docket No. 50-368."

7.3-11 "C-E Method for Control Element Assembly Ejection Analysis," CENPD-190-A, July 1976.

7.3-12 "User's Guide for the TACT5 Computer Code," NUREG/CR-5106, June 1988.

Table 7.3.0-1

Analysis Status of Design Basis Events, Cycle 16, 3026 MWt

SAR Section	Power Uprate Report Section	Section Title	Analysis Status
15.1.1	7.3.1	Uncontrolled CEA Withdrawal from a Subcritical Condition	Reanalyzed
15.1.2	7.3.2	Uncontrolled CEA Withdrawal from Critical Conditions: Hot Zero Power (HZP) Hot Full Power (HFP)	 Reanalyzed Reanalyzed
15.1.3	7.3.3	CEA Misoperation	Reanalyzed
15.1.4	7.3.4	Uncontrolled Boron Dilution Incident: Modes 1 and 2 Modes 3, 4, 5, and 6	 Reanalyzed Reanalyzed
15.1.5	7.3.5	Total and Partial Loss of RCS Forced Flow: Four Pump Loss of Flow Seized Rotor	 Reanalyzed Reanalyzed
15.1.6	None	Idle Loop Startup	Not Reanalyzed
15.1.7	7.3.6	Loss of External Load and/or Turbine Trip	Reanalyzed w/ RSG
15.1.8	7.3.7	Loss of Normal Feedwater Flow	Reanalyzed w/ RSG
15.1.9	7.3.8	Loss of All Normal and Preferred AC Power to the Station Auxiliaries	Reanalyzed w/ RSG
15.1.10	7.3.9	Excess Heat Removal Due to Secondary System Malfunction	Reanalyzed w/ RSG
15.1.11	None	Failure of the Regulating Instrumentation	Not Applicable
15.1.12	None	Internal and External Events Including Major and Minor Fires, Floods, Storms, and Earthquakes	Not Reanalyzed
15.1.13	7.3.10	Major Rupture of Pipes Containing Reactor Coolant up to and Including Double-Ended Rupture of Largest Pipe in the Reactor Coolant System (MHA)	Reanalyzed
15.1.14	7.3.11 7.3.11.1 7.3.11.2	Major Secondary System Pipe Breaks with or without a Concurrent Loss of AC Power: Main Steam Line Break (MSLB) Feedwater Line Break (FWLB)	 Reanalyzed w/ RSG Reanalyzed
15.1.15	7.3.12	Inadvertent Loading of a Fuel Assembly into the Improper Position	Reanalyzed
15.1.16	None	Waste Gas Decay Tank Leakage or Rupture	Not Reanalyzed
15.1.17	None	Failure of Air Ejector Lines (BWR)	Not Applicable

Table 7.3.0-1 (Cont.)

SAR Section	Power Uprate Report Section	Section Title	Analysis Status
15.1.18	7.3.13	Steam Generator Tube Rupture with or without a Concurrent Loss of AC Power (SGTR)	Reanalyzed
15.1.19	None	Failure of Charcoal of Cryogenic System (BWR)	Not Applicable
15.1.20	7.3.14	CEA Ejection: HZP HFP	 Reanalyzed Reanalyzed
15.1.21	None	Spectrum of Rod Drop Accidents (BWR)	Not Applicable
15.1.22	None	Break in Instrument Line or Other Lines from Reactor Coolant Pressure Boundary that Penetrate Containment	Not Reanalyzed
15.1.23	7.3.15	Fuel Handling Accident	Reanalyzed
15.1.24	None	Small Spills or Leaks of Radioactive Material Outside Containment	Not Reanlayzed
15.1.25	None	Fuel Cladding Failure Combined with Steam Generator Leak	Not Reanlayzed
15.1.26	7.3.16	Control Room Uninhabitability	Not Reanalyzed
15.1.27	None	Failure or Over pressurization of Low Pressure Residual Heat Removal System	Not Reanalyzed
15.1.28	(See 7.3.6)	Loss of Condenser Vacuum (LOCV)	Not Reanalyzed
15.1.29	(See 7.3.6)	Turbine Trip with Coincident Failure of Turbine Bypass Valves to Open	Not Reanalyzed
15.1.30	None	Loss of Service Water System	Not Reanalyzed
15.1.31	None	Loss of One DC System	Not Reanalyzed
15.1.32	None	Inadvertent Operation of ECCS during Power Operation	Not Reanalyzed
15.1.33	None	Turbine Trip with Failure of Generator Breaker to Open	Not Reanalyzed
15.1.34	None	Loss of Instrument Air System	Not Reanalyzed
15.1.35	None	Malfunction of Turbine Gland Sealing System	Not Reanalyzed
15.1.36	7.3.17	Transients Resulting from the Instantaneous Closure of a Single MSIV	Reanalyzed w/ RSG

Table 7.3.0.1-1

Initial Conditions for Safety Analyses		
Core Parameter	**Units**	**Analysis Value**
Core Power (nominal / with uncertainty) Rated	MWt	 3026 / 3087
Reactor Coolant Pump (total) Nominal Maximum	MWt	 10 18
Steady State Core Inlet Temperature (including uncertainty) Hot Full Power Hot Zero Power	°F	 $540.0 \leq Tin \leq 556.7$ $523.0 \leq Tin \leq 552.0$
Steady State Pressurizer Pressure (including uncertainty) [1]	psia	$2000 \leq Prz\ Press \leq 2300$
Steady State RCS Flow (including uncertainty)	gpm	$315{,}560 \leq Flow \leq 386{,}400$
Steady State Axial Shape	ASI	$-0.3 \leq ASI \leq +0.3$
Moderator Temperature Coefficient	$\Delta\rho$/°F	Figure 7.3.0.2-1
Maximum Linear Heat Rate	kW/ft	13.7
CEA Insertion Time	position vs. time	Figure 7.3.0.2-4
Steady State Linear Heat Rate for Centerline Melt Limit	kW/ft	21.0
DNB SAFDL CE-1 MacBeth		 1.25 1.30
Pressurizer Safety Valves Opening Setpoint Tolerance	 psia %	 2500 ± 3 [2]
Main Steam Safety Valves Opening Setpoints Bank 1 Banks 2 and 3 Banks 4 and 5 Tolerance	 psig %	 1078 1105 1132 ± 3 [2]

[1] Initial pressures are input as pressurizer pressure. Plots are of RCS pressure. Therefore the initial values on the plots are slightly higher by 20 to 30 psi than the value quoted in the "Assumptions" tables.

[2] Larger tolerances were conservatively used for some analyses.

Table 7.3.0.1-2

RPS/ESFAS Setpoints and Response Times

RPS / ESFAS Signal	Analysis Setpoint, Units	Response Time, seconds
High Containment Pressure		
RPS trip	20.7 psia	1.2[7]
High Logarithmic Power Level		
RPS trip	4% of rated	0.4
Low Pressurizer Pressure		
RPS trip	1400 psia	1.2
SIAS (time for HPSI pumps to reach speed and all valves to open)	1400 psia[1]	40[3]
High Pressurizer Pressure		
RPS trip		0.65[2]
Normal	2392 psia	
Harsh	2415 psia	
Low Steam Generator Level		
RPS trip		1.3
Normal	9 % of NR	
Abnormal	6 % of NR	
EFAS setpoint		
Normal	9 % of NR	
Harsh (FWLB only)	0 % of NR	
EFW Train A		97.4[3]
EFW Train B		112.4[3][4]/97.4 [3][5]
EFAS Isolation	220 psid	1.4
Low Steam Generator Pressure		
RPS trip		1.3
Normal	693 psia	
MSIS		
Normal	693 psia	
Adverse	658 psia	
Main Steam Isolation Valve		4.9[3]
Feedwater Isolation Valves		41.4[3][4]/26.4 [3][5]
Feedwater Backup Valves		34.9[3][4]/19.9 [3][5]

Table 7.3.0.1-2 cont.

RPS / ESFAS Signal	Analysis Setpoint, Units	Response Time, seconds
Core Protection Calculator System		
Low RCP Shaft Speed	0.95	0.4
ASGTP function - ΔTcold	11° F	0.4 [6]
Variable Overpower Trip		0.4 [6]
Floor	30 % of rated	
Ceiling	110 % of rated	
DELSPV (difference)	10 % of rated	
SPVMAX (rate),	1 % /minute	
Effective RTD Time Constant, seconds		
Hot Leg	-	13
Cold Leg	-	8

[1] SGTR conservatively uses a maximum setpoint of 1800 psia to maximize radiological doses.
[2] FWLB conservatively uses a response time of 0.9 seconds.
[3] Overall ESFAS response time as part of the specific ESFAS function, which is defined as part of the individual event section.
[4] Diesel generator starting and sequence loading delays included.
[5] Diesel generator starting delays not included, sequencing loading delays included. Offsite power available.
[6] Does not include two cycles of 0.1 seconds for the CPCS UPDATE subroutine execution time.
[7] A response time of 1.59 seconds has been conservatively used for some analyses.

Table 7.3.1-1

Assumptions for the Cycle 16 Uncontrolled CEA Withdrawal from a Subcritical Condition

Parameter	Units	Case 1 Conservative Assumptions	Case 2 Conservative Assumptions
Initial Core Power Level	MWt	$9.63 * 10^{-7}$	$9.63 * 10^{-7}$
RCP Heat	MWt	18	18
Core Inlet Coolant Temperature	°F	552	552
Reactor Coolant System Flow	10^6 lbm/hr	117.78	117.78
Pressurizer Pressure [1]	psia	2000	2000
Steam Generator Pressure	psia	1058	1058
Moderator Temperature Coefficient	10^{-4} Δρ/°F	+0.5	+0.5
Fuel Temperature Coefficient	-	BOC	BOC
CEA Reactivity Addition Rate	10^{-4} Δρ/sec	2.5	2.0
Total Nuclear Heat Flux Factor	-	6.8	9.0
Steam Bypass System	-	Manual	Manual
Feedwater Regulating System	-	Manual	Manual

[1] Initial pressures are input as pressurizer pressure. Plots are of RCS pressure. Therefore the initial values on the plots are slightly higher by 20 to 30 psi than the value quoted in the "Assumptions" tables.

Table 7.3.1-2

Sequence of Events for the Cycle 16 Uncontrolled CEA Withdrawal from a Subcritical Condition with a RIR of 2.5 * 10^{-4} $\Delta\rho$/sec

Time, seconds	Event	Setpoint or Value
0.0	Initiation of CEA bank withdrawal	- - -
256.5	High logarithmic power level trip condition	4 % of full power
256.9	Trip breakers open, and rod withdrawal stops,	- - -
257.3	Maximum power occurs	93.3 % of full power
257.5	CEAs begin to drop	- - -
257.6	Maximum heat flux occurs, and minimum DNBR	33.2 % of full power > 1.25
261.1	Maximum RCS pressure occurs (includes pump head)	< 2750 psia
300.0	End of transient	- - -

Table 7.3.1-3

Sequence of Events for the Cycle 16 Uncontrolled CEA Withdrawal from a Subcritical Condition with a RIR of 2.0 * 10^{-4} $\Delta\rho$/sec

Time, seconds	Event	Setpoint or Value
0.0	Initiation of CEA bank withdrawal	- - -
320.1	High logarithmic power level trip condition	4 % of full power
320.5	Trip breakers open, and rod withdrawal stops,	- - -
321.1	CEAs begin to drop and Maximum power occurs	- - - 73.8 % of full power
321.2	Maximum heat flux occurs, and minimum DNBR	23.4 % of full power > 1.25
324.7	Maximum RCS pressure occurs (includes pump head)	< 2750 psia
400.0	End of transient	- - -

Table 7.3.2-1

Assumptions for the Cycle 16
Uncontrolled CEA Withdrawal at Hot Full Power

Parameter	Units	Conservative Assumptions
Initial Core Power Level	MWt	3087
RCP Heat	MWt	18
Core Inlet Coolant Temperature	°F	556.7
Reactor Coolant System Flow	gpm	315,560
Pressurizer Pressure [1]	psia	2000
Steam Generator Pressure	psia	1044
Moderator Temperature Coefficient	10^{-4} Δρ/°F	0.0
Fuel Temperature Coefficient	-	BOC
CEA Worth on Trip	10^{-2} Δρ	-5.0
CEA Reactivity Addition Rate	10^{-4} Δρ/sec	1.0
Steam Bypass System	-	Manual

[1] Initial pressures are input as pressurizer pressure. Plots are of RCS pressure. Therefore the initial values on the plots are slightly higher by 20 to 30 psi than the value quoted in the "Assumptions" tables.

Table 7.3.2-2

Assumptions for the Cycle 16
Uncontrolled CEA Withdrawal at Hot Zero Power

Parameter	Units	Conservative Assumptions
Initial Core Power Level	MWt	0.0003026
RCP Heat	MWt	18
Core Inlet Coolant Temperature	°F	552
Reactor Coolant System Flow	gpm	315,560
Pressurizer Pressure [1]	psia	2000
Steam Generator Pressure	psia	1058
Moderator Temperature Coefficient	10^{-4} Δρ/°F	+0.5
Fuel Temperature Coefficient	-	BOC
CEA Worth on Trip	10^{-2} Δρ	-2.0
CEA Reactivity Addition Rate	10^{-4} Δρ/sec	1.8
Total Nuclear Heat Flux Factor	-	7.7
Steam Bypass System	-	Manual
Feedwater Regulating System	-	Manual
Automatic Withdrawal Prohibit	-	Inoperative

[1] Initial pressures are input as pressurizer pressure. Plots are of RCS pressure. Therefore the initial values on the plots are slightly higher by 20 to 30 psi than the value quoted in the "Assumptions" tables.

Table 7.3.2-3

Sequence of Events for the Cycle 16
Uncontrolled CEA Withdrawal at Hot Full Power

Time, seconds	Event	Setpoint or Value
0	Initiation of CEA bank withdrawal	- - -
6.5	CPCS VOPT trip condition occurs	112.4 %
7.1	Trip breakers open	- - -
7.7	Maximum power occurs, and CEAs begin to drop	114% of full power - - -
8.1	Maximum heat flux occurs, and minimum DNBR	111% of full power > 1.25
9.7	Maximum RCS pressure occurs (includes pump head)	< 2750 psia

Table 7.3.2-4

Sequence of Events for the Cycle 16
Uncontrolled CEA Withdrawal at Hot Zero Power

Time, seconds	Event	Setpoint or Value
0.0	Initiation of CEA bank withdrawal	- - -
22.4	CPCS VOPT trip condition occurs	36 % of full power
23.0	Trip breakers open and rod withdrawal Stops	- - -
23.2	Maximum power occurs	75.5 % of full power
23.6	CEAs begin to drop	
23.7	Maximum heat flux occurs, and minimum DNBR	38% of full power > 1.25
27.7	Maximum RCS pressure occurs (includes pump head)	< 2750 psia

Table 7.3.3-1

Assumptions for the Cycle 16 CEA Misoperation at Power

Parameter	Units	Conservative Assumptions
Core Inlet Coolant Temperature	°F	540 to 556.7
Reactor Coolant System Flow	gpm	315,560 to 386,400
Pressurizer Pressure	psia	2000 to 2300
Steady State Axial Shape	ASI	-0.3 to +0.3

Table 7.3.4-1

Assumptions for the Cycle 16
Uncontrolled Boron Dilution Event Mode 6 (Refueling Condition)

Parameter	Units	Conservative Assumptions
Reactor Vessel Volume to the Nozzles	ft^3	2457
Charging Rate	gpm	138
Initial Boron Concentration	Keff	0.95
Critical Boron Concentration	ppm	Figure 7.3.4-1

Table 7.3.4-2

Assumptions for the Cycle 16
Uncontrolled Boron Dilution Event
Mode 5 (Cold Shutdown)
Partially Drained

Parameter	Units	Conservative Assumptions
RCS Volume – Partially Drained Reactor Vessel to Nozzles plus One Shutdown Cooling System Loop	ft^3	2901
Charging Rate	gpm	138
Critical Boron Concentration	ppm	Figure 7.3.4-2
Initial Shutdown Reactivity *	10^{-2} Δρ	-5.0

* Note that a value of $-3.3 * 10^{-2}$ Δρ was actually used in the analysis. This is due to the boron dilution count rate monitor providing an alarm when the count rate reaches 1.5 times the background rate.

Table 7.3.4-3a

Assumptions for the Cycle 16
Uncontrolled Boron Dilution Event
Mode 5 (Cold Shutdown)
Alarms Inoperable

Parameter	Units	Conservative Assumptions
RCS Volume – Filled Reactor Vessel to Nozzles plus One Shutdown Cooling System Loop	ft^3	4647
Charging Rate	gpm	138
Critical Boron Concentration	ppm	Figure 7.3.4-3
CEA Worth on Trip	10^{-2} Δρ	-2.0

Table 7.3.4-3b

Assumptions for the Cycle 16
Uncontrolled Boron Dilution Event
Mode 5 (Cold Shutdown)
Alarms Operable

Parameter	Units	Conservative Assumptions
RCS Volume – Filled Reactor Vessel to Nozzles plus One Shutdown Cooling System Loop	ft^3	4647
Charging Rate	gpm	138
Critical Boron Concentration	ppm	Figure 7.3.4-4
Initial Shutdown Reactivity *	$10^{-2}\ \Delta\rho$	-5.0

* Note that a value of $-3.3 * 10^{-2}\ \Delta\rho$ was actually used in the analysis. This is due to the boron dilution count rate monitor providing an alarm when the count rate reaches 1.5 times the background rate.

Table 7.3.4-4a

Assumptions for the Cycle 16
Uncontrolled Boron Dilution Event
Mode 4 (Hot Shutdown)
Alarms Inoperable

Parameter	Units	Conservative Assumptions
RCS Volume – Filled Reactor Vessel to Nozzles plus One Shutdown Cooling System Loop	ft^3	4647
Charging Rate	gpm	138
Critical Boron Concentration	ppm	Figure 7.3.4-5
CEA Worth on Trip	10^{-2} Δρ	-2.0

Table 7.3.4-4b

Assumptions for the Cycle 16
Uncontrolled Boron Dilution Event
Mode 4 (Hot Shutdown)
Alarms Operable

Parameter	Units	Conservative Assumptions
RCS Volume – Filled Reactor Vessel to Nozzles plus One Shutdown Cooling System Loop	ft^3	4647
Charging Rate	gpm	138
Critical Boron Concentration	ppm	Figure 7.3.4-6
Initial Shutdown Reactivity	10^{-2} Δρ	-5.0

* Note that a value of $-3.3 * 10^{-2}$ Δρ was actually used in the analysis. This is due to the boron dilution count rate monitor providing an alarm when the count rate reaches 1.5 times the background rate.

Table 7.3.4-5a

Assumptions for the Cycle 16
Uncontrolled Boron Dilution Event
Mode 3 (Hot Standby)
Alarms Inoperable

Parameter	Units	Conservative Assumptions
RCS Volume – Filled Reactor Vessel to Nozzles plus One Shutdown Cooling System Loop	ft^3	4647
Charging Rate	gpm	138
Critical Boron Concentration	ppm	Figure 7.3.4-7
CEA Worth on Trip	10^{-2} $\Delta\rho$	-2.0

Table 7.3.4-5b

Assumptions for the Cycle 16
Uncontrolled Boron Dilution Event
Mode 3 (Hot Standby)
Alarms Operable

Parameter	Units	Conservative Assumptions
RCS Volume – Filled Reactor Vessel to Nozzles plus One Shutdown Cooling System Loop	ft^3	4647
Charging Rate	gpm	138
Critical Boron Concentration	ppm	Figure 7.3.4-8
Initial Shutdown Reactivity	10^{-2} $\Delta\rho$	-5.0

* Note that a value of $-3.3 * 10^{-2}$ $\Delta\rho$ was actually used in the analysis. This is due to the boron dilution count rate monitor providing an alarm when the count rate reaches 1.5 times the background rate.

Table 7.3.4-6

Assumptions for the Cycle 16
Uncontrolled Boron Dilution Event
Critical Operation (Startup Condition)

Parameter	Units	Conservative Assumptions
RCS Volume	ft^3	9040
Charging Rate	gpm	138
Critical Boron Concentration	ppm	Figure 7.3.4-9
Initial Shutdown Reactivity	$10^{-2}\ \Delta\rho$	-5.0

Table 7.3.5.1-1

Four Reactor Coolant Pump Flow Coastdown Resulting from an Electrical Failure

Time (Seconds)	Core Flow Rate (Normalized)
0.0	1.000
0.5	0.970
1.0	0.931
1.5	0.894
2.0	0.859
2.5	0.827
3.0	0.798
3.5	0.771
4.0	0.745
4.5	0.721
5.0	0.698

Table 7.3.5.1-2

Assumptions for the Cycle 16
4-Pump Loss of Coolant Flow Analysis

Parameter	Units	Minimum Subcooling Assumptions	Maximum Subcooling Assumptions
Initial Core Power Level	MWt	3087	3087
Core Inlet Coolant Temperature	°F	556.7	540.0
Reactor Core Mass Flow	* 10^6 lbm/hr	118.0	142.1
Pressurizer Pressure	psia	2000	2300
Radial Peak Factor, Fr	- - -	1.71	1.28
Axial Shape Index	- - -	0.3	0.3
Moderator Temperature Coefficient	10^{-4} $\Delta\rho$/°F	0.0	0.0
CEA Worth on Trip	10^{-2} $\Delta\rho$	-5.0	-5.0

Table 7.3.5.1-3

Sequence of Events for the Cycle 16
4-Pump Loss of Coolant Flow Analysis

Time (sec)			Setpoint or Value	
Maximum Subcooled	Minimum Subcooled	Event	Maximum Subcooled	Minimum Subcooled
0.0	0.0	Loss of power to all four reactor coolant pumps	- - -	- - -
0.8	0.8	CPC Low RCP Speed Trip	95% nominal speed	95% nominal speed
1.2	1.2	Trip breakers open	- - -	- - -
1.8	1.8	Shutdown CEAs begin to drop into core	- - -	- - -
3.10	3.05	Minimum CE-1 DNBR	≥ 1.25	≥1.25

Table 7.3.5.2-1

Assumptions for the Cycle 16
Loss of Coolant Flow Pump Shaft Seizure Analysis

Parameter	Units	Assumptions
Initial Core Power Level	MWt	3087
RCP heat	MWt	18
Core Inlet Coolant Temperature	°F	556.7
Reactor Coolant System Flow	gpm	386,400
Pressurizer Pressure[1]	psia	2300
Steam Generator Pressure	psia	967
Moderator Temperature Coefficient	10^{-4} Δρ/°F	-0.2
Fuel Temperature Coefficient	- - -	BOC
CEA Worth on Trip	10^{-2} Δρ	-5.0
Steam Bypass System	- - -	Manual
Feedwater Regulating System	- - -	Automatic

[1] Initial pressures are input as pressurizer pressure. Plots are of RCS pressure. Therefore the initial values on the plots are slightly higher by 20 to 30 psi than the value quoted in the "Assumptions" tables.

Table 7.3.5.2-2

Sequence of Events for the Cycle 16 (Typical Case)
Loss of Coolant Flow Pump Shaft Seizure Analysis

Time, seconds	Event	Setpoint or Value
0.0	Shaft seizure on one reactor coolant pump	- - -
0.3	CPC low RCP speed trip occurs	95% of Nominal
0.8	Reactor trip breakers open	- - -
1.3	DNBR falls below SAFDL	< 1.25
1.4	Shutdown CEAs begin to drop into the core	- - -
1.9	Minimum DNBR occurs	- - -
2.10	Core flow reaches asymptotic three-pump value	73% of Initial Flow
4.10	Maximum RCS pressure occurs	<< 2750 psia

Table 7.3.6-1

Inoperable MSSVs
Maximum Allowable MTC, Linear Power Level and High Trip Setpoint

Maximum Number of MSSVs Inoperable	MTC, 10^{-4} Δρ/°F	Maximum Allowable Linear Power Level and High Trip Setpoint, % of Rated Thermal Power[(1)]
1	-2.1	91
	-1.3	87
	-0.6	83
	0	79

Maximum Number of MSSVs Inoperable per Steam Generator	MTC, 10^{-4} Δρ/°F	Maximum Allowable Linear Power Level and High Trip Setpoint, % of Rated Thermal Power[(1)]
1	-2.5	87
	-1.6	83
	-0.81	79
	-0.17	75
	-0.0	71
2	N/A	43
3	N/A	25

[(1)] Percent of 3026 MWt

Table 7.3.10-1
Parameters Used in the LOCA Analysis

Parameter	Value
Power level for analysis MWt (102%)	3087
Fraction of iodine released from core	0.25 (50% release * 50% plateout)
Fraction of noble gases released from core	1.0
Iodine species distribution	0.91 elemental 0.04 organic 0.05 particulate
Reactor building free volume	1.778E6 ft^3
Sump volume	62898 ft^3
Sprayed volume	1.33E6 ft^3
Unsprayed volume	3.83E5 ft^3
Control room volume	40,000 ft^3
Initial fraction	0.22 to unsprayed 0.78 to sprayed
Exclusion area boundary (EAB) χ/Q	6.5E-4 sec/m^3
Low population zone (LPZ) χ/Q's	3.1E-5 sec/m^3 0-8 hrs 3.6E-6 sec/m^3 8-24 hours 2.3E-6 sec/m^3 1-4 days 1.4E-6 sec/m^3 4-30 days
Control room (CR) χ/Q's	9.77E-4 sec/m^3 0-2 hrs 5.76E-4 sec/m^3 2-8 hrs 2.56E-4 sec/m^3 8-24 hrs 1.68E-4 sec/m^3 1-4 days 1.25E-4 sec/m^3 4-30 days
Offsite breathing rates	3.47E-4 m^3/sec for 0-8 hours 1.750E-4 m^3/sec for 8-24 hrs 2.32E-4 m^3/sec for > 24 hours
Control room breathing rates	3.47E-4 m^3/sec in CR throughout
Dose conversion factors	ICRP30
Penetration room ventilation system filter efficiency	N/A (Not credited for Unit 2)

Table 7.3.10-1 cont.

CR unfiltered inleakage flow	10 cfm
CR filtered inleakage flow	333 cfm
CR recirculation flow	1667 cfm
CR occupancy factors	1.0 for 0-24 hours 0.6 for 1-4 days 0.4 for 4-30 days
CR intake filter efficiency	99%
CR recirculation filter efficiency	95%
Containment mixing rates between sprayed and unsprayed regions	11880 cfm
Containment leak rates	0.1%/day for 1st 24 hrs 0.05%/day >24hrs
Spray removal rates Elemental organic particulate	 20 hr^{-1} until DF = 200 then 0 hr^{-1} no removal 3.97 $^{hr-1}$ prior to recirc, 4.24 $^{hr-1}$ during recirc until DF = 50, then 0.424 hr^{-1}
Release Point	Ground Level
Leakage Rate from ESF Piping Components	2060 cc/hr
Leakage from Passive Component Failure Leakage rate Failure start time Duration	 5 gpm 24 hrs 30 minutes
Iodine Partition Fraction ESF leakage Passive component leakage	 0.1 1.0

Table 7.3.11.2-1

Assumptions for the Cycle 16
Feedwater Line Break

Parameter	Units	Conservative Assumptions
Initial Core Power Level	MWt	3087
RCP Heat	MWt	18
Core Inlet Coolant Temperature	°F	556.7
Reactor Coolant System Flow	gpm	315,560
Pressurizer Pressure[1]	psia	2300
Steam Generator Pressure	psia	999
Moderator Temperature Coefficient	10^{-4} Δρ/°F	-0.2
Fuel Temperature Coefficient	-	BOC
CEA Worth on Trip	10^{-2} Δρ	-5.0
Tolerance on PSV Setpoint	%	+3.2
Tolerance on MSSV Setpoint	%	+3.5
Number of U-tubes assumed plugged per Steam Generator	%	0

(1) Initial pressures are input as pressurizer pressure. Plots are of RCS pressure. Therefore the initial values on the plots are slightly higher by 20 to 30 psi than the value quoted in the "Assumptions" tables.

Table 7.3.11.2-2

Sequence of Events for the Cycle 16
Feedwater Line Break Event

Time, seconds	Event	Setpoint or Value
0.0	Feedwater line break occurs	-
33.3	Low steam generator level trip condition occurs on ruptured SG	40,000 lbm liquid inventory
33.7	High pressurizer trip condition occurs	2415 psia
34.6	Trip breakers open, loss of AC power occurs, RCPs begin coasting down	-
35.2	CEAs begin to drop	-
36.9	Pressurizer safety valves open	2580 psia
37.2	Maximum RCS pressure occurs	2647 psia [(1)]
38.9	Pressurizer safety valves close	2502.5 psia
40.7	EFAS occurs, EFW pump start	0% of NR
55.3	Ruptured steam generator empties	-
90.3	Steam generator low pressure trip condition and MSIS initiated	905 psia
90.3	Main steam isolation valves begin to close	-
90.3	Complete closure of main steam isolation valves terminating blowdown from the intact steam generator	-
96.0	Pressure difference reached between steam generators, EFAS to open EFW valves to feed the intact steam generator	220 psid
153.1	Emergency feedwater enters the intact steam generator	-

Table 7.3.11.2-2 (Cont.)

Time, seconds	Event	Setpoint or Value
190.1	Main steam safety valves open on intact steam generator (begin cycling long term)	1130.94 psia
222.1	Minimum liquid mass in the intact steam generator	117,100 lbm
3000.0	Case terminated	- - -

(1) Includes reactor coolant pump head.

Table 7.3.13-1

Assumptions for the Cycle 16
Steam Generator Tube Rupture with a
Concurrent Loss of AC Power

Parameter	Units	Conservative Assumptions
Initial Core Power Level	MWt	3087
Core Inlet Coolant Temperature	°F	556.7
Reactor Coolant System Flow	10^6 lbm/hr	117.6
Pressurizer Pressure[1]	psia	2300
Steam Generator Pressure	psia	960
Moderator Temperature Coefficient	10^{-4} Δρ/°F	-3.8
Fuel Temperature Coefficient	-	EOC
CEA Worth on Trip	10^{-2} Δρ	-5.0
Steam Bypass System	-	Inoperative
Feedwater Regulating System	-	Inoperative
Steam Generator Blowdown System	-	Inoperative
Steam Condenser	-	Inoperative

(1) Initial pressures are input as pressurizer pressure. Plots are of RCS pressure. Therefore the initial values on the plots are slightly higher by 20 to 30 psi than the value quoted in the "Assumptions" tables.

Table 7.3.13-2

Sequence of Events for the Cycle 16 Steam Generator Tube Rupture with a Concurrent Loss of AC Power

Time, seconds	Event	Setpoint or Value
0.0	Double-ended rupture of a steam generator u-tube and concurrent loss of AC power	- - -
0.6	CPC low RCP speed trip occurs	95% of nominal speed
1.6	Trip breakers open	- - -
2.2	CEAs begin to drop	- - -
4.8	Maximum RCS pressure occurs	2412 psia
5.5	Main steam safety valves open	1054.45 psia
7.4	Maximum secondary pressure occurs	1079 psia
10.4	Emergency feedwater is initiated to the intact SG,	41 % of NR
61.3	Main steam safety valves close	1002.0 psia
251.0	SIAS generated, Charging flow initiated to Primary	1800 psia
521.5	SIAS pumps reach full speed and begin injecting	- - -
1800.0	Operator isolates steam generator with ruptured u-tube, Controlled cooldown of NSSS is initiated	- - -

Table 7.3.13-3

Steam Generator Tube Rupture with a Concurrent Loss of AC Power Dose Results for No Iodine Spike and Event Generated Iodine Spike

Radiological Dose	No Iodine Spike, Rem	Event Generated Iodine Spike, Rem
Thyroid		
EAB	1.4	21.4
LPZ	< 0.1	1.2
Whole Body		
EAB	0.6	0.7
LPZ	< 0.1	< 0.1

Table 7.3.13-4

Steam Generator Tube Rupture with a Concurrent Loss of AC Power Pre-Existing Iodine Spike Radiological Dose Results

Radiological Dose	Pre-existing Iodine Spike, Rem
Thyroid	
EAB	70.0
LPZ	3.5
Whole Body	
EAB	0.9
LPZ	< 0.1

Table 7.3.14-1

Assumptions for the Cycle 16 CEA Ejection Event

Parameter	Units	Conservative Assumptions HZP	Conservative Assumptions HFP
Initial Core Power Level	MWt	30.3	3087
Core Inlet Coolant Temperature	°F	556.7	556.7
Reactor Coolant System Flow	gpm	315,560	315,560
Pressurizer Pressure	psia	2000	2000
Total Delayed Neutron Fraction (β)	-	0.0043414	0.0043414
Moderator Temperature Coefficient	10^{-4} $\Delta\rho$/°F	+0.5	0.0
Fuel Temperature Coefficient	-	BOC	BOC
CEA Worth on Trip	10^{-2} $\Delta\rho$	-2.0	-5.0
CEA Ejection Time	seconds	0.05	0.05

Table 7.3.14-2

Axial Power Distribution Used for the CEA Ejection Event

Fractional Distance from the Bottom of the Reactor Core	Power Fraction , Fz
0.025	0.5
0.075	0.8
0.125	1.0
0.175	1.1
0.225	1.1
0.275	1.1
0.325	1.1
0.375	1.1
0.425	1.1
0.475	1.1
0.525	1.1
0.575	1.1
0.625	1.1
0.675	1.1
0.725	1.1
0.775	1.1
0.825	1.1
0.875	1.0
0.925	0.8
0.975	0.5

Table 7.3.14-3

Cycle 16 CEA Ejection Analysis Results

Initial Power, % of 3026 MWt	Ejected CEA Worth, 10^{-2} $\Delta\rho$	Acceptable Ejected 3D Peak, Fq	Excore Detector Uncertainty, %
100	0.45	3.2	40
	0.25	3.8	
	0.15	4.6	
0	0.80	14.4	40
	0.60	16.5	
	0.45	22.0	

Table 7.3.14-4

Cycle 16 CEA Ejection Radiological Dose Results

Radiological Dose	Rem
Thyroid	
EAB	48
LPZ	15
Whole Body	
EAB	1
LPZ	0.2

Table 7.3.15-1

Gas Gap Activities for Fuel Assemble Drop Accident
Four Rows

Isotope	Four Rows (60 pins) Curies
Kr-85	8.207×10^{2}
I-131	2.099×10^{4}
I-133	2.010×10^{3}
Xe-131m	2.426×10^{2}
Xe-133m	5.392×10^{2}
Xe-133	2.766×10^{4}

Figure 7.3.0.2-1

Moderator Temperature Coefficient vs. Core Power

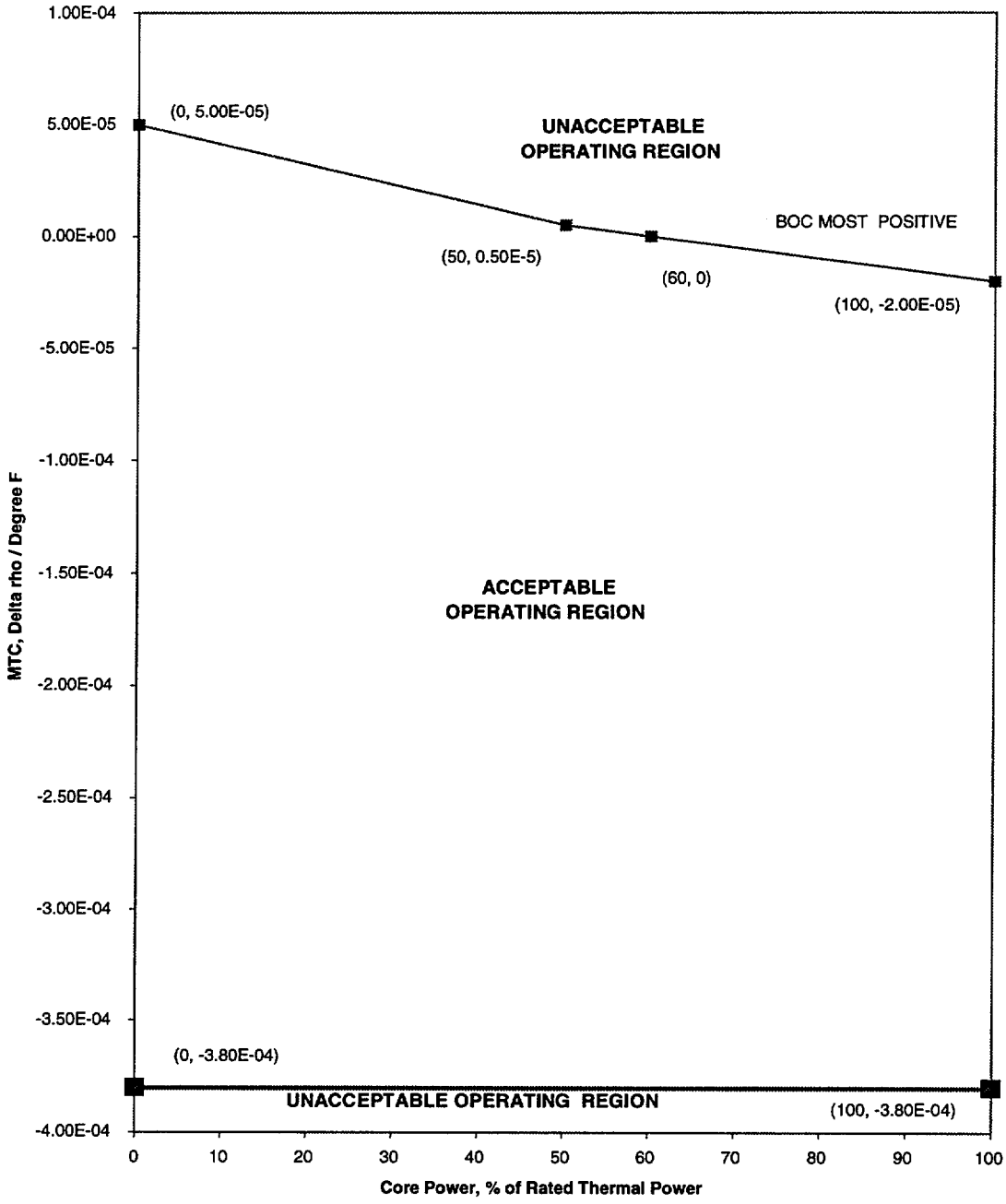

Figure 7.3.0.2-2

Doppler Reactivity vs. Fuel Temperature

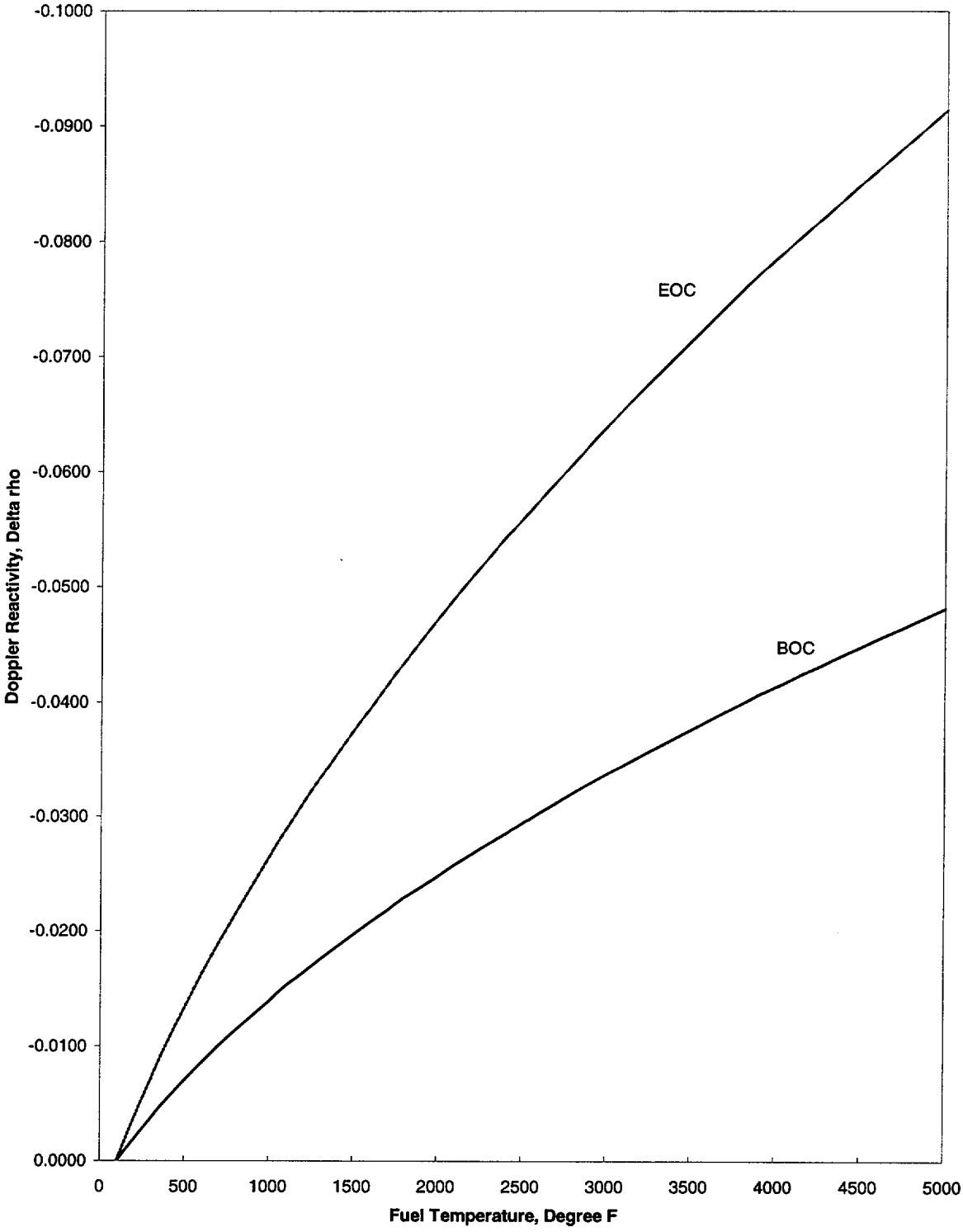

Figure 7.3.0.2-3

Reactivity Insertion vs. Time

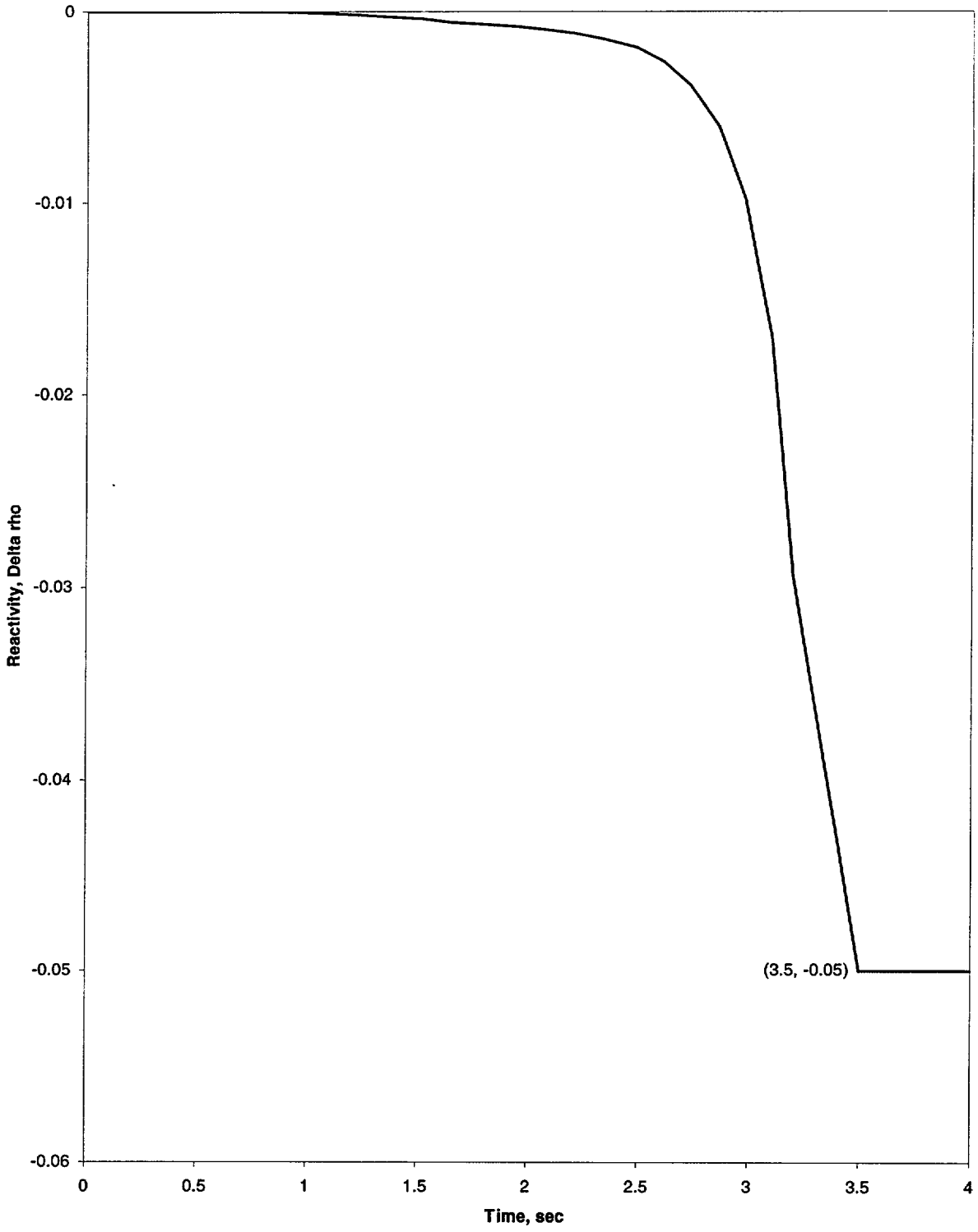

Figure 7.3.0.2-4

CEA Insertion vs. Time

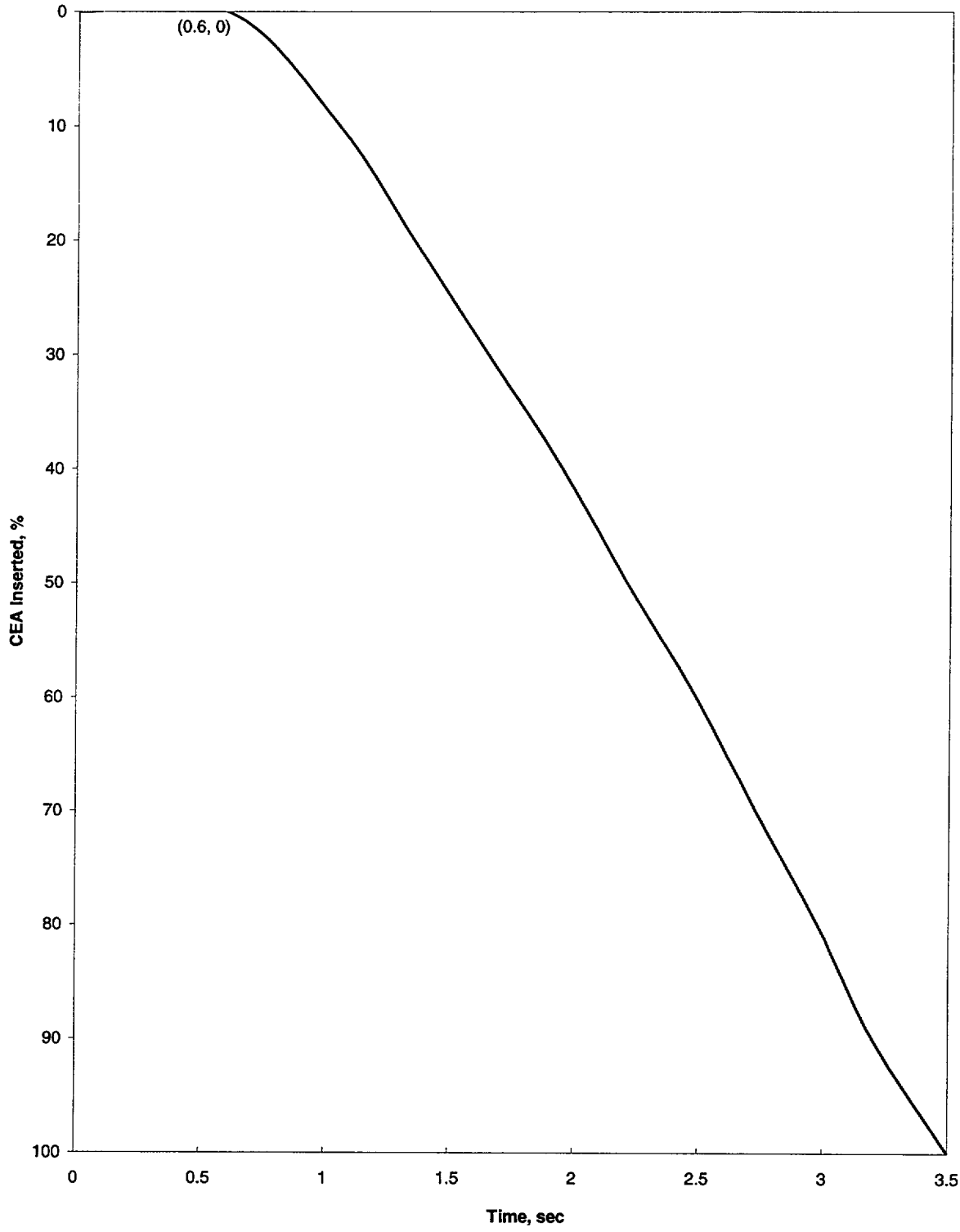

Figure 7.3.1-1

Uncontrolled CEA Bank Withdrawal from Subcritical Conditions with an RIR of 2.5 x 10^{-4} Δρ/sec Core Power vs. Time

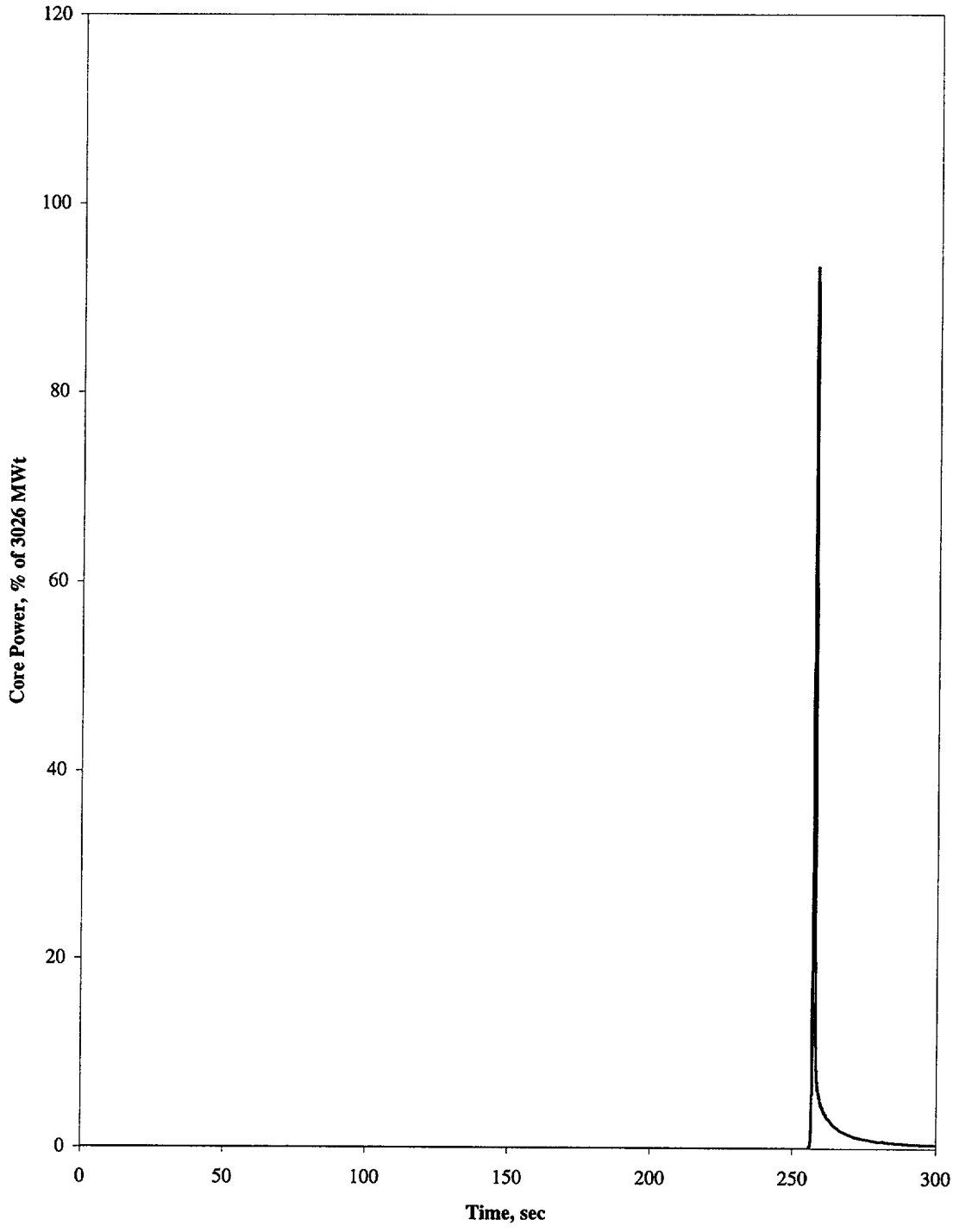

Figure 7.3.1-2

Uncontrolled CEA Bank Withdrawal from Subcritical Conditions with an RIR of 2.5 x 10^{-4} Δρ/sec Core Average Heat Flux vs. Time

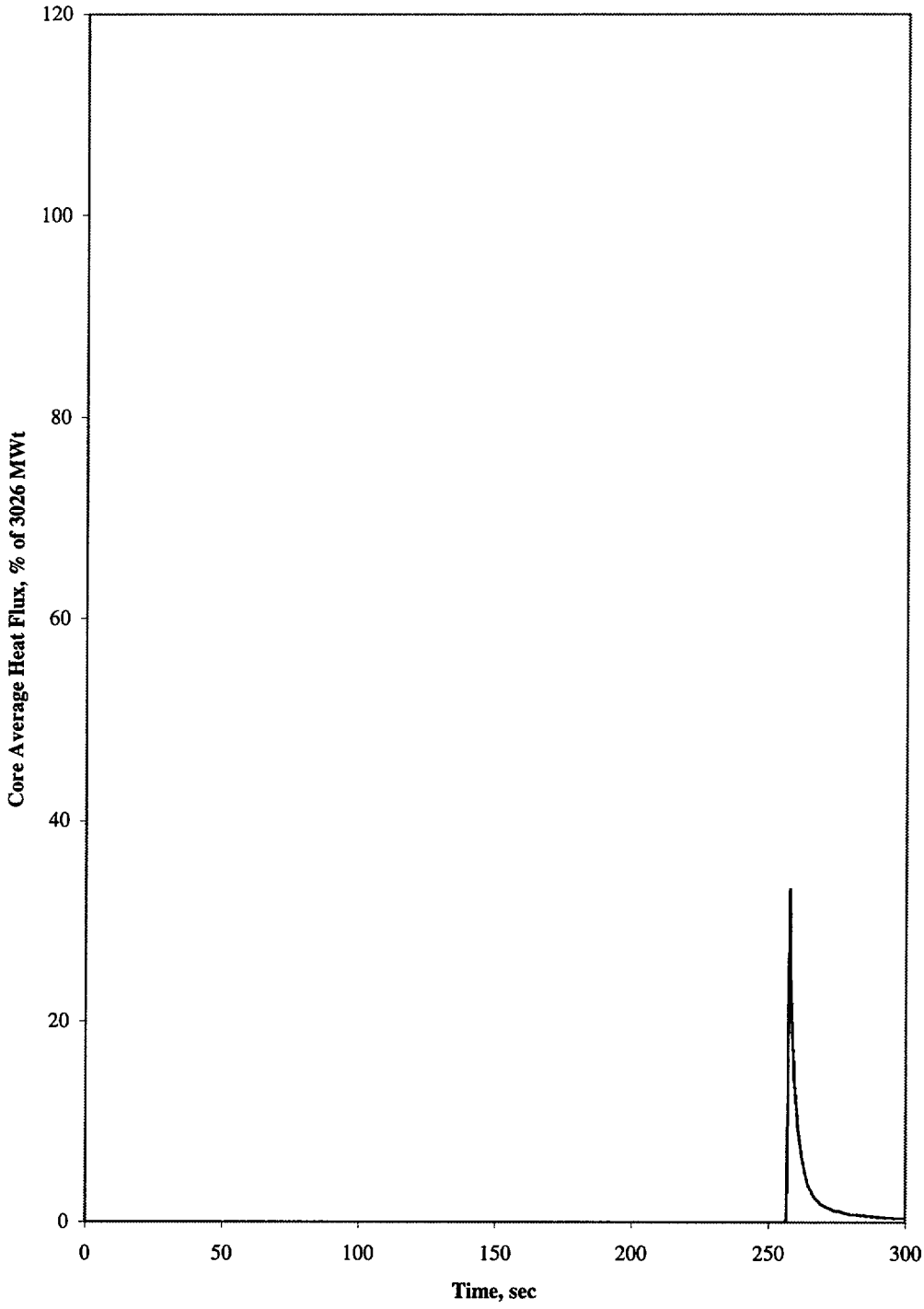

Figure 7.3.1-3

Uncontrolled CEA Bank Withdrawal from Subcritical Conditions with an RIR of 2.5 x 10^{-4} Δρ/sec Reactor Coolant System Pressure vs. Time

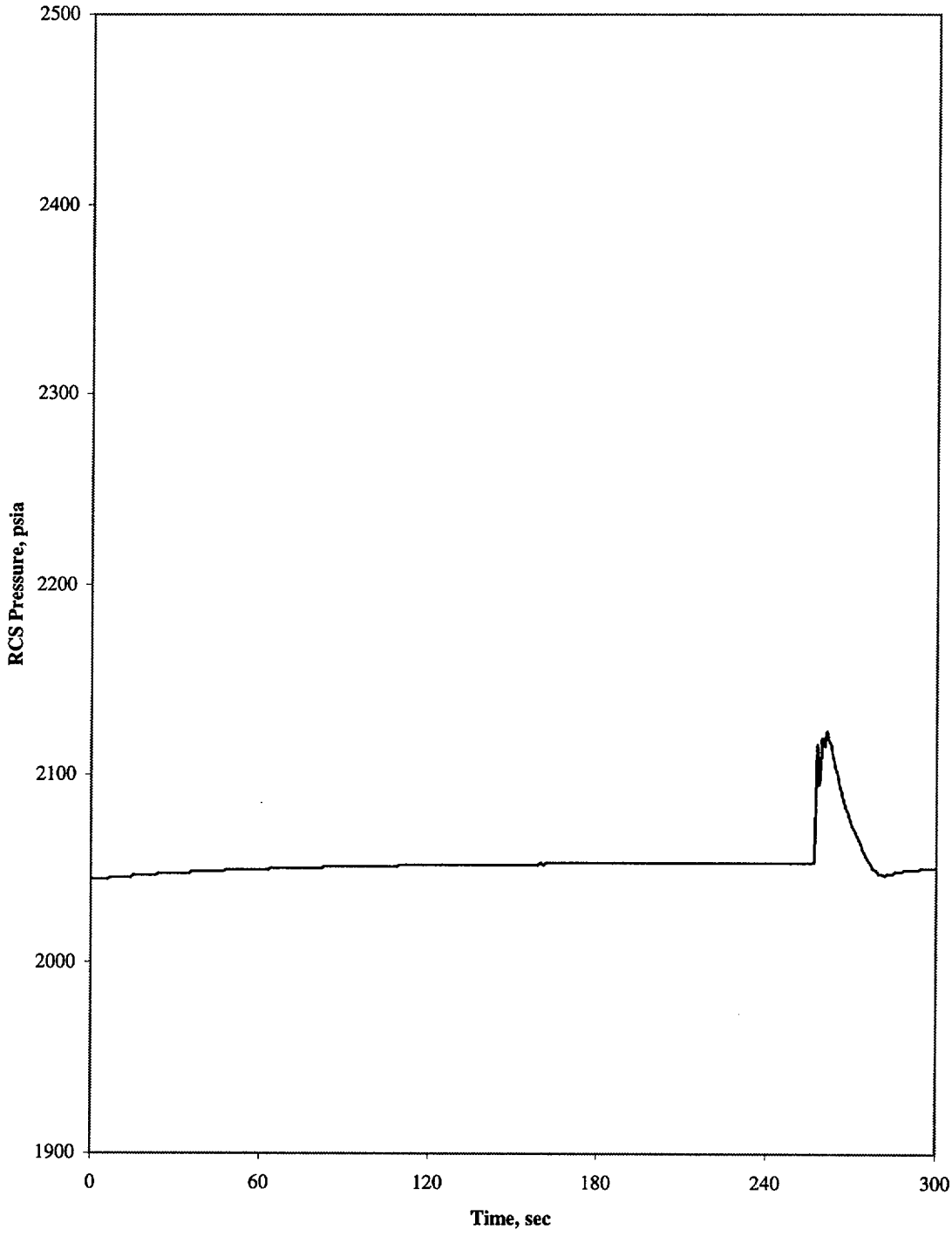

Figure 7.3.1-4

Uncontrolled CEA Bank Withdrawal from Subcritical Conditions with an RIR of 2.5 x 10^{-4} Δρ/sec Reactor Coolant System Temperature vs. Time

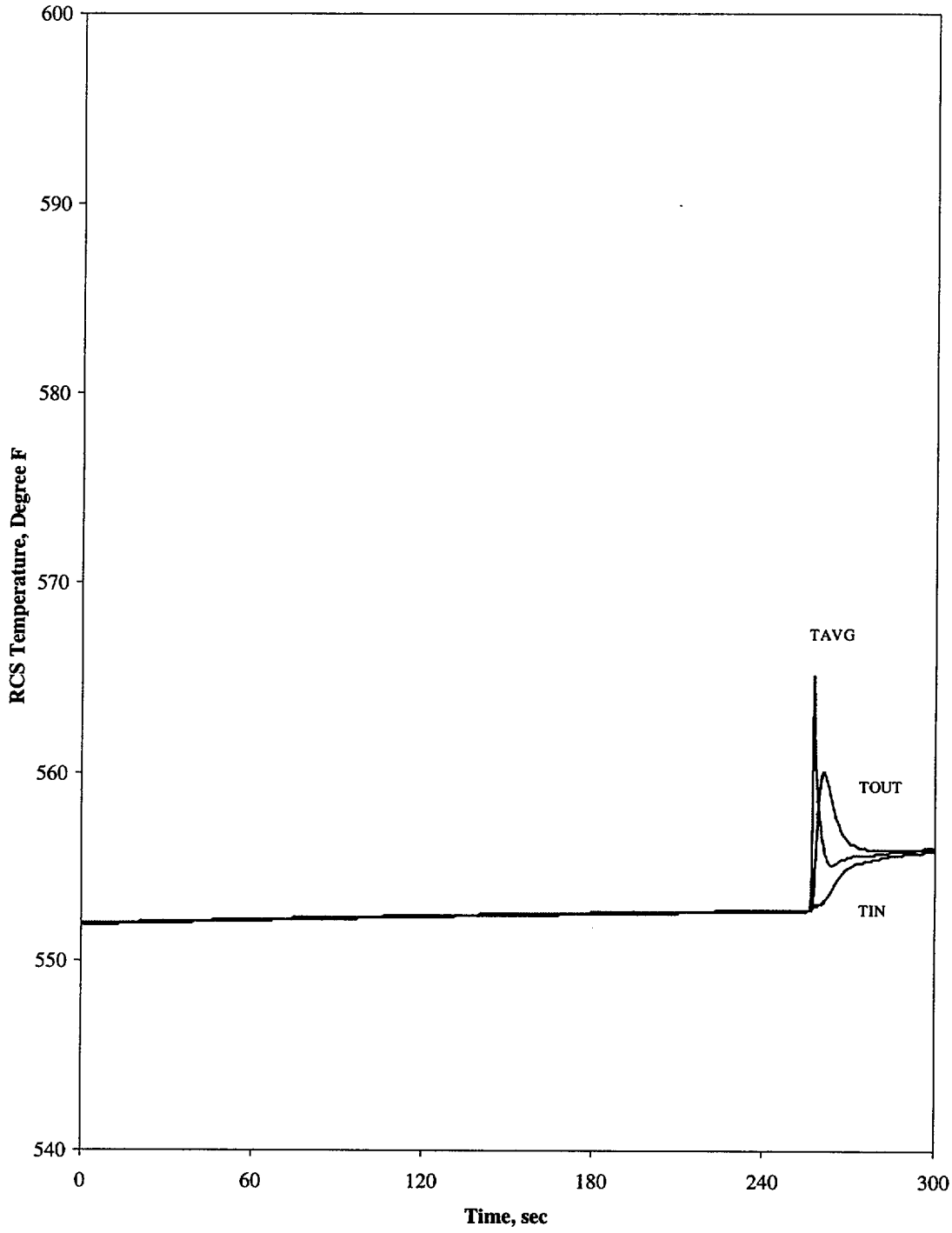

Figure 7.3.2-1

Uncontrolled CEA Bank Withdrawal from Hot Full Power
Core Power vs. Time

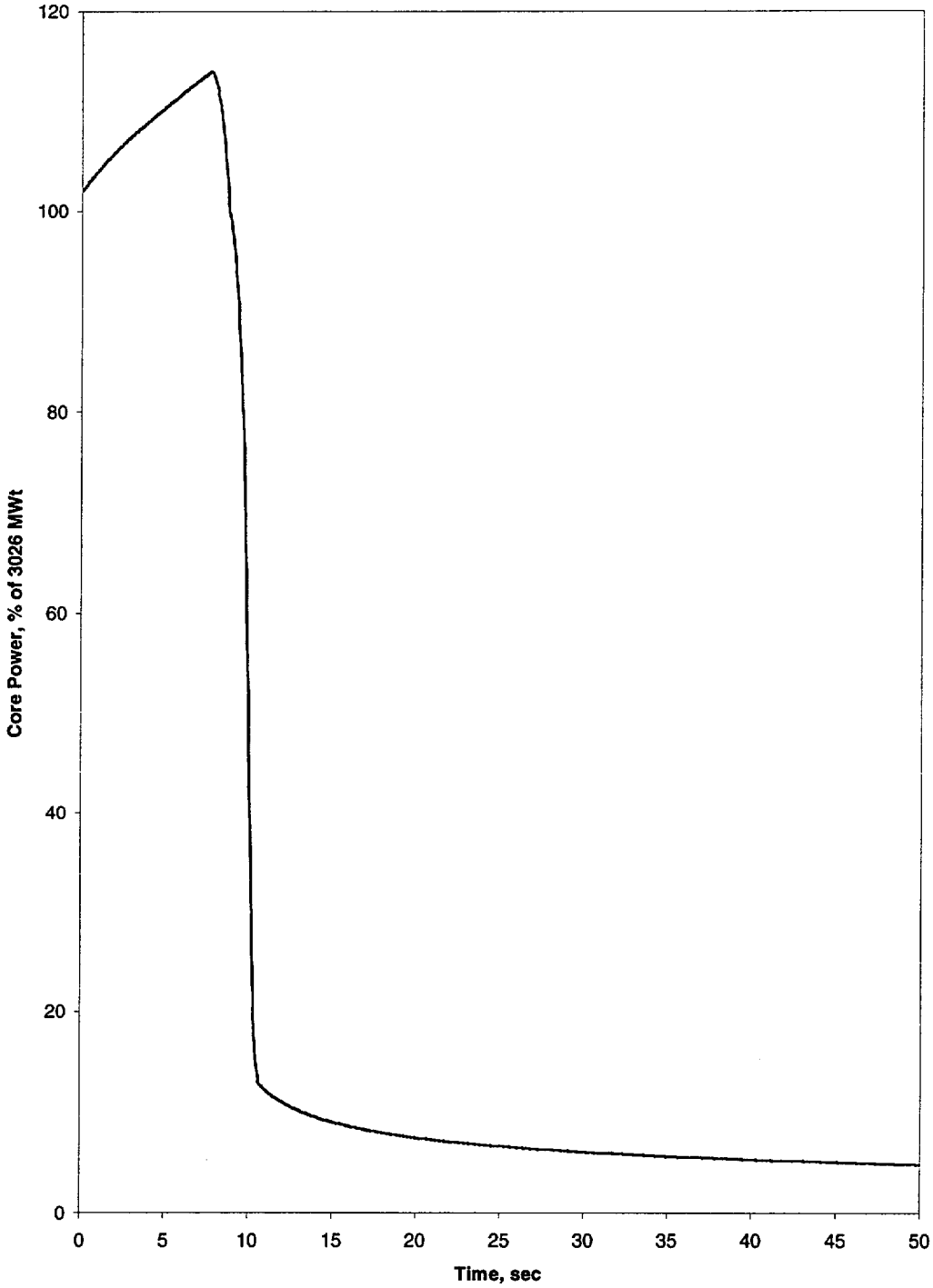

Figure 7.3.2-2

Uncontrolled CEA Bank Withdrawal from Hot Full Power
Core Average Heat Flux vs. Time

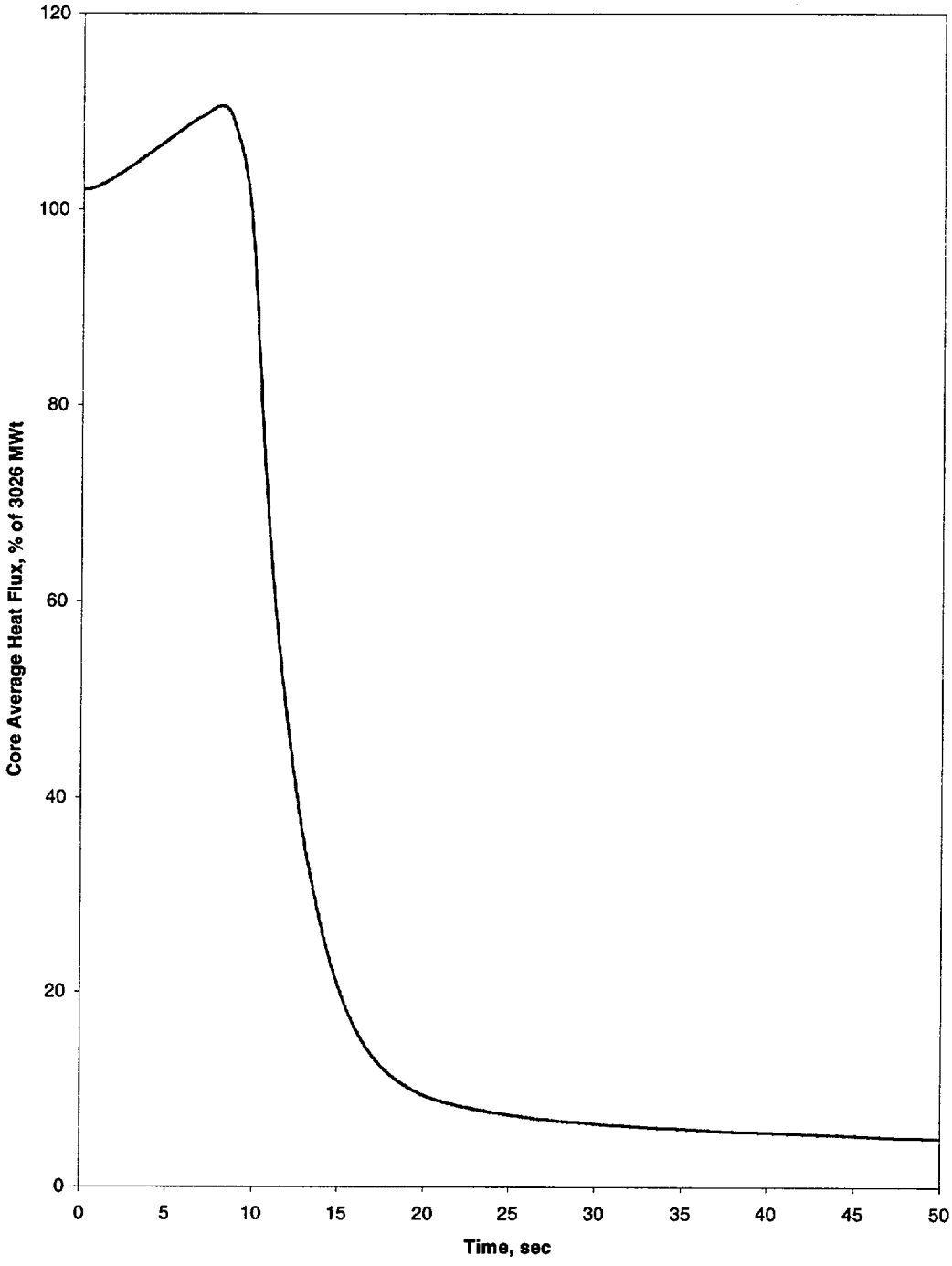

Figure 7.3.2-3

Uncontrolled CEA Bank Withdrawal from Hot Full Power
Reactor Coolant System Pressure vs. Time

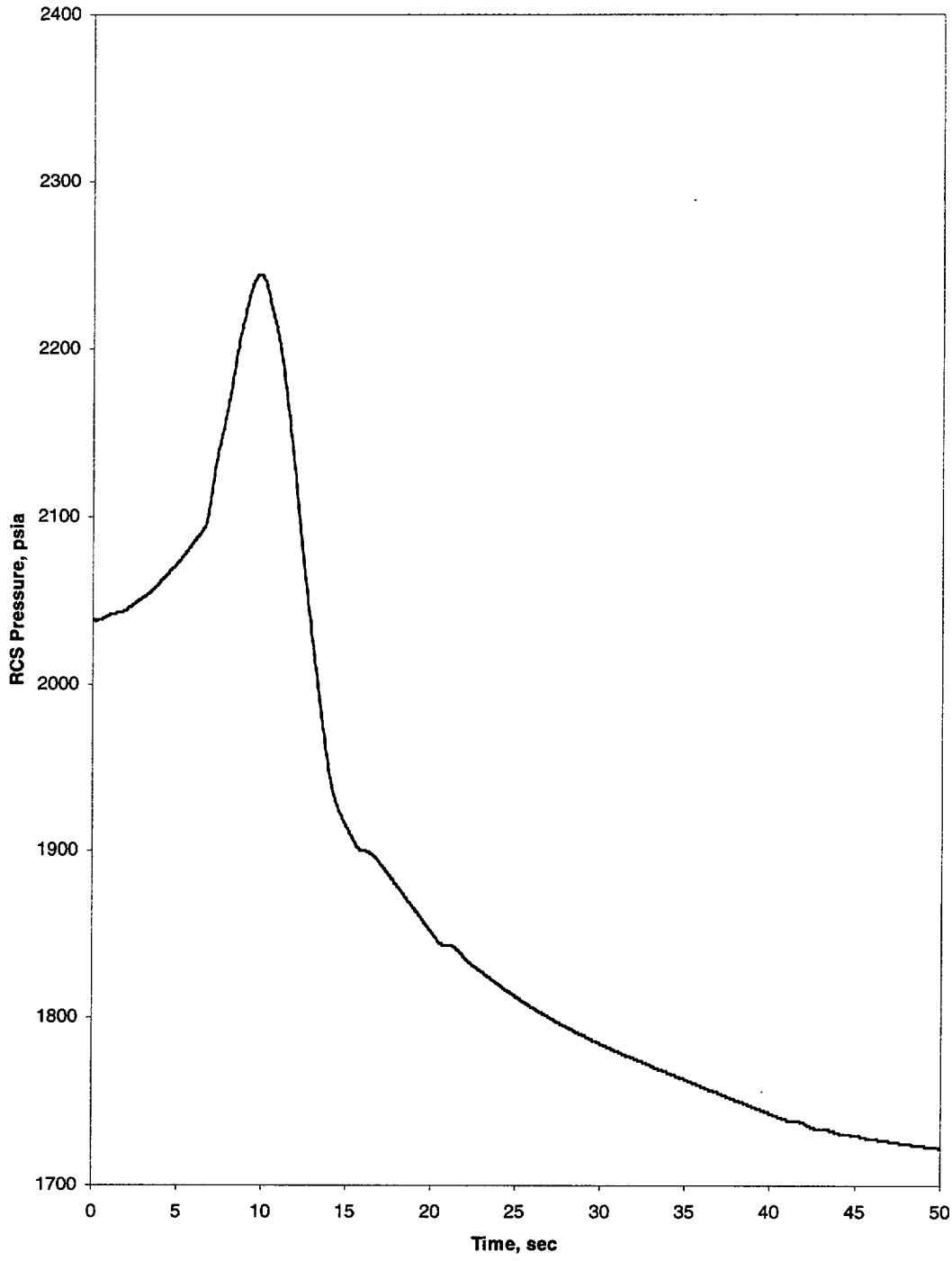

Figure 7.3.2-4

Uncontrolled CEA Bank Withdrawal from Hot Full Power
Reactor Coolant System Temperature vs. Time

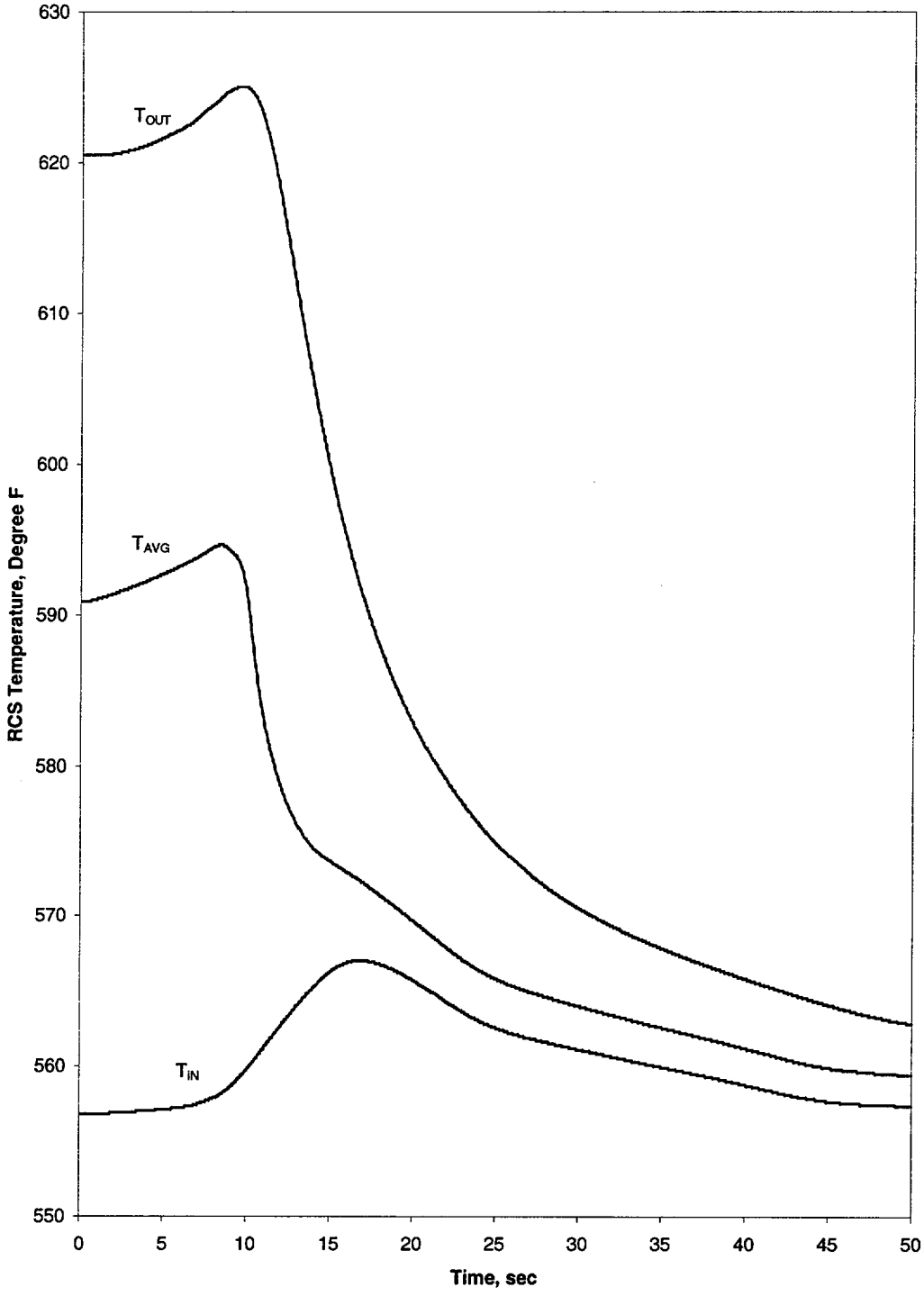

Figure 7.3.2-5

Uncontrolled CEA Bank Withdrawal from Hot Full Power
Steam Generator Pressure vs. Time

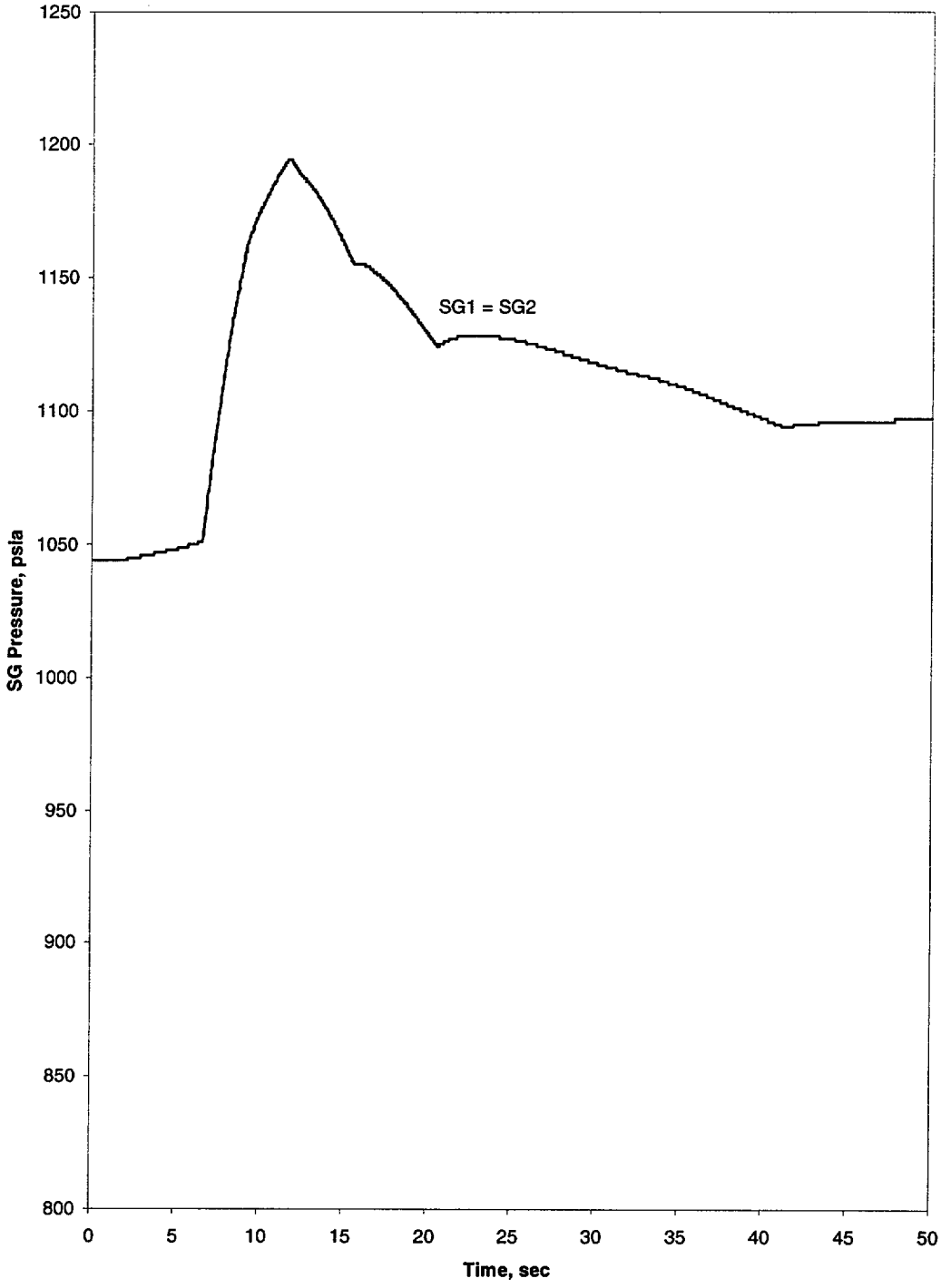

Figure 7.3.2-6

Uncontrolled CEA Bank Withdrawal from Hot Zero Power
Core Power vs. Time

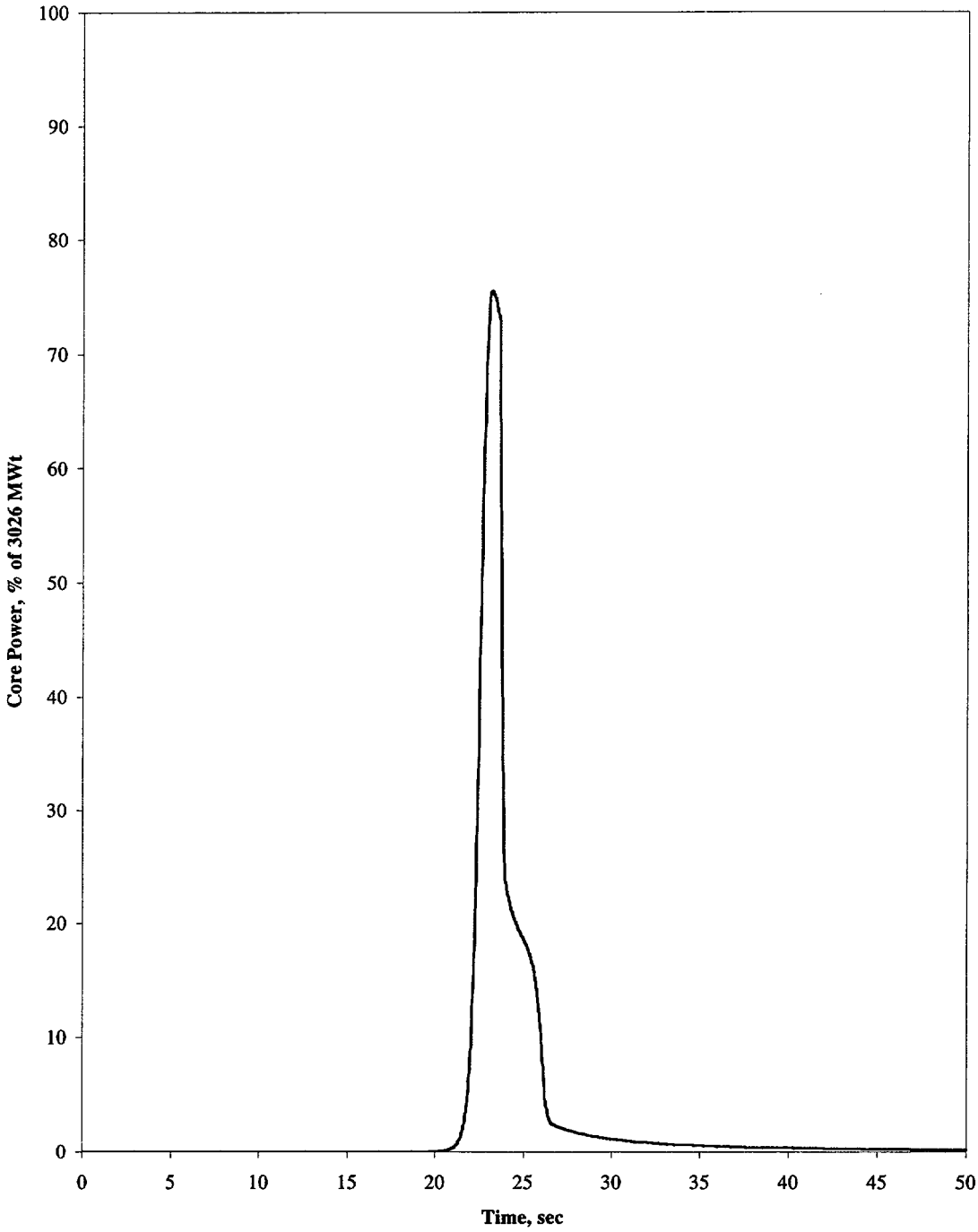

Figure 7.3.2-7

Uncontrolled CEA Bank Withdrawal from Hot Zero Power
Core Average Heat Flux vs. Time

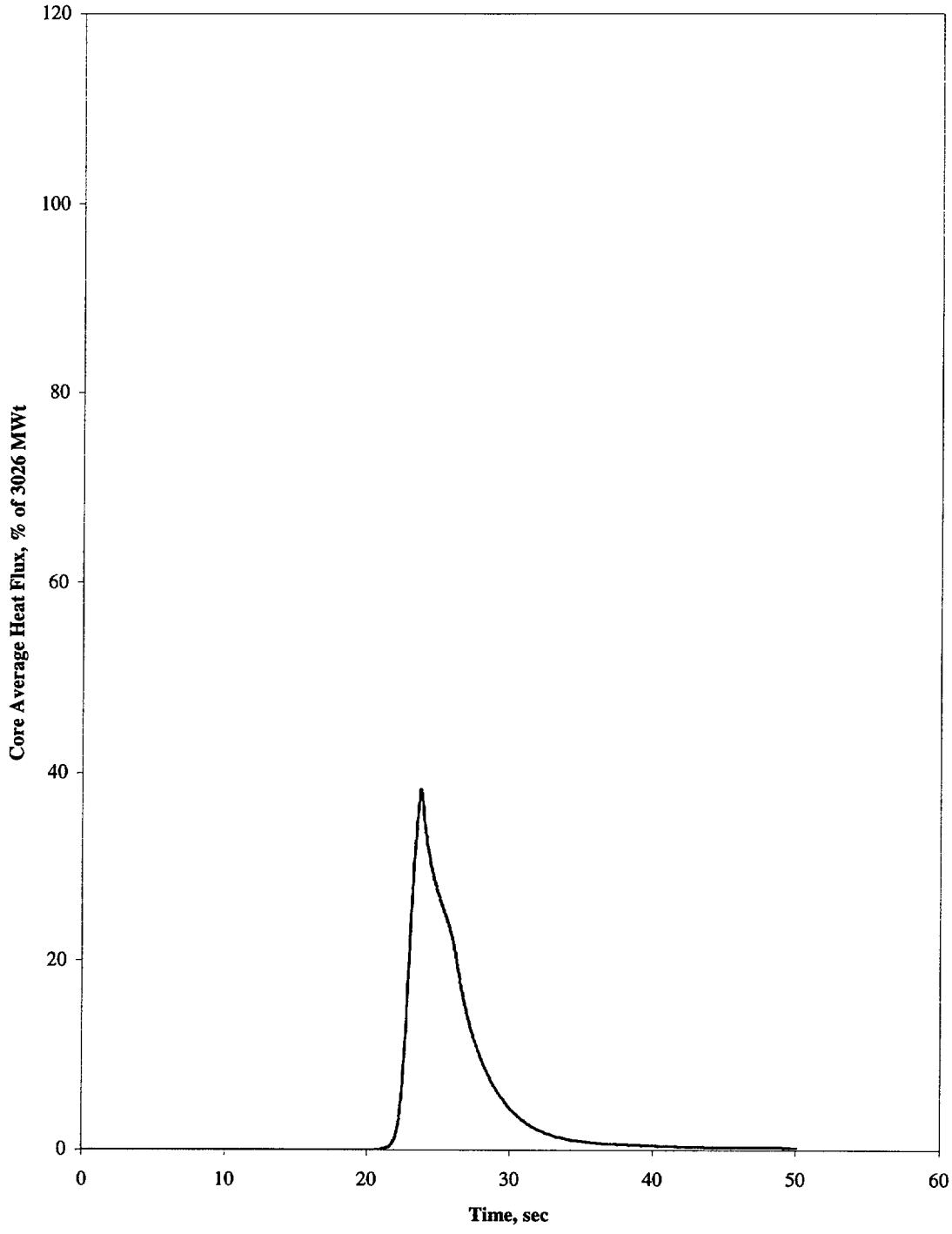

Figure 7.3.2-8

Uncontrolled CEA Bank Withdrawal from Hot Zero Power
Reactor Coolant System Pressure vs. Time

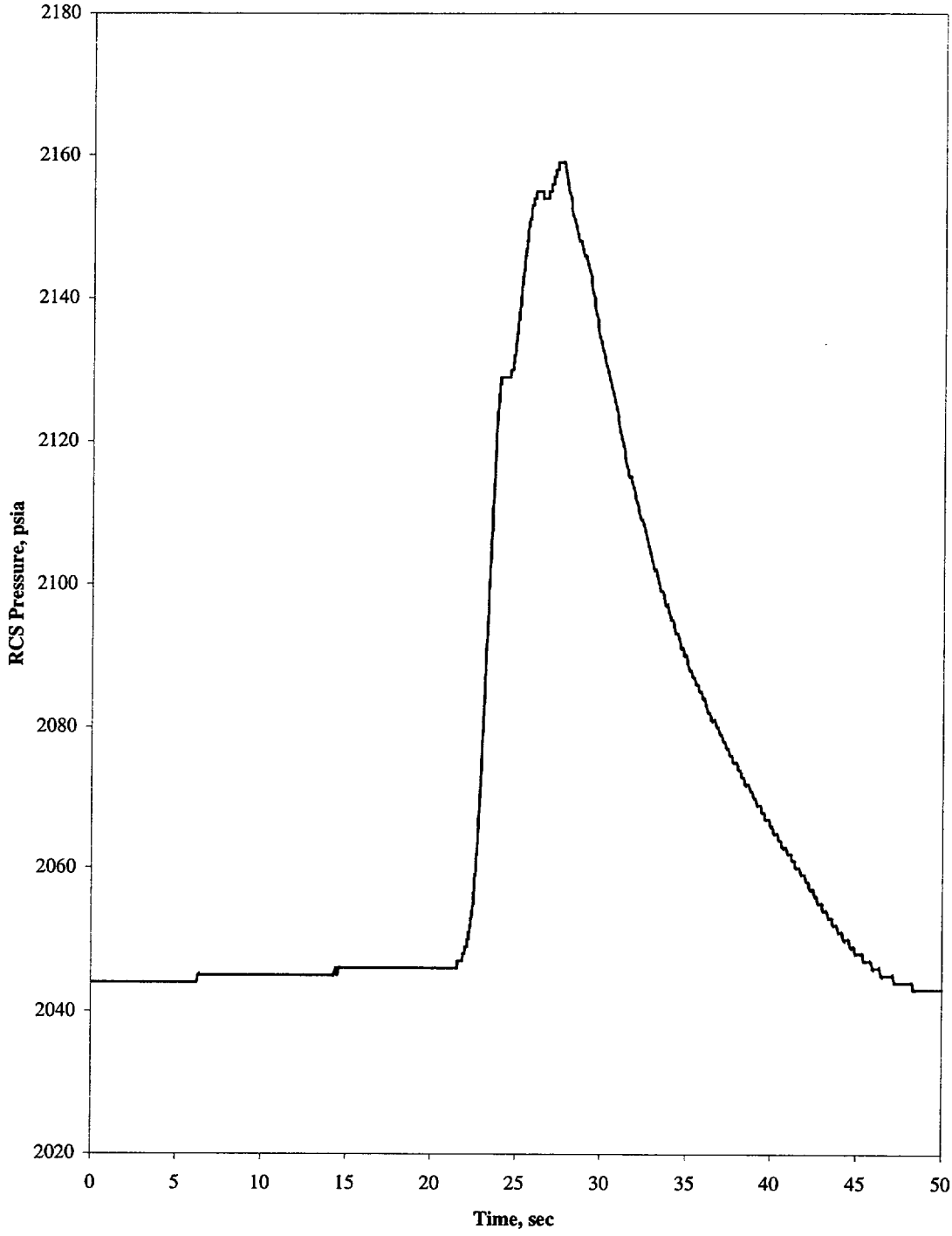

Figure 7.3.2-9

Uncontrolled CEA Bank Withdrawal from Hot Zero Power
Reactor Coolant System Temperature vs. Time

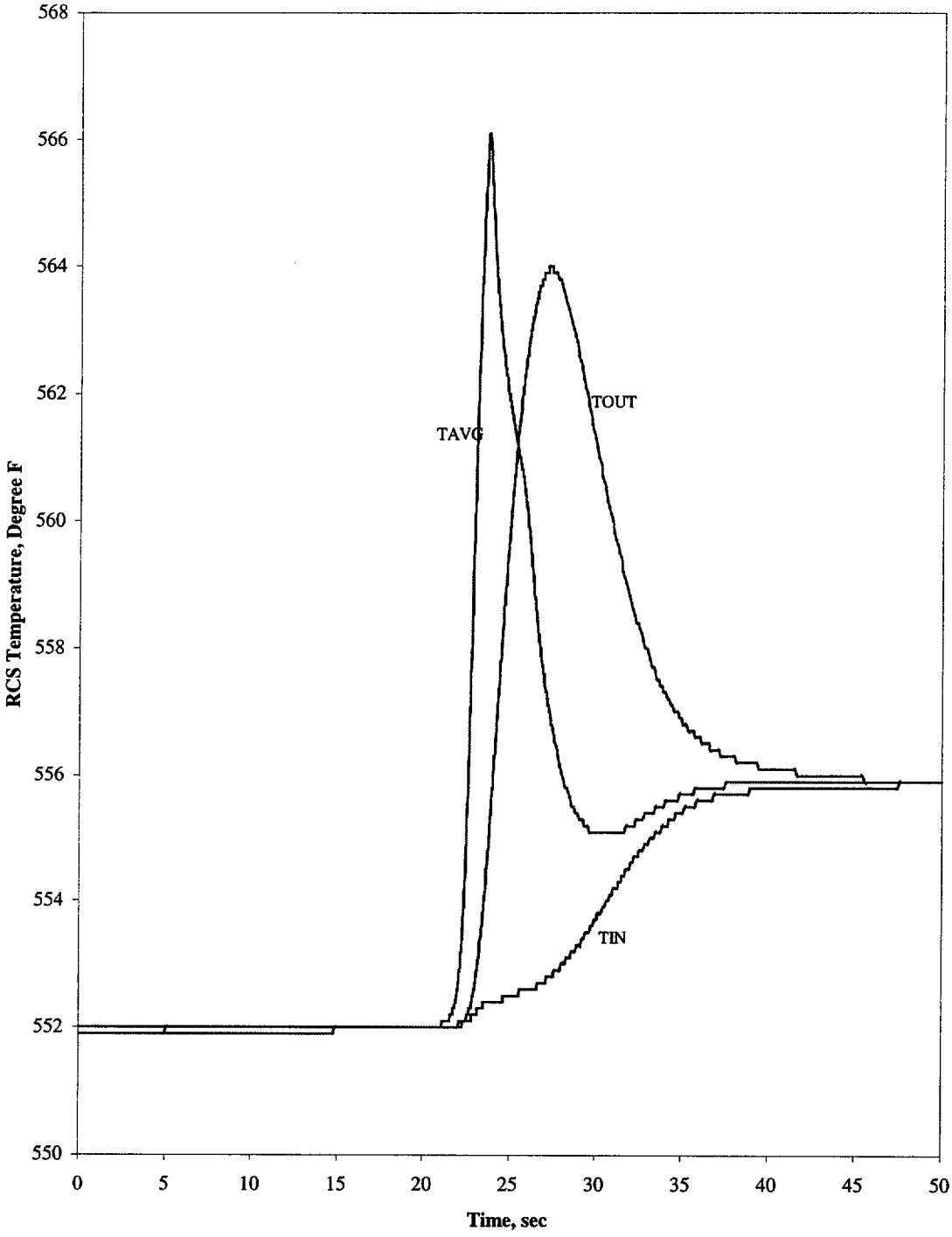

Figure 7.3.3-1

Required Power Reduction after Inward CEA Deviation*
(COLR Figure 2)

*When core power is reduced to 60% of rated power per this limit curve, further reduction is not required

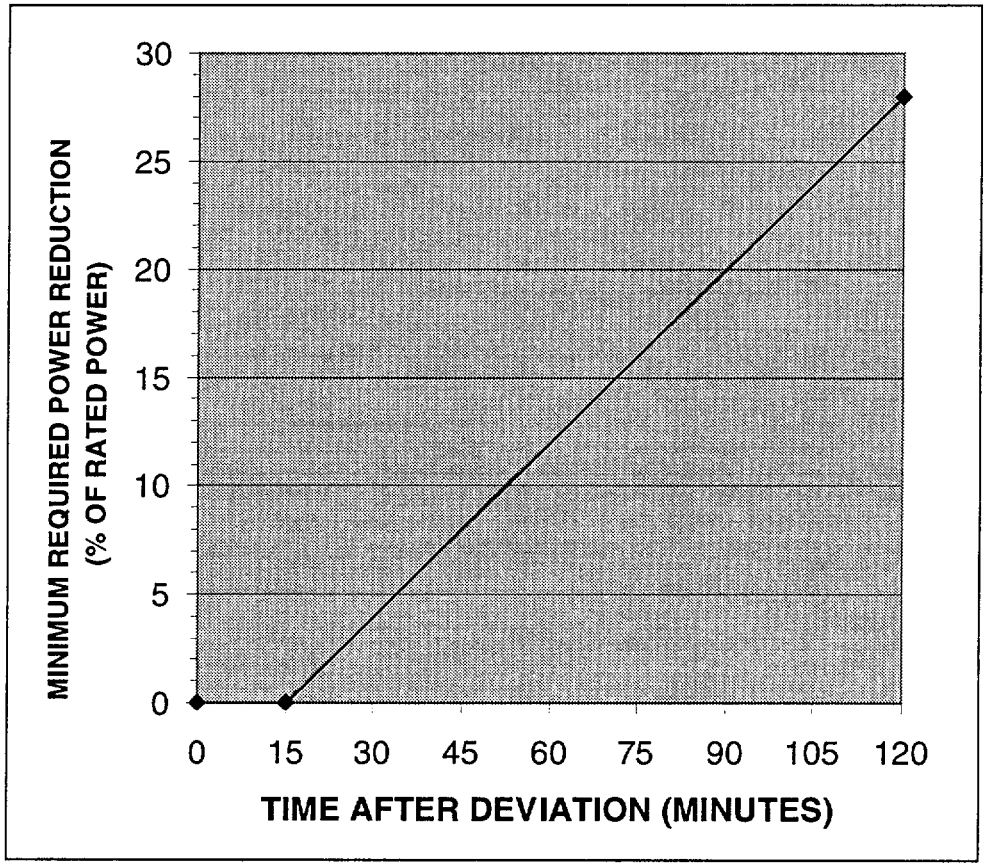

Figure 7.3.4-1

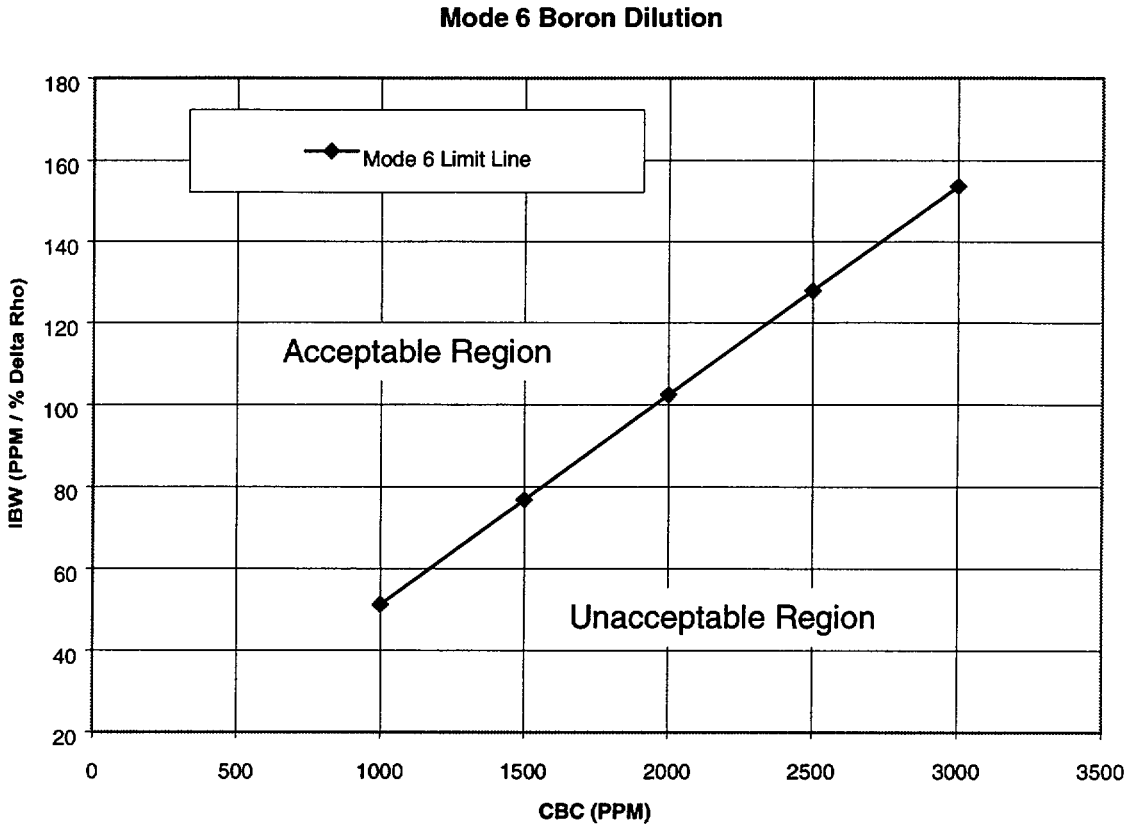

Mode 6 Boron Dilution Limit Line	
CBC (PPM)	**IBW (PPM / %Δρ)**
1000	51.2
1500	76.8
2000	102.4
2500	128.0
3000	153.6

Figure 7.3.4-2

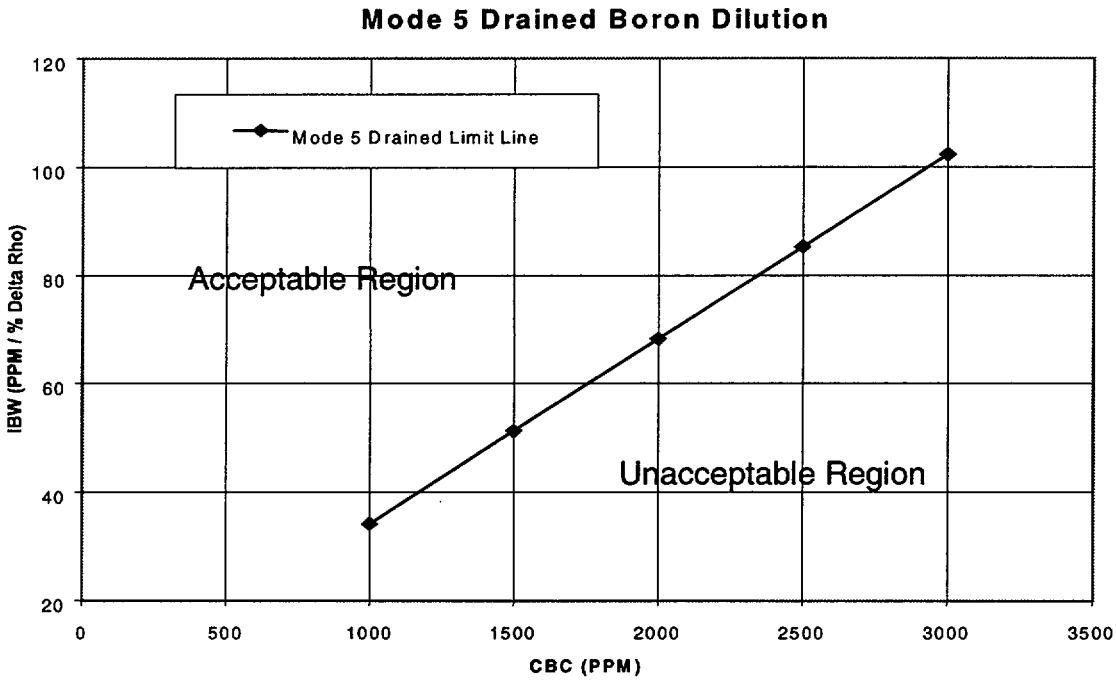

Mode 5 Drained Boron Dilution Limit Line	
CBC (PPM)	**IBW (PPM / %Δρ)**
1000	34.1
1500	51.2
2000	68.2
2500	85.3
3000	102.3

Figure 7.3.4-3

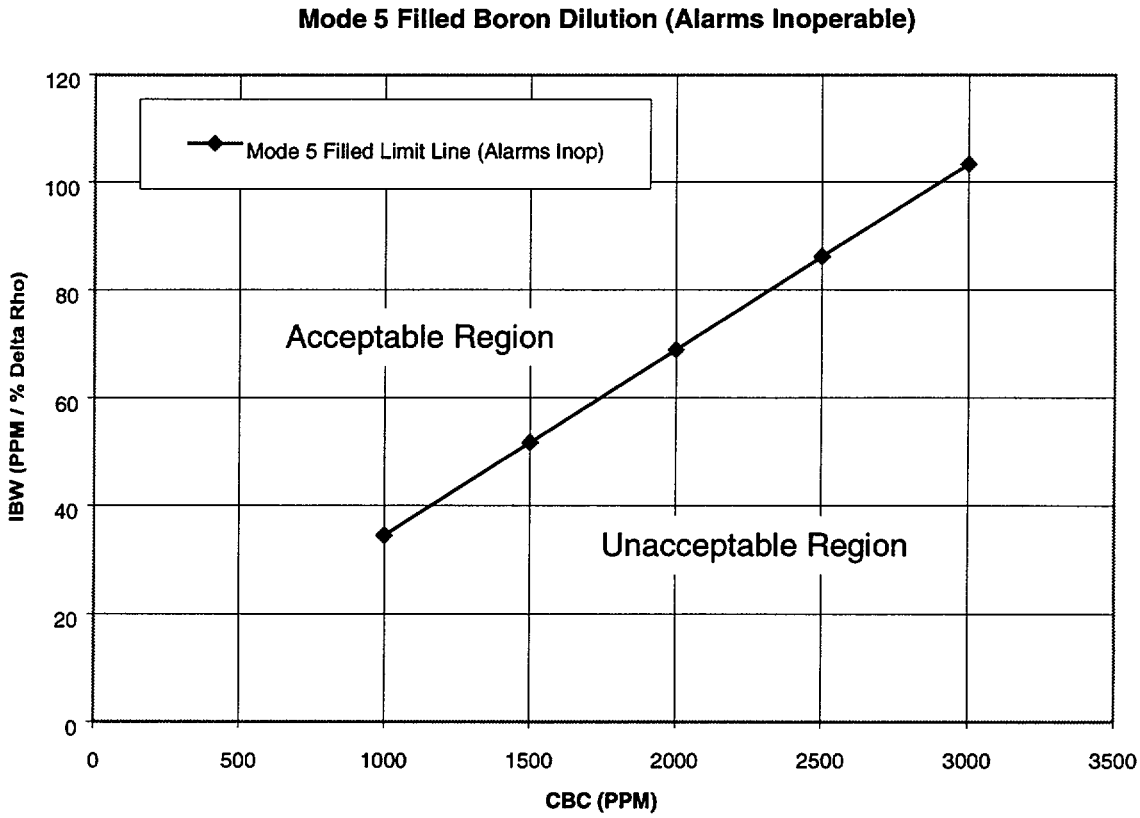

Mode 5 Filled Boron Dilution Limit Line (Alarms Inoperable)	
CBC (PPM)	**IBW (PPM / %Δρ)**
1000	34.5
1500	51.7
2000	68.9
2500	86.2
3000	103.4

Figure 7.3.4-4

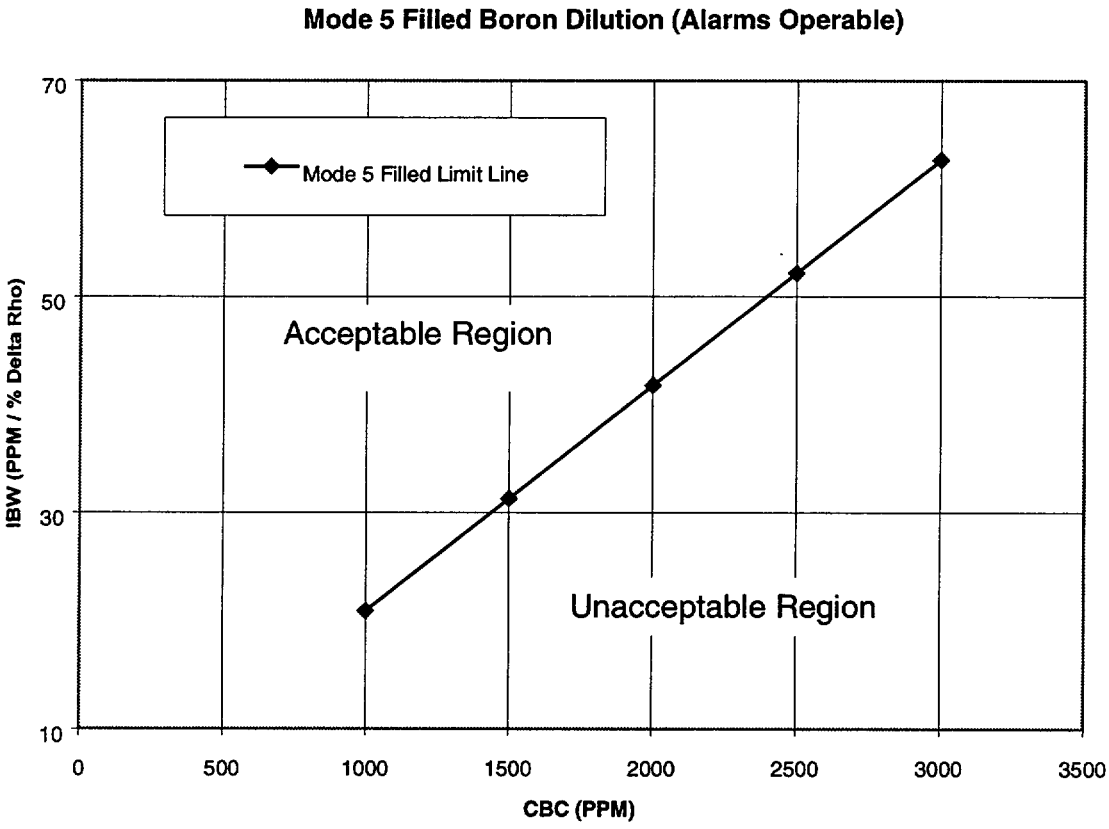

Mode 5 Filled Boron Dilution Limit Line (Alarms Operable)	
CBC (PPM)	**IBW (PPM / %Δρ)**
1000	20.9
1500	31.3
2000	41.8
2500	52.2
3000	62.7

Figure 7.3.4-5

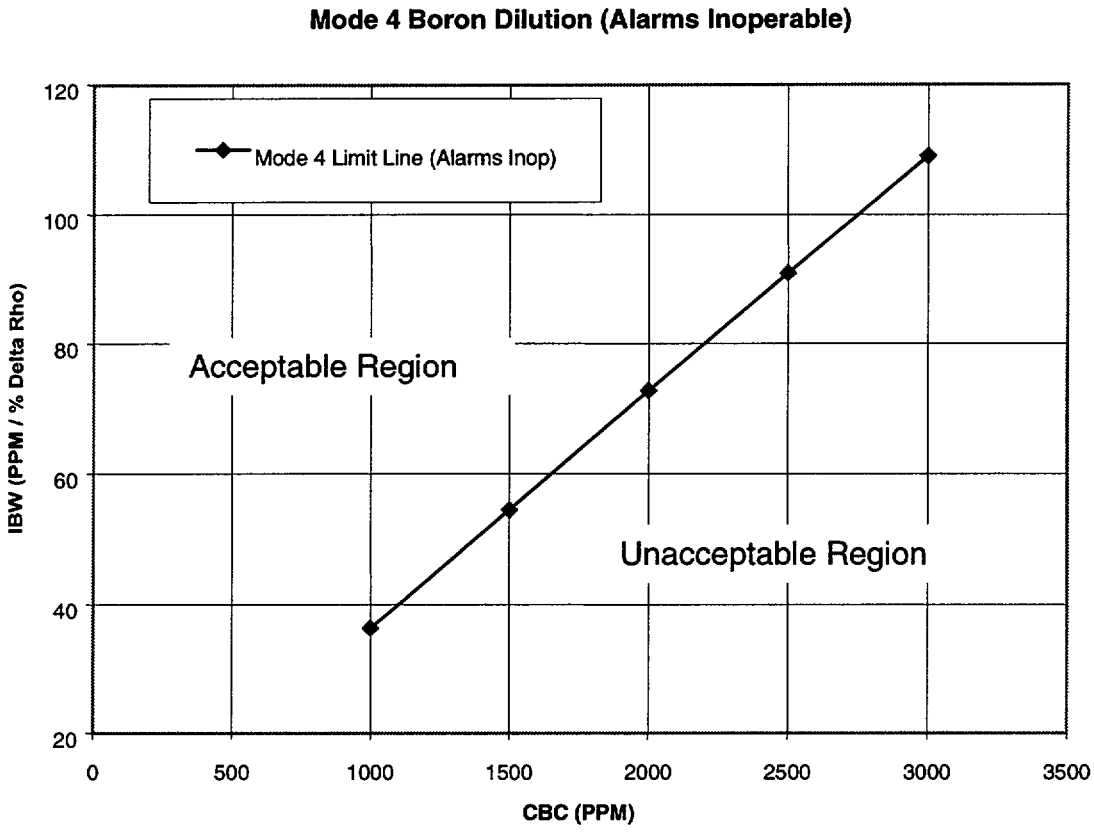

Mode 4 Boron Dilution Limit Line (Alarms Inoperable)	
CBC (PPM)	**IBW (PPM / %Δρ)**
1000	36.3
1500	54.5
2000	72.7
2500	90.9
3000	109.0

Figure 7.3.4-6

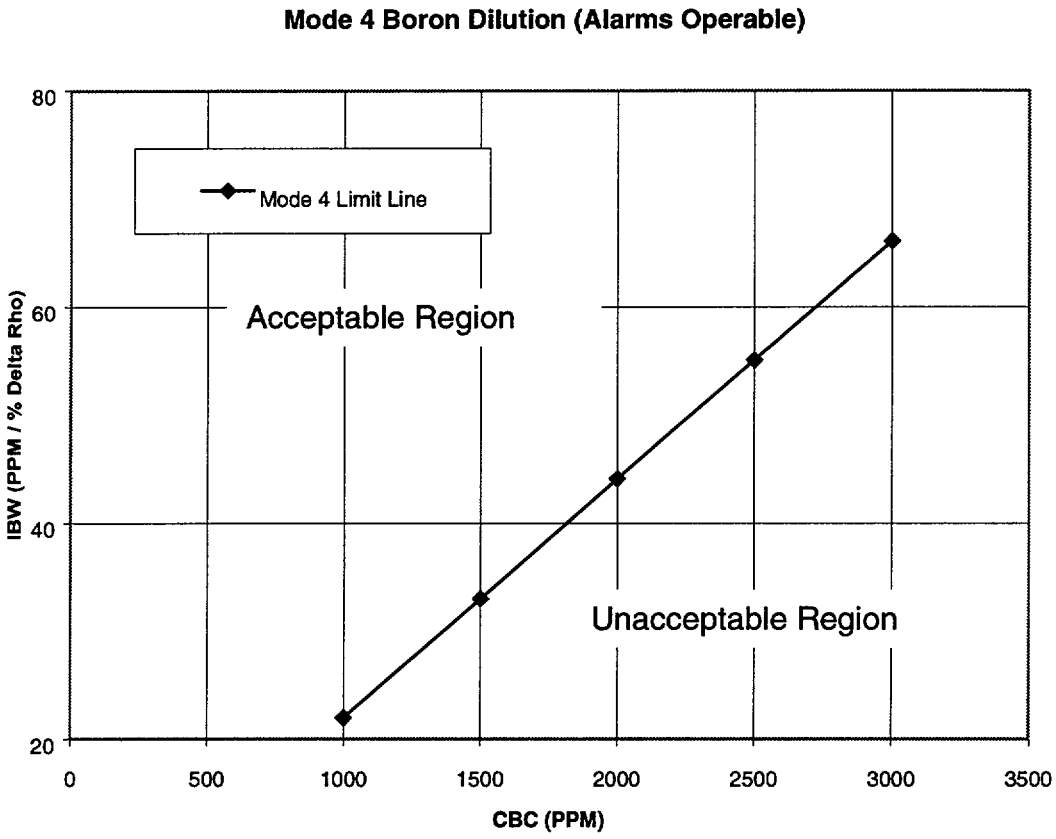

Mode 4 Boron Dilution Limit Line (Alarms Operable)	
CBC (PPM)	**IBW (PPM / %Δρ)**
1000	22.0
1500	33.0
2000	44.1
2500	55.1
3000	66.1

Figure 7.3.4-7

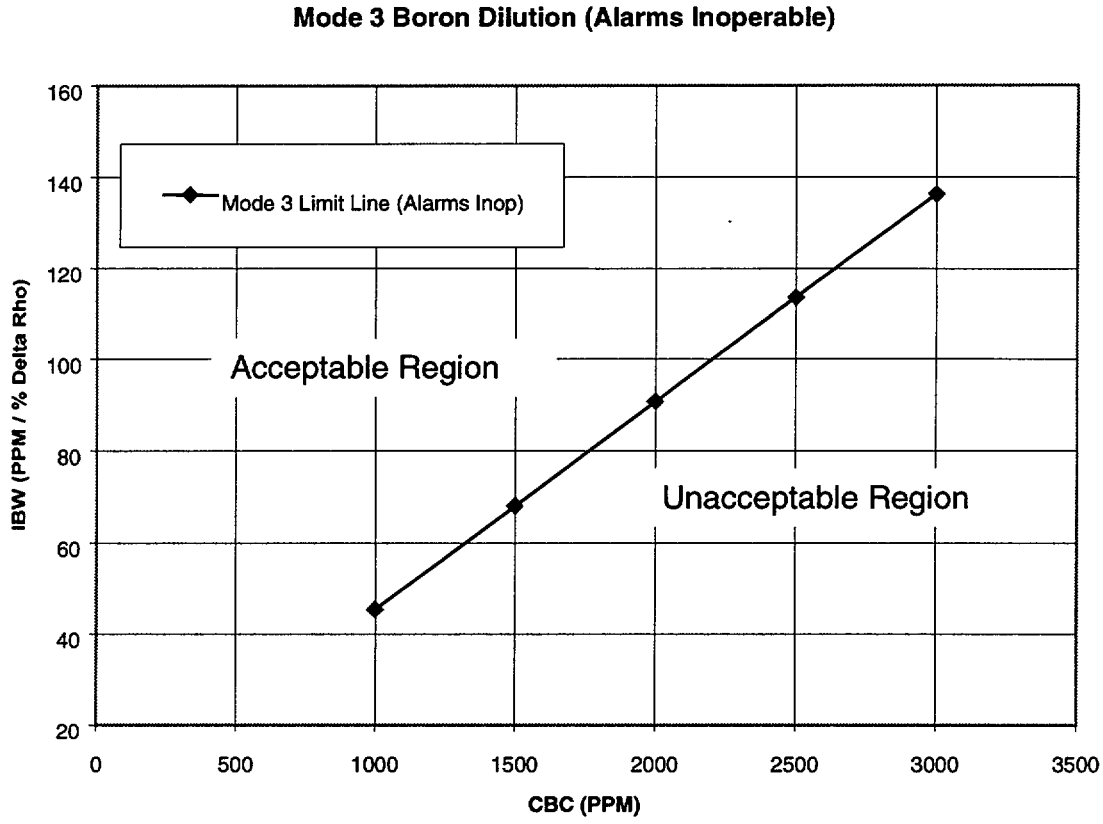

Mode 3 Boron Dilution Limit Line (Alarms Inoperable)	
CBC (PPM)	**IBW (PPM / %Δρ)**
1000	45.4
1500	68.1
2000	90.8
2500	113.6
3000	136.3

Figure 7.3.4-8

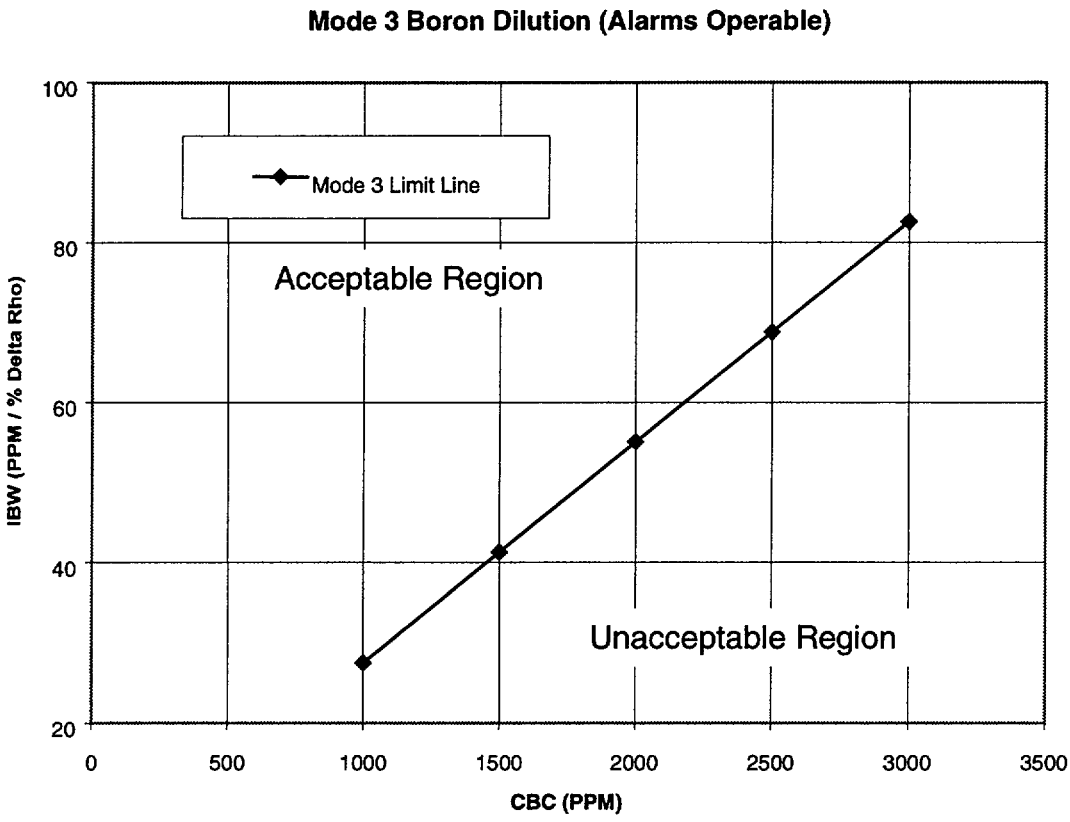

Mode 3 Boron Dilution Limit Line (Alarms Operable)	
CBC (PPM)	**IBW (PPM / %Δρ)**
1000	27.5
1500	41.3
2000	55.1
2500	68.8
3000	82.6

Figure 7.3.4-9

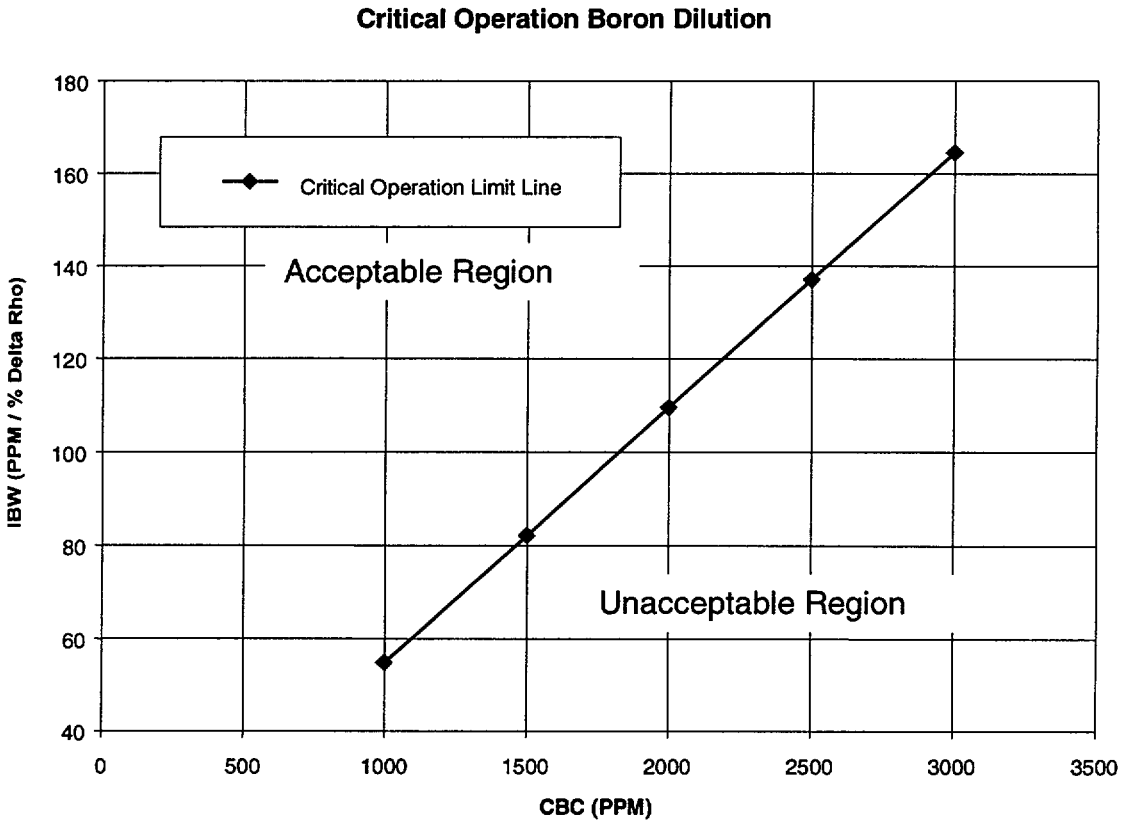

Critical Operation Boron Dilution Limit Line	
CBC (PPM)	**IBW (PPM / %Δρ)**
1000	54.8
1500	82.2
2000	109.6
2500	137.1
3000	164.5

Figure 7.3.5.1-1

4-Pump Loss of Coolant Flow
Core Flow vs. Time

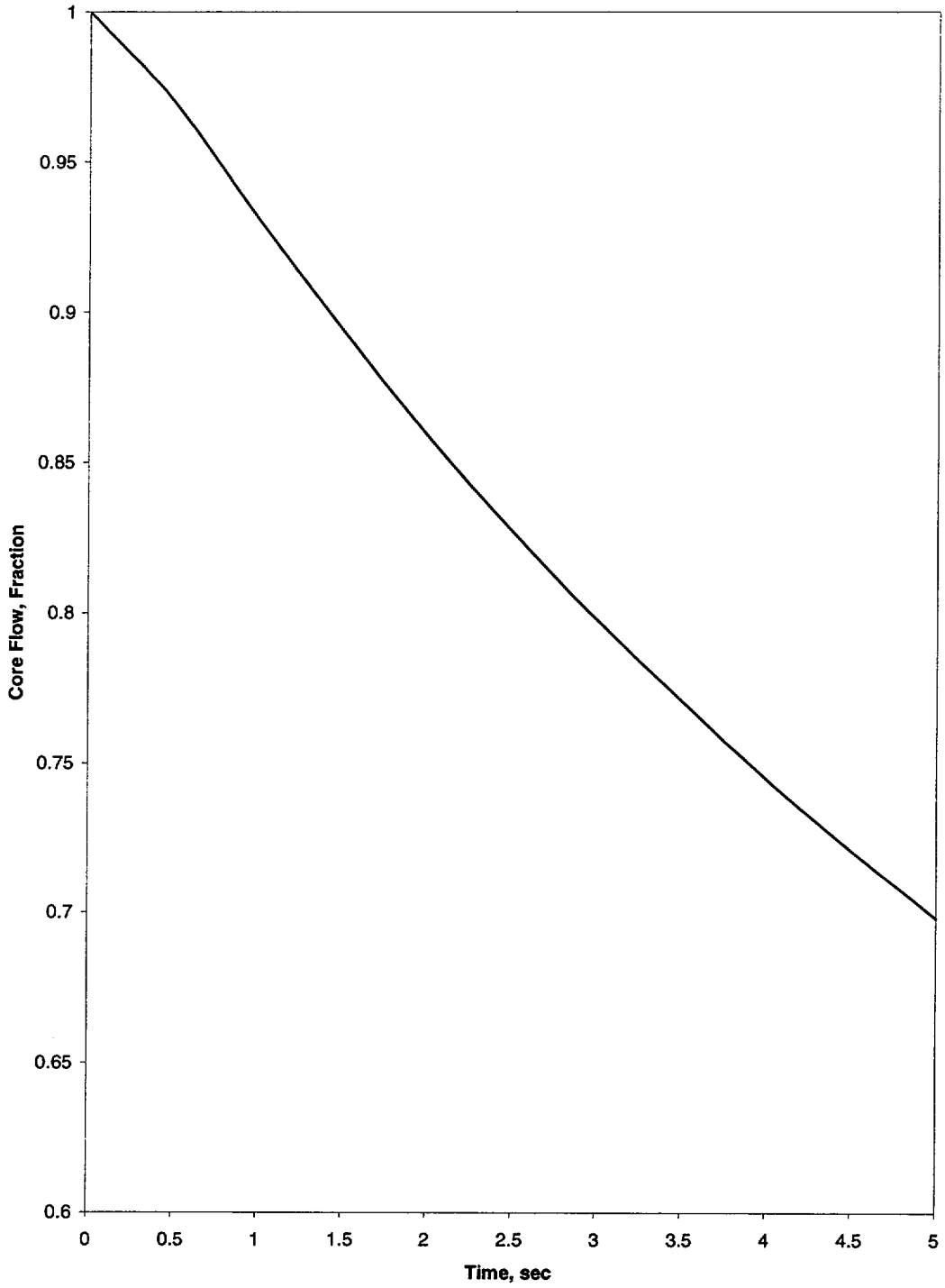

Figure 7.3.5.1-2
Cycle 16 4-Pump Loss of Coolant Flow
DNBR vs. Time
Maximum Subcooling Case

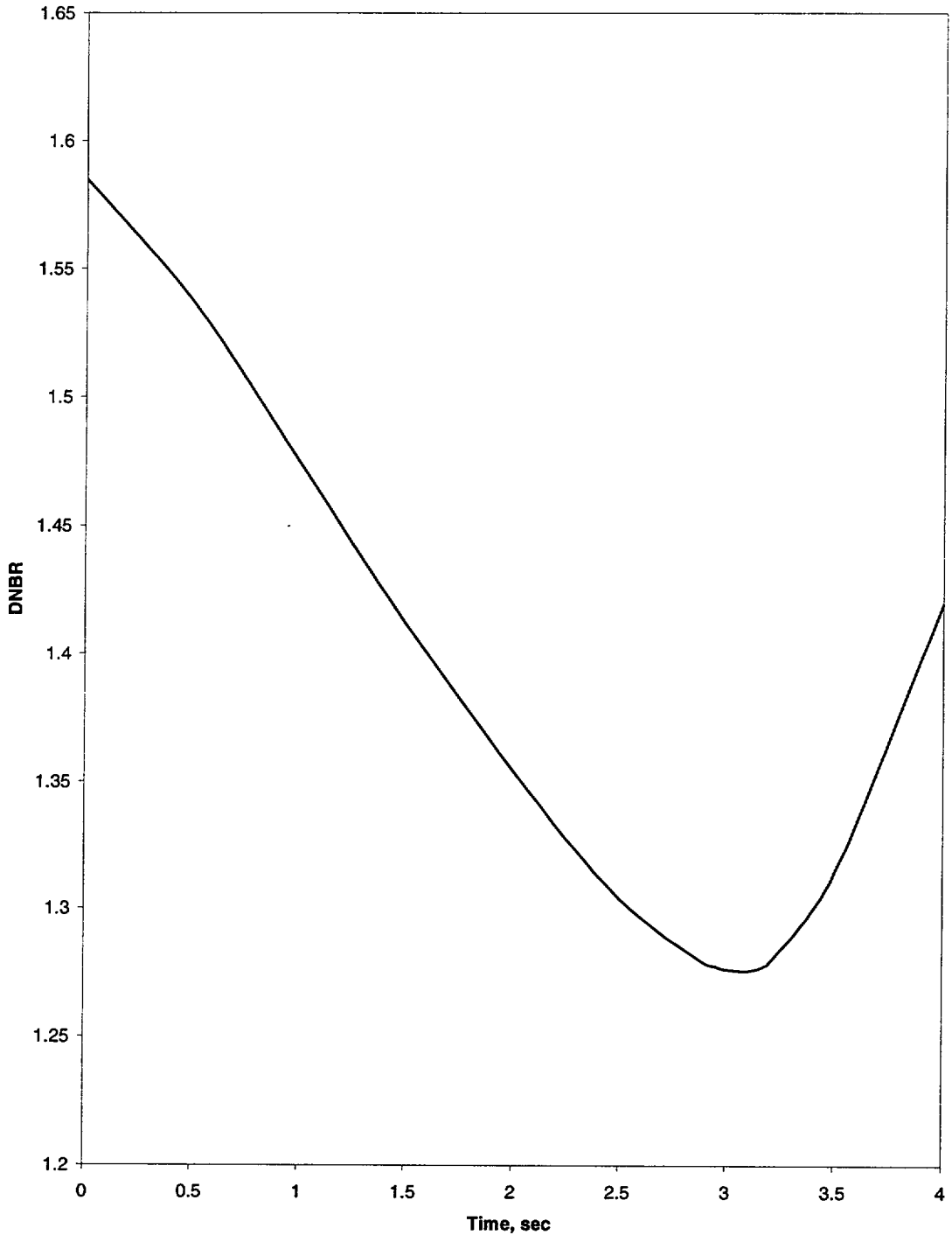

Figure 7.3.5.1-3

Cycle 16 4-Pump Loss of Coolant Flow
DNBR vs. Time (Minimum Subcooling)

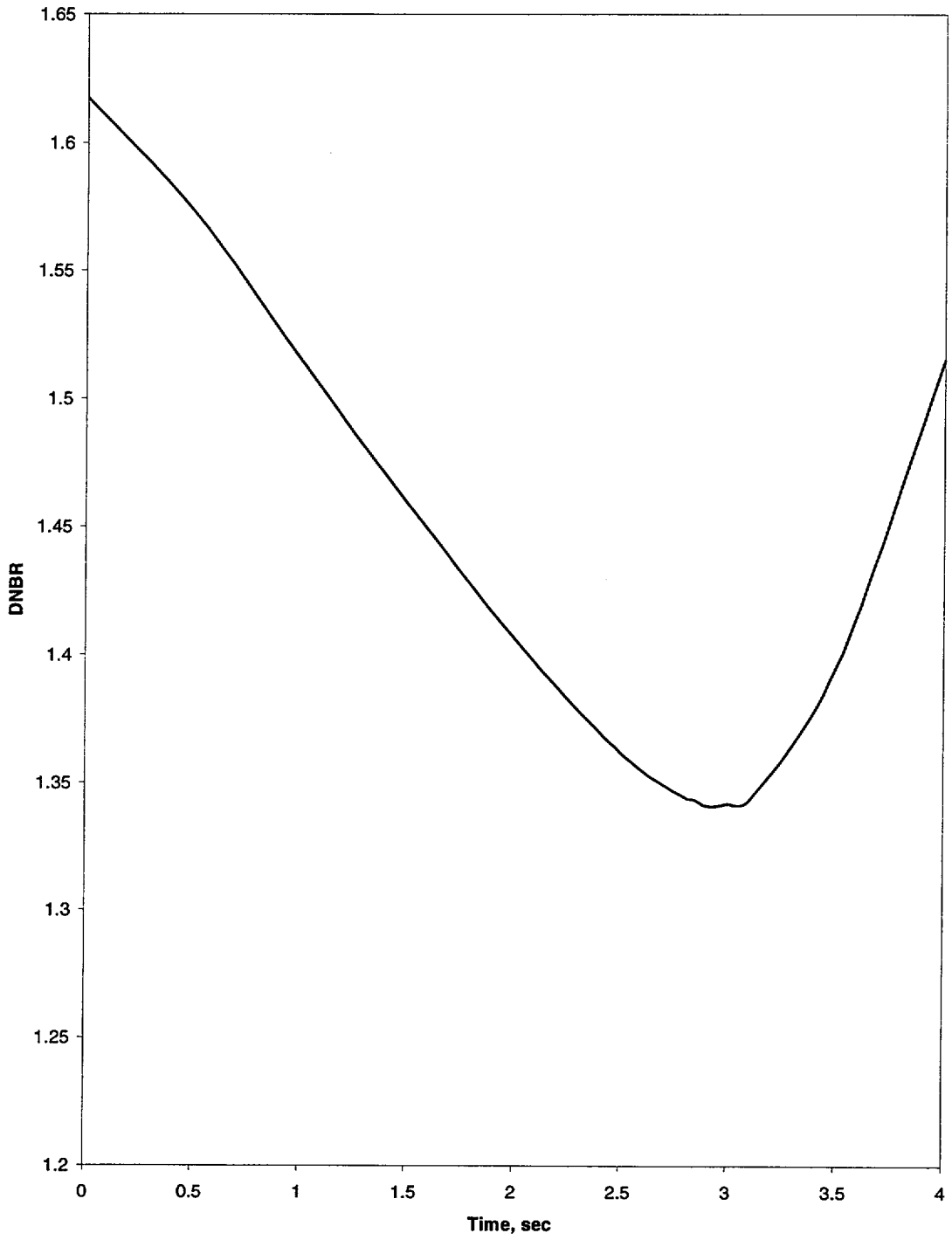

Figure 7.3.5.2-1

Loss of Coolant Flow
Pump Shaft Seizure
Core Flow Rate vs. Time

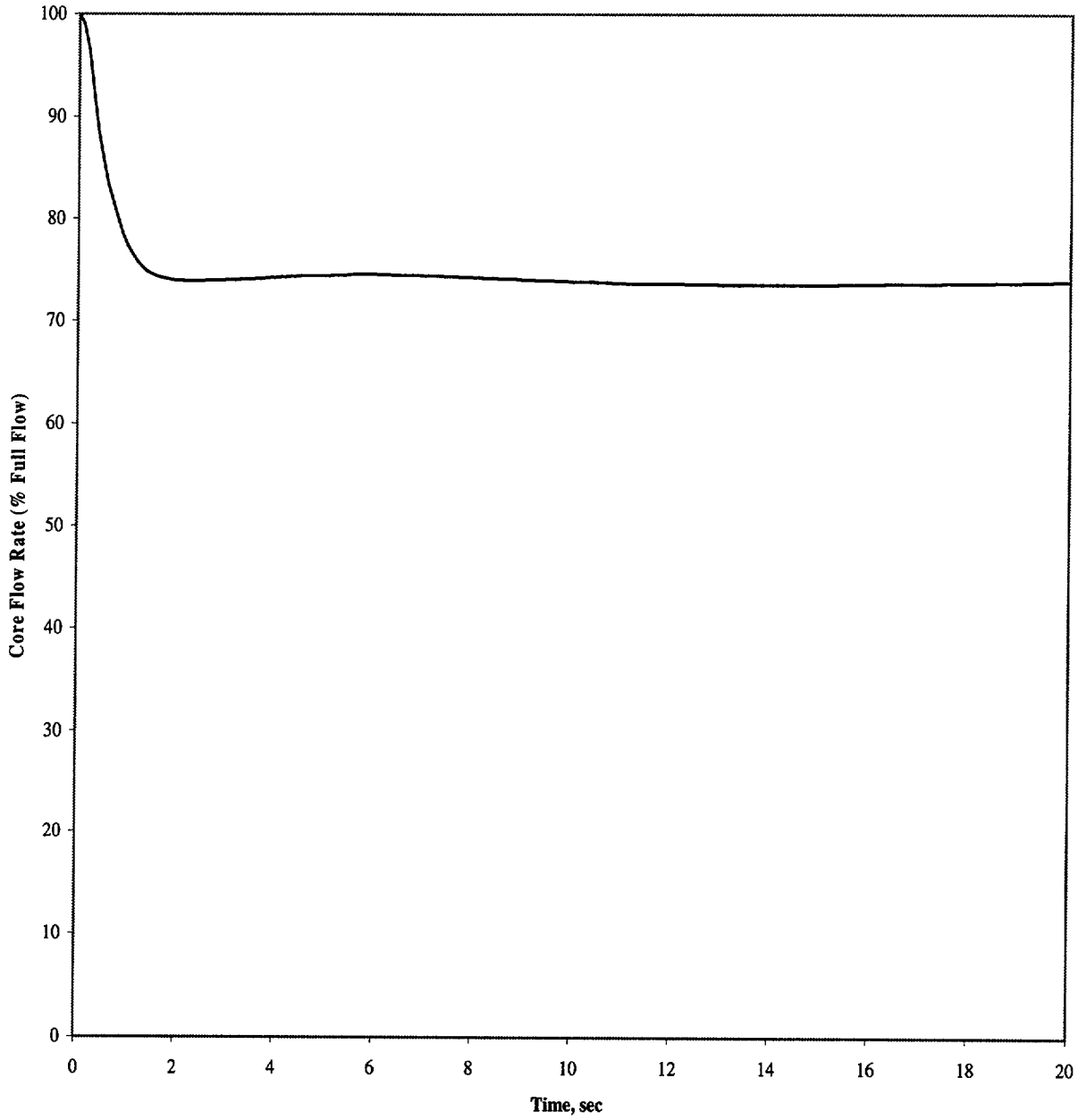

Figure 7.3.5.2-2

Loss of Coolant Flow
Pump Shaft Seizure
Core Power vs. Time

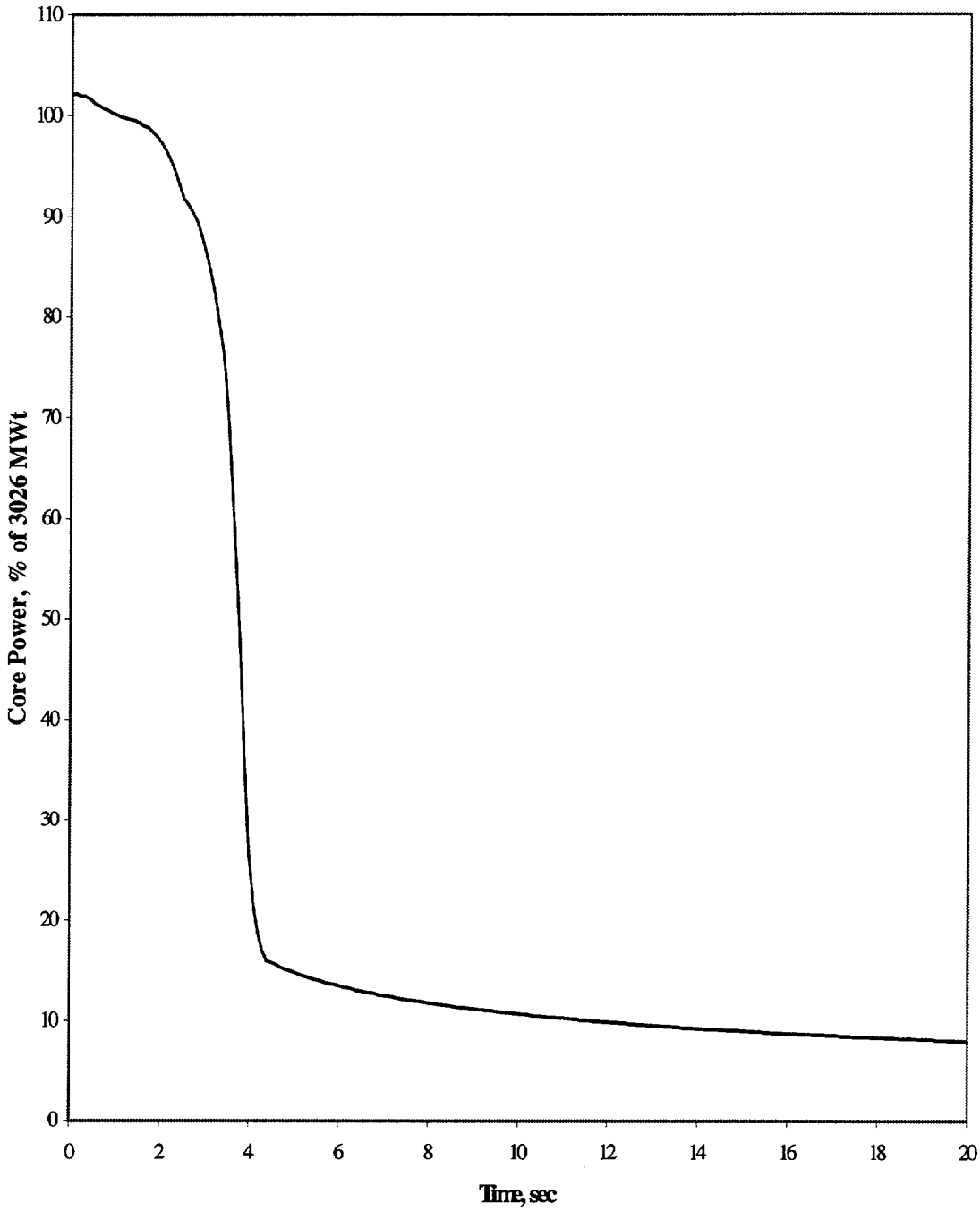

Figure 7.3.5.2-3

Loss of Coolant Flow
Pump Shaft Seizure
Core Average Heat Flux vs. Time

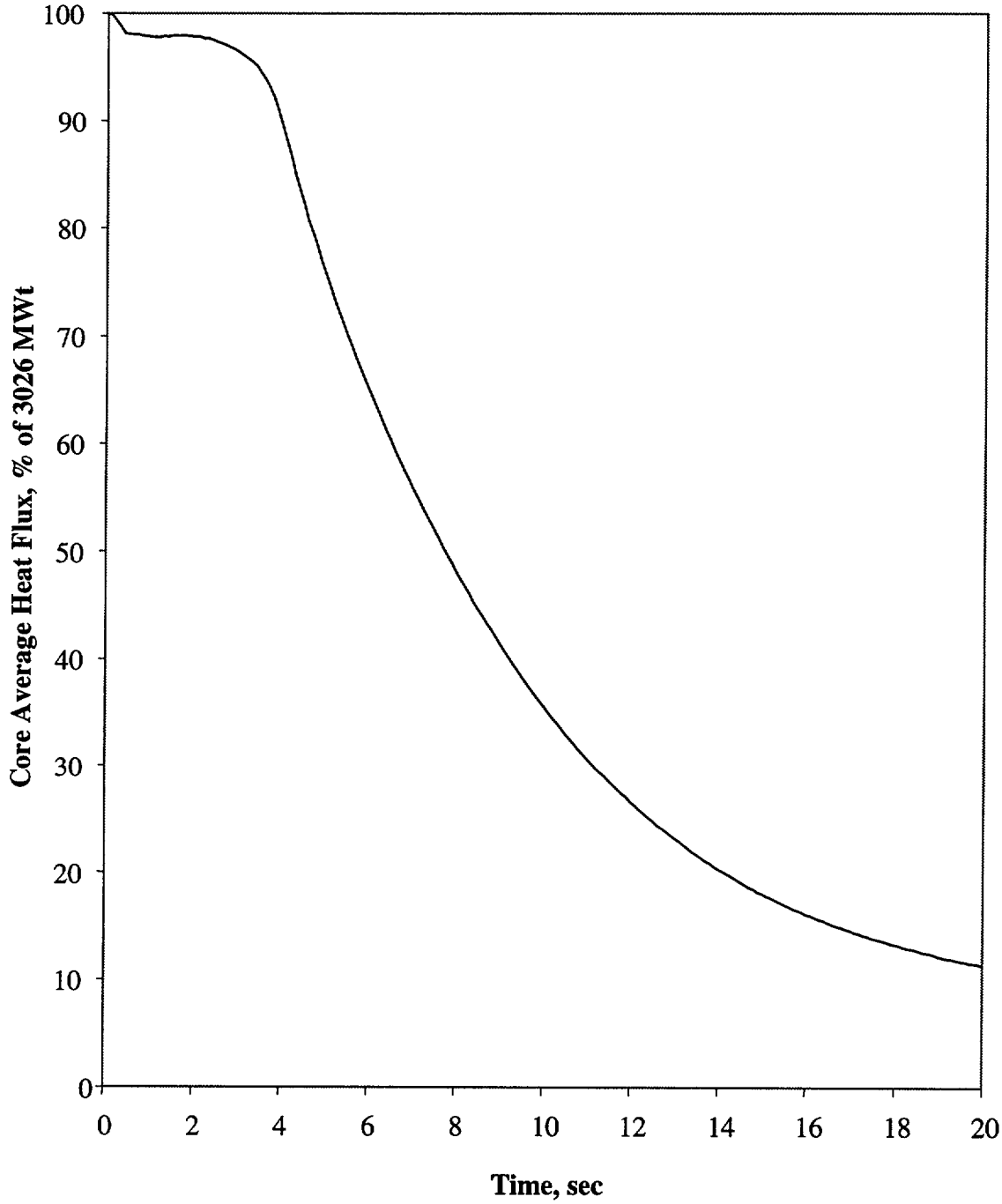

Figure 7.3.5.2-4

Loss of Coolant Flow
Pump Shaft Seizure
Reactor Coolant System Pressure vs. Time

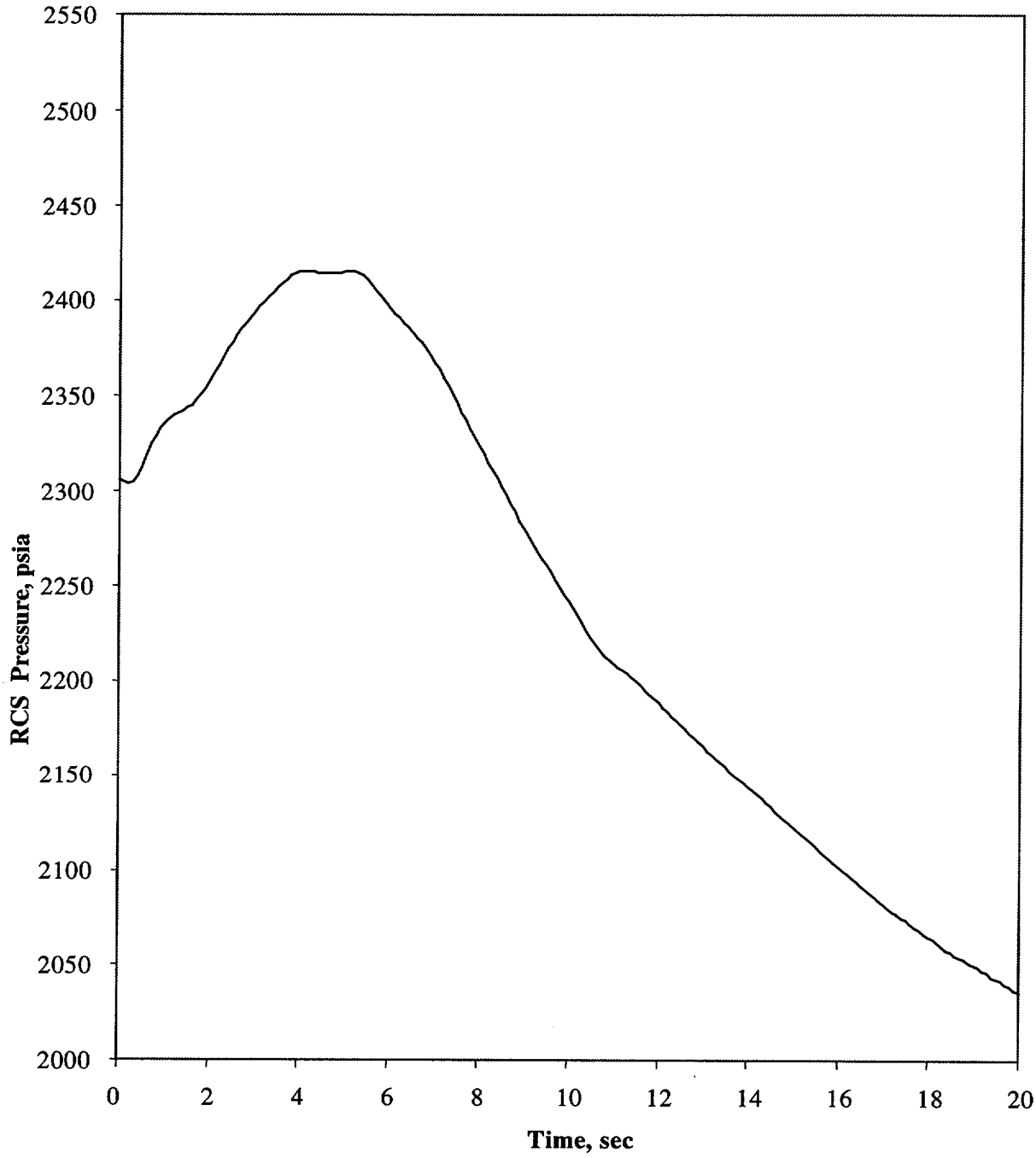

Figure 7.3.5.2-5

Loss of Coolant Flow
Pump Shaft Seizure
Reactor Coolant System Temperature vs. Time

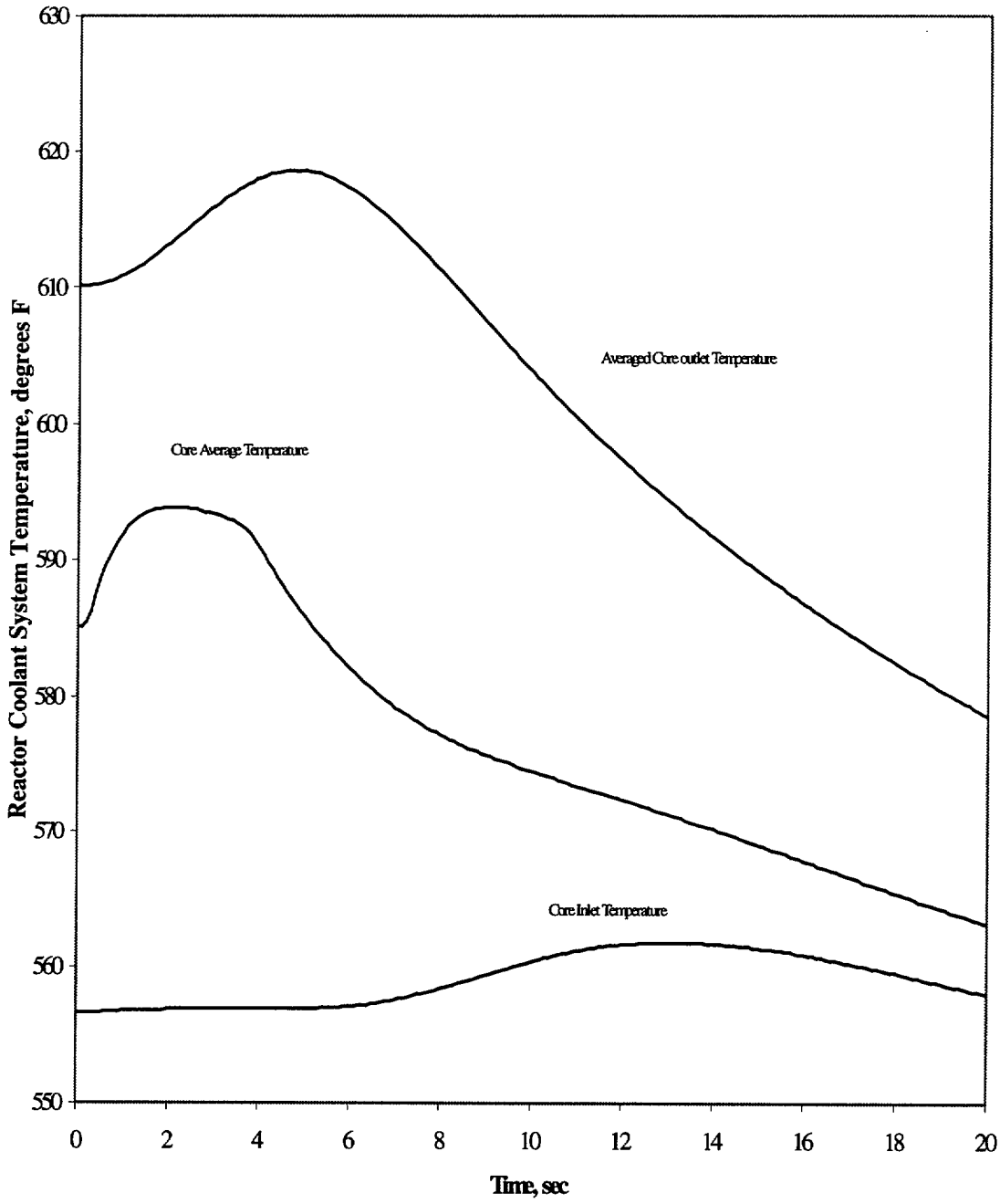

Figure 7.3.5.2-6

Loss of Coolant Flow
Pump Shaft Seizure
Fr vs. DNBR

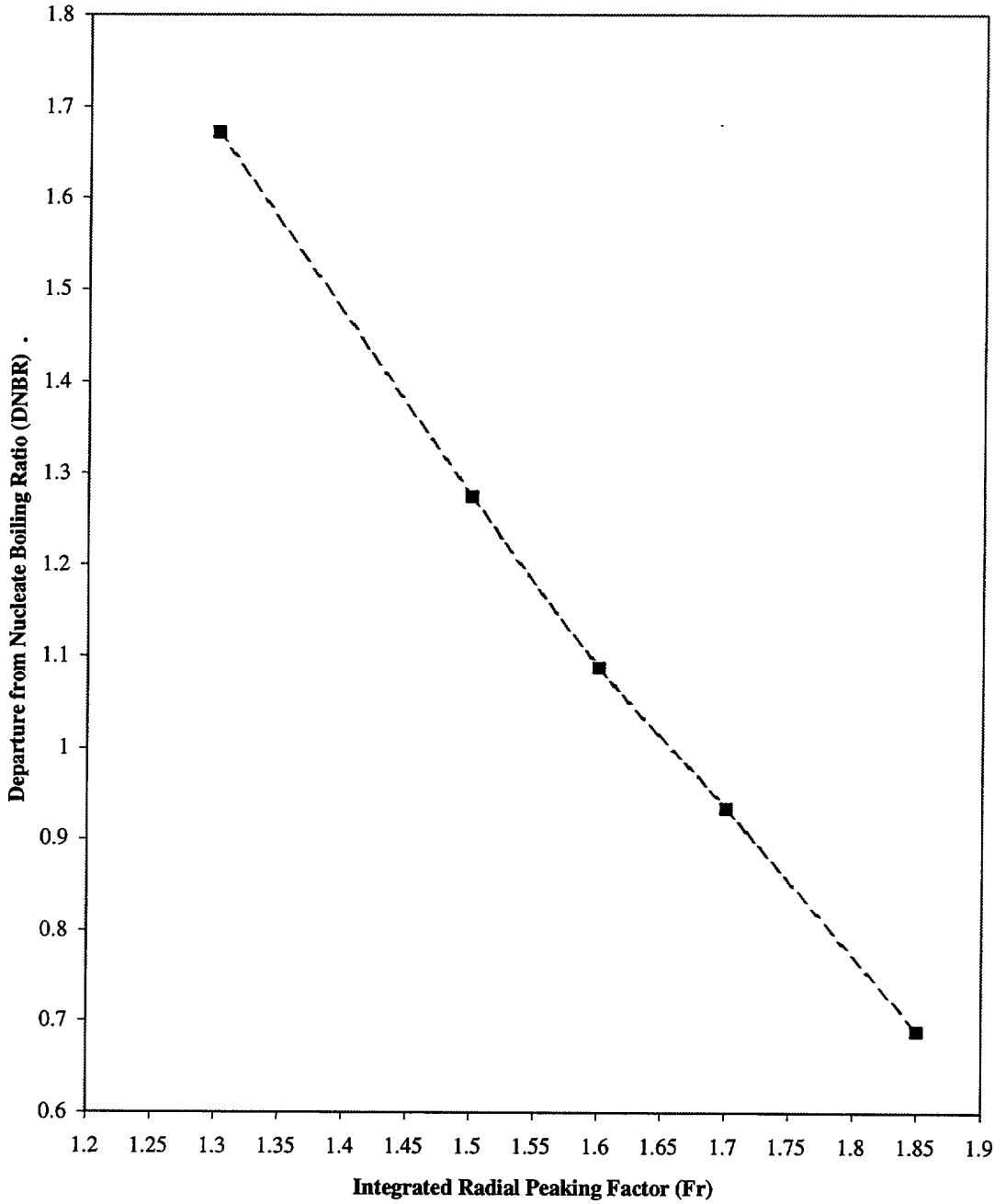

Figure 7.3.11.2-1

Feedwater Line Break
Peak RCS Pressure Vs. Break Size

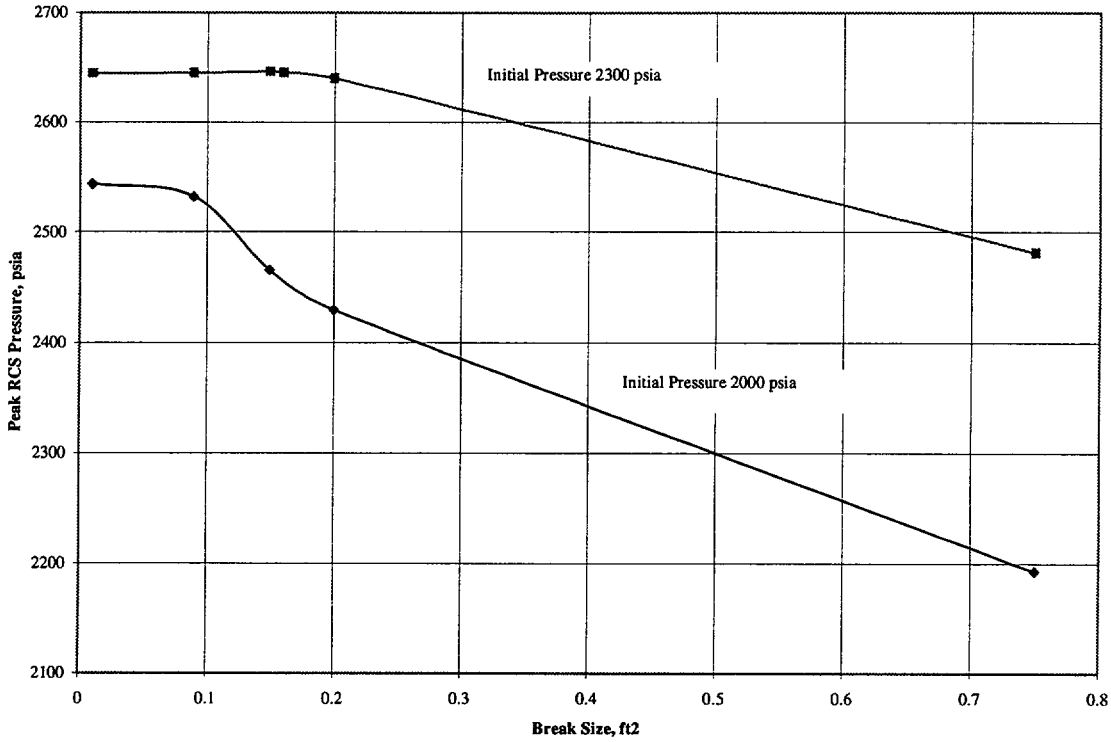

Figure 7.3.11.2-2

Feedwater Line Break
Core Power vs. Time

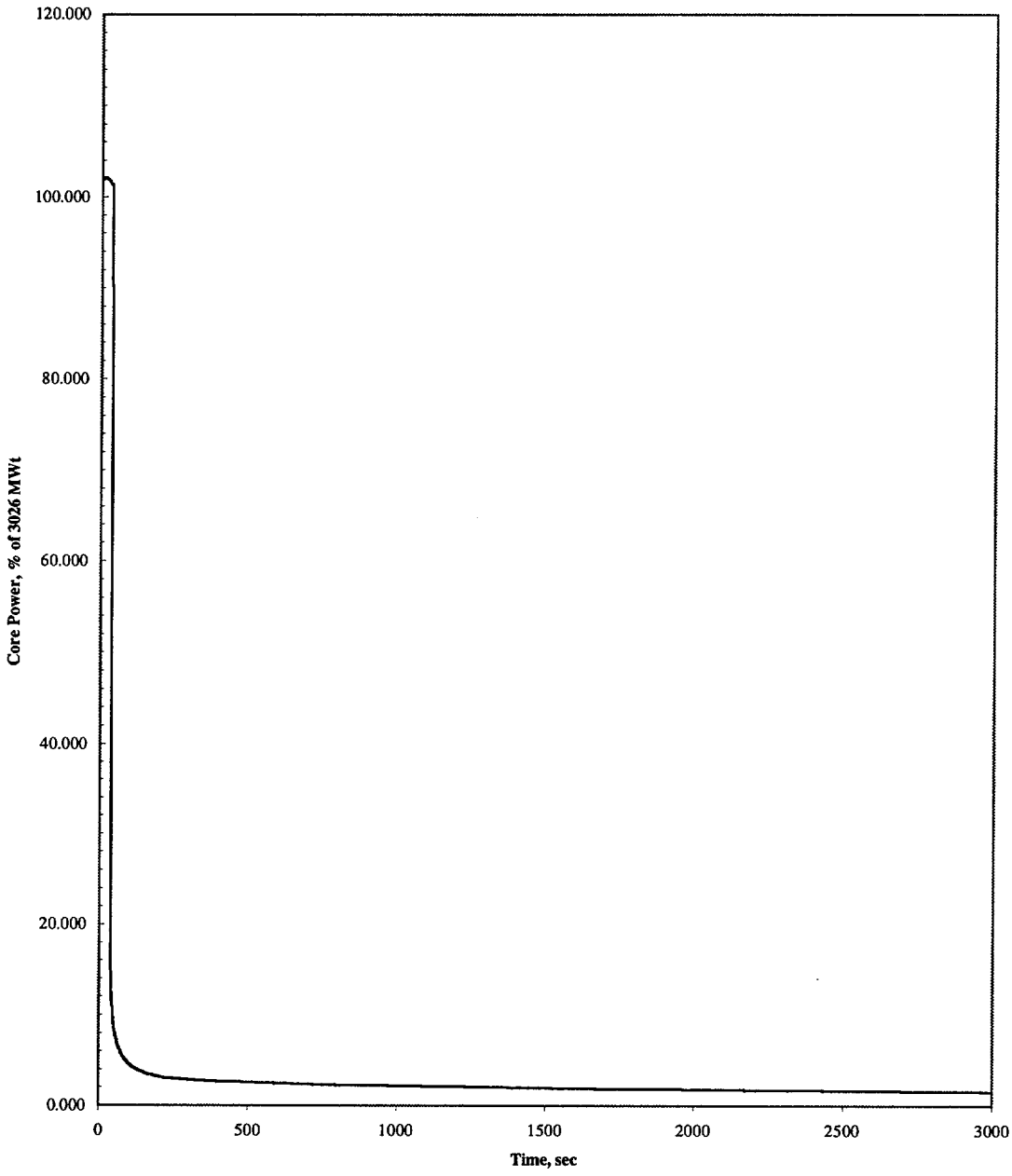

Figure 7.3.11.2-3

Feedwater Line Break
Core Average Heat Flux vs. Time

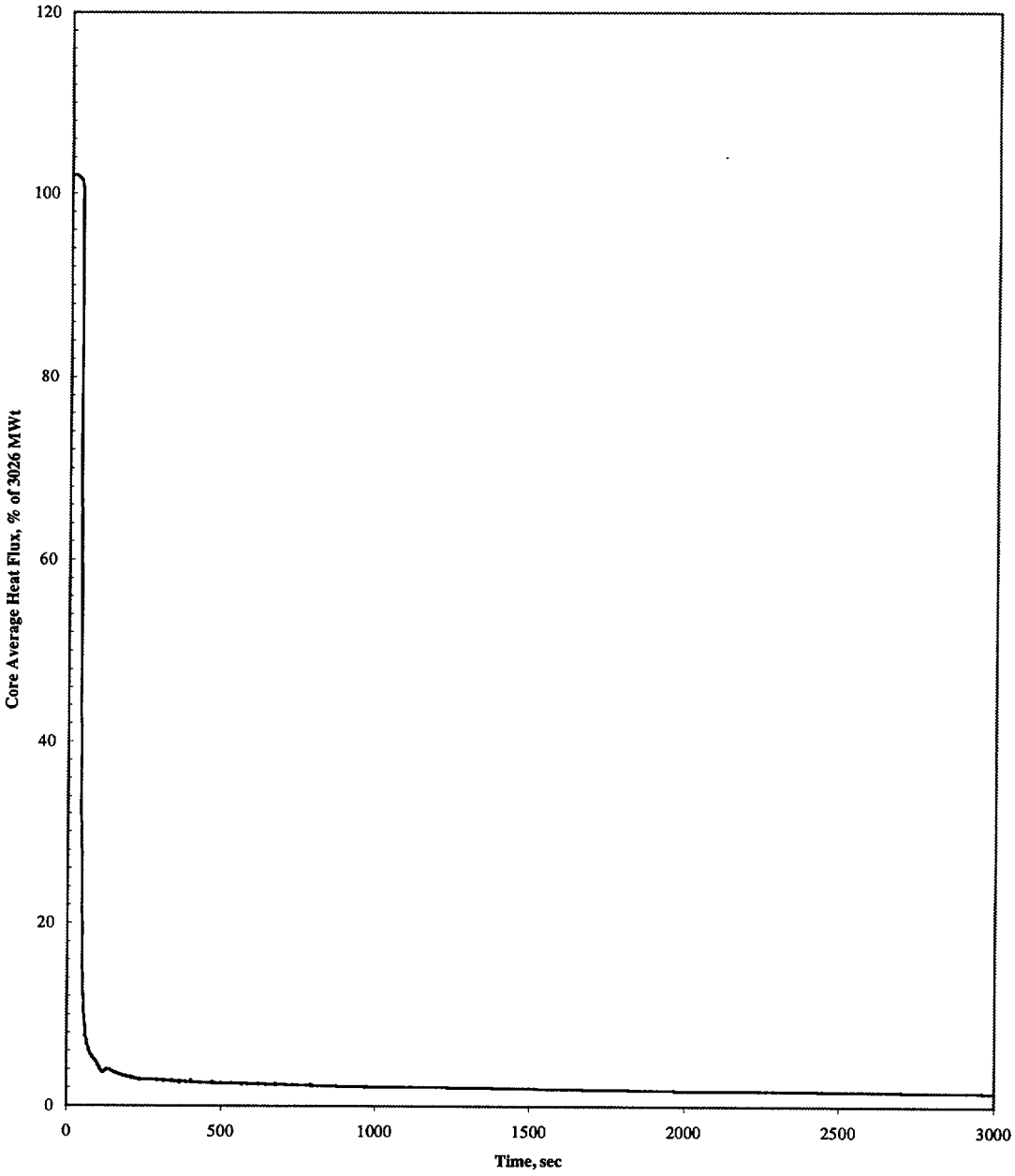

Figure 7.3.11.2-4

Feedwater Line Break
Reactor Coolant System Pressure vs. Time

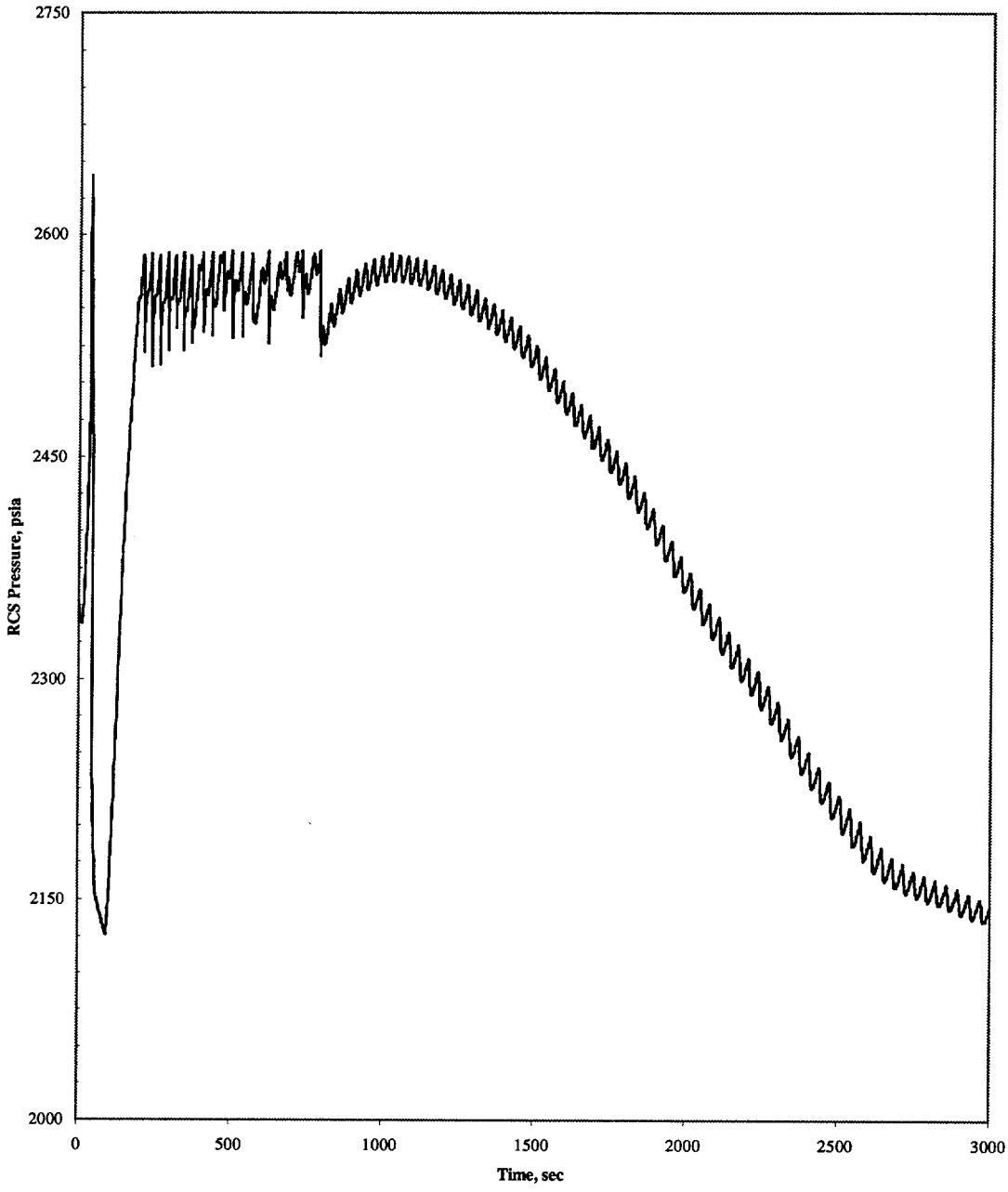

Figure 7.3.11.2-5

Feedwater Line Break
Reactor Coolant System Temperature vs. Time

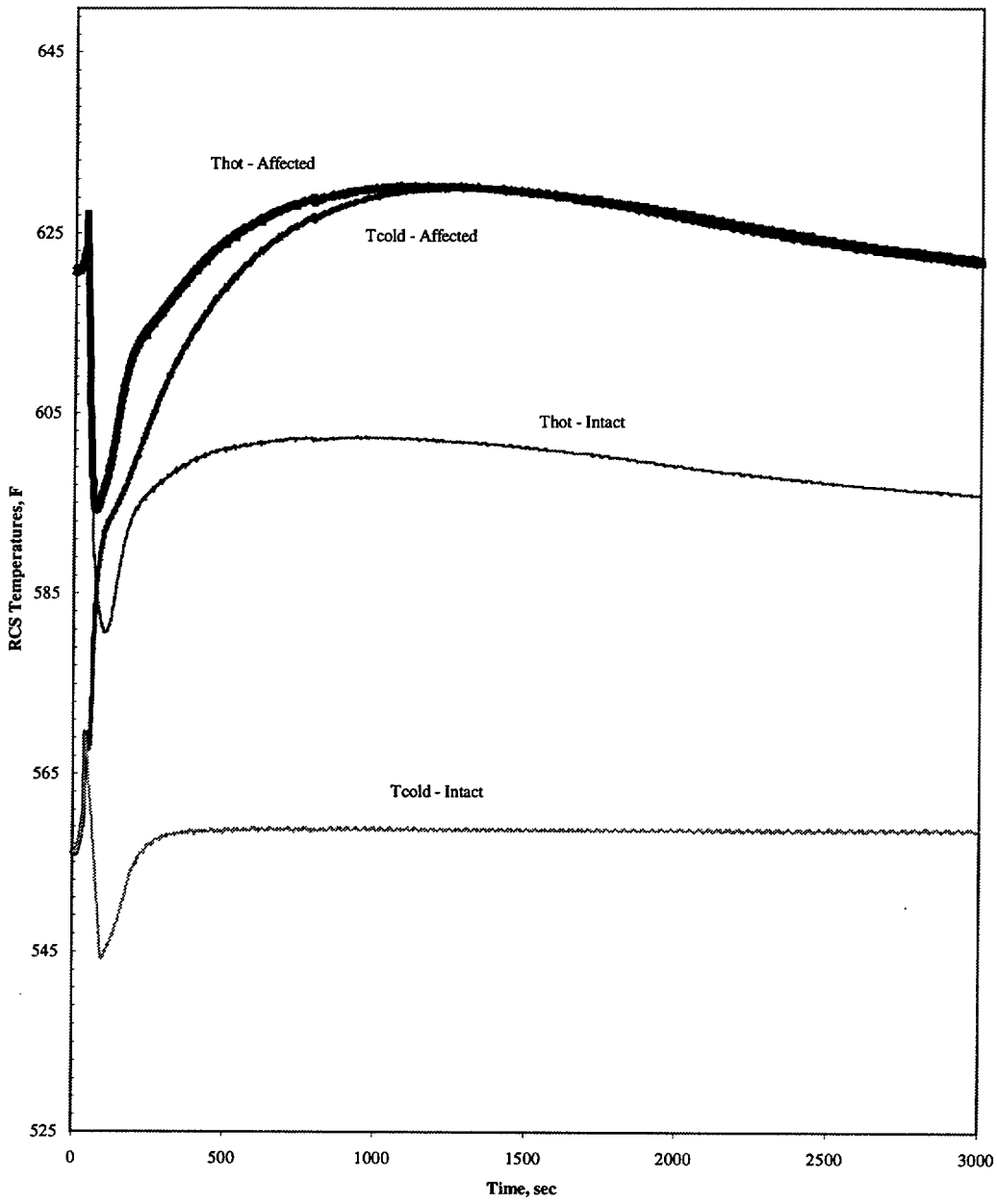

Figure 7.3.11.2-6

Feedwater Line Break
Steam Generator Pressure vs. Time

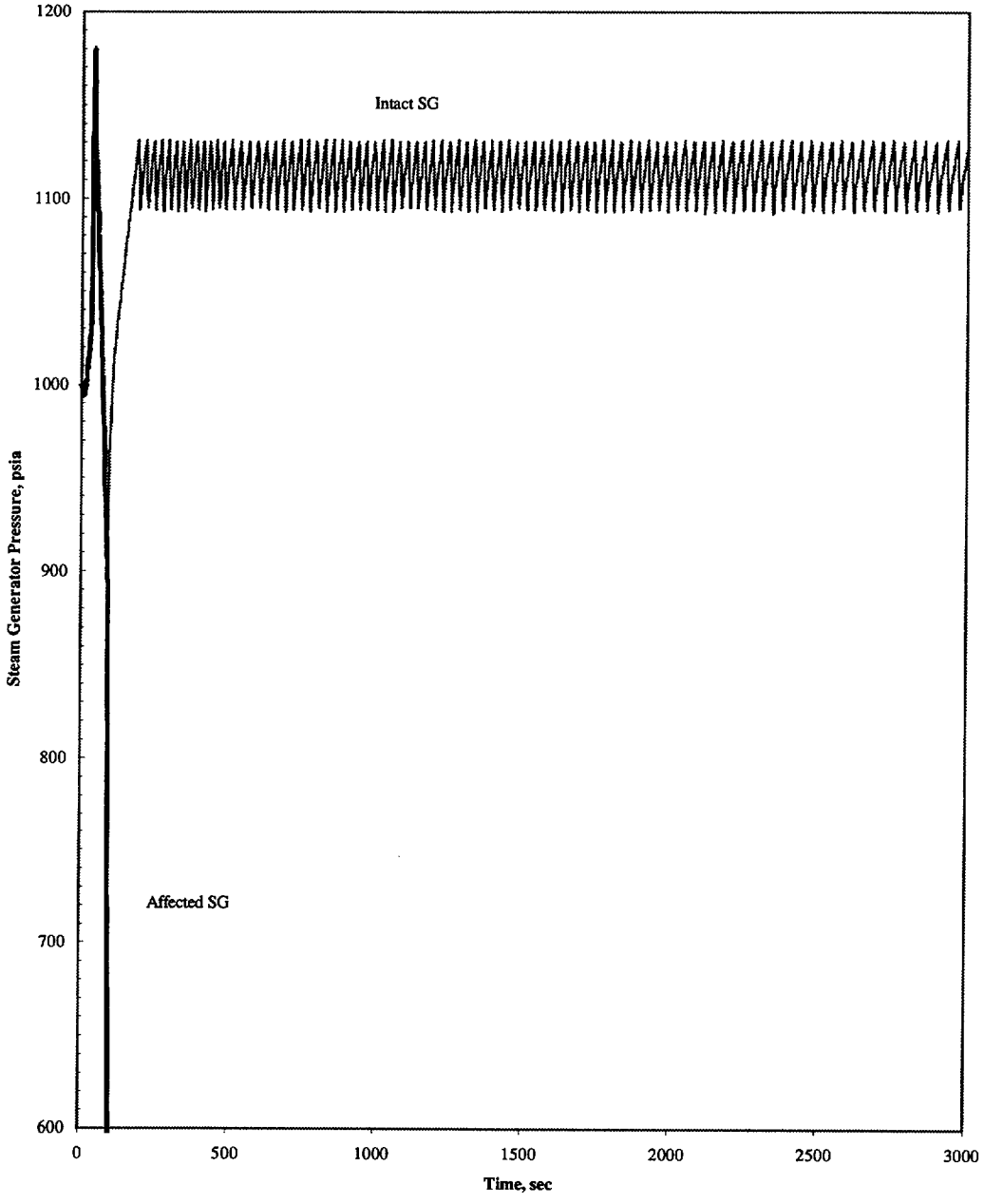

Figure 7.3.13-1

Steam Generator Tube Rupture with Concurrent Loss of AC Power
Core Power vs. Time

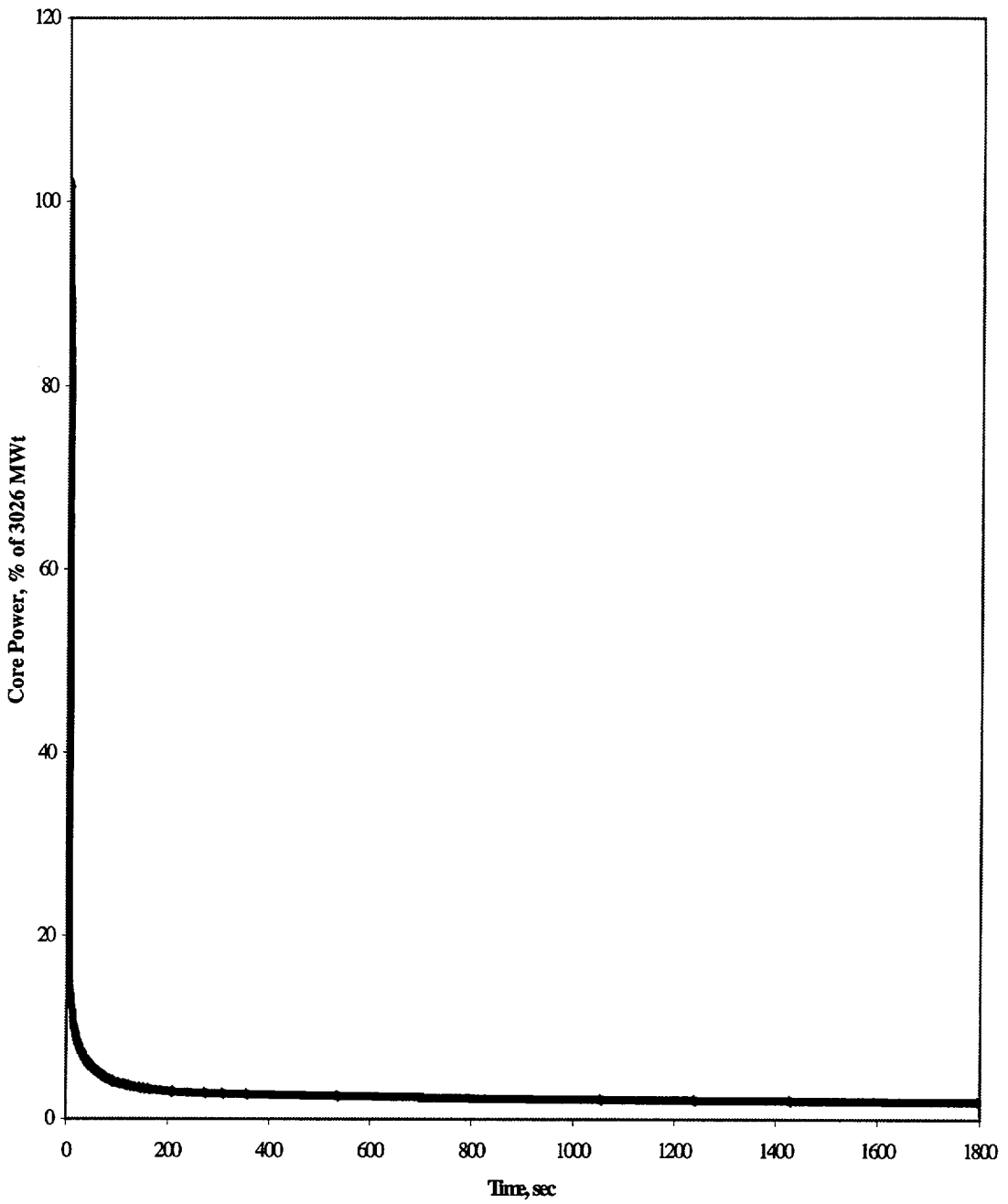

Figure 7.3.13-2

Steam Generator Tube Rupture with Concurrent Loss of AC Power
Reactor Coolant System Pressure vs. Time

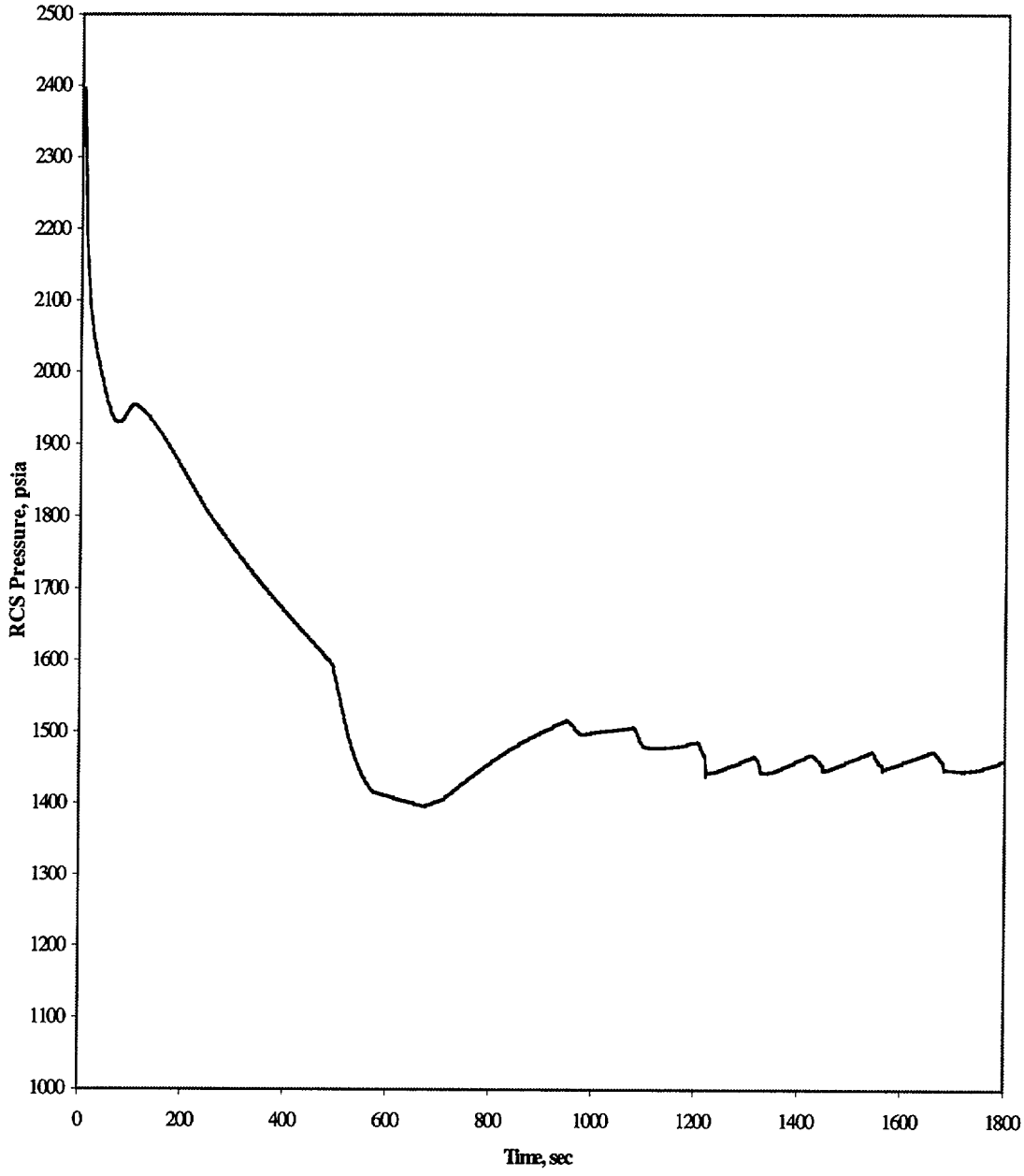

Figure 7.3.13-3

Steam Generator Tube Rupture with Concurrent Loss of AC Power
Reactor Coolant System Temperature vs. Time

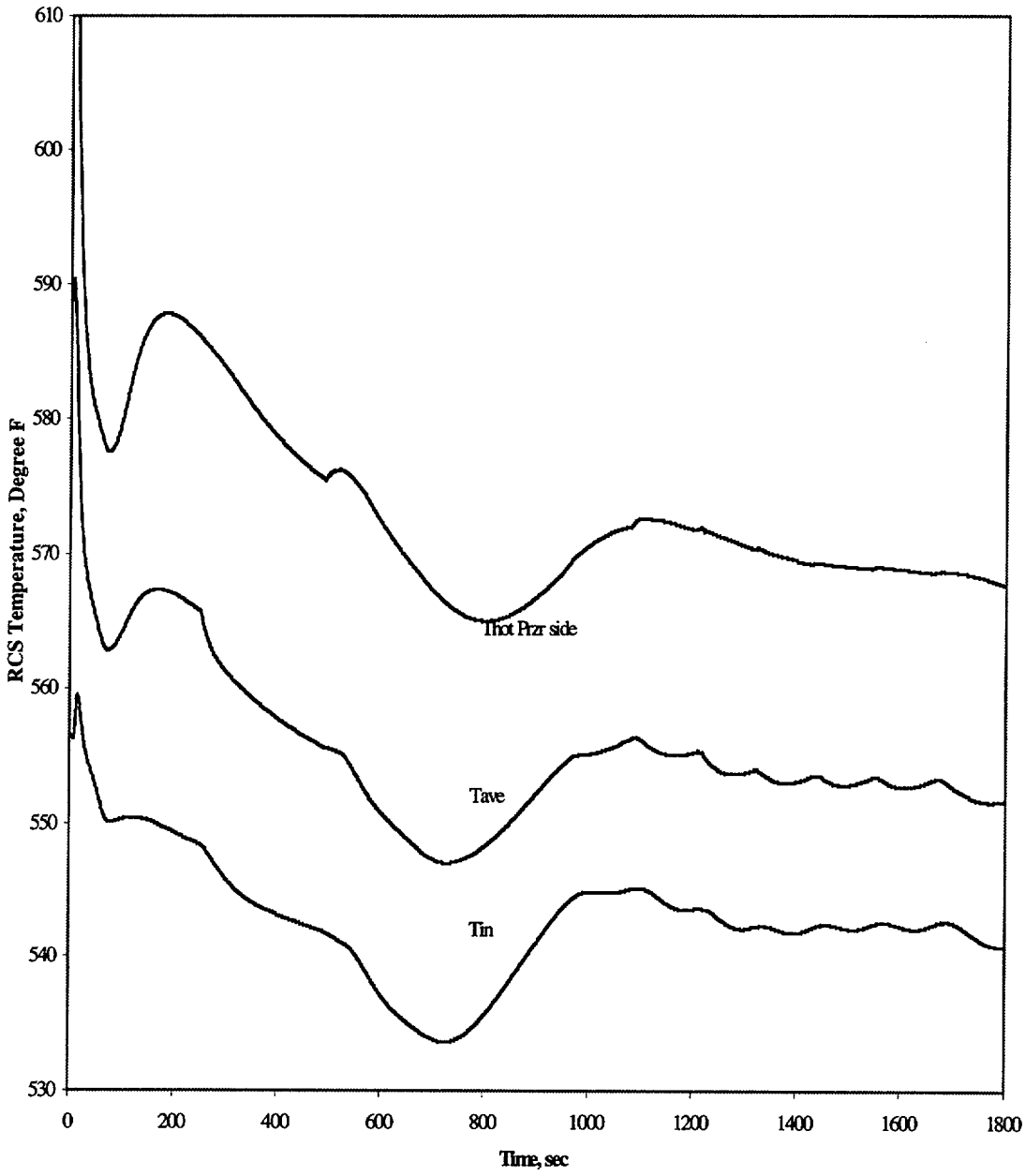

Figure 7.3.13-4

Steam Generator Tube Rupture with Concurrent Loss of AC Power
Steam Generator Pressure vs. Time

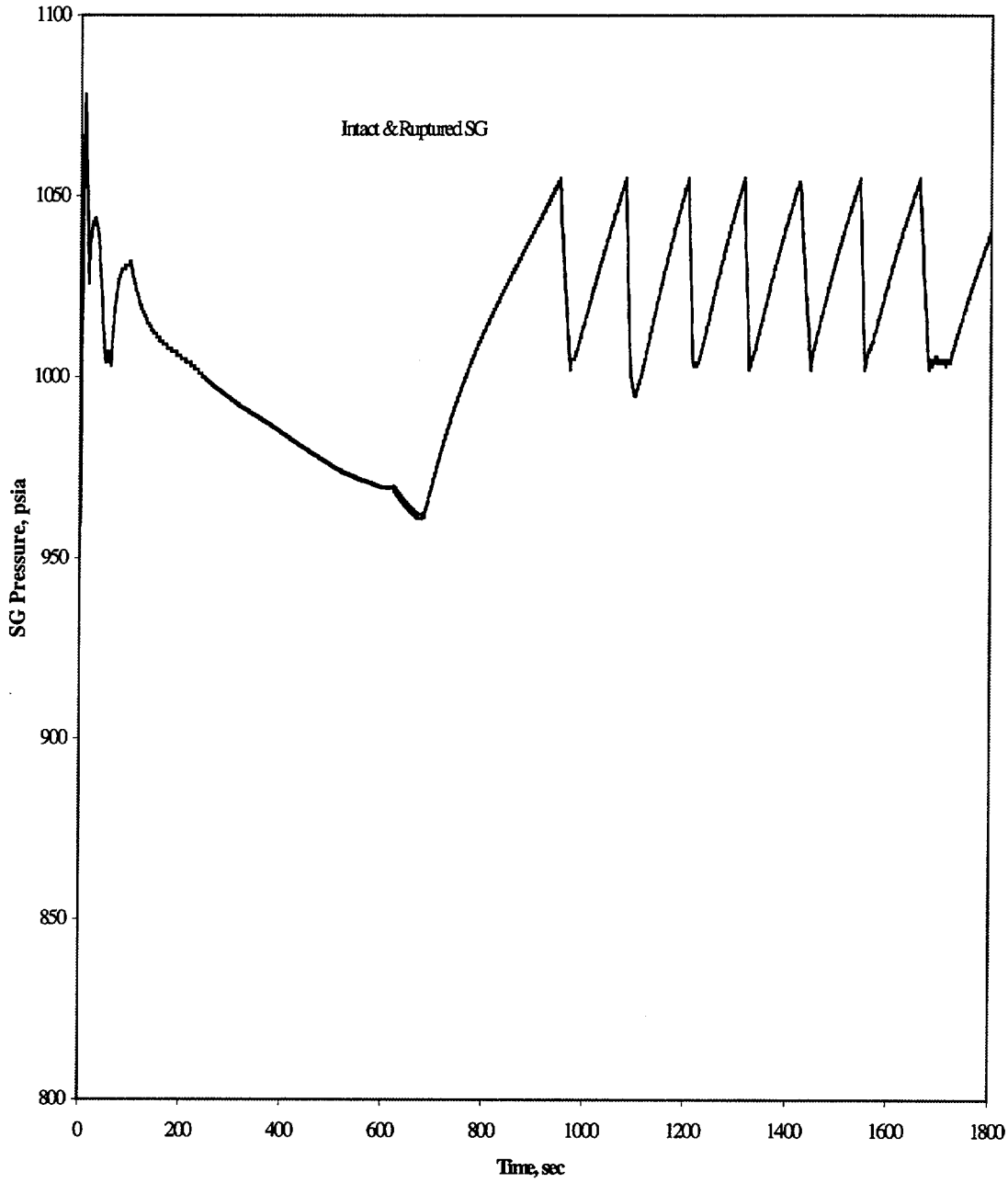

Figure 7.3.13-5

Steam Generator Tube Rupture with Concurrent Loss of AC Power
Leak Rate vs. Time

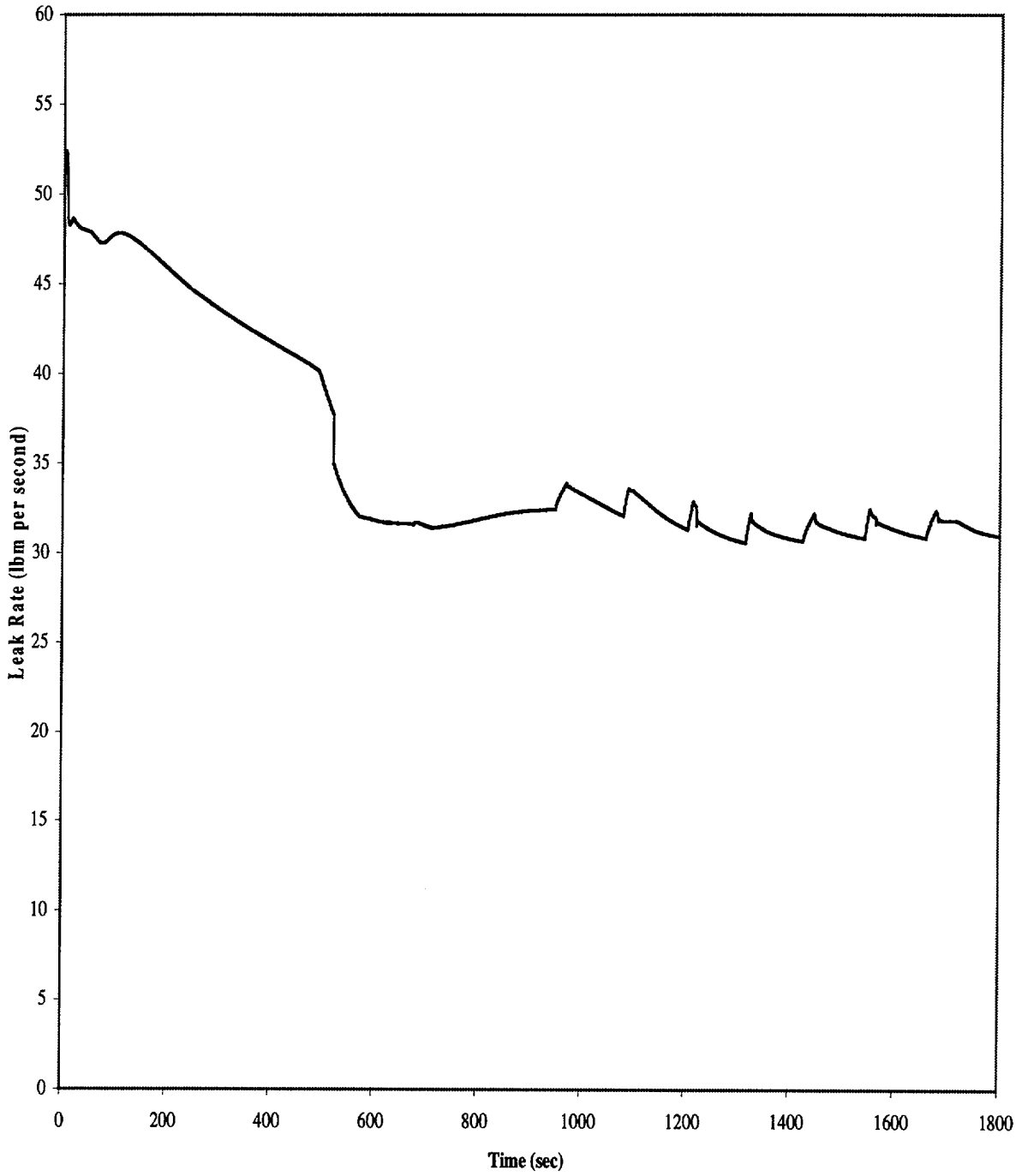

Figure 7.3.13-6

Steam Generator Tube Rupture with Concurrent Loss of AC Power
Pressurizer Level vs. Time

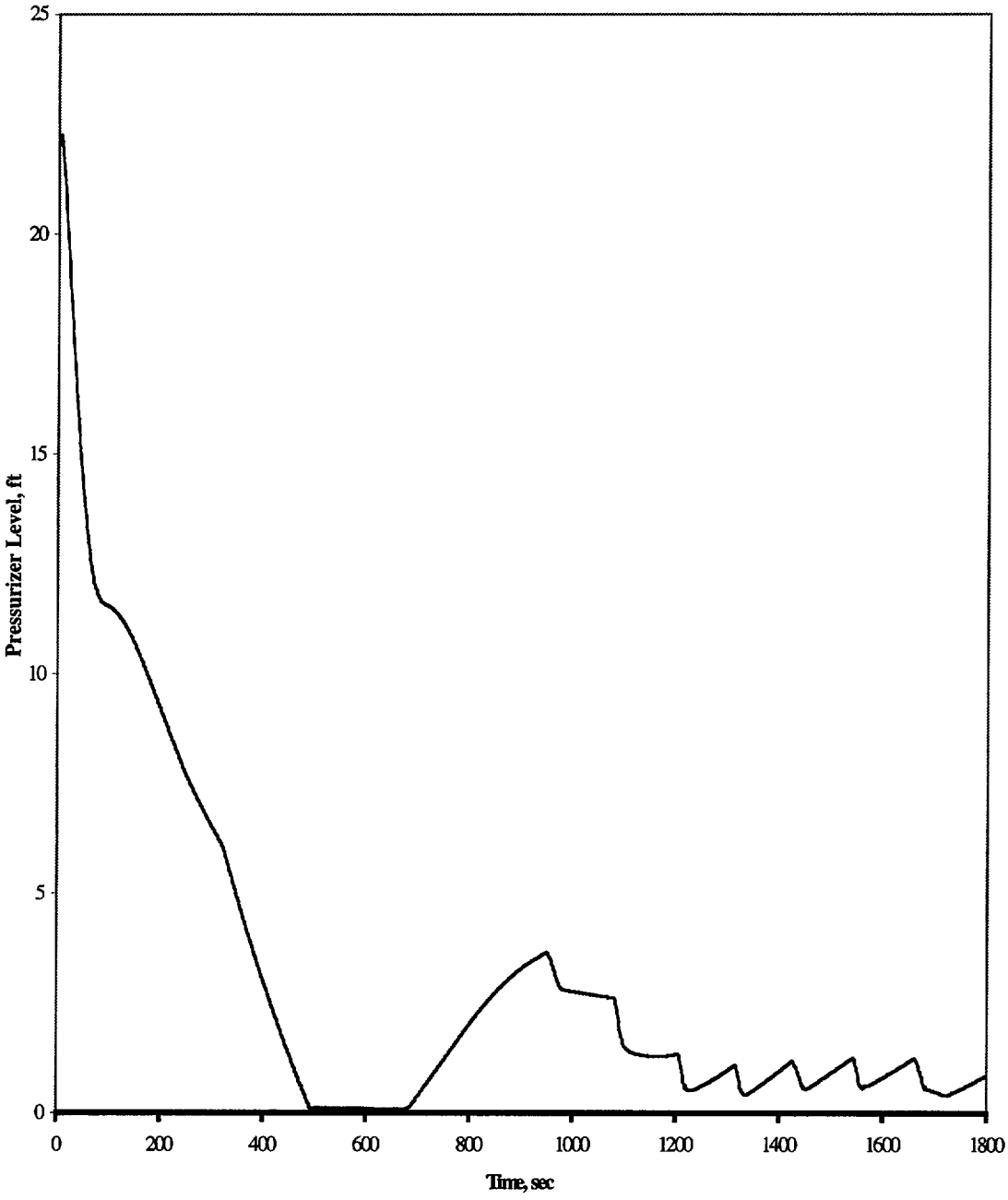

Figure 7.3.13-7
Steam Generator Tube Rupture with Concurrent Loss of AC Power
Steam Generator Liquid Mass vs. Time

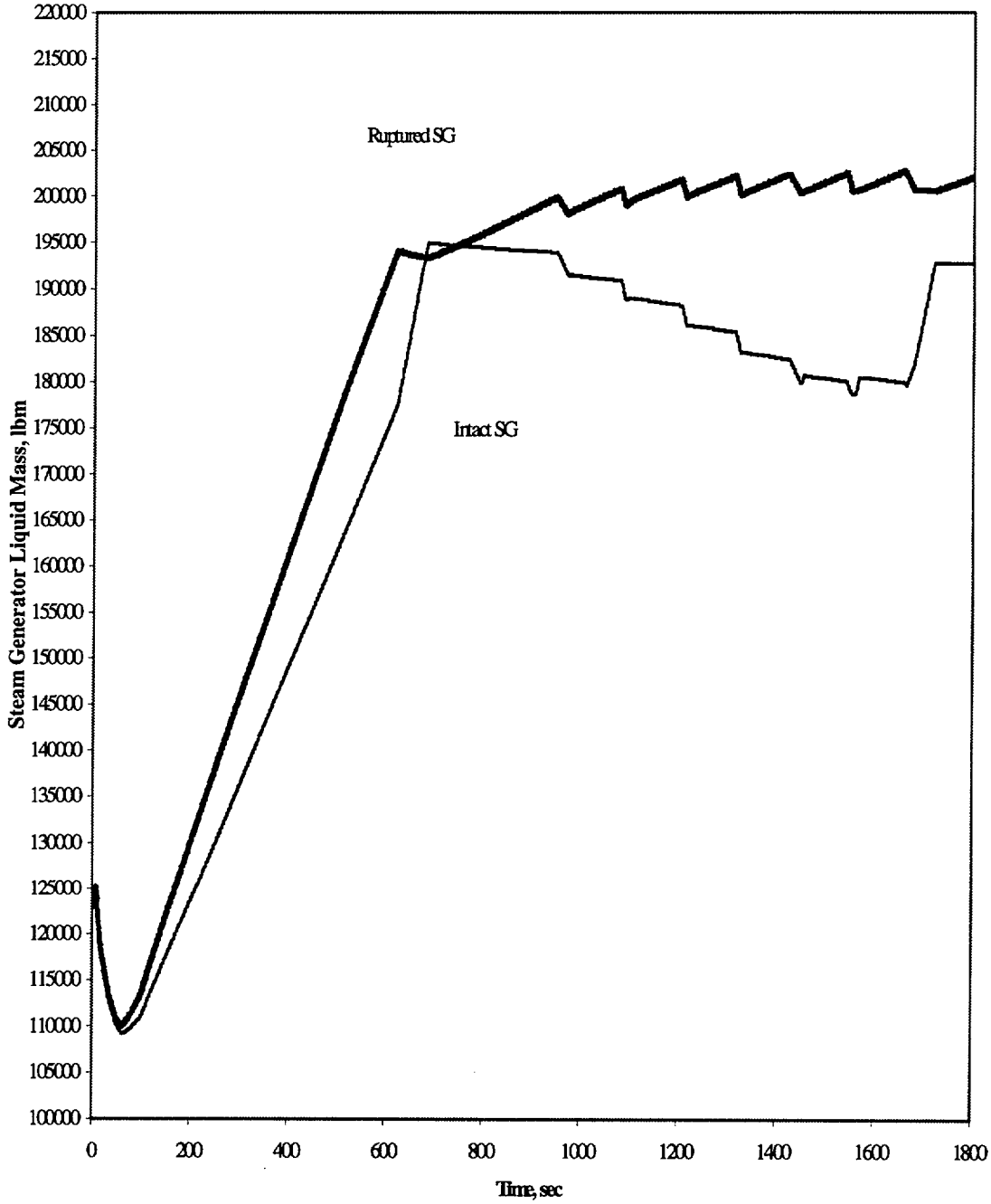

Figure 7.3.13-8

Steam Generator Tube Rupture with Concurrent Loss of AC Power
Secondary Safety Valve Flow Rate vs. Time

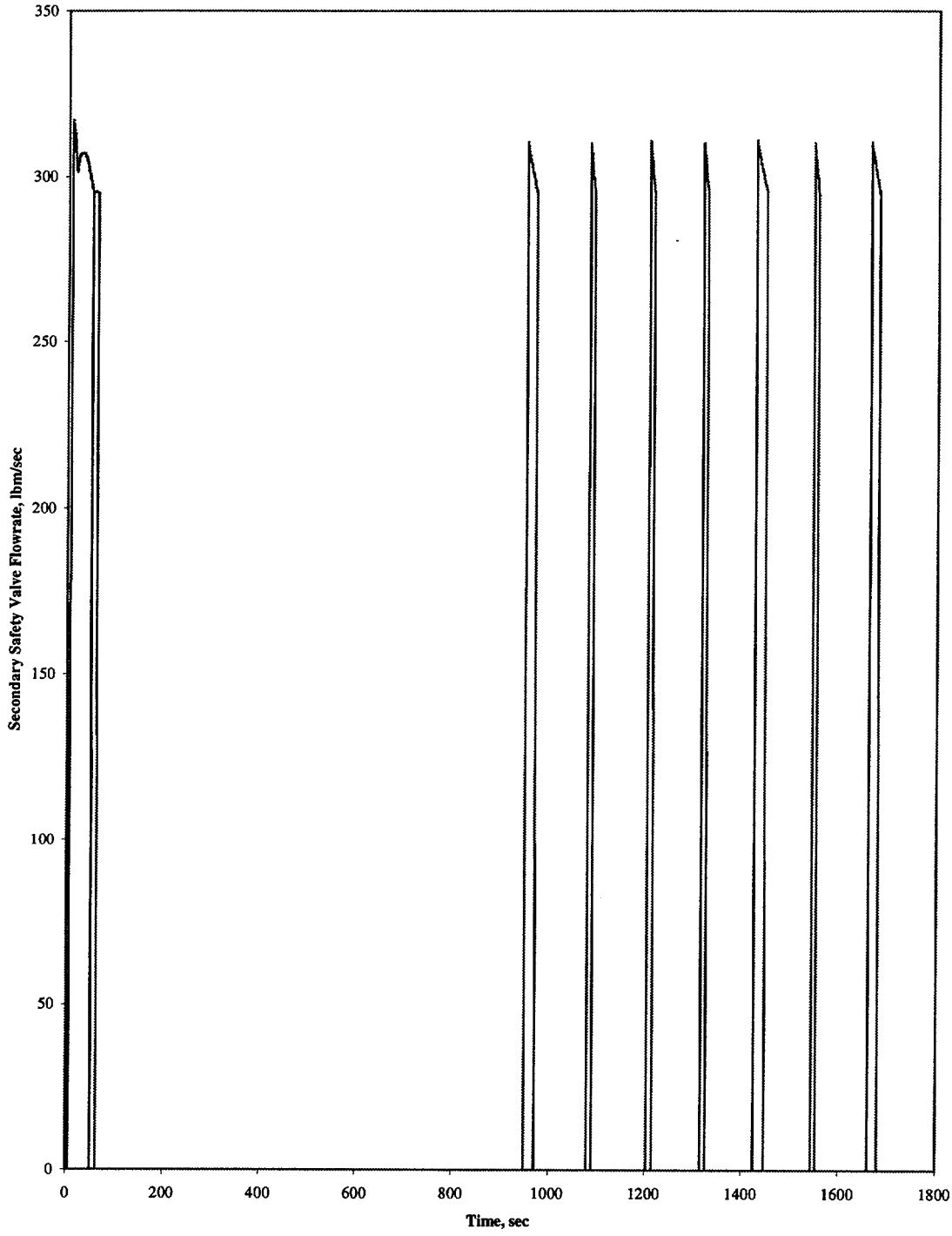

7.4 REACTOR MONITORING AND PROTECTION (RPS,ESFAS, AND COLSS)

As part of the evaluation for operation at an uprated power level, the setpoints for the reactor protection system (RPS), the engineered safety features actuation system (ESFAS), and the core operating limits supervisory system (COLSS) were reviewed to determine if changes were required.

Many of the RPS/ESFAS changes requested for Cycle 15 (correspondence dated November 29, 1999, 2CAN119901, approved by the SER for Amendment 222) included consideration of power uprate conditions. Therefore, of the RPS/ESFAS trip setpoints in the technical specifications, only the low pressurizer pressure setpoint is being changed for Cycle 16. This trip setpoint will be reduced to $\geq$ 1650 psia from $\geq$ 1675 psia to provide a comparable operating margin above the safety injection system actuation setpoint for the post-trip pressurizer pressure decrease after power uprate. The pressure decrease after an uncomplicated reactor trip is estimated to be slightly larger for uprate conditions and the setpoint is being reduced in order to avoid unnecessary safety injection system actuations. This setpoint change was supported by the use of a minimum setpoint of 1400 psia for the low pressurizer pressure safety injection actuation signal (SIAS) in the LOCA and steam line break analyses. The proposed TS values satisfy this setpoint assumption.

The steam generator high level trip setpoint was relocated to the Technical Requirements Manual (TRM) for Cycle 15. This trip setpoint is being reviewed for possible impact from the power uprate and the TRM will be revised as necessary.

Setpoints in COLSS and the core protection calculators (CPCs) will be adjusted to accommodate the power uprate operating conditions. The functional requirements imposed by the accident analyses are satisfied through the normal cycle reload process. Normal cycle reload analyses recognize changes in instrument uncertainties and make appropriate adjustments to necessary COLSS and CPC setpoints.

END OF SECTION

8 NUCLEAR FUEL

This section discusses the impact of power uprate on various aspects of the nuclear fuel.

8.1 THERMAL-HYDRAULIC DESIGN

The prime objective of the thermal and hydraulic design of the reactor is the assurance that the core can meet normal steady state and transient performance requirements without exceeding the design bases. For power uprate, the thermal margin for the cycle core design (Cycle 16) has been evaluated to ensure that the design bases have been met. Table 8.1-1 presents a comparison between the Cycle 15 and 16 parameters of interest for thermal-hydraulic design.

SAR Section 4.4 discusses the reactor thermal and hydraulic design. No changes to the SAR methodology were made in the evaluation of the thermal-hydraulic design under power uprate conditions.

8.1.1 Description of Analysis

8.1.1.1 Thermal Margin Analysis

Avoidance of thermally induced fuel damage during normal steady state operation and during anticipated operational occurrences (AOOs) is the principal thermal-hydraulic design basis. Steady state DNBR analyses of the bounding cycle design at the rated power level of 3026 MWt have been performed using the TORC computer code described in Reference 8.1-1, the CE-1 critical heat flux correlation described in Reference 8.1-2, the simplified TORC modeling methods described in Reference 8.1-3, and the CETOP code described in Reference 8.1-4 and approved in Reference 8.1-5.

Effects of fuel rod bowing on DNBR margin have been incorporated in the safety and setpoint analysis in the manner discussed in References 8.1-5, 8.1-6, 8.1-7, and 8.1-8. The penalty used for this analysis, 0.6% of MDNBR, is valid for assembly burnups up to 33 GWD/MTU. For assemblies with burnup greater than 33 GWD/MTU sufficient available margin exists to offset rod bow penalties due to the lower radial power peaks in these higher burnup batches. Hence, the rod bow penalty based upon Reference 8.1-8 for 33 GWD/MTU is applicable for all assembly burnups expected for the power uprate.

8.1.1.2 Coolant Flow Rate and Distribution

The lower limit on the total primary pump flow (given in Table 8.1-1) is utilized for all thermal margin analyses to assure that the core is adequately cooled. Uncertainties in system resistance, pump head, and core bypass flow are assumed to be in the adverse direction.

8.1.2 Conclusion

The thermal and hydraulic design of the reactor has been verified to be adequate under power uprate conditions such that the core can meet normal steady state and transient performance requirements without exceeding the design bases.

8.1.3 References

8.1-1 CENPD-161-P-A, "TORC Code, A Computer Code for Determining the Thermal Margin of a Reactor Core," April 1986.

8.1-2 CENPD-162-P-A, "Critical Heat Flux Correlation for CE-1 Fuel Assemblies with Standard Spacer Grids Part 1, Uniform Axial Power Distribution," April 1975.

8.1-3 CENPD-206-P-A, "TORC Code, Verification and Simplified Modeling Methods," June 1981.

8.1-4 CEN-214(A)-P, Rev. 1-P, "CETOP Code Structure and Modeling Methods for Arkansas Nuclear One-Unit 2," July 1982.

8.1-5 Robert A. Clark (NRC) to William Cavanaugh III (AP&L), "Operation of ANO-2 During Cycle 2," July 21, 1981 (Safety Evaluation Report and Licensing Amendment No. 26).

8.1-6 CEN-139(A)-P, "Statistical Combination of Uncertainties: Combination of System Parameter Uncertainties in Thermal Margin Analyses for Arkansas Nuclear One – Unit 2," November 1980.

8.1-7 CENPD-225-P-A, "Fuel and Poison Rod Bowing," June 1979.

8.1-8 CEN-289(a)-P, "Revised Rod Bow Penalties for Arkansas Nuclear One – Unit 2," December 1984.

Table 8.1-1
Arkansas Nuclear One Unit 2 Power Uprate
Thermal-Hydraulic Parameters at Full Power

General Characteristics	Units	Cycle 15	Cycle 16
Total heat output (core only)	MWt	2815	3026
	10^6 Btu/hr	9608	10328
Fraction of heat generated in fuel rod	---	0.975	0.975
Primary system pressure (nominal)	psia	2200	2200
Primary system pressure (minimum)	psia	2000	2000
Primary system pressure (maximum)	psia	2300	2300
Inlet temperature (maximum indicated)	°F	554.7	554.7
Total reactor coolant flow (minimum)	gpm	322,000	315,560
	10^6 lbm/hr	120.4	117.7
Coolant flow through core (minimum)	10^6 lbm/hr	116.2	113.6
Hydraulic diameter (nominal channel)	ft	0.039	0.039
Core average mass velocity	10^6 lbm/hr-ft^2	2.60	2.54
Pressure drop across core (at minimum steady state core flow rate)	psi	18.2	17.4
Total pressure drop across vessel (nominal dimensions and minimum flow)	psi	38.7	36.9
Core average heat flux (accounts for fraction of heat generated in fuel rod and axial densification factor)	Btu/hr-ft^2	179,772[1]	193,867[2]
Total heat transfer area (accounts for axial densification factor)	ft^2	52,094[1]	51,927[2]
Film coefficient at average conditions	Btu/hr-ft^2-°F	6200	6210
Average film temperature difference	°F	29.0[1]	31.24
Average linear heat rate of undensified fuel rod (accounts for fraction of heat generated in fuel rod)	kW/ft	5.26[1]	5.67[2]
Average core enthalpy rise	Btu/lb	82.7	90.9
Maximum clad surface temperature	°F	656.7	653.8
Engineering heat flux factor	---	1.025[3]	1.025[3]
Engineering factor on hot channel heat input	---	1.020[3]	1.020[3]
Rod pitch, bowing and clad diameter factor	---	1.05[3]	1.05[3]
Fuel densification factor (axial)	---	1.002	1.002

Notes:

(1) Based on 16 shims.

(2) Based on 150 shims.

(3) These factors have been combined statistically with other uncertainty factors at 95/95 confidence/probability level and included in the design limit on CE-1 minimum DNBR. These factors are the generic values based on fuel design drawing tolerances.

8.2 FUEL CORE DESIGN

In addition to the uprated power level, Cycle 16 will be the first cycle to use erbia as a burnable poison. Nuclear design analyses were performed to determine the impact on key safety parameters of the transition to UO_2-Er_2O_3 rod assemblies and the operation at an uprated core power of 3026 MWt. Key safety parameters are used as input to the SAR Chapter 15 accident analyses.

8.2.1 Description of Analyses and Evaluations

The nuclear design analyses employed a core power level of 3026 MWt. The preliminary design considered for Cycle 16 utilized typical values for the mechanical and thermal hydraulics data. The values of these parameters and others (enrichment, MTC, maximum burnup, etc.) were within the current licensed limits. The cycle-specific reload process utilizing approved methodologies will determine the final parameter values.

A Cycle 16 fuel management was constructed based on a typical fuel loading. The safety parameters were then evaluated such that the expected future range of potential fuel managements would be accommodated.

The methods and models have been used for other ANO-2 reload designs. No changes to the nuclear design philosophy, methods, or models are necessary due to the uprating.

The philosophy for the generation of physics data is to provide parameter values to the safety analyses that bound those actually expected within a given cycle. This includes items such as power distributions, fuel rod power histories, power peaking factors, reactivity coefficients, control rod worths, shutdown boron concentrations, neutron kinetics parameters, and neutron detector response.

All physics data for the ANO-2 power uprate have been evaluated and verified to be acceptable for a range of fuel managements. The parameter values used in the safety analyses bound the values expected in future core designs.

8.2.2 Conclusions

In summary, the key physics parameters for the power uprate have been evaluated to be acceptable for a range of fuel managements.

8.3 FUEL ROD MECHANICAL DESIGN AND PERFORMANCE

The fuel cladding is designed to prevent fuel element damage under steady state and transient operating conditions. The fuel rod design accounts for external pressure, differential expansion of the fuel and clad, fuel swelling, clad creep, fission and other gas releases, internal helium pressure, thermal stress, pressure and temperature cycling, and flow-induced vibrations. The purpose of this evaluation was to review the fuel rod design criteria to determine the acceptability of operating the ANO-2 fuel under power uprate conditions.

The fuel rod mechanical design and performance is discussed in SAR Section 4.2.1.

8.3.1 Description of Analyses, Acceptance Criteria, and Results

An evaluation was performed under power uprate conditions of the impact of the performance parameters in Table 8.3-1 on the ability to satisfy fuel rod design criteria for ANO-2. The evaluation accounted for the impact of cladding oxidation during the stress and collapse evaluations. Changes relative to previous ANO-2 fuel performance evaluations include an increase in the peak linear heat generation rate and application of the No-Clad Lift-Off methodology (Reference 8.3-10).

The parameters used in the fuel rod design criteria evaluation for the power uprate condition are summarized in Table 8.3-1.

The following sections summarize the impact of the power uprate conditions on key fuel rod design criteria relative to their corresponding acceptance limits and assess the resulting impact on anticipated design margin. The key criteria considered include rod cladding collapse, clad fatigue, clad stress and strain, rod maximum internal pressure, and clad corrosion. Other fuel rod design criteria are not significantly impacted by the proposed power uprate conditions.

8.3.1.1 Rod Cladding Collapse

Design Basis - The fuel rod will not collapse under operating compressive differential pressures for the specified residence time of the fuel.

Acceptance Limit - The minimum collapse time for the lead rod in the reactor will be greater than or equal to the target value of residence time specified in Table 8.3-1.

Design Evaluation - Margin to the fuel rod clad collapse limit is impacted by changes in the core power rating because higher power levels result in higher fuel operating temperatures and the resulting increase in oxide thickness levels. The NRC-approved collapse performance methodology and computer program CEPAN, References 8.3-1 and 8.3-2 , were used to evaluate rod collapse as a function of residence time. The results of this power uprate evaluation confirmed that rod collapse limits can be satisfied for the assumed residence time under power uprate conditions.

8.3.1.2 Clad Fatigue

Design Basis – The fuel system will not be damaged due to excessive fatigue from normal operating and upset transient conditions.

Acceptance Limit – The fuel rod clad EOL cumulative fatigue damage must be less than 0.8 for normal operating and upset condition transients of startup/shutdown and plant variations due to normal power changes and reactor trips from 100% power.

Design Evaluation - Margin to the fuel rod clad fatigue limit is impacted by changes in the core power rating because higher power levels result in higher fuel operating temperatures and the resulting increase in cyclic strain levels. The fatigue analysis evaluated rod fatigue as a function of burnup. The results of this power uprate evaluation confirmed that rod fatigue limits can be satisfied for the EOC burnup listed in Table 8.3-1.

8.3.1.3 Clad Stress

Design Basis - The fuel system will not be damaged due to excessive fuel clad stress.

Acceptance Limit - The maximum tensile stress in the cladding will not exceed two-thirds of the minimum unirradiated yield strength of the material at the applicable temperature.

Design Evaluation - Approved models and methodology were used to evaluate clad stress limits. The local power duty during anticipated operational occurrences (AOOs) is a key factor in evaluating margin to clad stress limits. The results of this evaluation show that the core power uprating will not impact the fuel's capability to meet clad stress limits for the uprated power conditions.

8.3.1.4 Clad Strain

Design Basis - The fuel system will not be damaged due to excessive fuel clad strain.

Acceptance Limit - Net unrecoverable circumferential strain in the fuel rod clad shall not exceed 1% as predicted by computations considering clad creep, pellet swelling, and pellet/clad differential thermal expansion under normal operating conditions.

Design Evaluation - Approved models and methodology were used to evaluate clad strain limits. The local power duty during AOO events is a key factor in evaluating margin to clad strain limits. The results of this evaluation show that the core power uprating will not impact the fuel's capability to meet clad strain limits for the uprated power conditions.

8.3.1.5 Rod Maximum Internal Pressure

The thermal performance of erbia and UO_2 composite fuel rods for Cycle 16 has been evaluated using the FATES3B version of the C-E fuel evaluation model (References 8.3-3, 8.3-4, 8.3-5, and

8.3-6). This analysis used a power history that enveloped the power and burnup levels representative of the peak fuel at each burnup interval, from beginning of cycle to end of cycle burnups.

In accordance with Reference 8.3-7, additional fuel performance analyses were performed to show that the gadolinia rods present in the uprate cycle are bounded by the urania rods with respect to rod internal pressure, fuel temperature and power-to-melt criteria during the uprate cycle.

The maximum predicted fuel rod internal pressure for the uprate cycle is below the no-clad-liftoff pressure (Reference 8.3-10). These results support a peak linear heat rate of 13.7 kW/ft to a peak rod average burnup of 50 GWD/MTU, and 13.0 kW/ft at higher burnups.

8.3.1.6 Cladding Waterside Corrosion

In accordance with Reference 8.3-8, an evaluation of waterside corrosion of W CENP fuel in ANO-2 was completed under uprated conditions. An evaluation was performed for the uprate cycle that used power histories expected to result in the highest predicted fuel cladding corrosion. Maximum oxide thickness levels for the uprate cycle are expected to be bounded by the waterside corrosion levels described for the highest burnup data of References 8.3-8 and 8.3-9. Therefore, the impact on thermal and mechanical performance will be acceptably described by these topical reports for those aspects dependent on the maximum oxide thickness.

8.3.2 Conclusions

The fuel rod design criteria most impacted by a change in core power rating have been reviewed with respect to the available margin to support the uprating. Although some design criteria are impacted, as stated above, the uprated conditions listed in Table 8.3-1 are supported. Finally, as in the past, cycle-specific fuel performance will continue to be evaluated for each fuel cycle to confirm that this assessment, and all fuel rod design criteria, are satisfied for the operating conditions specified for each cycle of operation. These evaluations support the reload safety evaluation which is performed for each cycle of operation.

8.3.3 References

8.3-1 "CEPAN, Method of Analyzing Creep Collapse of Oval Cladding," CENPD-187-P-A, March 1976.

8.3-2 "CEPAN Method of Analyzing Creep Collapse of Oval Cladding," EPRI NP-3966-CCM Volume 5, April 1985.

8.3-3 CEN-161(B)-P, Supplement 1-P-A, "Improvement to Fuel Evaluation Model," January 1992.

8.3-4 CENPD-139-P-A, "Fuel Evaluation Model," July 1974.

8.3-5 CEN-161(B)-P-A, "Improvement to Fuel Evaluation Model," August 1989.

8.3-6 CENPD-382-P-A, "Methodology for Core Designs Containing Erbium Burnable Absorbers," August 1993.

8.3-7 CENPD-275-P-A, Revision 1-P-A, "C-E Methodology for PWR Core Designs Containing Gadolinia-Urania Burnable Absorbers," May 1988.

8.3-8 CEN-386-P-A, "Verification of the Acceptability of a 1-Pin Burnup Limit of 60 MWD/kgU for Combustion Engineering 16x16 PWR Fuel," ABB Combustion Engineering, Inc., August 1992.

8.3-9 CENPD-384-P, "Report on the Continued Applicability of 60 MWD/kgU for ABB Combustion Engineering PWR Fuel," ABB Combustion Engineering, Inc., September 1995.

8.3-10 CEN-372-P-A, "Fuel Rod Maximum Allowable Gas Pressure," May 1990.

Table 8.3-1

Summary of ANO-2 Uprating Parameters Analyzed in Fuel Rod Design Evaluation

Parameter	Current Condition	Uprated Condition
Max fuel rod axially average fluence (10^{21}, n/cm^2)	13.0	13.0
Core inlet temperature (degree F)	554.7	554.7
Minimum flow rate (10^6, lbm/hr)	118.0	118.0
System pressure (psia)	2200	2200
Peak rod axial average burnup (MWD/MTU)	67,300	67,300
Residence time (EFPH)	41,200	41,200
Fuel design considered	Batches J-T	Batches M through U
Peak linear heat rate (kW/ft)	13.5	13.7 (Rods ≤ 50 GWD/MTU) 13.0 (Rods > 50 GWD/MTU)

8.4 NEUTRON FLUENCE

8.4.1 Description of Analysis

As requested in correspondence dated January 27, 2000 (2CAN010007), and approved by Amendment No. 213 to the facility operating license (correspondence dated April 4, 2000 (2CNA040002)), a reactor vessel surveillance capsule was withdrawn during 2R14 for analysis. As part of the analysis of this capsule, a revised fast neutron fluence will be calculated. Based on the analysis of the capsule, the Pressure/Temperature (P/T), Low Temperature Overpressure Protection (LTOP), and Pressurized Thermal Shock (PTS) analyses will be revised as necessary. The revised analyses will be the basis of a technical specifications change request to be submitted prior to Cycle 16. This change request will include new P/T curves based on the surveillance capsule and the projected fluence.

The current P/T curves in the technical specifications are applicable through approximately 17 EFPY, not 21 EFPY as stated in TS Figures 3.4-2A, 3.4-2B, and 3.4-2C. This is due to a change to the limiting plate and has been previously discussed with the NRC in correspondence related to Generic Letter 92-01 concerning reactor vessel structural integrity (see references below). The current TS curves are conservatively estimated to be applicable through the beginning of Cycle 16. At the beginning of Cycle 15, ANO-2 burnup is approximately 15.7 EFPY.

The estimated flux for Cycle 16 is within 7.5% of the flux for Cycle 15. Evaluations indicate that even with the power uprate, the expected Cycle 16 flux is approximately the same as the flux during Cycle 1 due to changes in fuel management.

Section 5.2.4 of the ANO-2 SAR discusses the fracture toughness of the reactor vessel and the impact of neutron fluence.

8.4.2 Conclusions

As discussed in the referenced correspondence, current estimates of neutron fluence are conservative. No difficulties are anticipated in incorporating the higher flux of Cycle 16 and beyond into acceptable P/T analyses based on the results of the surveillance capsule analysis.

8.4.3 References

8.4-1 Letter from Dwight C. Mims (Entergy Operations, Inc.) to U.S. Nuclear Regulatory Commission dated June 18, 1997 (2CAN069709), "Response to Generic Letter 92-01, Revision 1, Supplement 1, 'Reactor Vessel Structural Integrity,' for ANO-2, TAC Nos. M92642 and M77399."

8.4-2 Letter from M. Christopher Nolan (U.S. NRC) to C. Randy Hutchinson (Entergy Operations, Inc.) dated July 8, 1999 (2CNA079901), "Completion of Licensing Action for Closure of Generic Letter 92-01, Revision 1, Supplement 1, 'Reactor Vessel Structural Integrity,' Request for Additional Information for Arkansas Nuclear One, Unit 2 (TAC No. MA0524)."

8.5 SOURCE TERMS

Source terms for several different accident and normal operating conditions were determined for power uprate conditions. The results were used as input to dose and balance of plant analyses. The reanalyzed areas include source terms for uprated core power for use in the non-LOCA and Fuel Handling Accident (FHA) safety analyses. Each analysis assumes a core power of 3087 MWt (3026 MWt plus 2% measurement uncertainty). These analyses are summarized below.

8.5.1 Description of Analyses and Evaluations

8.5.1.1 Non-LOCA Source Terms

The scope of this analysis involves the calculation of the average volatile fission product activities (iodine, krypton, and xenon) per fuel rod. These source terms are used in the non-LOCA transient analyses to evaluate dose consequences resulting from failed fuel rods.

The average fuel rod isotopic activities of iodine and the noble gases krypton and xenon are calculated with the ORIGEN-II point depletion computer code. The calculations were performed at the uprated power. ORIGEN-II is an industry standard code that is generally accepted for the purposes for which it will be used in this evaluation and is therefore considered to be acceptable for application to ANO-2.

8.5.1.2 FHA Source Terms

The scope of this analysis involves the calculation of the maximum volatile fission product gas gap activities (iodine, krypton, and xenon). These source terms are used in the FHA analyses. This analysis covers burnups to 65,000 MWD/MTU, core power at 3087 MWt, and radial peaking of 1.70.

The maximum isotopic activities of volatile fission products are calculated with the ORIGEN-II point depletion computer code. The calculations were performed at the uprated power and 100 hours decay time.

8.5.2 Conclusions

8.5.2.1 Non-LOCA Source Terms

Table 8.5-1 contains the maximum volatile fission product activities for each isotope. The values given in Table 8.5-1 are valid for enrichments up to 5.0 w/o U-235 and for fuel management such that the maximum burnup of any rod within 10% of the limiting radial peaking factor (F_r) is less than 40,000 MWD/MTU, for an average power per fuel rod of 0.07247 MW, and the standard 16x16 pellet design. For a peak power pin, these values may be multiplied by the appropriate pin power peaking (F_r) required for the non-LOCA event analyzed.

8.5.2.2 FHA Source Terms

Table 7.3.15-1 contains the maximum volatile fission product gas gap activities for each isotope for four rows of a fuel assembly. These values include a 1.70 peaking factor for the "worst" assembly with a 100-hour decay following burnup to 65,000 MWD/MTU. The use of the 1.70 radial peaking factor gives a conservative value for the fuel handling accident.

Table 8.5-1

Volatile Fission Product Activities for Non-LOCA Transients

Isotope	Maximum Activity (Ci/Rod)
Kr-85	2.281E+01
Kr-85M	6.473E+02
Kr-87	1.279E+03
Kr-88	1.805E+03
I-131	2.002E+03
I-132	2.882E+03
I-133	4.072E+03
I-134	4.517E+03
I-135	3.788E+03
Xe-131M	2.249E+01
Xe-133	4.055E+03
Xe-133M	1.263E+02
Xe-135	1.055E+03
Xe-135M	7.993E+02
Xe-138	3.540E+03

END OF SECTION

9 MISCELLANEOUS TOPICS

9.1 POST-LOCA HYDROGEN GENERATION

Combustible gas control in containment is discussed in SAR Section 6.2.5. The SAR description of post-LOCA hydrogen generation is unaffected except as discussed below.

The increase in reactor power directly affects the hydrogen contribution from the radiolytic decomposition of water in the core and sump. The effect of power uprate on this reaction has been reviewed and found to be acceptable. The hydrogen contribution from the zirconium-water reaction is not affected by power uprate. The corrosion of metals within containment is not directly affected by the power uprate; it is indirectly influenced by the effect of power uprate on the containment pressure and temperature profiles.

9.1.1 Input and Assumptions

The containment post-LOCA hydrogen analysis was revised to support the installation of the replacement steam generators for Cycle 15. The revised analysis also addressed the effects of power uprate and the increased containment pressure and temperature profiles established for the containment uprate (see Section 6.2 of this report). The analysis methodology, which uses the COGAP computer program (NUREG/CR-2847), was unchanged from that described in the SAR (Amendment 15).

The assumptions used in calculating the amount of hydrogen produced from each source are the same as, or more conservative than, those suggested in Regulatory Guide 1.7. The power level assumed in the analysis increased from 2900 MWt to 3087 MWt.

The total hydrogen generation estimated from the zirconium-water reaction has been changed from 19,264 scf to 19,206 scf. The change resulted from a correction to the value for the zirconium mass: based on the current core design, the original value was overly conservative.

New metal corrosion rates were developed for Cycle 15 based on the post-LOCA containment pressure and temperature profiles developed for the containment uprate, which included consideration of power uprate. The new metal corrosion rates also reflected a containment spray pH profile based on the use of tri-sodium phosphate as a buffering agent instead of the former sodium hydroxide system. No additional revisions to the corrosion rates were necessary for Cycle 16. The net impact of these changes is an increase in the predicted rate of hydrogen production very early in the event, but a reduction in the total hydrogen produced by corrosion over the thirty days of the analysis.

A correction was made to the calculation of the value for dissolved hydrogen used in the previous analysis. This resulted in a decrease from 1680 scf to 500 scf.

9.1.2 Results of Analysis

The increase in the power level assumed in the analysis resulted in a 6.5% increase in radiolytic hydrogen generation throughout the 30 days of the analysis. In combination with the other analysis input changes and the revised containment pressure and temperature profiles, the results changed slightly from the previous analysis. Without consideration of recombiner operation, the total production of hydrogen over the thirty days of the analysis decreased by about 5%. The initial hydrogen release (from the zirconium-water reaction and dissolved hydrogen) was reduced but the early release from metal corrosion increased such that the time required to reach the concentration at which the Emergency Operating Procedures require startup of the recombiners, 2%, was unchanged. The time required for hydrogen to reach the concentration of 3.5%, at which the analysis assumed startup of one recombiner, decreased from 3.9 to 3.5 days. The peak hydrogen concentration assuming one recombiner increased from 3.5% to 3.8%, and the concentration at the end of 30 days increased from 2.3% to 2.4%.

9.1.3 Conclusions

The revised analysis demonstrates that the hydrogen recombiner system is still capable of performing its intended function of maintaining the containment hydrogen concentration below the 3.9% design limit established for the system. No change is required to the operator actions taken in response to a LOCA for combustible gas control in containment.

9.2 HIGH ENERGY LINE BREAK (HELB)

The high energy line break (HELB) analysis for pipe breaks located outside the containment was revised to include the replacement steam generator (RSG) configuration change. The HELB environmental analysis for the RSG configuration change used bounding break mass flow and energy values for the power uprate configuration. These changes have been incorporated into SAR Amendment 16 under 10CFR 50.59. Therefore, no additional HELB environmental impact analysis changes are necessary to specifically address the power uprate. The physical pipe break locations, evaluation of pipe whip, and jet forces have also been reviewed and any necessary changes incorporated into SAR Amendment 16 Under 10CFR 50.59. High energy line breaks are discussed in SAR Section 3.6.

The combined environmental impact of the RSGs and power uprate varied among the areas evaluated. Some rooms were not affected, and for others the estimated peak temperature and pressure actually decreased due to the effect of the flow restrictors in the RSGs which limit the rate of blowdown. For those areas where peak pressures and temperatures increased, the pressure increases were negligible, and most temperature increases were only a few degrees.

9.3 RADIOLOGICAL ASSESSMENT

The Safety Analysis Report (SAR) Sections 11 and 12 present the bases for radioactive waste management and radiation protection at ANO-2. The purpose of this assessment is to ensure that the radioactive waste systems will be able to handle the increase in radioactive materials and that the bases for the radiation shielding design remain valid for the power uprate.

9.3.1 Scope of Review

For normal plant operations the scope of review was limited since no changes are made to the normal reactor coolant system (RCS) or steam generator (SG) activity limits specified in the Technical Specifications. For design basis events revised source terms were prepared and evaluated for impact to radiation protection.

9.3.2 Design Requirements

Shielding for normal operations must meet the requirements of 10CFR20 as it relates to operator dose and access control. Regulatory Guide 8.8 provides additional guidance for shielding as described in SAR Section 12.1.1. Radwaste systems and equipment must be designed to be capable of maintaining offsite releases and the resulting doses within the requirements of 10CFR20 and 10CFR50, Appendix I. SAR Section 11 discusses how the design and operation of the radwaste system and equipment meet these design requirements. The Offsite Dose Calculation Manual (ODCM) controls the actual performance and operation of the installed radwaste system equipment and the reporting of actual releases and offsite doses.

9.3.3 Evaluation

9.3.3.1 Radioactive Waste Management

The radioactive waste management system is required to maintain normal plant and offsite doses within the limits prescribed in 10CFR50 and 10CFR20. For normal operation, no changes will be made to the allowable RCS or SG activity specified in the technical specifications; therefore, the demands made on the radioactive waste management system will not change.

9.3.3.2 Radiation Protection

For normal and shutdown operations, the shielding requirements will not change since the limits applied to RCS and SG activity in the technical specifications were not changed for power uprate. For design basis events, the shielding requirements have been evaluated and show that doses remain within limits delineated in 10CFR50 and 10CFR100.

9.4 ELECTRICAL EQUIPMENT QUALIFICATION

9.4.1 Scope of Review

Impact to the Environmental Qualification (EQ) Program from power uprate included changes in the containment loss of coolant accident (LOCA) temperature and pressure EQ profile, containment radiological conditions (both normal and accident), auxiliary building radiological conditions during accident conditions, and high energy line breaks (HELBs). SAR Section 3.11 discusses environmental qualification.

9.4.2 Containment Accident Conditions

Electrical EQ equipment located in containment was evaluated to the revised LOCA profile from the ANO-2 containment uprate and steam generator replacement efforts, which included power uprate. EQ equipment remains qualified to the revised LOCA temperature and pressure conditions. The containment analysis evaluations were included in the containment uprate submittal dated November 3, 1999 (2CAN119903), which has been reviewed and approved by the NRC in a safety evaluation dated November 13, 2000 (2CNA110002).

The normal and accident radiological conditions were evaluated using ORIGEN-II source terms developed for power uprate. The revised normal 40-year dose and 30-day accident doses (airborne, plateout, and sump) were determined. EQ equipment remains qualified to the revised containment radiological conditions.

9.4.3 High Energy Line Breaks (HELBS)

Revised HELB temperature and pressure conditions in the auxiliary building (see Section 9.2 of this report) were evaluated to determine impact to the current qualification of EQ equipment. EQ equipment located in the auxiliary building remains qualified to the revised HELB conditions.

9.4.4 Radiological Conditions - General Auxiliary Building

The accident radiological conditions in the auxiliary building were calculated for power uprate. The dose from recirculating fluid, released fission products from ESF component leakage, filter doses, and reactor building shine were calculated. With the exception of released fission products from ESF equipment leakage and containment shine, all revised doses are bounded by the current dose values. The general auxiliary building accident doses from ESF equipment leakage increased slightly but had no impact on the qualification of EQ equipment. The dose contribution from containment shine in the auxiliary building had negligible change and is not a significant contributor to the total auxiliary building equipment qualification dose.

The normal radiological conditions in the auxiliary building are not expected to change due to power uprate. Therefore, the normal 40-year dose values used in the EQ Program are

unchanged. This will be verified by the normal radiological surveys of the auxiliary building which will be conducted during Cycle 16.

9.4.5 Summary

The existing equipment qualification documentation was evaluated against the containment and auxiliary building environmental conditions postulated for power uprate (radiological, LOCA, and HELB). The result is that EQ equipment remains qualified for power uprate. The evaluation of revised LOCA temperature and pressure conditions from power uprate was performed with the containment uprate analysis work and submitted to the NRC with the containment uprate submittal. Subsequent to completion of these evaluations, non-conservatisms were discovered in some of the design inputs used in the radiological EQ dose calculations. The non-conservative design inputs were not related to the increase in power and the conclusions discussed above are not expected to be affected. Nonetheless, work is currently in progress to correct the calculations. This work is being performed in accordance with the station corrective action program. We will notify the NRC staff of the results.

9.5 MOV PROGRAM

The Unit 2 valves in the MOV program were evaluated for impact due to uprated conditions. Expected system pressures and temperatures were compared with the pressures and temperatures listed in MOV maximum expected differential pressure calculations, setpoint calculations, seismic and weak link calculations, and certified valve datasheets. Existing design assumptions were found to be bounding for uprated conditions.

9.6 FIRE PROTECTION PROGRAM

The impact of the power uprate on the Fire Protection Program was evaluated by reviewing specific impacts of plant modifications and the overall program impact. The review determined that the modifications required for power uprate will not adversely affect the ability to achieve safe shutdown during a fire scenario. SAR Section 9.5.1 discusses the Fire Protection Program at ANO-2.

The Fire Protection review included evaluation of such potential concerns as EDG loading and time available to ensure operation of the EDG transfer pumps, heat load in electrical equipment rooms, changes to the service water system (no other safe shutdown systems are affected by the power uprate related modifications), the effect on ambient temperatures in the plant, the effect of increased main steam pipe temperatures on seal material in associated fire barrier penetrations, etc. One case was identified in which the penetration seal material will need to be replaced. No other changes were found to be necessary for the fire protection systems.

The alternate shutdown procedure was determined to be adequate with no changes. The time available to perform certain manual actions was affected by the increased post-trip shrinkage in

the RCS. The increased shrinkage is caused by the increased inventory due to the replacement steam generators and by the higher T_{avg} under power uprate conditions. However, the current alternate shutdown procedure still accomplishes these actions within the required time.

9.7 CONTROL ROOM HABITABILITY

Power uprate does not affect normal ambient conditions inside the control room. Nor does it impact control room conditions during non-radiological events. Therefore, the only control room habitability (CRH) issue associated with a power uprate is the dose consequences associated with accidents at ANO-2.

As previously stated in Reference 9.7-1, the design basis LOCA (MHA) for ANO-2 provides bounding control room dose consequences. The bounding nature of this event was verified for power uprate through confirmatory control room dose calculations for other events (e.g., main steam line break, feedwater line break and seized rotor events). The results of the bounding dose analysis are presented in Section 7.3.10 of this report and meet the guidelines on 10 CFR 50, Appendix A, General Design Criterion 19.

Entergy is familiar with the ongoing discussions on CRH between the industry and the NRC and remains an active participant in development of the industry's CRH assessment guidance. Since this is an issue relating to the current MHA bounding control room dose calculation and considered a generic industry issue, resolution of this issue will be pursued through industry initiatives. In the interim, ANO has formed a CRH review committee to study the issue and develop an action plan to help resolve issues associated with the integrity of the control room envelope (the unfiltered control room in-leakage issue). Actions to date include inspection of the ANO-2 control room penetrations and additional sealing of any that are suspect. A comparable inspection, and sealing if necessary, of the ANO-1 penetrations will be performed during 1R16 in the spring of 2001. ANO is also studying methods of depressurizing two areas adjacent to the common control room envelope that may be pressurized following a MHA. Finally, by mid-2001, ANO intends to conduct a formal control room walkdown utilizing industry experts in this area to identify any additional vulnerabilities to unfiltered control room in-leakage. Any additional actions arising from the ongoing discussions between the industry and the NRC will be considered at that time.

9.7.1 References

9.7-1 Letter from Jimmy D. Vandergrift (Entergy Operations, Inc.) to U.S. Nuclear Regulatory Commission dated May 17, 2000 (2CAN050006), "Supplemental Information on Reactor Protective System Setpoint Changes – Probabilistic Safety Assessment Branch."

9.8 FLOW ACCELERATED CORROSION (FAC)

An evaluation was performed of the effects that the replacement steam generators, power uprate and the high pressure turbine upgrade would have on flow accelerated corrosion (FAC) wear rates. Power uprate results in increased flow rates; therefore, worst case conditions (i.e., valves wide open for maximum steaming conditions) were utilized to bound the effects on FAC wear rates.

In preparation for performing this study, an analysis was accomplished for the existing model. This analysis incorporated the most recent inspection data into the model, which allowed the model to adjust its predicted wear rate upward or downward to calibrate or correlate the predictions to the field data. This provided a baseline for comparing current wear rate predictions against the wear rates that would result from the changes in operating conditions.

This parametric study, which was performed using a copy of the original CHECWORKS model, addressed systems that are included in the FAC program and are classified as susceptible-modeled, which are main steam, main feedwater, reheat steam, high pressure extraction, low pressure heater vents and drains, high pressure heater vents and drains, condensate, and steam generator blowdown. Utilizing the CHECWORKS software, the study revealed that the worst case operating conditions for power uprate would have minimal impact on FAC wear rates. For the systems listed above, the average increases in wear, as predicted by the CHECWORKS model, would cause no need for physical modifications to the plant. As the operating parameters change to accommodate the uprated conditions, the original CHECWORKS model will require slight adjustments to reflect the new operating conditions. These program adjustments will be accomplished in accordance with the program guidelines.

9.9 IMPACT OF INCREASED POWER ON OPERATIONS, PROCEDURES, AND SIMULATOR TRAINING

9.9.1 Simulator Modifications

Simulator modifications are reviewed to determine the impact on training materials (e.g., System Training Manuals, Simulator Exercise Guides, Simulator Examination Scenarios, etc.) and on the simulator models for system and panel changes. Plant modifications that affect the primary systems, secondary system, and panel hardware or control systems will be incorporated into the simulator upon approval of the modification package.

After process model modifications are complete, simulator initial conditions are established at various power levels and times-in-life. Simulator operability testing occurs after the initial conditions have been established.

The simulator software offers flexibility in that the simulator parameters can be quickly changed to model either Cycle 15 or Cycle 16 parameters. The ability to change from the present cycle to Cycle 16 parameters in minutes provides flexibility for various training needs.

As a minimum, operability testing as described in ANSI/ANS 3.5 will be conducted for changes due to power uprate.

9.9.2 Pre-Outage Testing

As plant modifications are installed and control systems are changed, they are assessed by one or more of the following:

- Long Term Cooling (LTC) software (designed by ABB for control system testing)
- Combustion Engineering Nuclear Transient Simulator (CENTS)
- Feed Water Control System Stimulator
- Engineering reports on system response and new accident analyses
- Best Estimate data
- Supporting ANSI/ANS 3.5-1998 Post Modification Testing

9.9.3 Post-Outage Testing

The ANO-2 Simulator will be compared to actual plant startup and operating data. Data collection will be conducted by the simulator engineering and training staffs for validation of the simulator performance. This new data will become the baseline for the simulator in future ANSI/ANS 3.5 testing.

9.9.4 Operations Training

The training staff will provide classroom training and simulator training on the power uprate changes for the operations crews and staff prior to the 2R15 Refueling Outage. The classroom and simulator training will consist of plant changes, system response changes, new or revised technical specifications, startup testing, revised procedures (normal, abnormal, and emergency) and revised safety analyses.

Startup training will be conducted prior to the conclusion of the outage for the operations crews with emphasis on core reload, positive moderator temperature coefficient, Reactor Engineering interface and teamwork skills.

9.9.5 Operating Procedures

Existing procedures will adequately cover emergency scenarios, abnormal occurrences, or normal operations. New procedures are not expected to be required. Analyses and evaluations performed for power uprate made no change to the assumptions regarding operator actions that are required to mitigate the consequences of accidents. There are no new types of accidents, changes to accident scenarios, or changes to operator actions resulting from the power uprate other than those considered already. Adjustments to setpoints, which are consistent with analyses, are required due to the increase in power, hot leg temperature, and decay heat.

Operator actions that were assumed in the power uprate analyses are either consistent with or better than those assumed in the current analyses. There were no changes made to operator action assumptions in accident or transient analyses that resulted in reduced operator response times.

9.10 HUMAN FACTORS

Power uprate will result in some changes to indications and computer points available to the operator. For example, to accommodate the higher turbine power and pressure levels associated with power uprate, control room panel meters dealing with turbine status monitoring were replaced during 2R14 with new meters incorporating the revised scales/ranges. The increased level span between level taps associated with the replacement steam generators for the Regulatory Guide 1.97 steam generator wide-range level indication resulted in a scale range change. Another change directly related to flow increases expected for power uprate was the respanning of main steam and feedwater flow inputs to indicators, to the feedwater control system, and to COLSS. All of the above work was done during 2R14 in anticipation of the upcoming power uprate during 2R15. Because the design process prompts a human factors review when required, no additional reviews for human factor concerns are necessary for the applicable modifications implemented for power uprate.

9.11 TESTING

The power ascension test program for Cycle 16 will build upon the Cycle 15 program developed for steam generator replacement. Most of the plant modifications required for power uprate will have been installed during the steam generator replacement outage prior to Cycle 15. Baseline data on the modified NSSS and BOP systems will have been obtained during startup testing after that outage. These tests were designed to confirm that the affected systems/components operate within their design and licensing bases with some tests designed to determine that sufficient margins exist for the planned uprate conditions. These tests were also developed so that they may be used during the next cycle to demonstrate that plant systems/components perform as designed in the uprated conditions.

During the refueling outage prior to Cycle 16, the remaining design modifications required to support power uprate will be installed. The startup test program after that outage will include many of the same tests performed for Cycle 15 with data collection extended to the new uprated power level. These tests include vibration and thermal expansion measurements of primary and secondary systems; RCS flow measurements; primary and secondary chemistry; core power distribution and reactivity checks; and transient response of primary and secondary control systems, critical cooling systems, and secondary plant performance. Additional tests will also be performed to demonstrate appropriate design and licensing basis performance of the new modifications.

9.12 PROBABILISTIC SAFETY ASSESSMENT (PSA)

The ANO-2 plant risk model is an internal events Level-1, limited-scope Level-2 model. ANO-2 has no Level-3 PSA model. The model will be updated to match the as-built plant in accordance with the requirements of Maintenance Rule Paragraph (a)(4). The uprate of ANO-2 is not expected to have a significant impact on the ANO-2 plant risk.

The inputs and assumptions of the ANO-2 Probabilistic Safety Analysis (PSA) Core Damage Frequency (Level-1) model most affected by the uprate are judged to be the plant success criteria and the operator recovery probabilities. The uprate is not expected to change the success criteria. The uprate is expected to result in a reduction in the time available for operator response during some accidents. However, the treatment of operator recovery in the current ANO-2 Level-1 PSA model is conservative. One of the most significant conservatisms is the limited number of operator recoveries applied per cutset. A more realistic treatment of operator action is expected to have a much greater effect on the assessed risk than that of reduced available time for such action. Thus, the effect of the uprate on the assessed internal events Level-1 risk of operating ANO-2 is not expected to be significant. The effect of the uprate on the external events risk is expected to be similar to that of the ANO-2 internal events Level-1 risk.

The uprate is not expected to significantly affect the type of fission products released from the plant during a severe accident, the timing of their release, nor the magnitude of these possible releases. Thus, the proposed power uprate of ANO-2 is not expected to have a significant impact on the ANO-2 severe accident plant fission product release (Level-2) and severe accident public health impact (Level-3).

END OF SECTION

10 ENVIRONMENTAL IMPACT REVIEW

10.1 INTRODUCTION

This review evaluates potential environmental impacts associated with ANO-2 being licensed for 3026 megawatts thermal (MWt), a 7.5% increase above the current licensed NSSS power level of 2815 MWt. The gross electrical output corresponding to 3026 MWt is 1048 MWe. The review identified no significant new information for any of the issues when compared against the Final Environmental Statement for Arkansas Nuclear One Unit 2, prepared and issued by the U. S. Nuclear Regulatory Commission in June 1977 (NUREG-0254) and other available documents.

Since ANO-1 and ANO-2 share a common site, this review also references the draft to NUREG-1437, Supplement 3, September 2000, issued for the license renewal of ANO-1. The Generic Environmental Impact Statement (GEIS) and its addendum identifies 92 environmental issues and reaches generic conclusions related to environmental impacts for 69 of these issues that apply to all plants or to plants with specific design or site characteristics. Additional plant-specific review is required for the remaining issues. For ANO-1, these plant-specific reviews were included as Supplement 3 to the GEIS. Based on ANO's and the NRC's analyses that consider and weigh the environmental effects of the proposed license renewal action, the environmental impacts of alternatives to the proposed action, and alternatives available for reducing or avoiding adverse effects, impacts were of SMALL significance.

Similarly, this environmental review demonstrates that the request for a licensing amendment for an uprated power level of 3026 MWt NSSS power involves:

1. No significant hazards considerations,

2. No significant changes in the types or significant increase in the amounts of any effluents released offsite, and

3. No significant increase in individual or cumulative occupation radiation exposure.

Major refurbishment and plant maintenance activities identified as necessary to support the ANO-2 power uprate received an environmental review per ANO procedures during the planning stage and have been further evaluated. Although normal plant maintenance activities may later be performed for economic and operational reasons, no significant environmental impacts associated with such activities are expected.

Based upon the evaluations discussed in the review, Entergy Operations concludes that the environmental impacts associated with the ANO-2 power uprate are also of SMALL significance. The environmental impacts from continued operation of ANO-2 at uprated conditions are similar to those experienced during the original power level and as evaluated in the Final Environmental Statement.

When appropriate, analyses for power uprate used 3087 MWt as a bounding power level to account for a 2% measurement uncertainty.

10.2 ANO-2 ENVIRONMENTAL STATEMENT

The Final Environmental Statement concludes that ANO-2 would employ a pressurized-water reactor (PWR) "to produce up to 2825 megawatts thermal (MWt)...[and] the maximum design thermal output of the unit is 2908 MWt with a corresponding maximum calculated electrical output of 974 MWe." The 2908 MWt thermal is approximately 3% greater than 2825. At the outset of the original design phase, ANO-2 was to be sized at 2770 MWt. As the design developed, the plant design and size was increased and ANO-2 was granted an operating license for 2815 MWt. The 2825 MWt includes 10 MW from reactor coolant pump heating due to inefficiency, inherent in all pumps.

For the assessment of any change in the environmental impact caused by the ANO-2 dual-pressure condensers and cooling tower operating at uprated conditions, an adjusted heat balance for a calculated maximum electrical generation of 1084 MWe was used. The heat balance that was adjusted is the "valves-wide-open" (VWO) heat balance provided by turbine manufacturers to demonstrate that their turbines are designed with margin. The corresponding NSSS power to 1084 MWe is 3129 MWt, which is 103.4% greater than the requested licensed power of 3026 MWt. The VWO heat balance was adjusted by applying the highest expected condenser pressures in order to calculate maximum heat rejection from the turbine exhaust steam to the condenser cooling water. This increased heat transfer to the condenser cooling water was then calculated for the cooling tower. For the purpose of environmental impact assessment, the results for calculated evaporation, makeup, and cooling tower blowdown rates for 1084 MWe bound and provide margin to expected values.

10.3 SITE AND ENVIRONMENTAL INTERFACES

10.3.1 Site Information (Common to ANO-1 and ANO-2)

Location: Pope County, Arkansas
10 km (6 miles) WNW of Russellville
Latitude 35°-18'-36"N; longitude 93°–13'-53"W
Licensee: Entergy Arkansas, Inc.

Total Area: 471 ha (1164 acres)
Exclusion Distance: 1.05 km (0.65 mile) radius
Low Population Zone: 6.44 km (4.00 mile) radius
Nearest Major City: Little Rock; 1990 population: 175,795
Site Topography: flat
Surrounding Area Topography: hilly to mountainous
Land Use within 8 km (5 miles): wooded

Nearby Features: nearest town is London 3 km (2 miles) NW. Lake Dardanelle is 15,000 ha (37,000 acres) in size and is part of the Arkansas River. The Missouri Pacific Railroad and U. S. Highway I-40 are just north of the site.

Population within an 80-km (50-mile) radius:

1990	2000	2010	2020	2030
200,000	274,037	295,803	312,158	322,991

Sources: Draft version of NUREG-1437 (GEIS), Supplement 3 and "Applicant's Environmental Report – Operating License Renewal Stage

10.3.2 ANO-2 Information

Construction Permit	1972
Operating License	1978
Commercial Operation	1978
License Expiration	2018
Type of Reactor	PWR

Item	Original	Power Uprate
Licensed Thermal Power [MW(t)]	2815	3026
Design Electrical Rating [gross MW(e)]	958	1048
Nuclear Steam Supply System Vendor	CENP*	CENP

*CENP, formerly Combustion Engineering, Inc., a division of Westinghouse Electric Co. performed the NSSS analyses for both original and power uprate conditions.

10.4 ENVIRONMENTAL IMPACTS

The GEIS for License Renewal of Nuclear Power Plants, NUREG-1437, summarizes the approach and findings of a systematic inquiry into the potential environmental consequences of operating individual nuclear power plants. In regard to land use, water use, water quality, air quality, aquatic resources, terrestrial resources, radiological impacts and socioeconomic factors, generic conclusions were reached for 69 of the issues. The remaining 23 issues were evaluated in Supplement 3 to the GEIS, with both ANO and NRC concluding that impacts would be of SMALL significance.

Additional information on the environmental impact effects of the ANO-2 power uprate that support the continued assessment of SMALL significance is provided in the following discussions.

10.4.1 Condenser and Cooling Tower Evaluation Analysis of Environmental Impact

The ANO-2 condensers utilize closed-cycle cooling via a cooling tower. The condenser tubes and tubesheets were replaced during 2R13. The replacement resulted in slightly higher circulating water system resistance and a corresponding reduction in circulating water flow rate.

Lake Dardanelle, formed by damming the Arkansas River, serves as the water source for makeup to the tower.

Condenser/Cooling Tower System

Makeup source: Lake Dardanelle

Condenser type: Dual-pressure

Cooling Tower Design Atmosphere Conditions: 81 °F Wet Bulb @ 37% RH

Item	Cycle 13*	Cycle 16 forward**
Range at design conditions, °F	30.7	33
Approach at design conditions, °F	15.3	15.3
Circulating water temperature from the cooling tower basin at design conditions, °F	96.3	96.3
Rated circulation water flow rate, gpm	423,200	420,000
Operating circulation water flow rate, gpm	436,000	428,500
Condenser tube material	90/10 Cu/Ni	Titanium
Condenser tubesheets	Muntz	Titanium
Condenser/cooling tower duty, Btu/hr	6.2×10^9	6.9×10^9
Mixing dilution flow by Unit 1 circulating water, gpm	393,000	393,000

* Prior to replacing tubes and tube sheets and reconditioning the condensers in 2R13

** Evaluated at valves-wide-open (VWO) conditions (1084 MWe and 3129 MWt)

10.4.1.1 Cooling Tower Design

The cooling tower original design criteria of 81° F wet bulb and 37% relative humidity is conservative. These conditions of wet bulb and relative humidity lead to a maximum predicted cooling tower basin temperature of 96.3° F at the operating flow rate of 420,000 gpm. For example, the average daily cooling tower basin temperature from 1989 to 1996 did not exceed 92° F and the maximum basin for 1997 did not exceed 94° F. The meteorological worst day on record (July 17, 1934) shows the worst average 4-hour wet bulb temperature and relative humidity of 82.4° F and 59.20%. The wet bulb temperature on the worst 4-hour period exceeded the original tower design criteria by only 1.4° F and the relative humidity was 22.2% higher.

Cooling tower performance on hot summer days (above 70° F wet bulb) improves as relative humidity increases.

10.4.1.2 Circulating Water Makeup Rate and Blowdown

The increased temperature range across the tower evaluated for VWO conditions will result in an evaporation rate increase of 0.2% to 3.1% of circulating water flow at design conditions. At a circulating water flow rate of 420,000 gpm, approximately 840 gpm of additional makeup water will be required due to increased evaporation. Makeup due to evaporation will increase from 12,180 to 13,020 gpm. This additional evaporation will require a small increase in the cooling tower blowdown rate to maintain circulating water chemistry. However, the effect of a slight blowdown increase is negligible since the blowdown is normally mixed with the ANO-1 circulating water system discharge, which has a flow rate of 393,000 gpm with two of the four circulating water pumps in operation.

There are no blowdown flow limitations established in ANO NPDES Permit Number AR0001392, issued by the Arkansas Department of Environmental Quality. Other parameters such as pH, free available chlorine and total zinc will continue to be monitored in accordance with the permit to ensure that state water quality standards are met.

10.4.1.3 Liquid Discharge Temperature

The higher temperature range across the tower will not cause an increase in cooling tower basin temperature at ambient wet bulb temperatures above 70°F. However, at wet bulb temperatures below 70° F, this higher temperature range across the tower will result in slightly higher basin temperatures (<1° F). This small increase in basin temperature (hence blowdown temperature) is negligible since the blowdown is normally mixed with high flow rate ANO-1 circulating water system discharge as discussed above.

The temperature range after power uprate will be 32.90° F at a flow rate of 420,000 gpm. Correcting for the range changes due to power uprate results in a reduction in cooling tower basin temperature of 0.1° F at the design point (81° F wet bulb and 37% relative humidity). Therefore, the original design criteria bound the power uprate conditions for wet bulb temperatures above 70° F.

The discharge limits for ANO are currently established in NPDES Permit Number AR0001392, dated September 30, 1997. The effluent discharge limits are 43° C (110 F) daily maximum and 40.5° C (105° F) daily average. These limits apply to the point where the cooling water enters the discharge canal. A specific condition of NPDES Permit Number AR0001392 requires ANO to monitor water temperatures after the discharged cooling water passes through the discharge embayment and enters the main channel of Lake Dardanelle. Since 1973, when ANO was originally permitted to discharge cooling water to Lake Dardanelle, no violations of established thermal permit limits have occurred.

During the period from June to September, water temperatures are monitored twice a month at three locations in the lake within the influence of the ANO cooling water discharge. This is to ensure that the thermal water quality standard for the lake is not exceeded.

10.4.1.4 Air Particulate Emissions

Air emissions are regulated by the State of Arkansas Air Quality Standards. ANO Air Permit 0090-AR-2 regulates permitted emission sources at the ANO site. Based on previous emission calculations submitted to the Arkansas Department of Environmental Quality, the ANO-2 cooling tower was classified as a insignificant source and need not be regulated as an emission source under the permit.

Estimates of air particulate emissions use a standard drift value of 0.073 lb. drift/1000 gpm of circulating water. This is based on a recommended standard value taken from Table 13.4-1 of EPA's AP-42. Since the circulating water flow rate does not increase for Cycle 16 forward, air particulate emissions will not increase. (Circulating water flow rate actually decreased slightly after the condenser was refurbished during 2R13.)

Therefore, since there is no increase in air particulate emissions, the ANO-2 cooling tower classification as an insignificant source will not change.

10.4.2 Fuel Enrichment, Burnup and Transportation of Fuel and Waste

The current fuel enrichment and peak pin burnup limits for ANO-2 are 5.0 wt% U-235 and 60 GWD/MTU respectively. The NRC has previously approved these limits. There will be no changes to these approved limits for ANO-2 Cycle 16. The projected enrichments and burnup values for ANO-2 Cycle 16 are required to be within these limits. The preliminary average enrichment for ANO-2 Cycle 16 is 4.6 wt% U-235. In comparison, previous ANO-2 cycles have an average enrichment of approximately 4.5 wt% U-235. All analyses verifying these two NRC approved limits will be applicable to ANO-2 Cycle 16 forward and will be maintained.

10.4.3 Radiological Impacts

A review of historical data on ANO releases and the resultant dose calculations revealed that the dose to the maximally exposed individual for each pathway in the vicinity of ANO was a fraction of each of the limits specified in EPA's environmental radiation standards 40 CFR Part 190 as required by 10 CFR 20.1301(d). Entergy does not anticipate any significant changes to the radioactive effluent releases or exposures from ANO-2 operations as a result of the power uprate. Therefore, the impacts to the environment are expected to be similar to those in recent years.

END OF SECTION